SOFT TISSUE ATTACHMENT TO ORTHOPAEDIC IMPLANT MATERIALS

By

CATHERINE JANE PENDEGRASS

SUBMITTED FOR THE DEGREE OF DOCTOR OF PHILOSOPHY
DEPARTMENT OF BIOMEDICAL ENGINEERING INSTITUTE OF ORTHOPAEDICS UNIVERSITY COLLEGE LONDON

JULY 2005

THE CENTRE FOR BIOMEDICAL ENGINEERING
INSTITUTE OF ORTHOPAEDICS AND MUSCULO-SKELETAL RESEARCH
UNIVERSITY COLLEGE LONDON
ROYAL NATIONAL ORTHOPAEDIC HOSPITAL TRUST
STANMORE
MIDDLESEX
HA7 4LP
UNITED KINGDOM

ProQuest LLC
789 East Eisenhower Parkway
P.O. Box 1346
Ann Arbor, MI 48106-1346

CONTENTS **PAGE**

ABSTRACT

ABSTRACT: SOFT TISSUE ATTACHMENT TO ORTHOPAEDIC IMPLANT MATERIALS

Most orthopaedic endoprostheses are used to replace damaged joint surfaces and rely little on soft tissue attachment for their function. Massive bone tumour implants and solutions to attach external implants to the skeleton for amputees rely on soft tissue attachment for successful function. Massive implants require a tendon-metal attachment to preserve joint movement. Implants for amputees where the skeletally anchored implant penetrates the skin, require soft tissue attachment to produce an effective microbial seal which prevents infection.

My thesis aims to investigate the concept that biomimetic soft tissue-implant interfaces can be engineered using surface texturing, coatings and biological augmentation, to enhance the attachment and function of the soft tissues between:

1) Metallic implants and tendons, used for proximal tibial replacement

2) The epithelial and sub-epithelial soft tissues to transcutaneous implants used for amputation prostheses

I have shown that soft tissue derived cells' proliferative capacity, morphology and attachment are significantly affected by biomaterials and surface topography of the substrate used to support their growth, whilst biological substrate coatings can be used to optimise these functions to suit the requirements of an implant.

My findings have demonstrated that a functionally and morphologically successful tendon soft tissue – implant interface can be engineered using autologous cancellous bone and marrow graft combined with hydroxyapatite coatings in a clamp device, resulting in an interface that has significantly more bone attachment associated with fibrocartilage compared with hydroxyapatite alone.

My thesis demonstrates that the soft tissue – implant interface around intraosseous transcutaneous amputation prostheses can be optimised based on natural analogues. Deer antlers produce a microbial seal by engineering a region of thick dermal collagen fibres attached to the bone surface which supports the epithelium. Increasing the surface porosity and area of transcutaneous implants in the dermis results in significantly less epithelial down growth and significantly greater attachment of the epithelial and dermal tissue layers respectively.

ACKNOWLEDGEMENTS

ACKNOWLEDGEMENTS

I should like to thank my supervisor, Professor Gordon Blunn, Head of the Centre for Biomedical Engineering, for the opportunity to work in this exceptional department and for his vast contribution to my thesis. I am grateful for his colourful sense of humour, his patience, which I have tried to the full, and his continual support and guidance throughout my PhD.

It has been an honour to work with the people of this department. The support and friendship of my collegues has been immeasurable and I should like to thank them all for their contributions to my academic and personal achievements. I can not thank Annie Bartram enough for her help throughout my PhD – her ruthless approach with my comma obsession was especially appreciated. Special thanks must go to Keith Rayner for his technical expertise, impeccable timing, help and guidance in all of my "engineering" based undertakings, and of course to the girls, for laughter, lunches and conferences – you know who you are!

I should also like to thank Professor Allen Goodship, Head of the Institute of Orthopaedics and the staff in the Biological Services Unit at the Royal Veterinary College for their help and guidance. I would like to extend a special thank you to Gillian Hughes, for her friendship, chocolate biscuit scoffing sessions, and endless anaesthesia.

This thesis would not have been completed without Mike Oddy. I am indebted to him for his tireless hours of gait analysis, his surgical, academic and personal contributions, and for teaching me the merits of using "lab books" as apposed to "post-it notes". He has brought order to my chaos!

This thesis is dedicated to my family. Without their love and support throughout my life, I would be lost.

LIST OF FIGURES

LIST OF TABLES

CHAPTER ONE

INTRODUCTION

CHAPTER ONE: INTRODUCTION

1.1 AIMS AND HYPOTHESES

1.1.1 OVERVIEW

1.2 NATURALLY OCCURING SOFT-HARD TISSUE INTERFACES

1.2.1 TRANSCUTANEOUS INTERFACES

1.2.1.1 THE SKIN

1.2.1.2 THE TOOTH

1.2.1.3 THE BABYRUSSA TUSK

1.2.1.4 DEER ANTLERS

1.2.2 SUBCUTANEOUS INTERFACES

1.2.2.1 THE OSSEO-TENDINOUS JUNCTION

1.2.2.1.1 TENDON ANATOMY

1.2.2.1.2 THE TENDON-BONE INTERFACE

1.2.2.1.3 TENDON AND LIGAMENT HEALING

1.2.2.1.4 TENDON BONE – TUNNEL HEALING

1.3 ARTIFICALLY ENGINEERED SOFT-HARD TISSUE INTERFACES

1.3.1 IMPLANT MATERIALS

1.3.1.1 TEXTURING AND COATINGS

1.3.1.1.1 HYDROXYAPATITE COATINGS

1.3.1.1.2 BIOLOGICAL COATINGS

1.3.2 IMPLANT INTEGRATION WITH THE CONNECTIVE TISSUE

1 INTRODUCTION

1.1 AIMS AND HYPOTHESES

This thesis aims to investigate the concept that soft tissue-implant interfaces can be engineered to enhance their attachment and function using surface texturing, coatings and biological augmentation developed from research into natural analogues. My study aims to engineer the interfaces between:

1) **The soft tissue of tendons to implants, used for proximal tibial replacement**

2) **The epithelial and sub-epithelial soft tissues to transcutaneous implants used for amputation prostheses**

This thesis tests the general hypothesis that **successful soft tissue – implant interfaces can be engineered, by artifically simulating the morphological adaptations observed in soft – hard tissue interfaces of natural analogues.**

This chapter of my thesis gives an insight into the current status of research into soft tissue-implant interface engineering, a background into the biology of the soft tissues interfacing subcutaneous and transcutaneous implant materials and the problems associated with these interfaces.

Chapter Two presents a histological analysis of the soft-hard tissue interface that occurs naturally in deer antlers with the aim of developing an artificial transcutaneous interface. In deer antler, the skin forms an interface with the pedicle when the velvet is shed. **It is hypothesised that the bone surface of the antler and pedicle will be different.**

Based on the observations from Chapter Two, Chapter Three investigates the effects of titanium alloy substrate topography on the proliferative capacity, morphology and attachment of fibroblasts and epithelial cells *in vitro*. This chapter is designed to determine the optimal surfaces for soft tissue attachment *in vitro*. **The hypothesis that fibroblast and epithelial cells' proliferative capacity, morphology and attachment will be directly affected by the type and topography of the substrates used to support their growth is tested.**

From the observations in Chapter Two, Chapter Four examines the *additional* affects of two biological coatings, fibronectin and laminin, on fibroblast and epithelial cell attachment, proliferation and morphology in association with the biomaterials used for the development of soft tissue-implant interfaces, but essentially with the view to incorporation into other implants abutting soft tissues *in vivo*. **It is hypothesised that biomaterial topography will have a lesser effect on cell attachment and proliferation compared to adhesion protein coatings. The hypotheses that fibronectin will increase the attachment and proliferation of dermal fibroblasts, and laminin will increase the attachment and proliferation of dermal epithelial cells, will be tested.**

Chapter Five is an *in vivo* study of the development of an intraosseous transcutaneous amputation prosthesis. In Chapters Three and Four the effects of biomaterial topography and biological coatings were investigated *in vitro*. In Chapter five, emphasis is placed on engineering a successful skin-implant interface, examining the effects of different implant surface topographies, biomaterial and biological coatings to optimise the soft tissue seal surrounding transcutaneous implants. **It is hypothesised that implants designed to mimic naturally occurring transcutaneous structures provide surfaces that promote epithelial and sub-epithelial soft tissue attachment in an *in vivo* model.**

In the preceding chapters natural analogues, implant materials and biological augmentation were investigated. In Chapter Six, the principles developed were applied to enhance the attachment of tendon to metallic implants. This Chapter includes a functional and histological study of the reconstruction of the lower limb extensor mechanism *in vivo* and tests the **hypothesis that a tendon-implant neo-enthesis can be engineered *in situ*, using a suitable osteoconductive scaffold, bioactive material and autogenous cancellous bone and marrow graft augmentation.** It develops the concepts of tendon clamp design and implementation, enabling sufficient mechanical strength for early mobilisation, with biological fixation developing over time. It aims to achieve a fully functional extensor mechanism reconstruction by re-attaching the soft tissues of the patellar tendon to a metal implant used to simulate a proximal tibial replacement. It is hoped that once the concept is fully developed, it can be utilised as a universal method of re-attaching tendons and ligaments to orthopaedic implants irrespective of anatomical location.

The final chapter discusses the key findings of my thesis. It unites the principles of soft tissue attachment to orthopaedic implant materials in both subcutaneous and transcutaneous environments, which have been developed over the course of my research. It presents and discusses the benefits and drawbacks of the research included in my thesis and proposes possible future directions for research in the area of soft tissue-implant interface engineering, with the ultimate aim of artificially recreating the soft-hard tissue interfaces observed in nature.

It is hoped that some of the developments from my thesis will be incorporated into future implant designs to benefit patients suffering conditions requiring surgical orthopaedic intervention that rely on soft tissue re-attachment for good biological integration and function.

1.1.1 OVERVIEW

Introduction of a foreign material into the human body results in damage of the soft tissue scaffolds that support the body as a whole. Examples of this phenomenon include the disruption of soft tissue attachments as a result of bone replacement by massive prostheses used for bone tumour resection surgery, implantation of transcutaneous implants for dental, auricular and orthopaedic uses, and the subcutaneous implantation of medical devices. In all of these cases, soft tissue interfaces are disturbed, resulting in the need to restore continuity. The examples listed may appear unrelated, however our ability to re-establish soft tissue attachments remains restricted by our failure to successfully re-interface biological and implant materials. In order to redress this problem, a full understanding of soft tissues and interface biology is essential. *In vivo*, numerous soft – hard tissue interfaces exist in both subcutaneous and transcutaneous forms. The osseo-tendinous junction is an example of a natural, deep interface between the soft tissue of tendon and the hard tissue of bone, whilst the dento-epithelial junction is an example of a true, permanent transcutaneous structure, where the soft tissues of the gingiva interface with the hard enamel of the teeth. Understanding the biology and morphology of these natural interfaces may give insights into possible methods that could be employed to engineer interfaces with implant materials.

1.2 NATURALLY OCCURING SOFT-HARD TISSUE INTERFACES

1.2.1 TRANSCUTANEOUS INTERFACES

A number of conditions exist that necessitate the implantation of long-term skin penetrating devices. The introduction of transcutaneous devices can lead to a number of complications including inflammation, foreign body reaction, infection, marsupilization (pocket formation) and extrusion (epithelial migration through porous structures)(Von Recum and Park 1981, Grosse-Siestrup et al 1977). To date, a permanently successful transcutaneous interface between living and artificial materials has not been described; however naturally, a number of junctions between solid structures and soft tissues are observed. A number of structures which appear to penetrate the skin layers, for example hair, fingernails, hooves, horns and feathers, actually originate at the base of epidermal invaginations within the dermal layers, thus do not disrupt the epithelial layer continuity (Von Recum and Park 1981, Grosse-Siestrup and Affeld 1984). Examples of true, naturally occurring, transcutaneous structures include teeth, deer antlers and Babyrussa tusks. In these instances, nature has overcome the problems associated with transcutaneous devices by incorporating the numerous design criteria needed for artificial transcutaneous implant success, into a single structural element. Nature supplies the optimal biomaterial, to which soft tissues will adhere in a transcutaneous site, irrespective of the dynamic nature of the skin layers, where the rapid turnover of cell type and maturation present numerous problems for researchers aiming to artificially engineer this interface type.

1.2.1.1 THE SKIN

By definition, all transcutaneous structures penetrate the skin. In order to engineer an interface where the soft tissues of the skin layers are intimately associated with the transcutaneous implant material, a full understanding of the tissue types abutting the skin-penetrating segment of the implant is required. The epidermis is a multi-layered epithelium (Figure 1.1), composed largely of keratinocytes (named because of their ability to synthesise intermediate filament proteins called keratins). It is regenerated and replenished by a keratinocyte cell linage of stem cells from the basal layer, which differentiate as they migrate through the layers towards the surface of the skin. As the cells migrate, they change appearance from one layer to the next. The innermost layer contains basal cells attached to the underlying basal lamina via hemidesmosomes. Above the basal cells are several layers of prickle cells, whose numerous desmosomes (each a site of anchorage for thick keratin filaments) are visible under the light microscope as tiny

prickles around cell surfaces. Beyond the prickle cell layer, is a thin granular cell layer, which acts as a boundary between the inner metabolically active strata and the outermost layer of dead cells whose intracellular organelles have disappeared. The outermost cells are reduced to flattened scales, called squames (filled with densely packed keratin). This description is very 'static', however it is far from being so. While some basal cells are dividing, adding to the core number of basal cells, others are being released from the basal layer into the prickle cell layer, which is the initial step on the outward journey to the skin surface. When the cells reach the granular layer, they begin to loose their nuclei and cytoplasmic organelles, and are thus transformed into keratinised squames. These cells eventually flake away from the skin surface.

The skin is best viewed as a large organ composed of two main soft tissue types, epithelial tissue of the epidermis and connective tissue of the dermis. The connective tissue of the dermis consists of a loose layer (fibroblasts, collagen, mast cells, macrophages, lymphocytes) and a dense layer (fibroblasts, collagen, elastic fibres). There is also an underlying fatty hypodermis.

The basement membrane or basal lamina is a thin flexible mat, 40-120 nm thick, of specialised extracellular matrix that lies beneath all epithelial cell sheets (Stern 1965). The basement membrane separates these cells and cell sheets from the underlying or surrounding connective tissue. They are also found in other anatomical locations, for example the kidney glomerulus and lung alveolus, where they lie between two cell sheets and function as a selective filter. Basement membranes have more functional roles than merely structural and filtering, as they are capable of determining cell polarity, influencing cell metabolism, organising the proteins in adjacent plasma membranes, inducing cell differentiation and function as specific highways for cell migration (Alberts et al 1994). In skin, owing to the fact that basal cells are released from the basement membrane to migrate through the epidermal layers, it is thought that at least some components of the structure are involved in cell adhesion functions. The basement membrane is mainly synthesised by the cells that rest upon it, and consist of two distinct layers: an electron lucent layer, also called the lamina lucida, that is located adjacent to the basal plasma membrane of cells that rest upon it (typically epithelial cells), and an electron dense layer or the lamina densa below. In some cases, a third layer, the lamina fibroretularis, is present which connects the basal lamina to the underlying connective tissue.

The exact composition of the basement membrane varies between tissue types; however most contain type IV collagen, the heparin sulphate proteoglycan 'perlecan' and

glycoproteins laminin and entactin (Alberts et al 1994). Laminin is one of the initial extracellular proteins synthesised in a developing embryo. It is a large (approx 850,000 daltons) complex of three long polypeptide chains arranged in the shape of an asymmetric cross. It is held together by disulphide bonds, but as a whole, is a flexible structure. It contains many functional domains, one to bond collagen IV, one heparin sulphate, one entactin and two or more to bond to laminin receptor proteins on cell surfaces (Tryggvason 1993).

It is thought that one or more basement membrane components play a functional role in assisting cells adherence to transcutaneous structures, owing to their roles in cell attachment from the basement membrane (Wang et al 1997). Laminin is the most abundant glycoprotein in basement membrane and is both structurally and biologically active. Laminin binds to collagen IV, heparin sulphate proteoglycan, entactin and to itself, to create an integrated structure within the basement membrane. Due to its size and shape, it can span the membrane and bind to various substances on the surface of cells. These substances include a specific high-affinity membrane receptor (Mr = 67.000) and other ligands (heparin sulphate, gangliosides). Binding to laminin elicits cell-specific responses including polarization, migration and differentiation, hence it is an important structural and regulatory molecule. It has diverse effects on cultured cells, and can influence growth, survival, morphology, differentiation and motility (Kleinman et al 1985). These effects may be related to and proceed from the binding of cells to a laminin substrate.

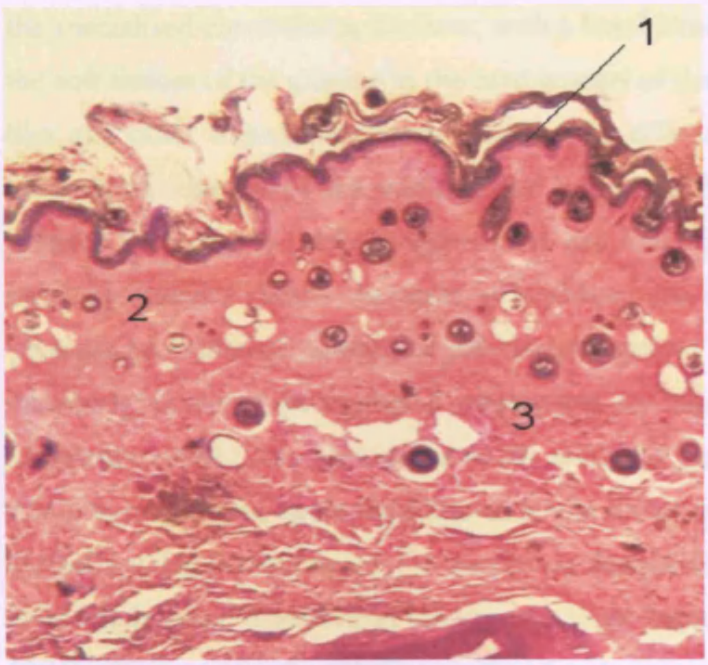

1- Epidermis – Surface keratinized layers
2- Dermis – Dense fibro-elastic connective tissue
3- Hypodermis – Loose connective tissue – mostly adipose

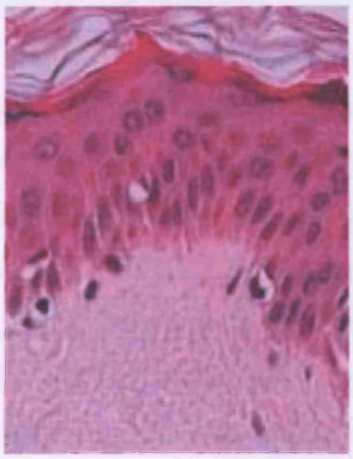

EPIDERMIS:

Stratum Corneum

Stratum lucidum

Stratum granulosum

Stratum spinosum

Stratum Basale

FIGURE 1.1 Histology of the skin

1.2.1.2 THE TOOTH

Since the 1960's we have been aware of the morphology of the structures that interface the natural tooth (Kobayashi et al 1976, Listgarten 1966, Schroeder 1969) (Figure 1.2). The teeth penetrate the stratified squamous epithelium of the gum, or gingiva. They are constantly surrounded by saliva containing microorganisms, and are also in contact with enzymes and globulins that repress pathologic organisms, fight infection and encourage healing (Bodner 1991, Varshney et al 1997, Gocke et al 1999). The skin penetrating section is made of hard, polished enamel. The periodontal ligament runs between the root of the tooth and the wall of the bony cavity in which the tooth resides, and reduces stress at the soft tissue – tooth interface. The region where the external environment, the tooth

and the soft tissues meet is maintained within a recess called the sulcus and is formed by the specialised crevicular epithelium, with a basal lamina and hemidesmosomes attaching the soft tissues of the gingiva to the hard enamel of the tooth. This is a dynamic interface like any other transcutaneous structure. The cells of the crevicular epithelium move towards the enamel of the tooth before migrating through the epithelial tissue layers towards the gingival surface, where they are found as dead cells that become washed away by sulcular fluids. In cases of irritation, the crevicular epithelium thickens and supports an increased number of polymorphonuclear leucocytes. Hemidesmosomes are intimately involved in epithelial attachment to natural teeth (Kobayashi et al 1976, Listgarten 1966). The attachment of the marginal gingiva to the tooth is mediated by a thin non-keratinized epithelium known as the junctional epithelium (JE). The junctional epithelium (JE) attaches to the tooth via hemidesmosomes and a basal lamina-like extracellular matrix known as the internal basal lamina (Hormia et al 1998, Marks et al 1994). The junctional epithelium is found to be in contact with both the hard surfaces of the tooth and the basement membrane adjacent to the connective tissues (Hormia et al 2001). This epithelium-tooth juncture is a unique interface in which the junctional epithelium achieves a tight attachment with the tooth, as well as accomplishing successful cell turnover, tissue permeability and the initial line of defence against oral pathogens. Mimicking the interface between soft and hard tissues observed in this natural example of a transcutaneous structure is the ultimate goal of artificial skin-penetrating implant development. The gingival soft tissues attach to the hard enamel covering the crowns of the teeth, and the cement layer covering the dental roots. Dental enamel is a mineralised cell secretion containing crystalline apatites. It is composed of densely packed enamel rods, each around 3-6μm wide, containing flattened hexagonal hydroxyapatite crystallites (Bannister et al 1995). At the enamel surface the rods are packed with their long axes parallel to form a continuous layer. At regular intervals along the length of each rod, swelling and shrinking can be observed under the light microscope, which result from growth. Cement is the bone-like covering of the dental roots. It is composed of 50% hydroxyapatite and amorphous calcium phosphates, by weight, and overlaps the enamel slightly in newly erupted teeth. Cement is perforated by collagen fibres, which extend into it from the periodontal ligament collagen fibres. New layers of cement are deposited over time to compensate for tooth movement, and these layers incorporate the collagen fibres further within the cement layer. In 1969, Schroeder described the ultrastructure of the junctional epithelium of human gingiva. Standardized areas of junctional epithelium were investigated using electron microscopy. All junctional epithelium specimens were

shown to possess a stratified squamous epithelium, twelve to eighteen cell layers thick, grouped into a stratum basale or basal cell layer and a stratum spinosum. In the tissue approaching the tooth, the cells' shape changes from cuboid to flat with cytoplasm rich in glogi apparatus, large cisternae of endoplasmic reticulum and sparse bundles of cytoplasmic filaments. The basement membrane and basal lamina were found to be indistinct with few desmosomal cell junctions. The connective tissue underlying the basement membrane was shown to contain an accumulation of cells directly below the basal lamina, where instead of a dense network of collagen fibres, fibroblasts, mast cells, neutrophilic granulocytes, macrophages, plasma cells and small lymphocytes were observed in abundance. Schroeder (1969) described the stratum basale as containing cells of a cuboid, flattened morphology with round, oval or flat nuclei, few desmosomes, and numerous hemidesmosomal junctions. In the stratum spinosum the cells adjacent to the enamel surface of the tooth were flat with a thin cytoplasmic content, few desmosomes and numerous neutrophilic granulocytes. Epithelial cells were not found to directly attach to the enamel surface (Schroeder 1969), instead 'a complex of organic layers' was observed, interposed between the cytoplasmic membrane of the epithelial cells and the tooth enamel. Schroeder (1969) termed this complex the Epithelial Attachment Lamina (EAL). He described the EAL as having two structurally and histochemically different layers, the EAL-1 and EAL-2. The EAL-1 was always observed, covering the epithelial cell layers, and was described as a moderately dense, slightly fibriliar, ruthenium-red positive (a stain for glycosaminoglycans) layer of between 0.1-0.2 microns thick. Towards the EAL-1, the cytoplasmic membrane of the abutting epithelial cells possessed what Schroeder then described as 'half-desmosomal junctions of varying length' now known as hemidesmosomes. The EAL-2 layer was located between the EAL-1 and the tooth enamel, and was not continuous with the tooth surface. It was described by Schroeder (1969) as, an electron dense, fibriliar, striated, ruthenium-red negative layer, ranging from 0.1-0.7 microns, varying both within and between patient specimens. The thickness of the EAL-2 layer was seen to increase where extensions of the epithelium-enamel towards the enamel were observed.

In 1967, Löe defined normal junctional epithelium as containing no inflammatory cells, with an underlying connective tissue free from inflammatory infiltrate. This finding was not collaborated by Schroeder (1969) who stated that in humans this was rarely the case, and an inflammatory cell population was always observed in the connective tissue layer beneath the junctional epithelium.

The gingival junctional epithelium is a stratified tissue, without a stratum granulosum or stratum corneum (McHigh 1964, Löe 1967, Schroeder 1969). The epithelial attachment to the tooth enamel is characterised by the presence of hemidesmosomes and an interposing epithelial attachment lamina. The hemidesmosomes are identical to those of basal cell membranes facing the basal lamina (Stern 1965). The 'basal lamina' between the junctional epithelium and the tooth surfaces is a multi-layered structure which mediates the attachment of epithelial cells to the tooth enamel via fine filaments that span between the interposing lamina, hemidesmosomes and tooth enamel, combining them to form a stable structural unit (Listgarten 1966, Schroeder 1969, Kobayashi et al 1976, Marks et al 1994, Hormia et al 2001).

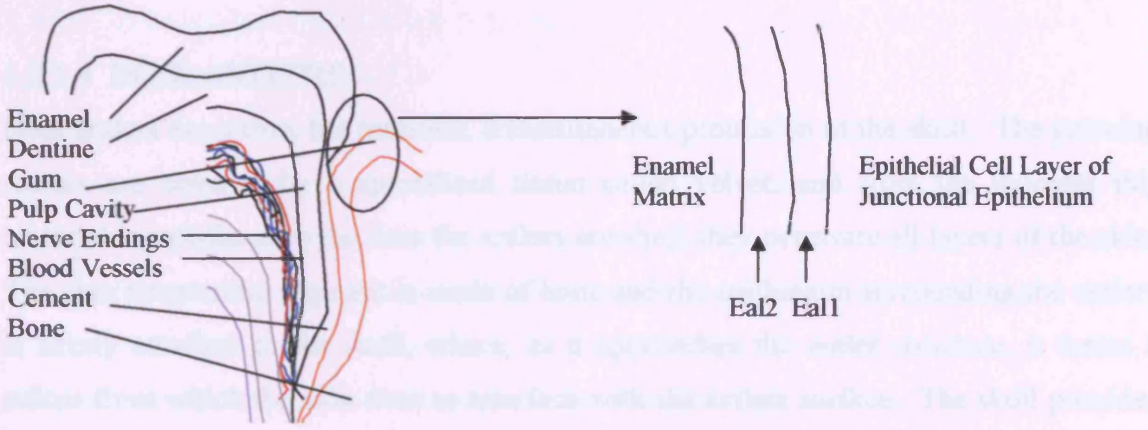

Figure 1.2 Schumatic of the natural tooth

1.2.1.3 THE BABYRUSSA TUSK

The only permanent naturally occurring transcutaneous structure is the tusk of the babyrussa, a very rare pig originating from the Celebes in South-East Asia. In this animal, the canine teeth of the upper jaw do not penetrate the gingiva like ordinary teeth; instead they grow in the opposite direction, piercing the external skin layers of the snout immediately beneath the animal's eyes. The tusk is a bone-anchored structure. In 1999, Knabe et al published a light microscopy, histological analysis of the transcutaneous interface of the babyrussa tusk. The tusk, consisting of dentin and a cement layer, is surrounded by an accumulation of keratin at the skin-penetrating region. It is anchored to the bone via a periodontal membrane, which contains a large blood vessel. In most cases, the epidermis is found to be in close adherence to the tusk, with no downgrowth. The

epidermis displays downward thickening regions, known as rete pegs, into the upper layers of the dermis. The tissues surrounding the tusk-skin juncture display signs of chronic inflammation, containing large numbers of lymphocytes, macrophages, plasma cells and polymorphonuclear leucocytes. To date no study has been able to characterise the ultrastructure of the attachment observed between the epithelium and the babyrussa tusk. It is possible that the structures that mediate epithelial attachment to the tooth, hemidesmosomes and the internal basal lamina, are also responsible for the junctional adherence observed in the babyrussa tusk. Certainly the observed pronounced thickening and keratinization are common to both interface structures, however they are more evident in the tusk model. It is postulated that the major contributing factor to the success of babyrussa tusk transcutaneous interface, is the subcutaneous bone attachment, which will greatly reduce interfacial stresses (Knabe et al 1999).

1.2.1.4 DEER ANTLERS

Deer antlers are a true, but transient, transcutaneous protrusion of the skull. The growing antlers are covered by a specialised tissue called velvet, and from the moment this material is exfoliated to the time the antlers are shed, they penetrate all layers of the skin. The skin penetrating segment is made of bone and the epithelium surrounding the antlers is firmly attached to the skull, where, as it approaches the antler structure, it forms a sulcus from which the skin rises to interface with the antlers surface. The skull provides the subcutaneous anchor for the antlers, and reduces the interfacial stresses around the skin-antler interface. This anchor system allows the animal to apply great stress on the antlers without adversely affecting the transcutaneous junction (Grosse-Siestrup and Affeld 1984). On the dermal level, collagen fibres penetrate the antlers' surface in a perpendicular orientation, which may reduce epithelial layer downgrowth into the underlying tissue layers (Winter 1974).

The morphology and interface biology associated with deer antlers will not be considered in any great detail in this section of my thesis as Chapter Four provides a detailed histological and scanning electron microscopy analysis of antlers as a model for the soft tissue attachment.

1.2.2 SUBCUTANEOUS INTERFACES

Implants designed to be integrated into the human body by tissue ingrowth have numerous applications, and in many cases are dependant on the infiltration of soft or fibrous connective tissue. The subcutaneous segment of skin penetrating implants and

cardiovascular devices depend on fixation by fibrous tissue ingrowth (Fernie et al 1977, Grosse-Siestrup et al 1979). Immobilisation of cardiac pacemaker electrodes is achieved by soft tissue integration (MacGregor et al 1979, Amundson et al 1979), as are the stabilisation of artificial larynx devices (Debreconi et al 1977), the attachment of avulsed ligaments and tendons (Amstutz et al 1976) and the resurfacing of the articular aspect of implants with cartilage-like tissue (Mears 1979). Finally, implants used in joint replacement rely on soft tissue attachments to supplement bone ingrowth for long-term stability (Pilliar et al 1981, Kent et al 1972, Jaffe et al 1978). In order to gain a better understanding of the interface biology associated with subcutaneous, soft-hard tissue interfaces, the osseo-tendinous junction is a good basis for the development of an engineered construct capable of soft tissue integration and incorporation.

1.2.2.1 THE OSSEO-TENDINOUS JUNCTION

1.2.2.1.1 TENDON ANATOMY

Tendons are anatomical structures that exist between muscles and bones. They transmit the forces generated in the muscles to the bones, thus enabling joint laxity. Tendon is a highly organised structure containing a sparse population of elongated fibroblasts, or tenocytes, within an extensive extracellular matrix; predominantly composed of type I collagen (~ 85% dry weight), with smaller quantities of other collagens (types III, V and XII), proteoglycans (Decorin, Biglycan, Fibromodulin) (Kastelic et al 1978, Blevins 1996) and elastin. Tendons are able to withstand both tension and compression, and the biochemistry of their extracellular matrix changes depending on the forces they encounter. In compression, tendons are often observed to be fibrocartilagenous in nature containing type III collagen (Gillard et al 1979), whilst the presence of fibrocartilage is also well documented at the tendon insertion sites or entheses, where it acts to reduce the stress concentration at the soft-hard tissue interface (Benjamin and Evans 1990, Ralphs et al 1991, Ralphs et al 1992).

In the tendon proper, the collagen molecules cross link to form fibrils, which grouped together make up collagen fibres, which in turn are the building blocks of primary (subfasicles), secondary (fasicles) and tertiary fibre bundles of which the tendon is composed.

In resting state, the collagen fibres and fibrils of the tendon display a wavy configuration that is clearly visible under the light microscope. Fibre orientation has been well defined (Rowe 1985, Whittager and Canham 1991) and is seen to disappear when the tendon is stretched, accompanied by a straightening of collagen fibres (Hess et al 1989). When the

tensile force is released, the normal wavy pattern is recovered provided the tendon is not stretched above approximately 4% elongation, otherwise the original wavy pattern will not return to its previous dimensions (Elliot 1965). If an elongation of greater than 8% is encountered, the tendon is subject to rupture (Jozsa and Kannus 1997). The collagen fibrils and fibres comprising the tendon structure run in a parallel orientation to the tendon, and are clearly visible under polarized light. A tendons matrix to collagen fibril ratio varies depending on its specific requirements. Tendons subject to predominately tensional forces with areas experiencing compression, for example flexor tendons, contain fibrocartilagenous regions with a high rate of glycosaminoglycan synthesis. They contain low collagenous and non-collagenous protein synthesis in the regions that encounter pressure as apposed to tensional forces (Abrahamsson et al 1989, Abrahamsson 1991). Glycosaminoglycan side chains attached to a core protein form proteoglycans, which joined via linking proteins, form hydrated space filling polymers found in extracellular matrix. The increased glycosaminoglycan content enables 'dampening' of the compressive forces that may otherwise irreversibly damage the tendon architecture. Hence the importance of a tendon's three dimensional structure can not be over emphasised. As previously stated, a tendon's function is to transmit the forces generated in the muscles to the bone, enabling joint motion, and it is the intricate micro- and macrostructure of a tendon that makes this possible. Tendons can be subjected to longitudinal, transverse and rotational forces, whilst being expected to withstand pressure and contusion. It is the internal three-dimensional architecture of fibrils and extracellular matrix that provides a buffer against these forces, and enables tendons to function successfully. Imposing a change in the physical forces affecting a tendon will undoubtedly result in a marked change in that tendon's composition and three-dimensional architecture (Abrahamsson 1991). It is a tendon's ability to respond to changes in physical forces and to regenerate following disruption of normal morphology that will determine whether it can be successfully re-attached to an implant *in vivo*.

1.2.2.1.2 THE TENDON-BONE INTERFACE

Tendons are connective tissues that attach muscles to bone, whilst ligaments are connective tissues that fulfil a stabilizing role between two bones across a joint. Tendons and ligaments display differences in matrix composition and organization (Amiel et al 1984), however their insertion sites into bone are structurally similar.

The term 'enthesis' has been applied to the attachment of a tendon or ligament to bone, and this juncture has been extensively studied (Cooper et al 1970, Benjamin et al 1986,

Kumagai et al 1994, Rufai 1995, Clark et al 1998, Waggett et al 1998, Benjamin et al 1998). The enthesis has been divided according to its morphology into Direct, also known as fibrocartilagenous or chondral (Evans et al 1990), and Indirect, otherwise known as fibrous or periosteal. Indirect attachments generally occur to the diaphysis or metaphysis of bones, where the superficial layers of the tendon merge with the periosteum whilst in the deeper layers Sharpey's fibres perforate the underlying bone. Epiphyseal tendon attachments, for examples the patellar tendon – tibial tuberosity interface, are of the Direct type. Here, there is a clear transition from the dense connective tissue of the tendon, through a fibrocartilage and then mineralised fibrocartilage region, to the sub-chondral bone. A 'Tidemark' at the calcification boundary is clearly visible under the light microscope and appears as a line of basophilic staining. Between the tendon and fibrobcartilage regions of the direct interface, the morphology of the resident cells changes. The elongated fibroblasts, characteristic of the tendon material, disappear and are replaced with round chondrocyte-like cells, in lacunae. The fibrocartilage and mineralised fibrocartilage regions differ as the name implies, by the laying down of mineralised areas between the lacunae. Stripping of the soft tissues disrupts a direct enthesis, and the interface separates through the tidemark, with the mineralised fibrocartilage remaining associated with the bone, which has a smooth surface. In contrast, in an indirect enthesis, lacking transitional zones, the bone at the interface displays ridges and fissures that accommodate the infiltrating collagen fibres (Benjamin et al 1986).

In 1999, Thomas et al described the variable nature of the direct insertion and its morphological dependence on anatomical location. The tissue composition and organization of the interface is largely dependant on the mechanical forces it experiences. For example, greater amounts of fibrocartilage and calcification are observed at entheses where the tendon is required to move through a wide range of angles and is subject to high tensile stresses (Evans et al 1990, Evans et al 1991). The fibrocartilage content of the osseo-tendinous interface also responds to compressive loading and is distributed according to the structural forces encountered at specific anatomical locations (Okuda et al 1987, Benjamin and Ralphs 1998). Morphological adaptations associated with immobilisation and physical activities have been well documented (Laros et al 1971, Woo et al 1987) and demonstrate that mechanical usage is a prerequisite for maintaining normal structure and morphology.

The unique interface that exists between tendon and bone demonstrates the ability of two tissue types with significantly different material and biomechanical properties, to unite

achieving a mechanically superior structure to either tendon mid-substance or sub-chondral bone, which are both observed to fail under mechanical loading prior to failure at the interface (Gao et al 1996).

Limited options for tumour control and the poor reconstructive surgical techniques of the nineteenth century meant that amputation was the treatment of choice for malignant bone tumours (Rubin 1971, Sweetnam et al 1971, Freidman and Carter 1972, Elton 1988, Checketts 1991). Since then, our understanding of, and ability to control tumours has greatly improved and earlier diagnosis, neoadjuvant therapies (Bacci et al 1976, Jaffe and Knapp 1983, Rosen and Marcove 1983, Goodnight and Bargat 1985, Rosen and Nirenburg 1985, Springfield et al 1988, Perek and Jurczyk-Procyk 1995, Thompson et al 2002) and a more concise comprehension of tumour biology (Enneking et al 1980, Simon 1984, Sundaram and McGuire 1986, Watt 1985, Grundmann 1995) has brought about radical changes in our approach to treating tumour patients. Currently, most patients receiving joint replacements report improved function and reduced pain (Walker et al 1989), resulting in reconstructive surgical techniques being the treatment of choice for many cases. Despite this, a clear need exists to reduce and repair the damage done to connective tissues during orthopaedic procedures.

1.2.2.1.3 TENDON AND LIGAMENT HEALING

Extra-articular tendons and ligaments heal via a four-stage process, including haemorrhage, inflammation, proliferation and maturation or remodelling. The stages are those of a regular healing response observed for all soft tissue injuries. Immediately following trauma, where blood vessels are damaged, blood plasma and tissue fluids infiltrate the affected area. Platelets bond to collagen, releasing phospholipids that stimulate the clotting mechanism (Houglum 1992). Fibrin and fibronectin are observed in the wound site within sixty minutes of initial injury (Lehto et al 1990), forming a glue-like substance at the wound site that provides a temporary plug to restrain local haemorrhaging and a provisional matrix to resist tensile stresses during early tendon healing. Fibrin and fibronectin act as a transient matrix for the infiltration of polymorphonuclear leukocytes, monocytes (Ciano et al, Lanir et al 1988) and later, fibroblasts (Grinnell et al 1980, Brown et al 1993). Chemotactic agents (specific substances produced to attract particular cell types) attract the cellular elements, polymorphonuclear leukocytes, monocytes and macrophages, into the wound site. Histamine is one such agent, produced by mast cells, platelets and granular leukocytes,

causing vasodilation and increasing vascular permeability. Fibronectin is a chemotactic agent for macrophages, leukocytes and fibroblasts (Grinnel et al 1980), whilst bradykinin increases vascular permeability and stimulates prostaglandin (PGE) release – PGE_1, which increases vascular permeability, and PGE_2, which attracts leukocytes. The inflammatory cells act to clear the area of necrotic tissue and debris, after which the proliferation and maturation phases can occur. Infiltration and accumulation of fibroblasts, myofibroblasts and endothelial cells into the injured tendon marks the beginning of the proliferation phase (Katenkamp et al 1976, Gelberman et al 1985). Platelets and macrophages secrete the growth factors required to cause migration and proliferation of these cell types (Houglum 1992), which then begin to synthesize the required collagenous and non-collagenous extracellular matrix components. These cells, the extracellular matrix and new capillaries, which form from buds and sprouting of the existing capillaries, are collectively known as granulation tissue. Hence, the provisional fibrin clot is gradually replaced with a more permanent structure, whose remodelling and maturation can take over a year from the time of injury (Clark and Henson 1988). During this phase, the number of fibroblasts, macrophages, myofibroblasts and capillaries decreases. This is accompanied by a decline in synthesis activity and a thickening of the resulting scar tissue as the vascularity and fluidity of the tissue is reduced. Glycosaminoglycan concentration decreases and tendon collagen becomes more densely packed, predominately Type I. The tensile strength of the tendon increases throughout this phase until the resulting collagen network has totally remodelled into a strong permanent structure (Leadbetter 1992). Scar formation occurs by a controlled programme of collagen and matrix synthesis that is mediated by gene expression and growth factor synthesis, and is similar to that seen in developmental processes. The resulting scar tissue is inferior to intact tissue, both mechanically and biochemically (Frank et al 1985, Liu et al 1995, Woo et al 1998, Lo et al 2000). Early research suggesting that tendons and ligaments have limited regenerative capacity for healing of mid-substance injuries, has been superseded by work showing that tendon fibroblasts have an intrinsic capacity to de-differentiate, proliferate and synthesize new extracellular matrix (Mast 1997).

Techniques for promoting soft tissue repair, in mid-substance or interface sites, have been well documented (Frank et al 1985) and a number of exogenous growth factors have been shown to enhance recovery *in vivo* and *in vitro* (Frank et al 1985, Natsu-Ume et al 1998). These include platelet derived growth factor (PDGF), insulin-like growth factor-1 (IGF-1), transforming growth factor-beta (TGF-β) and hepatocyte growth factor / scatter factor (HGF/SF). Preliminary results show the effects to be dose dependant, with additional

growth factor combinations (Hildebrand et al 1998, Letson and Dahners 1994) and tendon / ligament type (Spindler et al 1996) also being contributing variables. Tissue engineering approaches, re-introducing isolated culture-expanded, mesenchymal stem cells in collagen matrices to repair tendon defects, have yielded encouraging results (Awad et al 1999, Young et al 1998). Studies demonstrating the capacity for tendon and ligament regeneration have indicated that they have the potential to play active roles in healing processes that are required for the successful re-attachment of soft tissues to metal implants and bioactive surfaces.

1.2.2.1.4 TENDON BONE – TUNNEL HEALING

Methods employed to re-attach tendon to bone have also been examined to gain an understanding of soft tissue healing processes. In 1942, Kernwein postulated that the haemorrhage and trauma associated with drilling a hole into bone for tendon implantation would simulate the conditions of a fracture site. He concluded that the firm attachment resulting from such a technique was the direct result of gradual ossification of the tendon within the bone tunnel, which occurred by the infiltration of osteoblasts into the tendon proper and subsequent bone formation therein. Forward and Cowan (1963) described the lifeless appearance of the end of a detached tendon in an implantation model. They observed that healing of the tendon into a bone tunnel occurred in a similar manner to that of an undisplaced fracture, with an initial inflammatory phase (characterised by signs of degeneration of the tendon) and repair in the form of anchorage. This is initiated by an immature connective tissue sleeve of callus, followed by bone ingrowth into the tendon, with the collagen fibres of the tendon orientated along the line of mechanical pull, becoming 'buried in osseous tissue'. In 1960, Whiston and Walmsley described a bone tunnel implantation model *in vivo*. They too noticed the early degeneration of the detached tendon end, and described a loss of fibrocytes, myxomatous collagen fibre degeneration and formation of an amorphous poorly stained matrix five days post-operation. This phase was followed by a streaming of cells from the marrow spaces lining the bone tunnel, which invaded the edges of the degenerate tendon, replacing its structure from the periphery, inwards. They noted that a central core of degenerate tendon was slow to become repopulated. More recent research using a canine model has shown an early tendon-bone interface developing, consisting of immature connective tissue, which became anchored to the woven bone lining the bone tunnel by collagen fibres (Oguma et al 2001). However there was no evidence of a fibrocartilagenous layered enthesis during healing. In 1954, Skoog and Person also demonstrated the

degenerative changes associated with a cut tendon end and its recovery by ingrowth from surrounding tissues.

Rodeo et al (1993) used an *in vivo* canine model to study the development of the tendon-bone interface within a bone tunnel. They showed the maturation of a vascular cellular fibrous tissue at the interface, with the appearance of a 'basophilic tidemark' between calcified and non-calcified tissue by twenty-six weeks. Mechanical testing of load to failure in tension, demonstrated that at twelve weeks, failure occurred at the insertion of the tendon to the mechanical testing rig, or within the mid-substance of the tendon, but not at the tendon-bone interface. These findings oppose those of Jones et al (1987) who found that by twenty weeks, a tendon-bone interface consisted of tendon attached via a continuation of the periosteal cell layer without the formation of a layered enthesis in an *in vivo* model. Liu et al (1997) showed the formation of an indirect-like enthesis in a rabbit model after six weeks *in vivo*. The tendon-bone interface consisted of dense connective tissue, an interspersed fibroblast population, type III collagen fibres spanning the interface in a longitudinal orientation and neo-vascularisation. A fibrocartilage region was not observed, whilst the presence of a tidemark was not noted. Similar finding were described by Aoki et al (1998) following implantation of canine rotator cuff tendons six weeks post-operatively. At nine weeks, fibrocartilage was noted within the bone tunnel and a tidemark and layered enthesis had developed by twelve weeks. In contrast, in 1989 Hausman et al described little evidence of a tendon-bone union forming after twelve weeks, when tendon was attached through a metaphyseal bone tunnel in a Guinea pig model.

Other techniques have been employed to fix tendons to bone, the most successful, as defined by load to failure, being a screw and spiked washer device (Robertson et al 1986). It has been shown that the mechanical load to failure with this technique can be increased by increasing torque of the screw (Meriam et al 1995).

1.3 ARTIFICALLY ENGINEERED SOFT-HARD TISSUE INTERFACES

1.3.1 IMPLANT MATERIALS

Whether attempting to re-attach tendons to implants subcutaneously or successfully engineer a skin-implant interface in a transcutaneous device, one of the principle factors to consider is the type of biomaterial. The word 'biomaterial' refers to the synthetic or treated natural materials that can be used to replace or augment tissue functions. Biomaterials play a crucial role in orthopaedic procedures and an understanding of them allows the selection and implementation of a suitable material within a device, realistic

expectations of clinical performance and prediction of long term success rate. Metals possess properties that make them ideal for load bearing applications, thus they are regularly used to replace structural elements during skeletal repair and reconstruction. Metals have high strengths and are able to withstand plastic deformation under load, hence they are resistant to fracture. The biocompatibility of a metal is directly related to its corrosion resistance. A number of metals and metal alloys are well tolerated within biological systems. Metals are rarely used in their pure form owing to the fact that addition of other elements to form alloys can enhance metal properties.

The materials used for orthopaedic implants vary considerably and no optimal material has been described (Goldring et al 1990, Galante et al 1991, Black 1992, Wooley et al 1997).

Metals, polymers and ceramics are three of the material type groups used in implant manufacture. Commercially pure titanium and titanium alloy are the most commonly used metals in the fields of orthopaedics, dental implantology and cardiovascular medicine. Properties of the pure metal, including low density ($4.5g/cm^3$), high melting point (1668°C) high tensile strength (see Table 1.1), fatigue resistance, anti-corrosion characteristics, a low modulus of elasticity (107Gpa) and primarily its high biocompatibility, make titanium the most common material of choice for joint replacement (Rae 1975, Solar et al 1979, Albrektsson et al 1981, Kummer and Rose 1983, Linter et al 1986, Kodama 1989, Prigent et al 1998, Wang and Li 1998, Matsuno et al 2001). Titanium alloy properties include high tensile strength (947MPa) and ease of forging and machining. However poor wear resistance can result in the liberation of potentially toxic local metal debris into tissues surrounding implants (Buchanan et al 1987, Agins et al 1988). The principal limitation with the use of titanium is its chemical reactivity with other materials at elevated temperatures, which has resulted in the development of non-conventional refining techniques; consequently, titanium alloys are expensive. Table 1.1 summarises the properties of commercially pure titanium and titanium alloy Ti_6 Al_4V used in orthopaedic applications.

Alloy Type	Common Name	Composition	Tensile Strength (Mpa)	Yield Strength (Mpa)	Ductility (%EL in 50mm)
Commercially pure	Unalloyed	99.1 % Ti	484	414	25
Alloy	$Ti_6 Al_4V$	6 Al, 4 V, balance Ti	947	877	14

Table 1.1 - Properties of commercially pure and alloyed titanium for use in orthopaedic implant manufacture

More recently, titanium-tantalum alloys have been investigated as possible implant biomaterials. A titanium-5% tantalum alloy has been shown to support fibroblast and epithelial cell viability, adherence morphology and growth, with no significant differences from levels observed on titanium substrates (Prigent et al 1998). When alloyed with titanium (Young's Modulus 100-130GPa), tantalum (Young's modulus 3GPa) enhances the resulting alloy by increasing hardness, resistance to traction and corrosion (Mow and Hayes 1997). It is postulated that the alloying of titanium and tantalum could produce an implant material with a Young's modulus closer to that of bone (Young's modulus of cancellous bone 500-1500MPa), which has the potential to reduce stress shielding and enhance load transfer.

1.3.1.1 TEXTURING AND COATINGS

Texturing of implant materials can provide increased surface area for tissue attachment and a substrate that will enable tissue ingrowth, hence increase implant stability within the biological tissue in which it is placed. Texturing techniques include sintering, diffusion bonding and plasma spraying. The plasma spray process involves the spraying of molton or heat softened material onto a surface to provide a coating. The powder form of the coating material is injected into a very high temperature plasma flame, where it is rapidly heated and accelerated to a high velocity. The spray stream of molton particles is projected towards the substrate, where it cools forming the coating. The coating can be characterised by controlling the particle size of the material powder injected into the plasma flame and the pressure and temperature used to apply the coating (www.gordonengland.co.uk/ps.htm) (Wolke et al 1992). In 1987, Inoue et al postulated that the geometrical configuration of the surface of implants could influence whether a

capsule or an orientated fibrous attachment is developed. Since then, a number of authors have examined the nature of the soft tissue-porous implant interface. Characterisation of soft tissue bonding to porous coated implants has shown that pores of between 300 and 900 microns can support ingrowth, vascularisation and increased peel strength over time (La Berge et al 1990, Freels et al 2002).

The *in vitro* responses of cells isolated from the soft tissues to implant materials, coatings and surface topographies have also been extensively studied. Hydroxyapatite coatings have been shown to support and enhance bone and fibrous tissue cell attachment, growth, collagen matrix production and metabolism (Van Blitterswijk et al 1986, Ruano et al 2000).

1.3.1.1.1 HYDROXYAPATITE COATINGS

In the 1930's calcium phosphate ceramic hydroxyapatite ($Ca_{10}(Po_4)_6(OH_2)$)was identified as the main constituent of bone mineral (Engstrom 1972). Since then, synthetic hydroxyapatite and calcium phosphate materials have been developed that are structurally and chemically similar to bone, as well as being non-toxic and highly biocompatible (Jarco 1981, Klein et al 1983, Jarco 1986, Ducheyne and Lemons 1987, Manley 1993). Hydroxyapatite will support bone ingrowth and osseointegration when used in orthopaedics, dental and maxillofacial applications, and its beneficial biocompatible properties are well documented (Ducheyne et al 1980, Holmes and Roser 1987, De Groot et al 1987, Geesink et al 1987, Geesink et al 1988, Cook and Thomas 1988, D'Antonio et al 1992). Its properties make it one of the few materials that are classified as bioactive. The term bioactive refers to a substance that can be acted upon by a living organism or an extract from a living organism, and provides a surface that will form fixations via chemical bonds between the implant and host tissues. It is rapidly integrated into the human body without foreign body recognition, and bone will bond to it forming an indistinguishable union before undergoing degradation over time (Donath 1990). Despite the numerous advantages of hydroxyapatite it cannot be used in bulk for load bearing applications because of its poor mechanical properties (de Groot et al 1981), hence it is usually plasma sprayed onto a metal substrate. Hydroxyapatite coatings are beneficial because they can employ the biocompatible and bonding properties of the ceramic, whilst exploiting the mechanical properties of their metal substrate. When applied to orthopaedic implants, a hydroxyapatite coating provides an osteophilic substrate for bone to bond with and can direct (osteoconduction) and induce (osteoinduction) bone growth (Bauer et al 1991). The bone-hydroxyapatite interface stabilises the implant, enabling the

transference of the loads generated in the muscles to the skeleton, thus reducing atrophy. Osteoblasts and osteoclasts have been shown to attach to, and proliferate on hydroxyapatite coated implant materials (Bauer et al 1991, Kirschenbaum 1991), and it is thought that the coating adsorbs bioactive factors that assist in the initiation of bone formation. Mesenchymal stem cells have been observed at different stages of differentiation on hydroxyapatite coatings (Hardy et al 1991).

In vivo soft tissue responses to hydroxyapatite have also been documented. Complete soft tissue ingrowth into porous hydroxyapatite blocks has been observed after fourteen days (Butts et al 1989) and when used to replace bone defects, connective tissue can invade and totally replace porous HA within sixteen weeks (Lindholm and Lindholm 1993). Sintered porous hydroxyapatite blocks implanted in rat tendons show no inflammatory or calcification response (Ozawa 1991), whilst hydroxyapatite powder in a collagen gel has been shown to bond directly to rat tendon tissue without fibrous tissue capsule formation (Ishikawa et al 2001). More recently, mesenchymal stem cells sub-cultured on hydroxyapatite constructs for two weeks, prior to subcutaneous implantation in a rat model, develop into bone within thirteen weeks (Dong et al 2002).

1.3.1.1.2 BIOLOGICAL COATINGS

Biological coatings have been applied to implant materials in the hope of increasing their integration with and affinity for human tissue cell types and to enhance attachment with the soft tissues. Epithelial cells have been shown to proliferate and attach to titanium substrates *in vitro*, whilst laminin initiates early attachment of gingival epithelial cells (Wang et al 1998). Extracellular matrix components can affect the cellular response observed in relation to implant materials (Park et al 1998). Collagen IV coated titanium is a superior substrate compared with uncoated titanium, for encouraging epithelial cells attachment, proliferation, morphological pattern, differentiation and cytoskeletal organisation, whilst fibronectin coating promotes the adhesion of fibroblasts *in vitro*.

Fibronectin is an adhesive protein (Hynes 1986, Ruoslahti and Pierschbacher 1987). The extracellular matrix contains a number of non-collagenous adhesive proteins that have multiple domains, each with a specific binding site for other matrix macromolecules and for cell surface receptors. Hence these proteins contribute to the organization and cell adhesive properties of the matrix. One such protein is fibronectin, which is a large glycoprotein found in all vertebrates. It is a dimer composed of two large subunits joined by a pair of disulphide bonds. Each subunit folds into a series of distinct rod like domains, separated by regions of polypeptide chain. Each domain consists of smaller

modules, each serially repeated. Fibronectin can be analysed by chopping it into pieces to determine the functional role of each domain. This can be achieved by treatment with low concentrations of a proteolytic enzyme to cleave the polypeptide chain in the regions connecting the domains, leaving the domains intact, hence their individual binding activities can be established. This method has been used to demonstrate that in fibronectin, one domain binds to heparin, one to collagen and another to specific receptors on the surface of various cell types. Once isolated, a domain with cell-binding abilities amino acid sequence can be determined and synthetic peptides corresponding to different segments of the domain can be prepared. These peptides can be used to localize the main region responsible for cell binding (Hynes 1986). For fibronectin, this sequence is Arg-Gly-Asp or RGD and can be found in one of the type III repeats as a central feature of the binding site. Short peptides containing the RGD sequence will compete with fibronectin for the cellular binding site and thus inhibit attachment of cells to a fibronectin matrix. If these peptides are coupled to a solid surface, they will cause cells to attach to it. The RGD sequence is not limited to fibronectin and can be found in a number of other extracellular matrix proteins (Ruoslahti and Pierschbacher 1987).

There are numerous isoforms of fibronectin, one of which is plasma fibronectin which is soluble and circulates in the blood and bodily fluids, where it is supposed to enhance blood clotting, wound healing and phagocytosis. All other isoforms assemble on the surface of cells before being deposited in extracellular matrix as highly insoluble filaments. In cell surface forms, fibronectin molecules are cross-linked together and can assemble into filaments on specific cell surfaces (Degasne et al 1999). This information suggests that fibronectin may have a positive effect at the soft – hard tissue interface. If the RGD sequence in fibronectin can bind to connective tissue cell surface receptors and encourage adhesion, it could increase the degree of soft tissue attachment to implant materials if utilised as a biological implant coating. Fibronectins characteristic enhancement of blood clotting, wound healing and phagocytosis may also prevent bacterial invasion of the epidermal tissues exposed to the external environment on implantation of transcutaneous implants.

Cell attachment to extracellular matrix components is primarily mediated by integrins, a widely expressed family of transmembrane receptors (Hynes 1986). Integrins are heterodimeric receptors, consisting of alpha and beta subunits that are non-covalently associated and interact to bind specific amino acid sequences in the ligand, for example the RGD sequence of fibronectin. Integrin mediated adhesion is a highly regulated, complex process involving receptor-ligand interactions and subsequent adhesion

strengthening and cell spreading. Integrin binding to fibronectin involves a conformational change and activation in the receptor that results in mechanical coupling to the ligand. Bound receptors rapidly associate with the actin cytoskeleton and cluster together giving rise to focal adhesions, discrete complexes that contain cytoplasmic structural proteins and signalling molecules. Cell adhesion to the extracellular matrix is essential in development, wound healing and tissue remodelling. In addition to anchoring cells to provide structure and integrity, cell adhesion triggers signals that regulate survival, cell cycle progression and differentiation. Many pathological conditions, including blood clotting defects and tumour metastasis involve abnormal adhesion processes (Hynes 1986). Adhesion proteins could be used as biological coatings to assist the integration of implant materials into soft tissues in orthopaedic procedures.

1.3.2 IMPLANT INTEGRATION WITH THE SOFT TISSUES

Acceptance and integration of implants within soft tissues depends on the relationship between the implant material and the constituent parts of the specific soft tissue concerned. *In vivo*, cell populations and interactions remain in a stable equilibrium through proliferation, apoptosis and cell-cell interactions (Meffert 1997). Mechanical strength is a necessity for all soft tissues and is provided by fibroblasts, which secrete the supporting scaffold of extracellular matrix; a complex network of polysaccharides (glycosaminoglycans) and proteins. A blood supply is essential to bring nutrients to, and remove waste products from the tissues, whilst macrophages, white blood cells and lymphocytes are observed to dispose of dying cells and surplus extracellular matrix and combat infection. All tissues are a mixture of numerous cell types that are distinguishable from one another, whilst coexisting in the same environment. The fundamental properties of cells make possible the retention of tissue form and function. 'Cell memory' enables cells to maintain their individual characteristics and pass them on to their progeny, whilst constantly sensing their surroundings and adjusting their properties to suit the function that is required (Alberts et al 1994). All cells depend on signals from other cells and from their surroundings. When a foreign implant material is introduced into the body, all of the aforementioned parameters are affected. *In vitro* experiments demonstrate that even when cells are removed from their 'normal' environment, they and their offspring generally retain their original instructions, however cell behaviour is not totally independent of environment. *In vivo* most specialised cell types act as if their basic character has been irreversibly determined. For example, epidermal cells injected into an alien bodily environment will grow and form cysts lined with epidermis, suggesting

retention of characteristics in the most abnormal surroundings. Despite this, the character of many differentiated cells can be strongly influenced by their environment. Introduction of an orthopaedic implant could potentially be fatal or beneficial to soft tissue cell populations. Fibroblasts and their relatives, the connective tissue cell family, including osteoblasts/osteoclasts, chondrocytes, adipocytes and smooth muscle cells, are an exceptionally adaptive cell family and can undergo numerous interconversions (Alberts et al 1994). These conversions play key roles in the processes of fracture healing and wound repair, and have the potential to determine the fate of an implanted medical device.

Stem cells can generate differentiated cells in the adult form. These cells are precursors that have no mature differentiated state, but are able to divide to yield progeny that do. In adults, most populations of cells are not permanent and are constantly dying and being replaced. In the adult form, new differentiated cells can be produced in two ways, simple duplication or generation from an undifferentiated stem cell. Human mesenchymal stem cells are influenced by the materials and coatings used in orthopaedic applications and have the potential to enhance the acceptance of implant materials *in vivo* (Rust et al 2003).

To be successful, when implant materials are introduced to the soft tissues, they must become integrated through host tissue ingrowth, otherwise they become encapsulated within an unattached tissue pocket. Porous and textured surfaces, both metal and ceramic, have been shown to support connective tissue ingrowth. Research into the relationship between bone ingrowth and implant pore size has shown that optimal mechanical fixation is achieved using pores in the region of fifty to six hundred and fifty micrometers in diameter (Bobyn et al 1980, 1980, 1999, 1999, Roberetson et al 1976). Bobyn et al (1982) have also demonstrated that pore diameters between four hundred and eight hundred micrometers are associated with fibrous tissue ingrowth. Interface movement inhibits bone ingrowth and results in fibrous interposition, with the collagen fibres of the fibrous capsule running parallel to the implant surface (Pilliar et al 1981).

In 1982, Bobyn et al evaluated the peel strength of soft tissues from porous implants, from subcutaneous locations. Peel strength was seen to significantly increase with implant duration and also with pore sizes ranging from fifty to two hundred micrometers, compared with those of between five and twenty, and twenty and fifty micrometers. Hacking et al (2000) showed that subcutaneous soft tissue ingrowth into porous tantalum (Hedrocel) with pores of between four hundred and six hundred micrometers, consisted of

densely ordered collagen rich bundles with good vascularity, and a mechanical strength at the resulting interface that exceeded that of the tissue alone.

LaBerge et al (1990) used a model in which the femoral mid-shafts were replaced with porous coated cobalt-chrome, to study the problems of soft tissue attachment to porous implants. Pore sizes between three hundred and nine hundred micrometers, of cobalt-chrome implants were examined. Mechanical fixation was seen to be superior in the largest pore sizes, with the development of a vascularised interface at four months. The smaller pores supported a covering of nonvascularised, pseudoepithelial membrane.

Bioactive hydroxyapatite coatings have also produced encouraging results for tissue attachment and integration. Significant increases in bone ingrowth and mechanical shear strength, as demonstrated by push-out tests, compared with uncoated surfaces have been demonstrated both clinically and experimentally (Meffert et al 1997, Ducheyne et al 1980, Soballe et al 1990, Kienapfel et al 1999, Geesink 1990). *In vivo* versus *in vitro* variations in the behaviour of hydroxyapatite coatings may be due to the deposition method, and the physico-chemical properties of the applied layer (Geesink et al 1990, Lavos-Valereto et al 2001, Massaro et al 2001). Hydroxyapatite will support mineralisation directly onto an implant surface (biointegration), unlike uncoated implants that can demonstrate areas of attachment interspersed with thin fibrous membranes (Cook et al 1988, Yan et al 1997).

Soballe et al (1992) have shown that a fibrous connective tissue membrane will form at a bone-implant interface that is subject to micro motion of five hundred micrometers. Under similar conditions, a hydroxyapatite coating on the titanium implant will produce a significantly greater shear strength (push-out). Shear strength results of a hydroxyapatite coated unstable implant were comparable with those of a stable uncoated titanium implant, leading Soballe et al (1992) to conclude that in addition to its osteoconductive properties, hydroxyapatite may induce collagen synthesis.

The clinical success of an oral implant can only be guaranteed if the integrity of the permucosal area is maintained by an adequate gingival soft tissue-implant attachment (Listgarten et al 1991). *In Vitro* studies concerning the gingival tissue-implant interface include the effect of the physical and chemical properties of implant materials, the influence of topographic surface configurations, the type of attachment mechanism between cells and implant materials, and the effect of surface composition and configuration on the mechanical strength of attachment.

The replacement of extracted teeth by bone anchored synthetic tooth substitutes has been one of the principle areas of research for the dental profession. Numerous research

groups have shown that bone will infiltrate suitable materials, to provide a successful bone-implant interface (Hulbert et al 1970, Galante et al 1971, Karagianes et al 1982). However, the interface between the junctional epithelium of gingiva and the surface of a dental implant is essential because it is the potential biological seal that protects the underlying bone and soft tissues from pathogens present in the oral and external environments.

In 1984, Gould et al demonstrated that *in vivo*, epithelial cells attach to titanium implanted in human gingiva in a similar manner to that observed *in vitro* and in the natural dento-gingival interface, via hemidesmosomes and a basal lamina. Junctional epithelium abutting surgically implanted ceramic dental implants, develop an external interposing basal lamina between the epithelial cells and the implant surface, with hemidesmosomes at regular intervals, similar to those in natural tissue interfaces (McKinney et al 1985). A 'natural-type' interface has also been described as developing between grooved titanium implants *in vivo* in a rat model (Chehroudi et al 1989) and between titanium dental fixtures and junctional epithelium *in vivo* in dogs (Berglundh et al 1991).

Wang et al (1997) showed that *in vitro* spreading of primary human gingival epithelial cells was greater on titanium surfaces coated with a basement membrane than on titanium alone. Based on these findings, it was postulated that attachment of gingival epithelial cells to titanium can be enhanced by coating with a basement membrane.

Laminin-5 is a major component of the internal basal lamina observed between the junctional epithelial cells and the teeth (Hormia et al 1998). Tamura et al (1997) demonstrated that the laminin-5 component of basement membranes promotes gingival epithelial cell attachment to a titanium alloy *in vitro*. They concluded that being a constituent of the basement membrane, laminin-5 may play a role in the formation and maintenance of hemidesmosomes, which could be used in clinical applications to improve the biological seal around dental implants. Clinically it has been shown that the epithelial cell adhesion to dental implant materials is vital in retaining the successful condition of an implant (Kawahara et al 1998).

It has been shown that a natural-type interface can be recreated between the soft tissues of the gingiva and a dental implant surface. However it should be noted that the external environment immediately encountered at the neo-interface of a dental implant is very different from that of an implant penetrating the external skin of the body.

Following the reported, long-term success of skin penetrating titanium dental implants (Adell 1985), bone anchored titanium transcutaneous implants were developed, with the

first clinical application being that of the bone-conducting hearing aid. In 1977 three patients underwent procedures to implant bone-conducting hearing aids at the Ear Nose and Throat Department of the Sahlgren's Hospital in Gothenburg, Sweden. Since 1979 the same type of implants have been utilised for the retention of external head and neck prostheses (Brånemark et al 1977, Holgers et al 1987 and 1988). In 1990, Tjellström published results of patients with auricular prostheses, quoting no adverse skin reactions in 89.3% of 2458 observed cases, 92.5% of 1739 observations were in bone-conducting hearing aid recipients. In 1989, Holgers et al stated that over 26 years of clinical experience of transcutaneous titanium implants in the head and neck, a subcutaneous tissue reduction appears to be of vital importance in the maintenance of a reaction-free skin abutting the implants surface. It was postulated that a reduction in subcutaneous tissue could result in reduced mobility of skin surrounding the implant surface, which is a prerequisite for healing and attachment of the soft tissues to the abutment surface. Subcutaneous tissue reduction may also decrease the contact area between the implant material and the host tissues, hence minimising the possible effects of the metal on the biological tissues. The possible elimination of biological factors that can stimulate epithelial cell proliferation and migration are also considered to be advantages of subcutis removal (Squier and Kammeyer 1983). The interface between bone-anchored auricular prostheses and soft tissues has been shown to be successful with the necessary removal of subcutaneous tissue mass (Holgers et al 1989), and a failure rate of 0.14% has previously been reported (Holgers et al 1987).

Despite the successful findings of the aforementioned studies, all surgically positioned implants evoke an inflammatory reaction in the surrounding tissues as a direct result of the normal healing response. When the implant also breeches the skin, the system is subjected to a further complexity, since the skin barrier function is disrupted and extrogenous agents have the potential to colonise the implant material and infiltrate the surrounding soft tissues. Although this has been shown not to occur in transcutaneous implants of the head and neck, it is postulated that in a weight bearing environment the soft tissue - implant interface may be less stable due to increased radial stresses and micromotion at the interface, which may increase the potential for failure due to infection and soft tissue migration. The success of transcutanoeus implants for weight bearing applications will predominately rely on the integrity of the soft tissue – implant attachment.

To date, implant integration with the soft tissues has been demonstrated in both subcutaneous and transcutaneous environments, however is still subject to numerous

complications and limited applications. The aim of my thesis is to overcome some of these limitations, and improve the attachment of soft tissues to orthopaedic implant biomaterials.

CHAPTER TWO

DEER ANTLER: A MODEL FOR THE DEVELOPMENT OF BONE ANCHORED AMPUTATION PROSTHESES

2.1 INTRODUCTION AND HYPOTHESES

Following amputation, patients achieve close to normal limb use with made to measure false limbs, however problems are generated by the attachment of the external prosthesis. Interface pressures and stresses on the soft tissue of the stump are often high. The limb can be subject to periods of disuse following tissue breakdown and in extreme cases patients may require revision surgery. Small problems can often be amplified by mismanagement causing numerous drawbacks for the patient, which have been discussed in detail by Levy in 1995. The stump that results from amputation is a heterogeneous amalgamation of soft tissues, fat, muscle and bone. This affects the biomechanics of the stump, which is different for every patient, and produces non-uniform pressure distribution at the socket-stump interface with focal points of high stress (Lee et al 1997). The socket is vital as it forms the interface between the body's soft tissues and the external prosthesis required for "normal" motion. Thus, the problems associated with current designs and limb management are important factors for the function of the prosthetic. One means of achieving this goal would be to try to protect areas that are sensitive, whilst redistributing higher stresses to regions that are able to tolerate them. Shear stresses are detrimental to the skin and research has focused on maintaining low shear at the skin-socket junction (Radcliffe 1955, Appoldt et al 1968, Pritham 1990, Buis and Convery 1997).

There are two main socket designs, the quadrilateral socket and the ischial containment socket (Schuch and Pritham 1999, Pritham 1990). The need to improve designs is detailed in the study by Sherman in 1999. Stump infection is a common occurrence and can be brought about by the natural microbial inhabitants of the skin. High humidity and poor mechanical conditions enhance this phenomenon. One main concern is the development of an unnatural microbial environment that could be detrimental to the success of the stump-socket interface and lead to infection (Kohler et al 1989). A further concern is the lack of adaptability of the sockets that are currently available. The present designs cannot accommodate changes in stump size, and a once well fitting socket can become poorly fitting in a short time. In 1995 Levy outlined the detrimental factors of badly fitting prostheses and concluded that if the socket is too loose, the stump can sink in too far when the limb is used and it is abnormally fixed and loaded. This can cause occlusion of the stump's blood vessels, which leads to odema, ulceration and eventually necrosis of the stump. Pain is associated with friction and sweating at the interface and causes skin irritation.

If the socket is tight, pain and bruising of the stump tissues occurs. If the stump sits too high in the socket, the bone will be unable to reach its designated place in the junction. This leads to skin lesions, which have been shown to be the principle problem encountered by lower limb amputees (Canale 1998).

Problems associated with load transmission could be reduced and possibly eliminated by anchoring the prosthesis to bone. However this would introduce a breach in the skin's protective barrier to infection, allowing bacterial entry to the exit site. The main question is whether it is possible to develop a bone anchored percutaneous prosthesis, without destroying the barrier function of the skin. Development of intraosseous transcutaneous amputation prostheses (ITAP) is a research concept that will be examined in Chapter Five of my thesis. The main goal of the ITAP concept is to overcome the problems associated with current amputation prosthetics by attaching the external prosthesis directly to the bone via an intraosseous anchor system. The prosthesis will anchor into bone and the soft tissues will be attached to the implant. It will require a sufficient tissue-implant seal, on all tissue levels, which will prevent infection and provide a load transmission system capable of withstanding the stresses and loading associated with normal limb function.

Currently there are numerous non-loaded percutaneous devices in use. Their life spans are governed by foreign body reactions, infection of the exit site, inflammation, marsupilisation (where the implant becomes enclosed within a pocket, reminiscent of the marsupial pouch, caused by migration of the host tissues around the whole implant surface), permigration (epidermal migration through a porous implant leading to implant failure) and avulsion (tearing away). One focal point of past research has been the disruption of the soft tissue seal surrounding implants of a percutaneous nature and has been discussed by Winter in 1974, Von Recum and Park in 1981 and Grosse-siestrup and Affeld 1994. It is still one of the principle concerns in the development of bone anchored percutaneous prostheses. Currently, percutaneous devices are employed as both auricular and dental implants.

Bone anchored percutaneous titanium implants are attached to bone conducting hearing aids (Holgers et al 1995 (i)). They have a high success rate, which may be attributed to the fact that they are not loaded. In 1992 Holgers et al observed immune cells, able to respond to antigens, and phagocytic cells in the connective tissue surrounding the soft tissue-implant interface in patients with hearing aids with and without skin irritation.

In 1995, Holgers et al (ii) found no epithelial or connective tissue attachment around titanium implants of a successful or non-successful nature. The conclusion drawn from these findings was that inflammatory cells provide a cellular barrier that prevents

infection and is thus of paramount importance in the successful performance of transcutaneous implants. However, in 1995 Holgers et al (i) found no significant differences in the amount of T and B lymphocytes surrounding irritated and non-irritated cases, which indicates that the reasons for the success or failure of such implants is still not known. The statistics concerning the success rate of these implants are encouraging; in that 95% of bone anchored auricular implants are successful (Snik et al 1998).

Literary reviews concerning dental implants of a transgingival nature have been available since the 1960's (Branemark et al 1969). Unlike hearing aids, transgingival implants appear to have epithelial adhesion, as demonstrated by Listgarten and Lai in 1975 and Schroeder et al in 1981. It is important that there is a strong attachment between the implant and bone, and the implant and soft tissue. However it is crucial that the epithelium provides a barrier between the internal and external environments.

At the implant-bone interface there is osseointegration as demonstrated by Steflick et al 1991. Dental implants traverse bone, soft tissues and project into the oral cavity, which has a microbial rich environment. Saliva contains antimicrobial agents, however it is still important that epithelial and underlying connective tissues form a barrier to prevent bacterial invasion of the host's tissues and thus circulatory system (Berglundh et al 1991).

Many studies, including those by Squier and Collins in 1981, Baier and Mayer in 1988 and Brunette in 1988, discuss the implications of titanium and biomaterial composition, topography, charge density, ion release, corrosion, protein adsorption, oxide layer formation and physical factors on implant-cell interactions and cellular behavior.

In 1993, Majeska et al discussed the possibilities of material coatings to enhance and promote the attachment of certain chosen cell populations, in the hope of increasing overall levels of cellular attachment to implant biomaterials. For example, dental and orthopaedic implants could be coated with factors that increase connective tissue cell attachment at the site where the implant breaches the soft tissue layers (Lowenberg et al 1988). Collagen IV was shown to be a suitable coating to encourage epithelial cells to attach to titanium in a 1998 study by Park et al, whilst vitronectin appears to deter epithelial cell adherence.

Transgingival and orthopaedic implants are not totally comparable. Gingival soft tissues differ from those that an orthopaedic implant would be traversing because they are maintained within the oral environment. However, an understanding of dental implant technology may aid the development of intraosseous transcutaneous amputation prostheses. Dental implant failure is generally attributed to implant rejection and/or apical epithelisation, for reasons unknown. Two factors are known to influence the

epithelisation process. Firstly, macro/micro structure of the implants surface affects adhesion, orientation and proliferation of epithelial cells (Kawahara et al. 1995 and Chehroudi et al. 1998). Secondly, biochemical and physical factors of implant surfaces affect adhesion of epithelial and connective tissues to implant materials (Kawahara et al 1998).

It is understood that in cases of gingival-implant success, a zone of epithelial attachment approximately 200nm thick consisting of a basal lamina, focal contacts and hemidesmosomes, is observed. Inflammatory cell activity may also contribute to the success or failure of the implant. In 1989, Seymore et al illustrated the presence of inflammatory cells in dental implants of both a stable and unstable nature. Whereas Berglundh in 1991 observed no inflammatory cell reaction around titanium gingival implants in beagles. Hence the history of inflammatory presence surrounding percutaneous implants is not consistent and is thus questionable.

For ITAP to be successful, a number of obstacles need to be overcome. The bone-implant and connective tissue-implant interfaces need to be maintained. The mechanical properties acting at the soft tissue-implant junction need to be reduced to protect the delicate tissues from large stresses, as motion at the interface has been shown to be detrimental to the interface success (Von Recum 1984). In 1980, Daly demonstrated that even low forces acting at the interface between percutaneous implants and the soft tissues could lead to local inflammation and infection. It is obvious that if implants are subject to loading, the forces about the interfaces will be increased. This problem must be addressed for ITAP to be successful. One may question the differences between gingival and non-gingival connective tissues, owing to the fact that loading of gingival percutaneous implants appears not to be associated with the problem of motion at the interface. This may be due to the fact that gingiva is designed to withstand the loading associated with eating and biting as a normal phenomenon, and thus differs from non-gingival connective tissue. A full understanding of how dental and auricular implants function successfully, and study of the effects of loading implants on the living-alien material interfaces will aid a number of avenues of research. These include ITAP, catheters, external fixation pins/screws and cardiovascular devices.

Antlers are bony protuberances arising from the skull of most members of the deer family, or Cervidae. They are restricted to Cervidae and generally to the male of the species. Antlers are a natural analogue of ITAP and are a good model for study as, unlike teeth, they exist in a non-gingival environment. Antlers have been referred to as horns, however they are a structurally different anatomical features. Horns, fingernails, teeth,

hair and hooves all appear to be analogues of percutaneous structures. However they originate from the base of epidermal invaginations of the dermis and hence do not penetrate the epidermis. Antlers grow in pairs, annually and emanate from permanent bony pedicles arising from the frontal bones of the skull. During growth they are covered with a soft hairy skin, called velvet and are provided with an abundant supply of blood vessels. On completion of growth, the skin dies and is shed, leaving the antler bare. After a designated time period, which is dependent on the species, the antlers are cast, epidermal continuity is re-established and the process begins again. Antlers are thus transient, true naturally occurring analogues of the percutaneous devices we are attempting to mimic. Once the velvet is shed, the antler penetrates all of the skins layers for approximately four months, during which time they may be heavily loaded and hence they overcome the problems associated with ITAP (Grosse-Siestrup and Affeld 1984). A second example of a true permanent natural percutaneous device is the tusk of the Babyrussa, which is a small pig that originates from the Celebes, South East Asia, and is extremely rare (Knabe et al 1999). Instead of piercing the gingiva and entering the oral cavity, its upper jaw canine teeth pierce the external skin of the snout beneath the eyes. The skin penetrating component is the circular cross sectional tusk, and there is a slight down growth of hairless epithelium around the tusk that serves to reduce stress in the area. Knabe et al (1999) described the epidermis as "closely adhered to the tusk surface" and the surrounding tissues were seen to contain large numbers of lymphocytes, plasma cells and macrophages. The structure of mature antler is comparable to that of the diaphysis of long bones, with an outer cortical layer which varies in thickness dependant on the species, and a central trabecular core. Fluctuating testosterone levels in males determine the cyclical nature of antlers. Antler growth coincides with deer infertility in spring and summer, when the sex hormones are at low levels (Goss 1985), and they grow on average at an astounding 1.75cm per day mid-season (Goss 1983). Towards the end of the summer testosterone levels increase, leading to the maturation of the antler and the velvet is shed (Brown 1983). During the rutting season males fight to maintain their hierarchical position in society and this places great forces on the antler structures. Decreasing testosterone levels after the rutting season causes the antler to be shed.

The velvet is thought to convey a good blood supply to the underlying antler and hence most authors consider the antlers to be dead once the velvet is shed. Rolf and Enderle argue this point in their 1999 study and maintain that antler is living bone until casting.

The pedicle is living bone, which becomes evident around the onset of puberty and grows from frontal bone cells of the deer skull (Chapman 1975, Goss1985). Li and Suttie 1994

studied the histology of pedicle development and first antler growth in detail, and Banks and Newbrey (1982) discussed the development of antler as a modified form of mammalian endochondrial ossification. Knowledge and understanding of these sites may aid our progress with ITAP. Antlers are natural transient percutaneous structures once the velvet is shed and can act as a model for the development of amputation prostheses.

This chapter aims to determine the nature of the interface that exists between the antler and the skin, and describes the surface morphology of the antler-pedicle juncture. The information gained will aid the development of ITAP. **It is hypothesised that the skin forms an interface with the pedicle at the antler-pedicle junction when the velvet is shed, and it is this attachment that maintains a stable union. It is hypothesised that the bone surface of the antler and pedicle will be different.** There are three main objectives, firstly to describe the histology of the soft tissue seal around the antler-pedicle interface. Secondly, to qualify and quantify the differences in surface morphology of the antler and pedicle at and near the junction between the two and finally, to review the findings and their implications in terms of ITAP.

2.2 MATERIALS AND METHODS

2.2.1 HISTOLOGY PROCESSING FOR LIGHT MICROSCOPE ANALYSIS

Eleven deer antler pairs were obtained from the Rayne Institute and evaluated histologically, to qualify the interfaces between antler and pedicle. Three of the sections possessed the pedicle-epithelium junction, one showed velvet attached to the antler and all sections had pedicle-skin junctions. The samples were dehydrated in an ascending alcohol series over two weeks and chloroform was used to clear the specimens for 24 hours. They were then washed in 100% ethanol and placed in 50:50 LR white (Hard grade acrylic resin – Agar Scientific) : alcohol for three days. For a further two weeks the samples were placed in 100% LR white, with one resin change, and then polymerized with accelerator in LR white resin. The blocks were cut to size, prior to histology (see figure 5 = specimen in LR white block). The blocks were glued to Perspex slides and thick sections were cut using an Isomet 2000 with a diamond edge saw blade. The sections were then ground to between 60-80 microns using a Motopol 2000 and graded wet silicone carbide paper. They were then polished and stained with toluidine blue and paragon. The sections were covered with Pertex mounting medium (Xylene) and clean cover slips prior to light microscope evaluation.

2.2.3 SCANNING ELECTRON MICROSCOPY PROCESSING FOR ANTLER - PEDICLE SURFACE MORPHOLOGY STUDY

Five antlers were thawed and the skin and fascia were removed with care to prevent scratching of the bone surface. The frontal bone was partially removed and the antlers were macerated by treatment with 0.2M NaOH at 60°C until the soft tissue had dissolved, taking up to 48 hours. The specimens were then washed and slices were taken of the antler-pedicle interface and the pedicle-skull interface. The specimens were dried at 60°C and mounted onto Scanning Electron Microscopy (SEM) stubs, prior to sputter coating with a 10-15 nm gold layer and visualization under SEM (JEOL JSM 35C) at 20 Kv acceleration voltage.

The number and size of pores on either side of the interfaces were counted and the sizes of the pores were measured using an Olympus BH2 microscope linked to Zeiss KS300 3.0 computer image software. To establish continuity of the results, all measurements were taken from 1cm either side of the interface. The results were analysed quantitatively using statistical analysis and qualitatively with descriptional analysis.

Figure 6 shows the left macerated antler-pedicle interface from one of the specimens prior to sputter coating. The figure demonstrates the raised antler area close to the pedicle and the interface between the two.

2.2.4 STATISTICAL ANALYSIS

The numbers of pores observed over 40 antler and pedicle samples were counted and the data was tested for normality using a Kolmogorov-Smirnov test. To maintain continuity and accuracy of results, all of the measurements were taken at least 1 cm from the antler – pedicle interface and within a $1cm^2$ area. The data was normally distributed and a Student T test was used to determine whether there was a statistical difference in number of pores between the antler and pedicle surfaces.

Pore size was determined using Zeiss KS300 3.0 Image Analysis software for 70 randomly selected pores over antler and pedicle surfaces. The distribution of the data was found to be non-normal using a Kolmogorov-Smirnov test. A Mann Whitney U test was used to determine if the pores observed over the antler and pedicle surfaces were significantly different in terms of size.

2.3 RESULTS

2.3.1 ANTLER PREPARATION RESULTS

The antler were prepared for processing on arrival. Figures 2.1 and 2.2 demonstrate the appearance of two intact whole antler specimens. Figures 2.3a-d show the antler - pedicle interface with velvet absent (2.3a), velvet present (2.3b), in longitudinal section in London hard grade resin (2.3c) and as a macerated sample (2.3d).

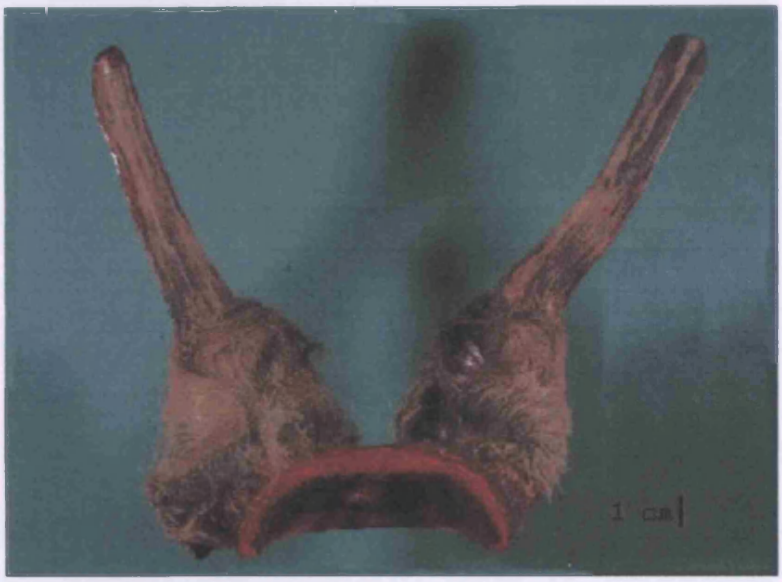

FIGURE 2.1 Whole antler specimen - frontal bone with the antler and pedicle skin intact.

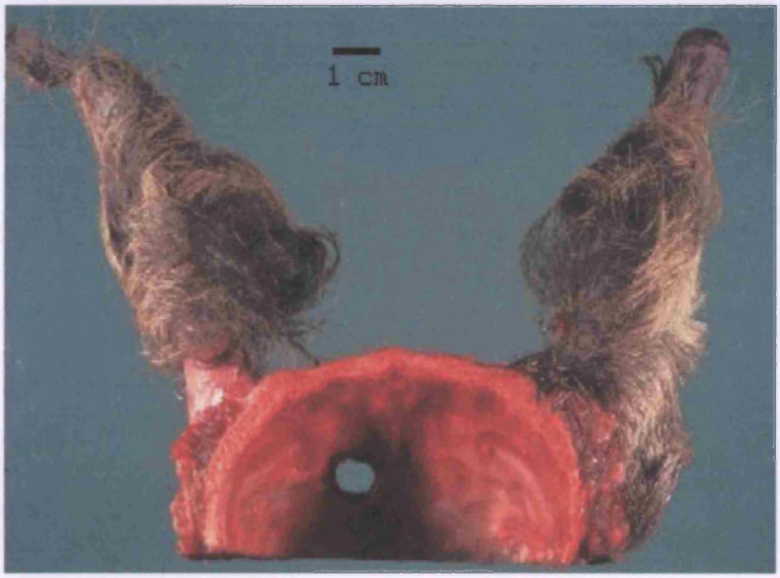

FIGURE 2.2 Whole antler specimen with velvet.

FIGURE 2.3

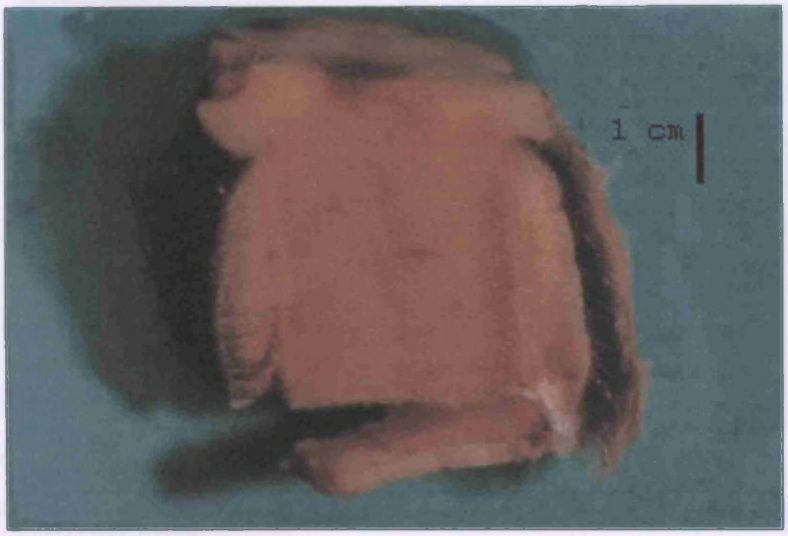

FIGURE 2.3a Antler – pedicle interface with no velvet.

FIGURE 2.3b Antler – pedicle interface with velvet.

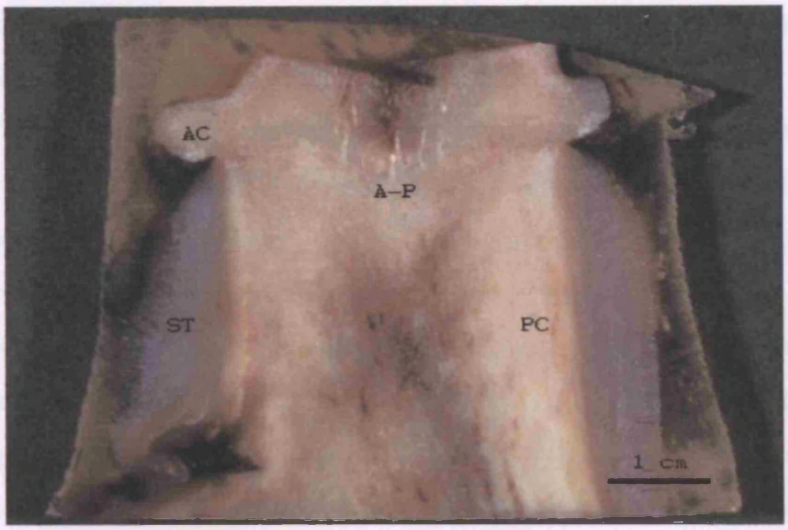

FIGURE 2.3c Antler – pedicle interface in longitudinal section - cast in london hard grade resin (AC – Antler coronet, A-P – Antler to pedicle interface, ST – Soft tissues, PC – Pedicle cortex).

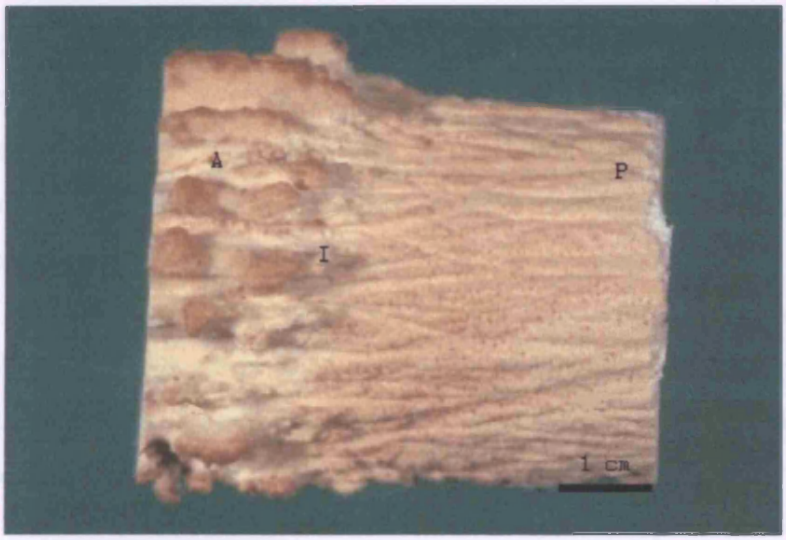

FIGURE 2.3d Macerated antler – pedicle section (A – Antler proper, P – Pedicle, I – Antler to pedicle interface region).

2.3.2 HISTOLOGY – RESULTS OF PROCESSING FOR LIGHT MICROSCOPY

2.3.2.1 HISTOLOGY OF THE SOFT TISSUE – PEDICLE INTERFACE

Where the soft tissues abut the bone of the pedicle, the bone appears highly invaginated, dense in nature and composed of Haversian systems (channels through which the blood vessels run in bone). The pedicle appears to be associated with a thick hypodermal connective tissue layer, which is distinctly different from the overlying dermis. The dermis possesses numerous longitudinally orientated collagen fibres, which are identified within the tissue sections by their dark pink coloration. The density of collagen fibres is less in the hypodermal connective tissue. Below the epidermis, the soft tissue abutting the pedicle is rich in collagen fibres, which run through the soft tissue and into the adjacent bone. These fibres enter the bone at an angle perpendicular to the bone surface, and are orientated differently from the fibres seen in the dermis above. These observations were found in all of the sections evaluated. Figures 2.4a-c present the findings of the histological analysis.

2.3.2.2 HISTOLOGY OF THE EPIDERMAL – PEDICLE INTERFACE

The epidermis is a thin, 1-2 cell thick, layer that forms an interface with the pedicle of the antler. In some of the sections observed, no epithelial attachment is evident. The epidermis thins as it nears the bone interface, and the epidermis always approaches the antler at the pedicle below the antler coronet. At the juncture, there is a collection of plasma cells and lymphatic cells that appear to form weak connections with the underlying bone. One can observe this phenomenon in all of the epidermal-pedicle interfaces when velvet is absent. Figures 2.4 to 2.9 give a visual insight into the epithelial-pedicle interface.

2.3.2.3 HISTOLOGY OF THE ANTLER – VELVET INTERFACE

One of the sections evaluated in this study possessed velvet attached to the antler. There is one marked difference between this interface and the one that exists between the epidermis and the pedicle (B), in that the velvet-antler interface appears far less invaginated. It was also observed that fewer collagen fibres, of smaller diameter, intersperse the interface between the velvet soft tissues and the antler. As in the pedicle-dermis interface, the collagen fibres orientate in a longitudinal manner along the length of the antler. The velvet appears not to have a clearly distinguishable hypodermal connective tissue layer between itself and the antler surface, and the antler surface is

highly organised in terms of active osteoblasts. The interface appears less structured than that of the tissue – pedicle interface. See figures 2.10 and 2.11.

FIGURE 2.4

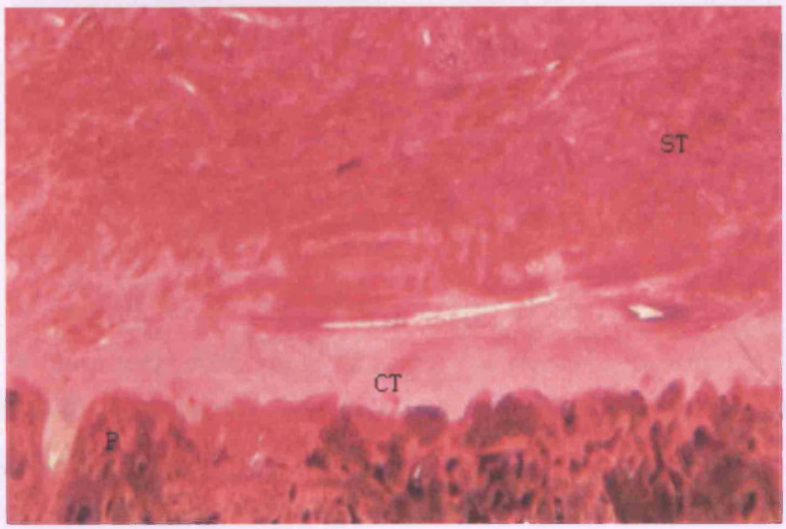

FIGURE 2.4a Soft tissue-pedicle interface at a magnifiation of x4. Figure demonstrates the hypodermal connective tissue layer (CT) that interposes the pedicle bone (P) and the soft tissue of the dermis (ST).

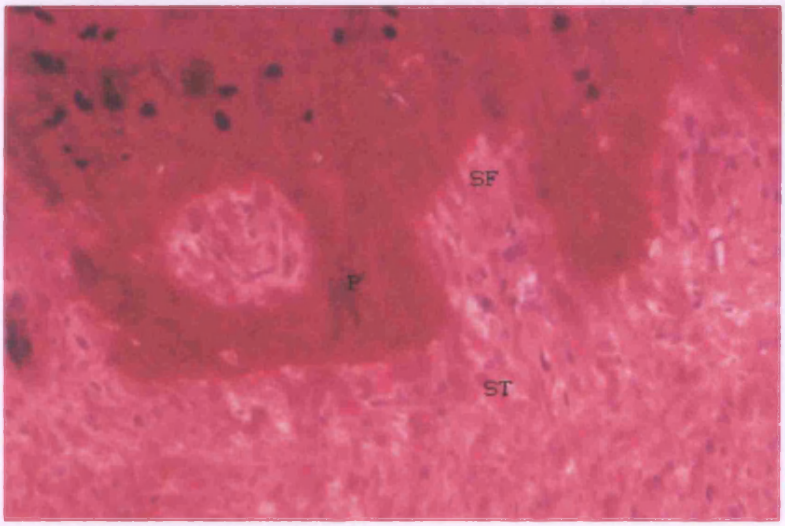

FIGURE 2.4b Soft tissue-pedicle interface at a magnification of x20. Figure demonstrates the numerous thick collagen fibres that run from the soft tissues into the pedicle bone in a perpendicular manor - they can be described as Sharpey's Fibres.

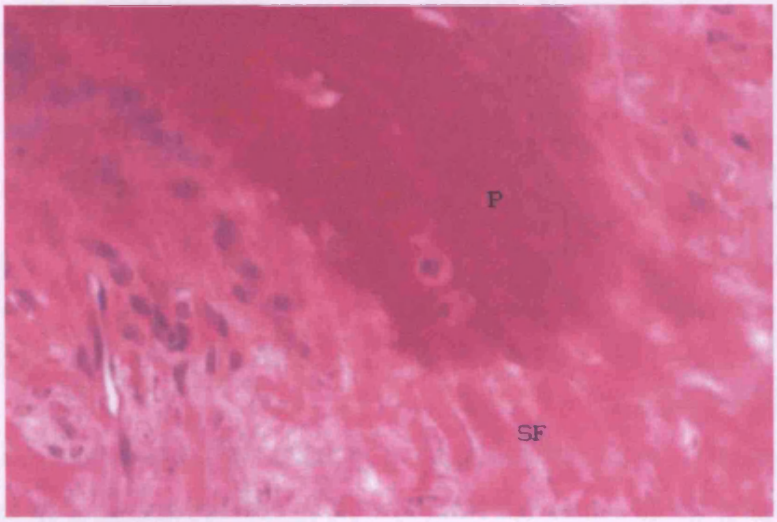

FIGURE 2.4c Soft tissue-pedicle interface at a magnification of x40. SF = Sharpey's Fibres inserting perpendicularly into the pedicle bone (P).

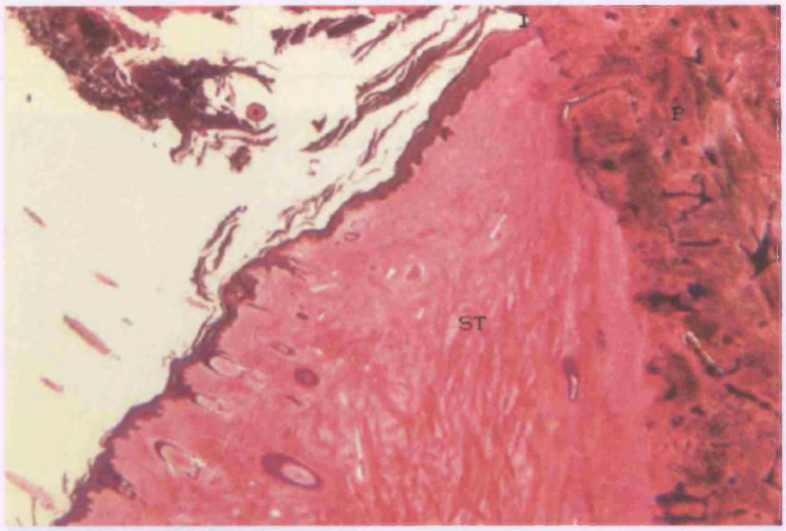

FIGURE 2.5 Epidermal-antler interface at a magnification of x4. Observe the thinning of the epidermis as it approaches the pedicle (P) and the nature of the interface that exists between them (I). Collagen fibres can be seen running longitudinally in the soft tissues of the dermis (ST).

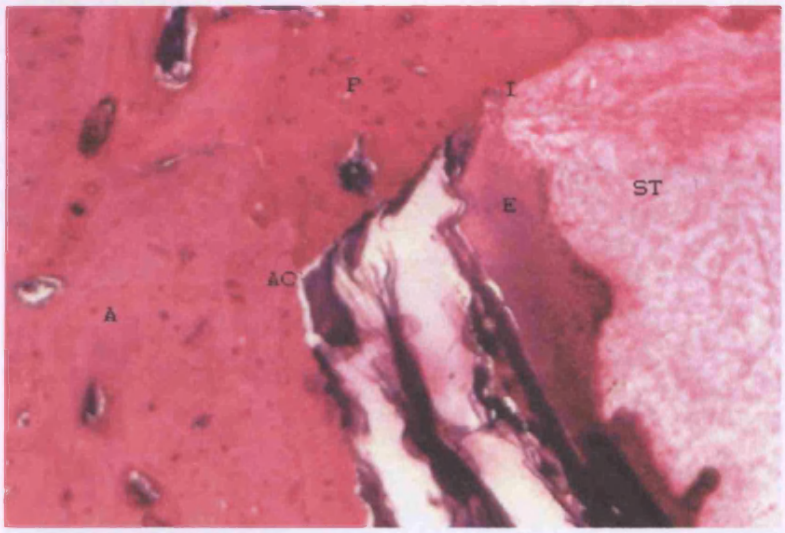

FIGURE 2.6 Epidermis-bone interface at a magnification of x10. The epidermis (E) approaches the pedicle bone (P) near to the widening of the antler (A) into the antler coronet (AC). However the interface between them (I) is exceedingly thin. The darkly stained region where the epidermis interfaces with the pedicle is a collection of inflammatory cells. This can be seen at a higher magnification in Figure 2.7a.

FIGURE 2.7

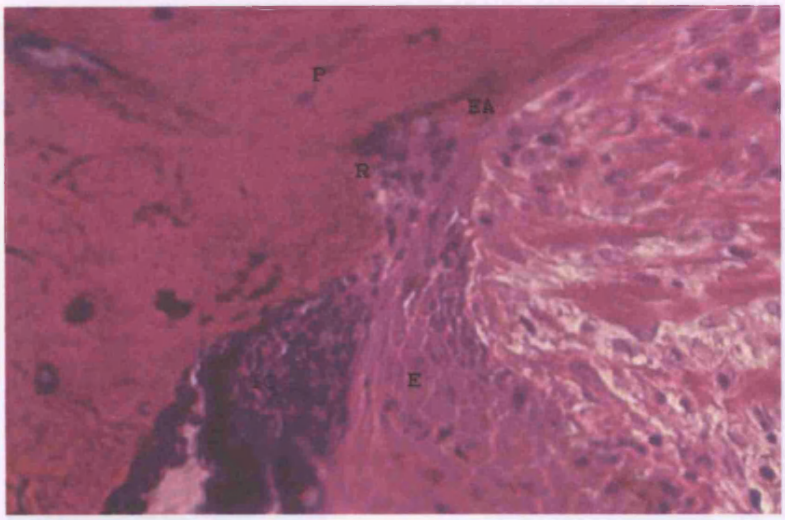

FIGURE 2.7a Epithelial-pedicle junction at a magnification of x 20. The epithelium (E) thins as it approaches the pedicle (P), to a single epithelial cell attachment (EA). The epithelial cells are affiliated with inflammatory cells (IC) which attach to the bone base in an area of resorbed bone (R). This area is shown in more detail, at a higher magnification, in figure 2.7b.

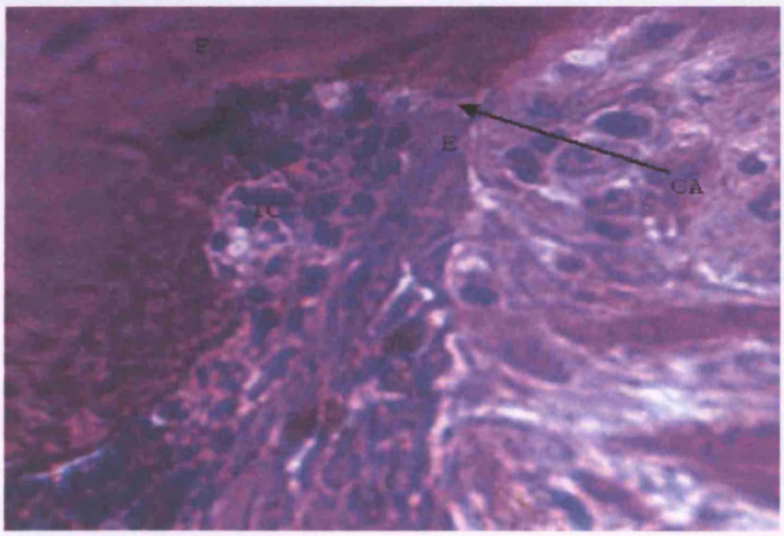

FIGURE 2.7b Epidermal-pedicle interface at a magnification of x40. CA represents the single cell attachment that exists between the epithelium (E) and the pedicle bone (P). Inflammatory cells (IC) abutting and attached to the bone bed.

FIGURE 2.8

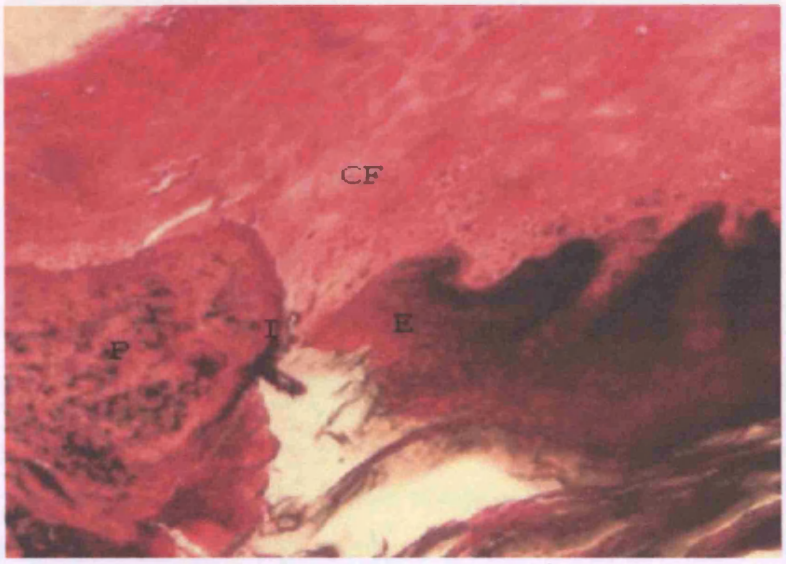

FIGURE 2.8a Lack of epithelial attachment at a magnification of x10. At the interface (I) between the epithelium and the pedicle bone, a tight epithelial attachment is not a prerequisite for a healthy antler. In Deer No. 11, there is no attachment seen between the epithelium (E) and the pedicle (P). The underlying connective tissue contains collagen fibres (CF) that are closely associated with both the epithelium and the pedicle bone. There is not an excess of epithelial downgrowth, which would be a tunnel for infection from the external to internal environments. Figure 2.8b examines this interface at a higher magnification. In the sections from Deer No. 11 the lack of epithelial attachment could be a result of artefacts generated during histological processing.

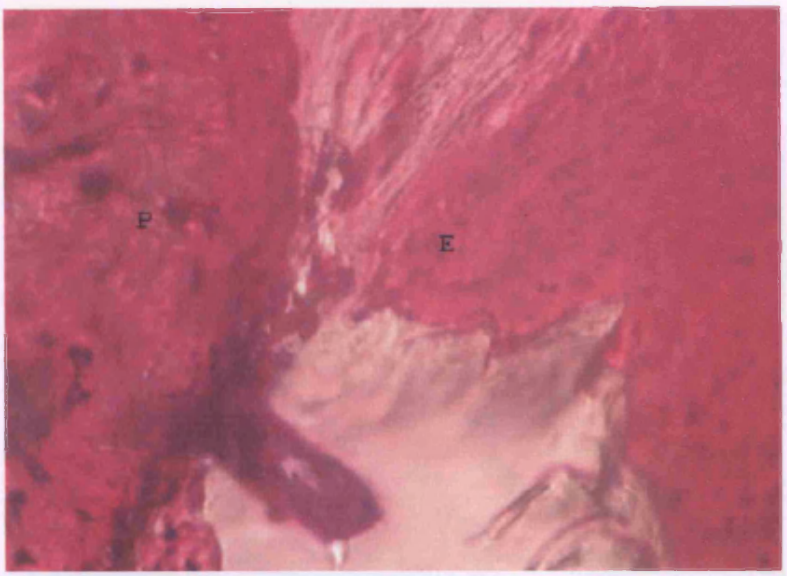

FIGURE 2.8b Lack of Epithelial Attachment at a magnificantion of x40. The epithelial – pedicle interface is examined at a higher magnification. One can observe a slight amount of epithelial downgrowth. However this appears to be limited by the collagen fibres in the connective tissue adjacent to the epidermis and pedicle bone. The collagen fibres appear to run virtually perpendicular to the pedicle bone, and as such there is an element of ingrowth of the fibres into the adjacent bone to prevent further epithelial downgrowth.

FIGURE 2.9

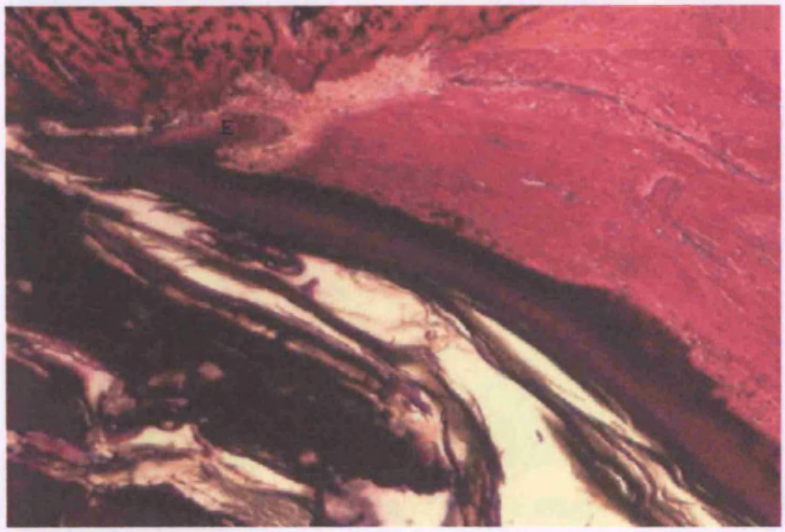

FIGURE 2.9a Increased epithelial downgrowth at a magnification of x4.

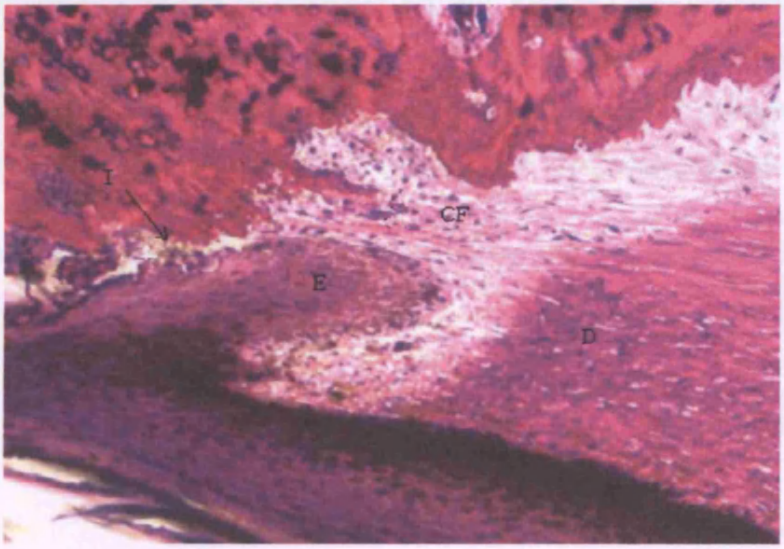

FIGURE 2.9b Epidermis (Figure 2.9a) at a magnification of x20. Figures 2.9a and 2.9b show the epithelial-pedicle interface with no epithelial attachment at the interface (I), and collagen fibres (CF) in the underlying tissue adjacent to the epidermis (E) and pedicle bone (P). Collagen fibres appear to be inhibiting further epithelial downgrowth by obstructing the path of the epithelium and inserting into the pedicle bone.

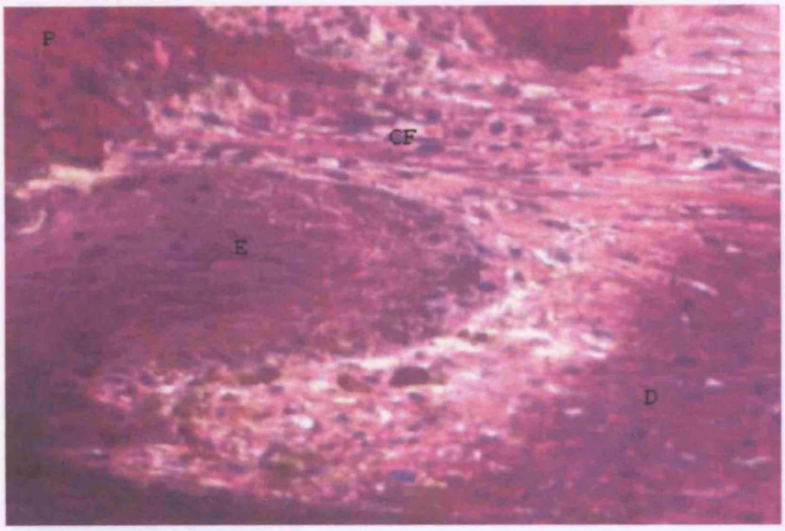

FIGURE 2.9c Attachment zone from Figure 2.9b at a magnification of x40. This image at a higher magnification reinforces the hypothesis that the collagen fibres (CF) in the connective tissue below the epithelium (E) actually inhibit the downgrowth of the epithelial layer. The fibres can be observed actually growing into the pedicle bone, thus creating a physical barrier between the external and internal environments. One can observe large round cells with darkly stained nuclei surrounding the collagen fibres, and it is expected that these cells are active fibroblasts that are producing collagen matrix.

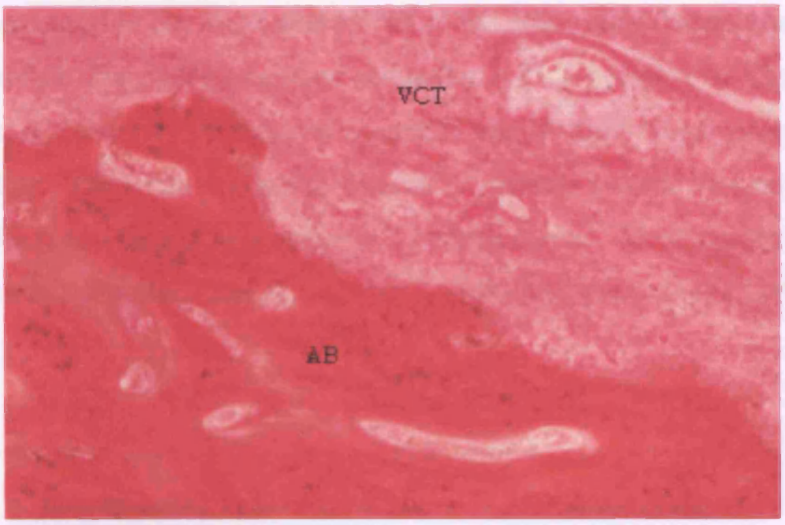

FIGURE 2.10 Antler – velvet interface at a magnification of x20. Antler bone appears mildly invaginated and few collagen fibres can be seen between the antler and the velvet tissues. VCT = Velvet connective tissue AB = Antler bone.

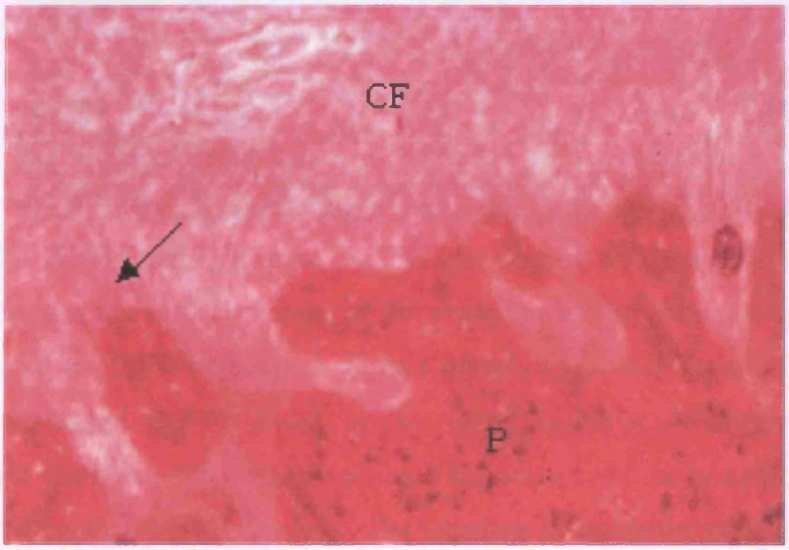

FIGURE 2.11 Pedicle – connective tissue interface at a magnification of x20. This image is presented as a comparison to be drawn against figure 2.10. At the same magnification one observes a more organised collagen fibre network at the pedicle interface than that which exists between the antler and the velvet. The pedicle is more invaginated and the collagen fibres can be seen to grow into the pedicle in a perpendicular orientation. The whole structural appearance is more defined than that seen in figure 2.10.

2.3.3 SCANNING ELECTRON MICROSCOPY RESULTS

Five antlers were used in the SEM study. All of the specimens demonstrated a dramatic alteration in surface morphology between the antler and the pedicle (see figure 4.4d). The pedicle surface is extremely porous and possesses significantly larger pores compared to the antler surface. The antler possesses distinctive grooves present near the junction with the pedicle, which decrease in size as the two regions merge. More pores are observed in the pedicle than in the antler. The surfaces were evaluated qualitatively in figure 2.12.

FIGURE 2.12

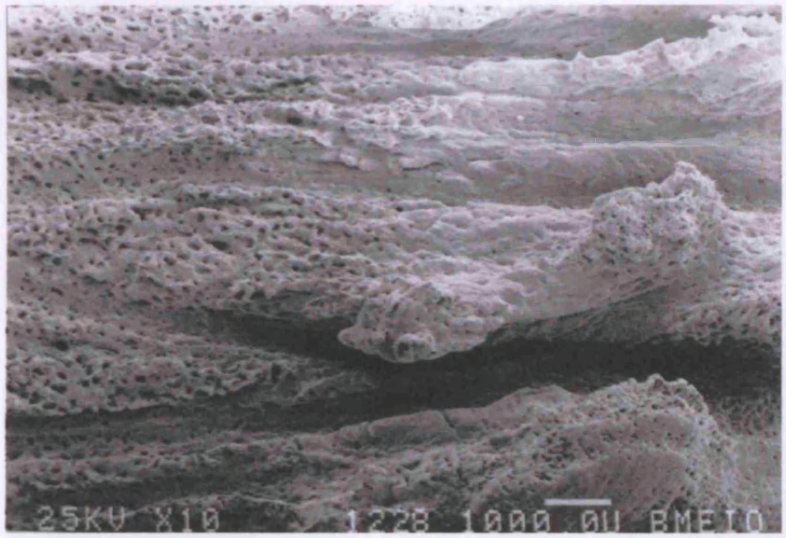

FIGURE 2.12a SEM Image of antler-pedicle interface at a magnification of x10. This figure demonstrates the surface nature of the structure as the antler and pedicle merge. One can observe the distinct change in surface morphology from the pedicle, on the left-hand side of the image, and the antler, on the right. The pores of the pedicle are clearly larger and more numerous than those visible on the antler, and the pronounced ridges and grooves are visible on the antler surface. The interface between the two shows a decrease in the ridges and grooves and an increase in porosity as the antler merges into the pedicle.

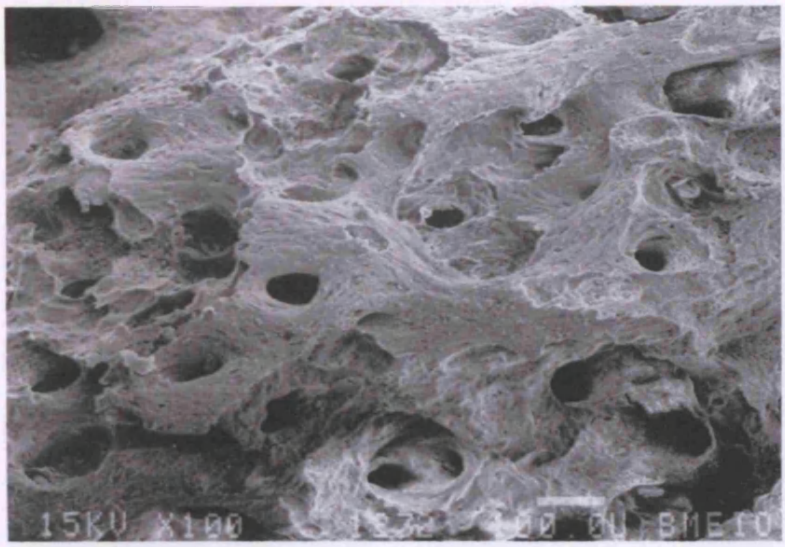

FIGURE 2.12b SEM Image of the pedicle at a magnification of x100. The pedicle surface possesses large and numerous pores. At a high magnification these pores are visible and can be compared to figure 2.12c which demonstrates the porous nature of the antler surface, showing smaller pores with clearly defined borders.

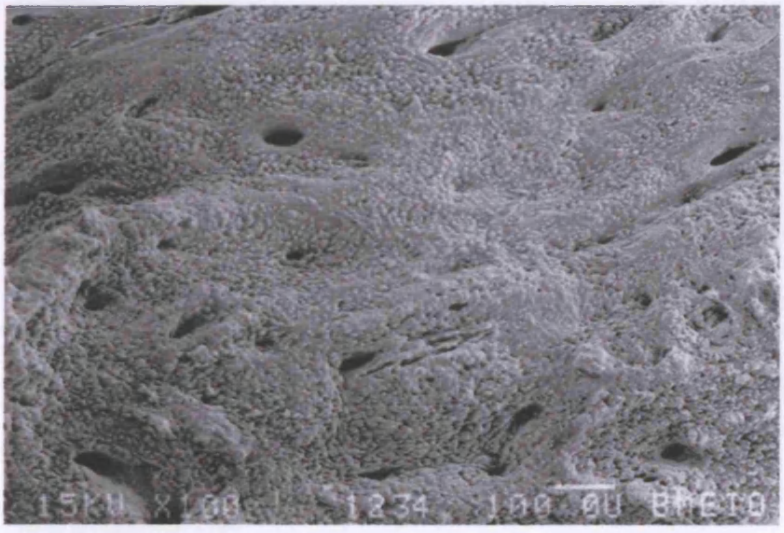

FIGURE 2.12c SEM Image of the antler surface at a magnification of x100.

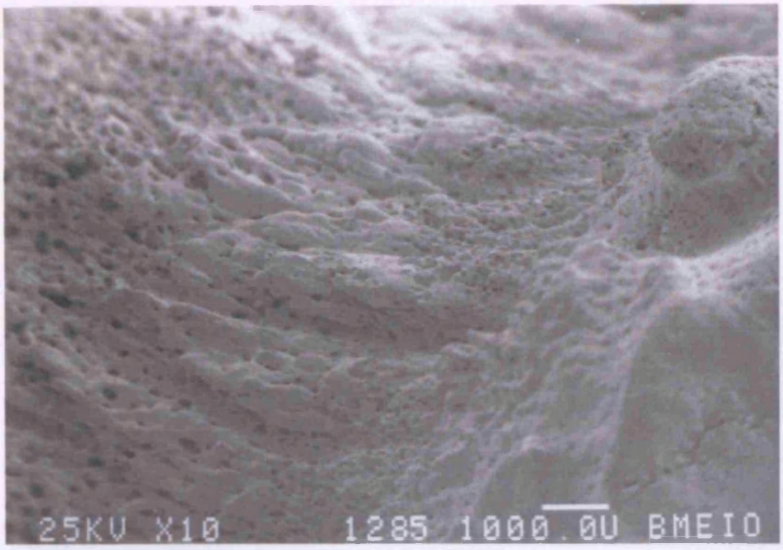

FIGURE 2.12d SEM Image of the antler – pedicle junction at a magnification of x10. This image demonstrates the rise of the antler coronet (right hand side of picture) as the structure develops from the pedicle (left) to the antler proper (right). Figure 2.12e indicates the pedicle nature closer to the interface than that shown in figure 2.12b.

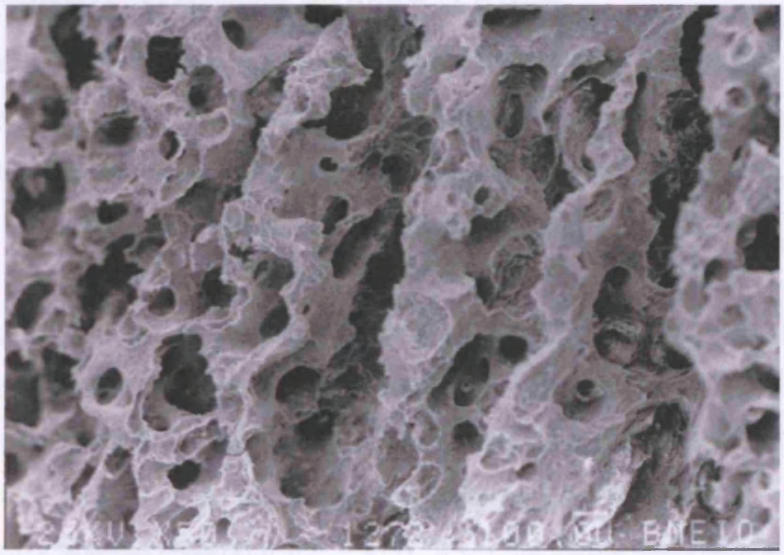

FIGURE 2.12e SEM Image of the pedicle surface close to the antler – pedicle junction at a magnification of x50. The porous nature of the pedicle continues proximally until it reaches the interface with the skull. Here the porosity undergoes a change in structure that is demonstrated in figure 2.12f, where the large pedicle pores diminish into fewer smaller pores visible on the surface of the frontal bone of the skull.

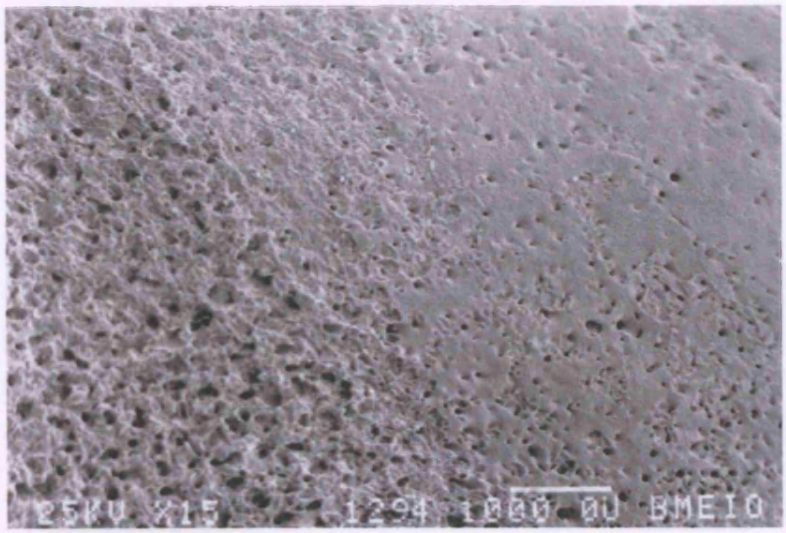

FIGURE 2.12f SEM Image of the pedicle – skull juncture at a magnification of x15. Image demonstrates the decreasing porosity from the pedicle (left) to the frontal bone of the skull (right).

2.3.4 STATISTICAL ANALYSIS

2.3.4.1 STATISTICAL ANALYSIS OF PORE NUMBER

This analysis was carried out to determine whether there is a statistical difference in the number of pores associated with the antler and pedicle surfaces. Counts were carried out in five antler specimens across forty different antler and pedicle regions. Figure 2.13 presents a box plot of the data obtained and the raw data can be observed in Appendix 1.1.

Normality tests carried out on the data suggest that the data is normal in nature and is thus suitable for parametric testing, hence a Student T test was carried out.

The result of the Student T Test suggests that there is a significant difference in the number of pores observed in the antler and pedicle interfaces ($P = 0.000$).

From the box plot and the results of the T Test, it can be stated that there are significantly more pores present on the pedicle surface than on the antler surface.

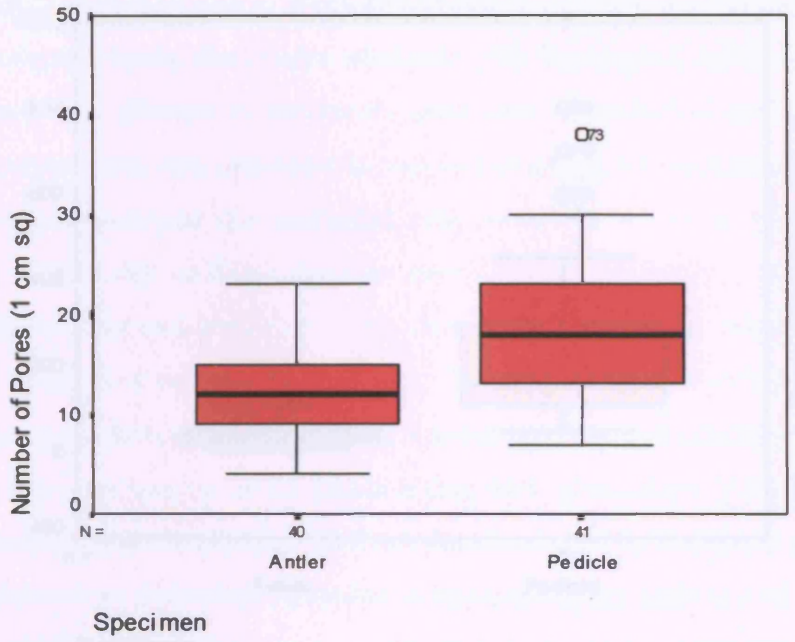

FIGURE 2.13 Box plot comparing the number of pores in the antler and pedicle (within 1mm^2). The boxes indicate the interquartile range. The horizontal lines within the boxes represent the median. The whiskers show the range of data within one and a half interquartile ranges of the interquartile range, and the data points beyond these appear individually.

2.3.4.2 STATISTICAL ANALYSIS OF PORE SIZE

Having established the significant differences in the number of pores between the antler and pedicle structures, it was decided to determine whether any differences exist in terms of the pore size between the two. Seventy randomly selected pores over antler and pedicle regions were measured in five antler pairs. Figure 2.14 presents a box plot summary of the data obtained, and the raw data can be observed in Appendix 1.2. The normality tests showed that the data does not conform to the assumptions that are generally accepted for the use of parametric statistical testing, hence a Mann-Whitney U non parametric test was used to analyse the data. The Mann-Whitney U test gave a P value of 0.000, hence it can be stated that the pores observed in the pedicle structure are significantly larger than those observed in the antler. Figure 2.15 gives a representation of the data distribution of pore size between the antler and pedicle structures.

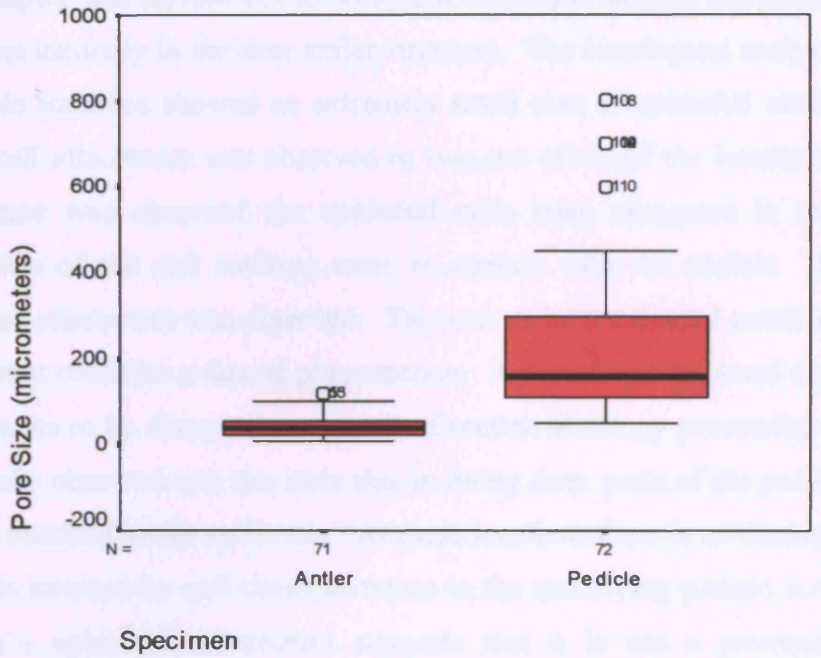

FIGURE 2.14 Box plot showing the data for pore size anaylsis.

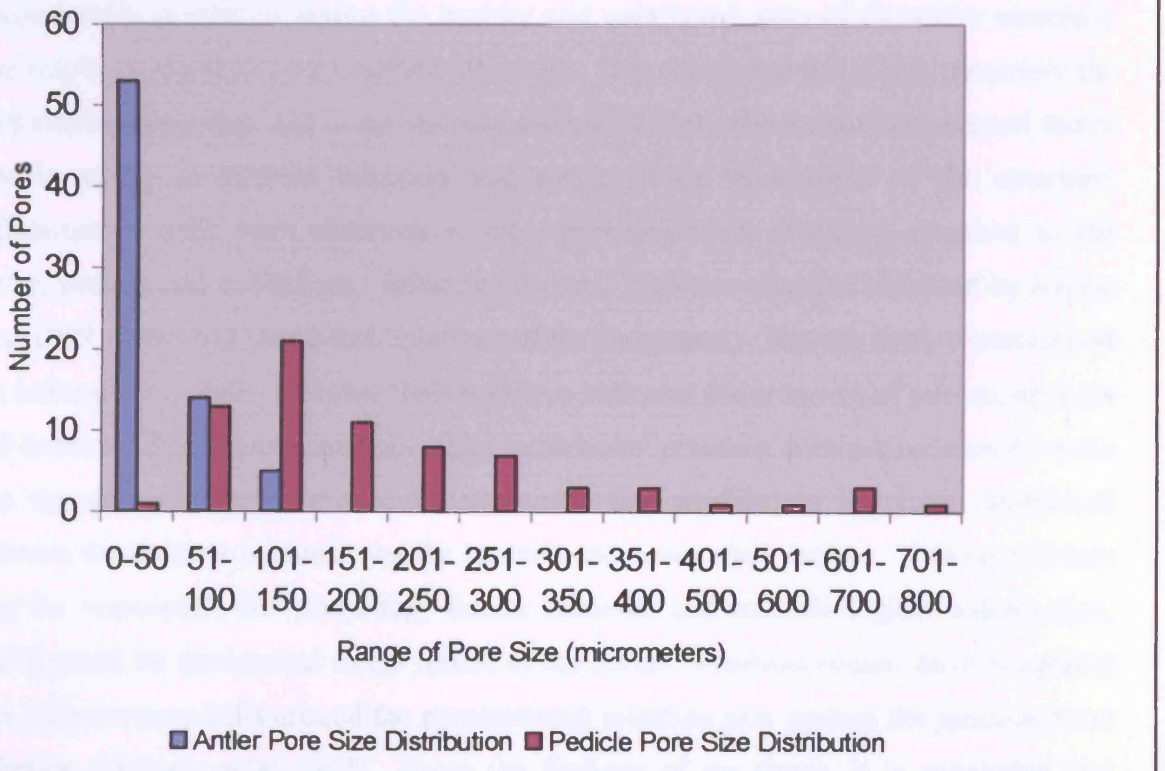

FIGURE 2.15 Distribution of the pore size data.

2.4 DISCUSSION

This chapter was carried out to study the histology, surface morphology and interfaces that exist naturally in the deer antler structure. The histological analysis of the epithelial – pedicle interface showed an extremely small area of epithelial attachment, if any. A single cell attachment was observed in two out of six of the interfaces studied. Where attachment was observed the epithelial cells were elongated in nature and a small proportion of the cell surfaces were in contact with the pedicle. In one section no epithelial attachment was observed. This cannot be considered conclusive, as the lack of attachment could be a natural phenomenon. It should also be noted that it is possible for attachments to be disrupted as a result of routine histology processing techniques. From the results observed one can state that in living deer, parts of the pedicle at the interface are not attached to the epidermis. At these locations there is an element of downgrowth, which is arrested by soft tissue adhesion to the underlying pedicle surface. The lack of pedicle – epidermal attachment suggests that it is not a prerequisite for infection prevention or longevity of the interface in Red Deer. This finding contradicts those of Knabe et al 1999, who state that close adherence of the epidermis to the tusk is observed in the Babyrussa model. One would assume a seal between the external and internal environments is vital to ensure the healthy and uninfected state of the antler structure. The results of my thesis demonstrate otherwise. It is concluded that if it is not solely the epidermal-pedicle seal that is maintaining the antler form, there must be a second factor that is acting to prevent infection and assist in the sustenance of the structure. Inflammatory cells were observed at the epithelial-pedicle interface, attached to the antler, pedicle and epithelium. Inflammatory cell presence was also observed by Knabe et al 1999, at the soft tissue-tusk interface of the Babyrussa. Neither study characterised the inflammatory cells, however their presence indicates the presence of microorganisms and bacteria. The bacterial and microbial inhabitants' presence does not necessarily mean that the site is infected, and it is conceivable that equilibrium has been established between the immune response and the bacteria colonising the interface. This equilibrium may be responsible for preventing further bacterial and microbiological colonisation, which could be detrimental to the health of the antler. Previous studies have suggested that inflammatory cells around the percutaneous interface may protect the junction from infection (Holgers et al 1994). From the findings of my thesis, it is concluded that inflammatory cells are important in preventing infection at the soft tissue – antler interface.

The weak epidermal attachment to the pedicle bone is in contrast with the strong attachment between the pedicle bone and the sub-epidermal tissues for the entire antler evaluated. Numerous thick collagen fibres are evident, connecting the pedicle with the soft tissues.

The pedicle surface is invaginated, which increases its surface area for fibrous attachment. It is thought that the strong attachment seen here may protect the soft tissue-pedicle interface and the supporting epithelium from the forces encountered during loading in the rutting season. The fibrous network may also play a part in preventing infection by maintaining the dermal-bone junction in tight contact, thus preventing bacterial invasion into the underlying bone. The collagen fibres in the sub-epidermal tissues appear to prevent further epithelial migration and downgrowth. Where epithelial attachment is absent, there is a certain element of downgrowth, which is a result of epidermal cell characteristics. Epidermal cells strive to establish layer continuity and are stable when surrounded by other epithelial cells on all sides. When at least one side of the cells abutting the pedicle are free from any attachment to another epithelial cell, those cells migrate proximally along the pedicle surface.

Cell migration appears to be discouraged by the presence of a tight sub-epidermal tissue – pedicle barrier. Fewer collagen fibres with smaller diameters are visible within the antler-velvet interface. The antler surface is smooth in nature; therefore less surface area is available for fibrous ingrowth. Strong attachment of the velvet to the antler is not required because the velvet is shed at continuous intervals throughout the life of the deer, thus firm adhesion would serve no beneficial function. Whilst the velvet is attached to the antler, the epidermal-pedicle interface is not percutaneous, hence strong adhesion of the velvet to the antler is not needed to prevent downgrowth or infection. The surface morphology study was carried out using SEM analysis. The results indicate that the surface morphology of the antler and pedicle are significantly different in terms of the number and size of pores present on their surfaces ($P < 0.05$ for both parameters). The pedicle possesses large poorly defined pores, which reflects its highly invaginated nature, whilst smaller well-defined pores were visible on the antler surfaces. The high porosity seen on the pedicle surface is not a phenomenon that is generally associated with bone of such a hard nature, however it is a prerequisite for a tight soft-tissue seal. The juncture between the antler and pedicle is clearly defined. The porosity of the structure increases dramatically from the antler to the pedicle. It is postulated that the reason for this is to maintain the strength in the antler, where it is required during fighting. Were the porosity

to remain constant throughout the bone, the antler would be mechanically compromised and would not withstand the forces encountered during rutting.

The change in morphology between the antler and pedicle may also play a role in the prevention of downgrowth, increasing in surface area where a strong soft tissue attachment is required. The ridges and clefts found in the antler-pedicle interface are thought to assist infection control. It is thought that the ridges guide the soft tissues to the areas where strong attachment is crucial for the health of the antler. SEM images were used to examine the surface morphology at the pedicle-skull interface. The number of pores decreases from the pedicle to the skull at a definable region. It is assumed that the nature of the soft tissue attachment to the pedicle differs from that of the skull, and that the pedicle is a morphological adaptation generated by the need for strong support around the soft tissue-pedicle interface. This is to protect the interface from mechanical stresses encountered by the lifestyle of the deer species. At the soft tissue-skull interface such dampening effects are not required and thus the surface morphology is restored to a smoother form.

The aim of this chapter was to establish the histological morphology of a non-gingival, natural percutaneous structure and relate the findings to the development of an artificial amputation prosthesis. The deer antler is a natural transitory percutaneous structure and as such, can act as an analogue for limb replacement prostheses. Previous research on percutaneous devices is mainly limited to non-bone anchored devices. However studies of bone anchored percutaneous hearing aids indicate the success of the implants in the absence of epithelial attachment to the biomaterial traversing the living tissues (Snik 1998). Sniks' results were consistent with the findings of Knabe et al in their 1999 analysis of catheters for peritoneal dialysis. Deer are notorious for having an exceptional immune system (Goss 1983), however the extent to which this protects the pedicle-soft tissue interface is as yet unknown. This factor should be taken into account when developing percutaneous implants for immuno-compromised patients, as they are undoubtedly more prone to infection. For other patients, immune system function effects on the success of loaded bone-anchored percutaneous implants should be further investigated. Owing to the success of the antler as a natural percutaneous structure, it is thought that the development of the ITAP concept should begin by recalling the surface characteristics and histological morphology of antler. Hence a device should include, a porous, roughened surface for bone anchorage, a largely invaginated surface with small grooves and ridges for epidermal and soft tissue attachment, and a smooth "non-sticky" surface externally. This chapter has shown that the attachment of the skin with the

pedicle at the antler – pedicle junction maintains stable union, which supports the antler as a non-gingival percutaneous structure. To maximise the chances of success for ITAP, it would be desirable if the material used to traverse the soft tissues encouraged collagen fibre attachment, ingrowth, proliferation and maturation.

Numerous factors must be considered in the development of ITAP, including surface properties, surface chemistry and mechanical properties of biomaterials. For antler to be successful, a number of factors are considered vital. Thick collagen fibres anchored to the pedicle from the adjacent tissues, provide strong attachment at the interface, prevent downgrowth and deter infection. The highly porous nature of the pedicle and smoother properties of the antler proper, provide ideal surface characteristics at different points along the length of the whole structure. Finally, the ridges and grooves at the antler-pedicle interface mediate soft tissue adherence. These factors should be introduced to the amputation prosthesis design to maximise efficiency and longevity. The pedicles' properties appear to be ideal for traversing the bodily tissues and breaching the skin barrier without detrimental effects, thus it is this natural structure that we should attempt to recreate artificially. It is possible that coating the biomaterials used in ITAP with various growth factors, surface finishes/materials and chemical/artificial materials may enhance the attachment of the designated tissues to the desired areas of the implant, as well as discouraging attachment of bacterial pathogens in the external environment. A quantitative and qualitative analysis of the epithelial interaction with the pedicle may give an insight into the importance of ITAP longevity and infection prevention. It is thought that the main focal point of research for ITAP should be the attachment of the sub-epidermal tissues to the biomaterials employed, as it is attachment at this level that appears to enable deer antler to function so successfully.

CHAPTER THREE

THE EFFECTS OF TITANIUM AND DIAMOND-LIKE CARBON SURFACE PROPERTIES ON THE ATTACHMENT AND PROLIFERATION OF FIBROBLASTS AND EPITHELIAL CELLS *IN VITRO*

CHAPTER THREE: THE EFFECTS OF TITANIUM AND DIAMOND-LIKE CARBON SURFACE PROPERTIES ON THE ATTACHMENT AND PROLIFERATION OF FIBROBLASTS AND EPITHELIAL CELLS *IN VITRO*

3.3.6 CELL MORPHOLOGY AND DESCRIPTIVE ANALYSIS

3.3.6.1 IMMUNOLOCALISATION IMAGES

3.3.6.2 SCANNING ELECTRON MICROSCOPY IMAGES

3.3.6.2.1 FIBROBLAST CELL CULTURE – 48 HOURS

3.3.6.2.2 EPITHELIAL CELL CULTURE – 48 HOURS

3.4 DISCUSSION

3.4.1 PROLIFERATION RATES – FIBROBLASTS 24/48 HOUR CULTURE

3.4.2 PROLIFERATION RATES – EPITHELIAL CELLS 24/48 HOUR CULTURE

3.4.3 CELL SURFACE AREA

3.4.4 NUMBER OF VINCULIN MARKERS PER UNIT CELL AREA

3.4.5 CELL MORPHOLOGY AND DESCRIPTIVE ANALYSIS

3.4.6 GENERAL CONCLUSIONS

3.1 INTRODUCTION AND HYPOTHESES

A stable connection between orthopaedic implants and their surrounding tissues is one of the most important prerequisites for their long-term success. Micro motion at the interface can lead to cellular damage, production of a soft tissue capsule and inflammation around the implant (Von Recum 1990). Transcutaneously, epithelial down growth can occur as a result of lack of cellular attachment, contact inhibition, the 'free edge effect' (see below), and tissue damage at the soft tissue-implant interface (Von Recum 1984). Thus, both strong cellular attachment and local stabilisation of the implant are vital applications where the principle aim is attachment of the soft tissues to the implant body.

In 1911, Harrison proposed that fibroblasts respond to the topography of the substratum. This phenomenon is known as "contact guidance". Contact guidance suggests that cells grown on a material surface will align in relation to the microstructures of the substratum surface. The term also refers to alterations in cell shape, polarity and orientation (Abercrombie et al 1971). Advancements in biomaterial science have produced substrates with definable and controllable surface geometries with uniform chemical and physical properties, thus allowing *in vitro* studies of cell orientation, attachment and migration (Brunette 1986).

One key feature in determining the nature of the interaction between cells and their substrata is the type of attachment. In 1958, Abercrombie and Ambrose were the first to describe the ultrastructure of fibroblast adhesion plaques on a glass substratum. From these early experiments it is now accepted that focal adhesions, or plaques, are locations at which a very close contact exists between the membrane of a cell and the substratum (typically 15nm). An adhesion plaque is made up of actin and intermediate filaments that are linked via proteins, for example vinculin, talin, alpha-actinin and paxillin, to transmembrane integrin receptors and to extracellular matrix (Turner et al 1990). Thus focal adhesions can be thought of as sites of contact, forming a stable connection between extracellular and intracellular fibre systems (Figure 3.1).

Many studies have been carried out using techniques to locate and visualise cell attachment plaques on biomaterial substrata *in vitro* (Hunter et al 1995, Eisenbarth et al 1996).

Contact guidance has been observed to occur in fibroblasts cultured on microstructured surfaces (Meyle et al 1993), whilst surface roughness has been shown to influence cellular behaviour (Richards 1996). Past research has shown inconsistencies in

observations concerning cellular response to material type and topography. In 1996, Richards presented results suggesting that material roughness is independent of fibroblast attachment, whilst in 2000 Anselme et al found that a negative correlation exists between titanium surface roughness and proliferation and attachment of primary mouse osteoblasts. Cambell and Recum (1989) demonstrated that alterations in surface patterns in the micrometer range would encourage different tissue reaction when implanted subcutaneously. Some research has been aimed at the role of cell shape and its relation to cell proliferation and attachment. Folkman and Moscona (1978) hypothesise that appropriate cell shape is vital for DNA synthesis of normal cells, and that this theory explains anchorage dependence. Anchorage dependence describes the inability of normal cells to grow unless attached to a substratum. It is based on the principle that primary fibroblasts will proliferate if attached to plastic or glass, but will not in suspension culture. This phenomenon indicates that DNA synthesis is coupled to cell attachment and the effect of any biomaterial on cell attachment will consequently alter DNA synthesis and proliferation rates.

For my thesis the emphasis is placed on fibroblast and epithelial cell attachment for subcutaneous soft tissue, including tendon attachment and ITAP development respectively. This chapter examines the attachment, proliferation and morphology of fibroblasts and epithelial cells cultured on materials *in vitro* that will be selected and used in *in vivo* studies in subsequent chapters (see Chapters Five and Six). The principle advantage of using cell culture techniques to determine biocompatibility is the increased definition of the criteria to be evaluated. In culture, each variable that could affect cell behaviour can be altered individually, thus determining the consequence of changing that parameter independently of the others. The cells physiochemical environment, namely pH, temperature, pressure and tension of gases such as oxygen and carbon dioxide can be controlled and monitored. *In vitro* cell populations are more homogenous than those observed in living tissue, and as such the culture conditions can be altered to ensure that a specific cell type will grow more rapidly. Agents to be tested *in vitro* can be utilised at much lower concentrations as the cells are exposed to them directly rather than by injection *in vivo*. *In vitro* studies are a cheaper alternative to *in vivo* models and the need to use animals for preliminary studies is significantly reduced.

There are, however, drawbacks to using cell culture as an indication of cellular activity, mainly because the cells are subjected to an environment in which they are unaffected by the normal *in vivo* parameters. Cells cultured on traditional substrates adopt a flattened morphology, losing any type of physiological three-dimensional structure and polarity. In

a culture environment cells undergo a selective process whereby those that are most suited to survival *in vitro* proliferate, while others undergo programmed cell death. Over time this process produces a uniform population of cells that is useful for reproducibility in results, but is considerably different from *in vivo* conditions, principally because cells are deprived of heterotypic cell interactions.

When epithelial cells or fibroblasts are cultured on plastic surfaces, they attach, spread and divide until they form a confluent monolayer in which all neighbouring cells are in contact with one another. This is a phenomenon known as contact inhibition. When there is no more space for cells to occupy, division ceases. If cells are removed from the monolayer, the remaining cells divide and fill the gap (Alberts et al 1994). *In Vivo*, epithelial cells in the skin carry out similar behaviour. When the skin layer is interrupted (for example, in a cut or wound), the epithelial cells abutting the interruption migrate beneath the clot formed to heal the breach in the skins protective layer. In transcutaneous implants, one of the principle hurdles is epithelial down growth; also known as marsupialization. The epithelial cells on the surface layers of the skin traverse the surface of the protruding implant and attempt to travel beneath its structure to heal the breach in the skin layers. All of these observations are due to contact inhibition. It is postulated that using a material with surface properties that promote epithelial cell attachment, the cells on the wound margin surrounding the transcutaneous implant will attach to the implant surface and this attachment will prevent their migration into the underlying soft tissues.

The material surface properties best suited to fibroblast and epithelial cell attachment, proliferation and morphology must be determined to further promote integration of implants with soft tissues, either in a subcutaneous or transcutaneous site.

Titanium is the obvious material of choice for any *in vitro* research owing to its use in orthopaedic surgery. Diamond like carbon (DLC) coatings can be applied to numerous substrates, and studies have demonstrated its high biocompatibility, durability and wear- and corrosion-resistance (Kornu et al 1996, Tang et al 1995, Allen et al 2001). DLC has a very low surface energy, typically between 40-50mN/m, and possesses few free electrons on its surface. It is thought that these properties would make it difficult for a cell to spread across a titanium surface coated with DLC, as the weak bonds formed (H-bonds, electrostatic forces) which are essential in the early phase of cell spreading and attachment, will be inhibited.

This chapter attempts to determine the effects of titanium and DLC on epithelial and fibroblast cell attachment, proliferation and spreading. The role of surface topography in influencing these cellular activities is also investigated.

The hypotheses for this chapter are threefold. Firstly, fibroblast and epithelial cells' proliferative capacity, morphology and attachment will be directly affected by the topography of the substrate used to support their growth. Secondly, DLC is a low surface energy coating that will prove detrimental to the maintenance of fibroblast and epithelial cell populations *in vitro*. Finally, innate properties of cell populations can outweigh the properties instigated by changing the substrate topography, with the emphasis being placed on contact inhibition and contact guidance.

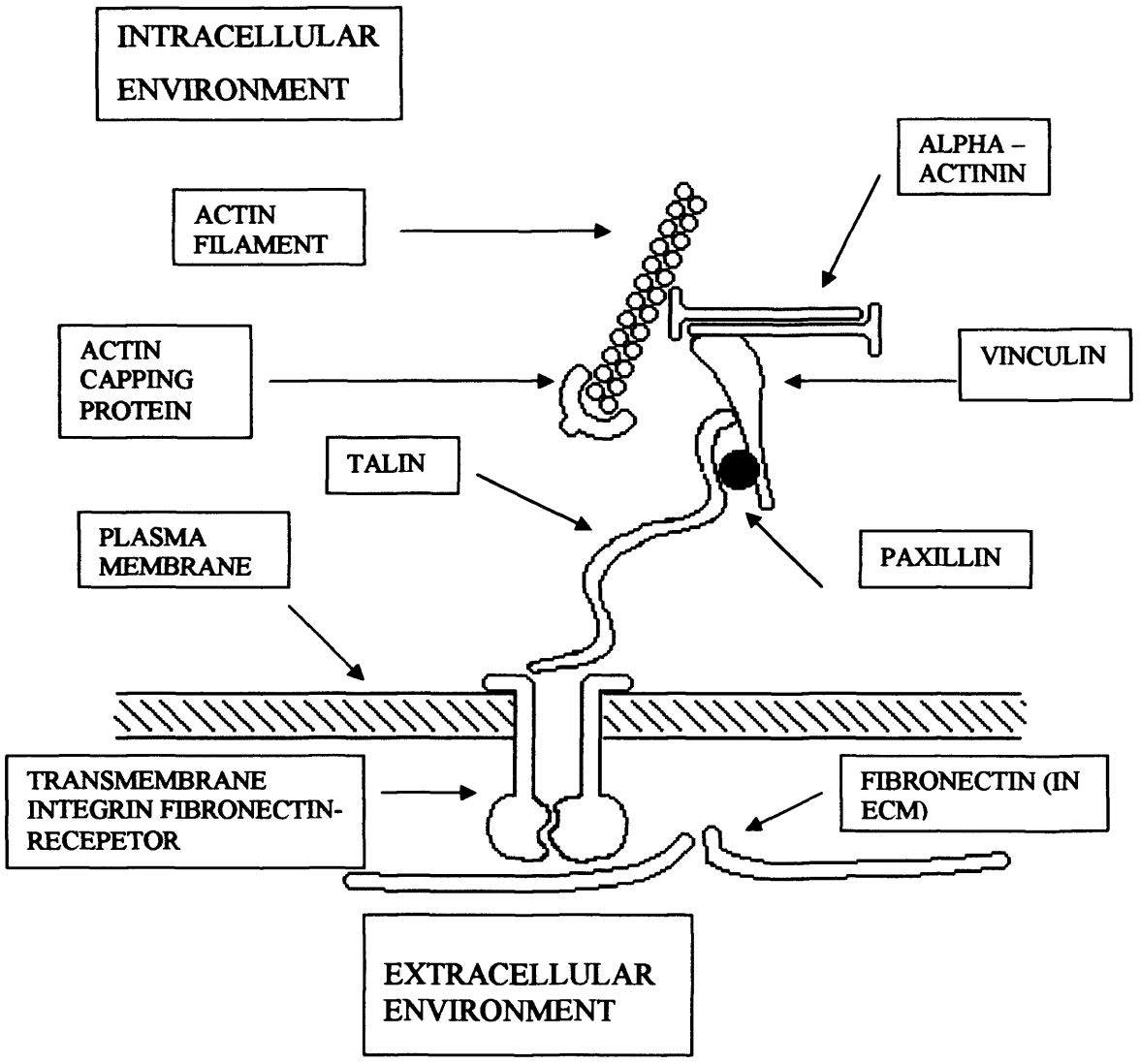

FIGURE 3.1 Schematic diagram of a focal adhesion plaque.

Integrins are a large family of homologous transmembrane linker proteins that allow the cytoskeleton and extracellular matrix to communicate across the plasma membrane. Many matrix proteins are recognised by multiple integrins, for example eight integrins bind to the RGD sequence in fibronectin (see Chapter One). Integrins are made of two noncovalently associated transmembrane glycoprotein subunits called heterodimers – as seen here in the transmembrane integrin fibronectin receptor, which serves as a receptor for proteins containing the RGD sequence.

3.2 MATERIALS AND METHODS

3.2.1 MATERIAL PREPARATION

Smooth Polished Titanium (SPTi) (Ra 0.026 μm, Ry 0.71 μm, Rz 0.47 μm), Machine Finished Titanium (MFTi) (Ra 0.210 μm, Ry 1.35 μm, Rz 1.27 μm), Rough Sand Blasted Titanium (RSBTi) (Ra 0.404 μm, Ry 2.56 μm, Rz 1.34 μm) and DLC Coated Smooth Polished Titanium discs (SPDLC) (Brunel University) (Ra 0.040) were prepared.

A 10.1mm diameter stock bar of medical grade titanium (Ti_6Al_4V)(BS7252 part 3) was machined on a lathe with carbide tooling to a diameter of 9.9mm. The resulting bar was sectioned into discs; 3mm in thickness and the sharp edge of each disc was removed. This process produced discs of a machine-finished type. A holding device was designed to polish the machine finished discs to a smooth polished finish, which was achieved by rubbing the machine finished discs vigorously over wet 1200 grade polishing paper and then repeating the process on a jean-type material using Buehler Micropolish (1.0 micron alumina) and water, mixed to a paste. The smooth polished discs were rough sand blasted in a sealed cabernet containing 0.2mm diameter aluminium oxide grit. A number of smooth polished discs were sent to Brunel University for DLC coating. The roughness average value (Ra) of each disc type was established using a Taylor Hobson Talysurf Ra Machine. Five measurements were taken from five randomly selected discs from each material type group.

The materials were then cleaned to the level required for orthopaedic implantation.

The three titanium finishes were used to determine the effects of surface roughness and topography on cell response (contact guidance, cell attachment, morphology and proliferation).

The DLC coated discs were used to determine the effects of lowering surface energy on cell response respectively.

3.2.2 CELL CULTURE TECHNIQUES

3.2.2.1 MATERIAL SET-UP

The following 24 well plates were set up for testing each cell line:

24-Hour SEM Plate

SPTi	RSBTi	MFTi	SPDLC
SPTi	RSBTi	MFTi	SPDLC

48-Hour SEM Plate

SPTi	RSBTi	MFTi	SPDLC
SPTi	RSBTi	MFTi	SPDLC

48-Hour FM Plate

SPTi	RSBTi	MFTi	SPDLC
SPTi	RSBTi	MFTi	SPDLC
SPTi	RSBTi	MFTi	SPDLC

3.2.2.2 CELL LINES AND SEEDING TECHNIQUES

The materials were all seeded at a rate of 30,000 cells per disc. The two cell lines were obtained from the ECACC. The fibroblasts used were 84-BR, human skin fibroblasts derived from a biopsy of a radiosensitive female (Ref No. 90011805). The epithelial cells were PNT-2 cells established by immortalisation of normal adult prostatic epithelial cells by transfection with a plasmid containing SV40 genome with a defective replication origin. The primary culture was obtained from a prostate of a 33-year-old male at post mortem. (Ref No. 95012613). The cells were resuscitated from frozen vials and cultured to the numbers required. The cells were stored in a standard incubator at 37°C, 5%CO_2, and the medium was changed every other day:

84-BR:	PNT-2:
350ml DMEM	90ml RMPI-1640 (sigma)
40ml FCS	10ml FCS
4ml Pen/Strep	1ml Pen/Strep
4ml L-Glutamine	1ml L-Glutamine
4ml NEAA	

All cell culture techniques were carried out in a laminar flow hood using standard sterile techniques. When the cells had reached sufficient numbers, they were trypsinised, centrifuged and re-suspended in medium to produce a cell suspension of suitable cell density. The cells were seeded at 30,000 for SEM/FM, onto the discs in the minimum

amount of medium (50µl). The cells were dropped in suspension, onto the surfaces and the discs were placed in the incubator for one hour, to allow the cells to attach. The discs were then flooded with medium and incubated for 24 / 48 hours.

3.2.2.3 DETERMINATION OF PROLIFERATION RATES – ALAMAR BLUE

After 24 hours the medium was removed from the wells of the 48-hour plates. 10% Alamar Blue in phenol red free medium was added to the wells and the discs were incubated for 4 hours. Two 100µl aliquots of Alamar blue/medium solution were removed from each disc's well and plated into a 96 well plate for analysis on a Dynatech Plate Reader (570nm, ref 630nm). The Alamar blue was washed from the discs using sterile PBS and the discs were suspended in fresh medium. The procedure was repeated at 48 hours prior to processing for SEM / FM.

3.2.3 CELL MORPHOLOGY - SCANNING ELECTRON MICROSCOPY PROCESSING

The medium was removed from the wells containing discs for SEM processing. The discs were washed with sterile phosphate buffered saline (PBS) prior to addition of medium and placed in a refridgerator at 4°C for 20 minutes. The plates were removed from refrigeration and the cells were fixed in a solution of 1.5% gluteraldehyde in 0.1M sodium cacodylate (stock buffer). The plates were left in a refridgerator over night. The buffer was removed and replaced with 1% osmium tetroxide in 0.1M buffer for one hour. The discs were then subjected to 2x5 minute buffer washes. A filtered 1% tannic acid in 0.05M buffer was applied and left for 1 hour. The discs were then washed 4x5 minutes in buffer wash prior to dehydration in an ascending alcohol series. After the 70% alcohol stage, the discs were subjected to 0.5% uranyl acetate in 70% ethanol for 30 minutes prior to completion of the dehydration process. The discs were then chemically dried using Hexamethyldisilazane (HMDS), mounted onto SEM stubs and gold sputter coated prior to examination under SEM.

3.2.4 IMMUNOLOCALISATION OF VINCULIN

The medium was removed from the wells containing discs for processing. The discs were washed (2x5mins) in sterile PBS and fixed in 10% formal saline for 5 minutes. The discs were washed (4x5mins) in sterile PBS prior to application of the primary antibody solution: 0.2ml monoclonal anti-human clone HUV-1 (Sigma V9131 = Anti-vinculin) + 0.01% Triton X-100 + 40ml sterile PBS – for a duration of 2 hours. The discs were re-

washed (3x10mins) and soaked in secondary antibody solution – 0.5ml FITC conjugate (Sigma F2883) + 50ml PBS – for a duration of 45 minutes. The discs were washed in PBS (3x10mins) and examined under a Weiss fluorescent microscope.

3.2.5 COUNTING VINCULIN MARKERS

Vinculin markers were counted for 10 randomly selected cells on each material tested. Photographs were taken to give a visual image of the appearance of the cells – see Figure 3.14.

3.2.6 MEASURING CELL AREA

SEM images were taken from five typical cells from each material tested. The negatives were analysed using the Zeiss KS300 image analysis package, and the cell area for each cell was determined.

3.2.7 STATISTICAL ANALYSIS

The data obtained was examined and analysed using the SPSS software package. Normality tests (Kolmogorov-Smirnov) were used to determine whether the data fitted the assumptions for parametric (normally distributed data i.e. symmetrically distributed into a bell shaped curve) or nonparametric testing (data not fitting into a standard bell shaped curve). Values <0.05 generated using the Kolmogorov-Smirnov normality test were considered to be non-normally distributed data sets and were analysed using nonparametric tests, including Mann Whitney U (a nonparametric equivalent to the t test) and Spearman R (a nonparametric equivalent to standard correlation coefficient analysis).

3.2.7.1 STATISTICAL ANALYSIS OF MULTIPLE COMPARISONS

For some data sets it was necessary to carry out a number of hypothesis tests. Clearly, if one were to carry out a large number of tests, each with the significance level set at the 5% level, then even in the absence of any real effects, some of the tests would appear to be significant. This is a type I error. The method employed in these cases to avoid the type I error was simple. When conducting n significance tests, to achieve an overall type I error rate of α, one would only declare any of them significant if the p value was found to be less than α/n. Thus, if 5 tests were carried out the result would not be declared significant unless the p value for that result was found to be less than 0.01. For these, and all following multiple analyses, the 0.05 value was divided by the number of

comparisons being made to the particular data set of interest, to avoid error in the findings.

Data sets demonstrating no significant differences between means using Mann-Whitney U tests were not statistically analysed further.

3.3 RESULTS

3.3.1 ANALYSIS OF SURFACE ROUGHNESS

The data did not fit the assumptions required for parametric testing, hence Mann Whitney U tests were carried out to determine the significance of the findings. Significant differences were observed in the average surface roughness (Ra) values between the three titanium-finished discs tested. The rough sand blasted titanium discs were found to possess an Ra value significantly higher than both the machine finished and smooth polished groups ($p < 0.01$), whilst the machine finished discs were observed to have a significantly higher Ra than the smooth polished discs ($p < 0.01$). There was no statistical difference observed in Ra value between the smooth polished titanium and the smooth polished DLC discs ($p = 0.09$). The box and whiskers plot (figure 3.2) displays a visual summary of the data, where the boxes represent the interquartile range, the horizontal lines inside the boxes represent the median value, the whiskers demonstrate the range of data that falls within one and a half interquartile ranges, with data points beyond the whiskers appearing individually.

Tables of summary data can be referred to in Appendix 2 (2.1 and 2.2).

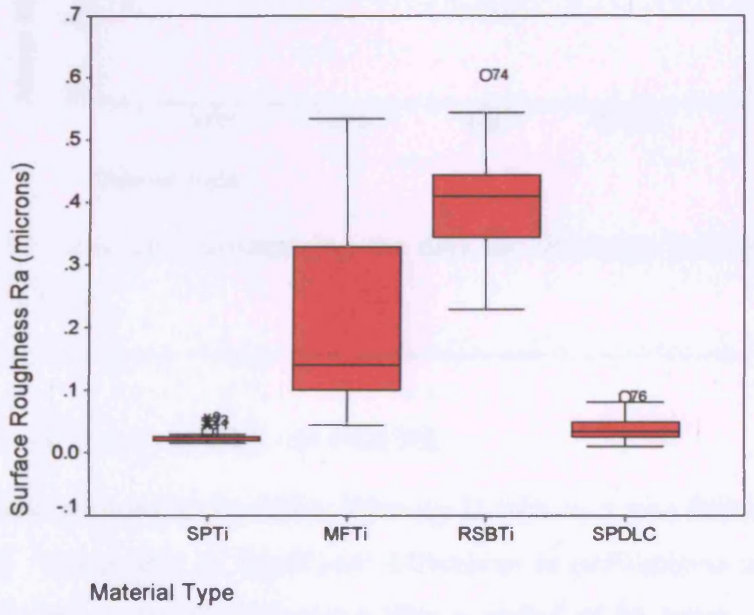

FIGURE 3.2 Box plot summarising the data for surface roughness analysis.

3.3.2 PROLIFERATION RATES – ALAMAR BLUE

3.3.2.1 FIBROBLASTS - 24 HOURS

The data did not fit the assumptions required for parametric testing, thus Mann Whitney U tests were used to demonstrate the statistical significance of the findings. The numerical data for the results is presented in Appendix 2 (2.3 and 2.4) and the box and whiskers plot in Figure 3.3 summarises the data obtained. There were no significant differences observed in proliferation rate of fibroblasts cultured on any of the materials tested after a period of 24 hours ($p>0.01$)

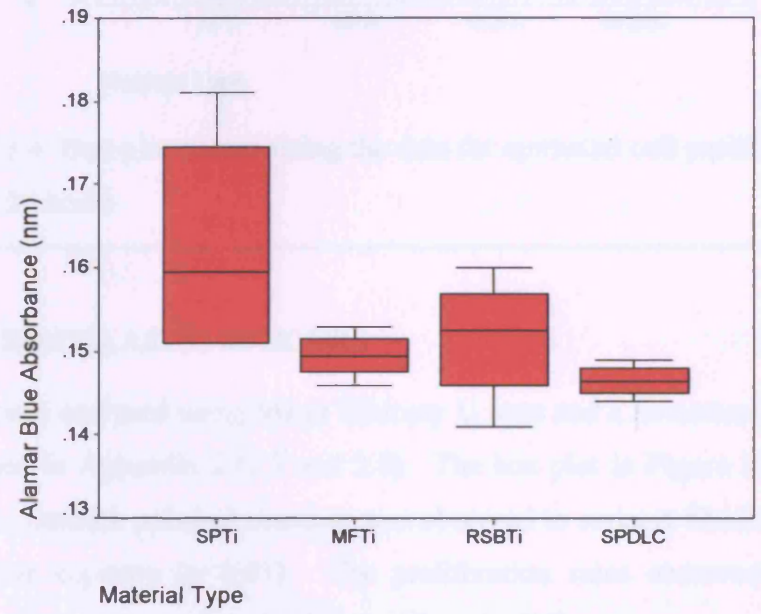

FIGURE 3.3 Box plot summarising the data for fibroblast proliferation after a culture period of 24 hours.

3.3.2.2 EPITHELIAL CELLS - 24 HOURS

The data was analysed using Mann Whitney U tests as it was found to be non-normally distributed. There were no significant differences in proliferation rate of epithelial cells cultured on any of the test substrates after a period of 24 hours. The numerical data summary is presented in Appendix 2 (2.5 and 2.6) and the box and whiskers plot in Figure 3.4 summarises the data obtained.

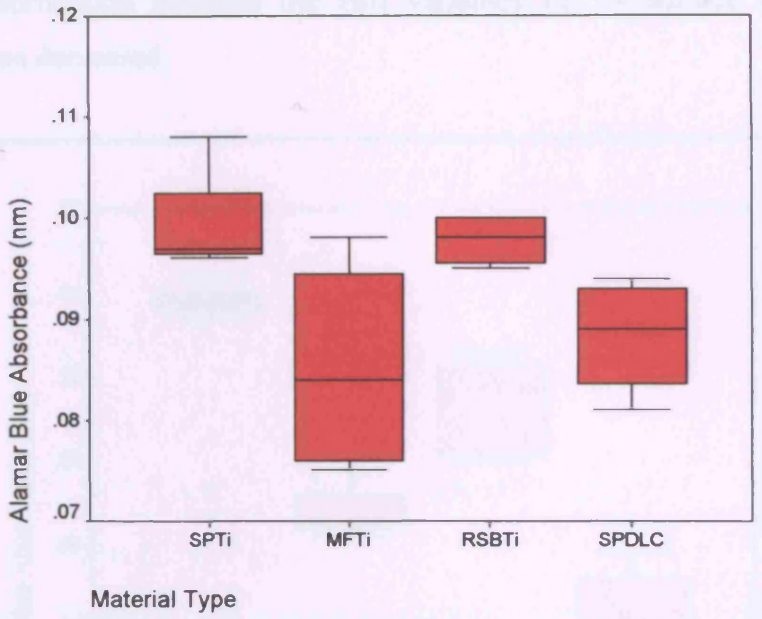

FIGURE 3.4 Box plot summarising the data for epithelial cell proliferation after a culture period of 24 hours.

3.3.2.3 FIBROBLASTS - 48 HOURS

The data was analysed using Mann Whitney U tests and a numerical summary of the data can be seen in Appendix 2 (2.7 and 2.8). The box plot in Figure 3.5 gives a visual data summary. Smooth polished titanium was observed to support fibroblasts with the highest proliferative capacity ($p<0.01$). The proliferation rates observed between all of the material substrates were found to be significantly different.

Correlation between surface roughness and fibroblast proliferation was determined using the Titanium groups – SPTi, MFTi and RSBTi. Surface roughness values were evaluated against the Alamar Blue Absorbance result. To express a relationship between two variables, one usually computes the correlation coefficient. Non-parametric equivalents to the standard correlation coefficient are Spearman R, Kendall Tau and coefficient Gamma. Here, the Spearman R test was used to express the nature of the relationship between surface roughness and fibroblast proliferation. The data table is presented in Appendix 2 (2.9). The correlation between the two variables was found to be significant at the 0.01 level. The correlation coefficient reflects the degree of linear relationship between two variables. It ranges from +1 to -1. A correlation of +1 means that there is a perfect positive linear relationship between variables. A correlation of -1 means that there is a perfect negative linear relationship between variables. A correlation of 0 means there is no linear relationship between the two variables. Here there was a significant

negative correlation between the two variables i.e. as surface roughness increased proliferation decreased.

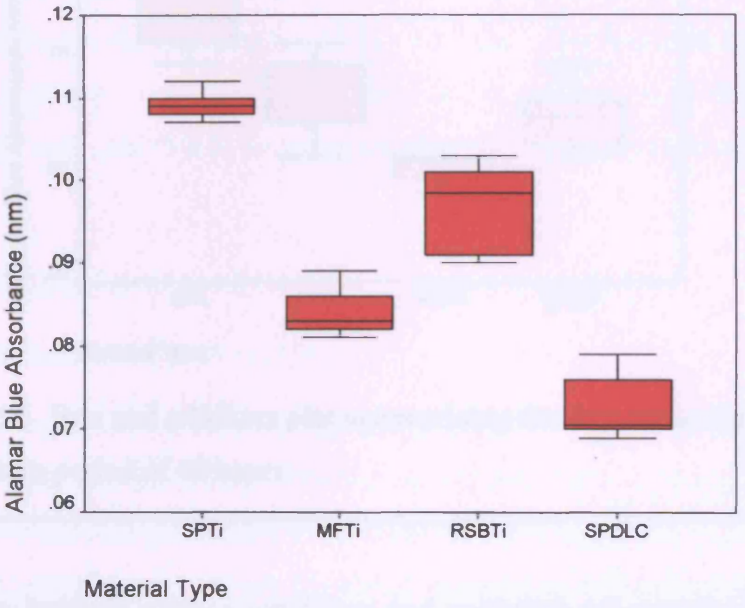

FIGURE 3.5 Box plot summarising the data for fibroblast proliferation after a culture period of 48 hours.

3.3.2.4 EPITHELIAL CELLS - 48 HOURS

The data did not fit the assumptions for parametric testing, hence Mann Whitney U tests were carried out to determine the significance of the findings. From the box and whiskers plot in figure 3.6 it is clear that the proliferation rate of epithelial cells cultured on titanium substrates, decreases as surface roughness increases. The statistical analysis showed a significant decrease in proliferative capacity of epithelial cells cultured on SPTi and MFTi ($p = 0.00$) and MFTi and RSBTi ($p = 0.000$). No significant differences were observed between MFTi and SPDLC ($p = 0.223$). The numerical data summary and Mann Whitney U test results can be observed in Appendix 2 (2.10 and 2.11).

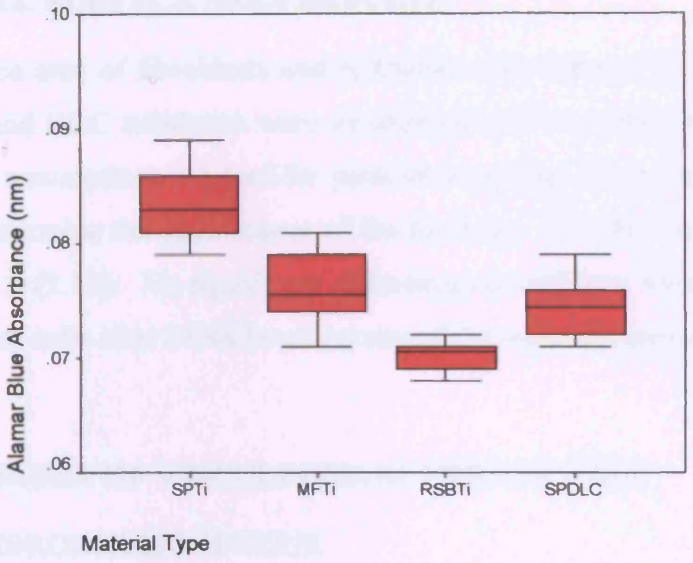

FIGURE 3.6 Box and whiskers plot summarising the data for epithelial cell proliferation after a culture period of 48 hours.

Correlation between surface roughness and epithelial cell proliferation was determined for the Titanium groups using a Spearman's rho analysis. The relationship between the two variables was found to be significant at the 99% level, with Figure 3.7 showing that as the surface roughness of epithelial cell substrata increases the proliferative capacity decreases.

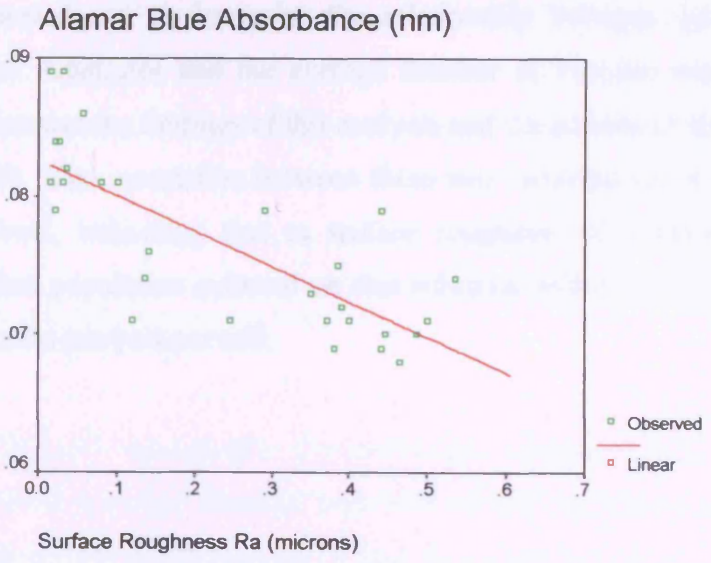

R Squared = 0.616

Sig of R value = $\frac{r\sqrt{n-2}}{\sqrt{1-r^2}}$

$= \frac{0.616 \times 5.292}{0.620} = 5.26$

5.26 significant at the 99% level.

FIGURE 3.7 Curve estimation for the relationship between alamar blue absorbance and surface roughness (Summary data – Appendix 2 (2.12)).

3.3.3 CELL SURFACE AREA RESULTS

The surface area of fibroblasts and epithelial cells cultured for 24 and 48 hours, on the titanium and DLC substrates were established and evaluated statistically. The data did not fit the assumptions required for parametric testing, hence Mann Whitney U tests were used to determine the significance of the findings. The data summaries are presented in Appendix 2 (2.13). No significant differences in cell area were observed for fibroblasts or epithelial cells after 24/48 hours on any of the material types tested.

3.3.4 NUMBER OF VINCULIN MARKERS PER CELL

3.3.4.1 FIBROBLASTS 48 HOUR

The results were analysed statistically using Mann Whitney U tests as the data was found to be non-normally distributed. The box and whiskers plot in Figure 3.8 demonstrates the findings and the numerical data can be referred to in Appendix 2 (2.14 and 2.15). There were more vinculin markers per fibroblast cultured on SPTi than on RSBTi and SPDLC substrates (all p values < 0.01). There was no significant difference in the number of vinculin markers per cell in fibroblasts cultured on SPTi and MFTi (all p values > 0.01). MFTi supported a fibroblast population with significantly higher numbers of vinculin markers per cell than RSBTi ($p < 0.01$).

Figure 3.8 shows the relationship between numbers of vinculin markers and surface roughness within the titanium substrate materials. Spearman's rho correlation analysis was carried out to determine the relationship between the surface roughness of the titanium substrates and the average number of vinculin markers per cell. Figure 3.9 demonstrates the findings of this analysis and the numerical data is presented in Appendix 2 (2.16). The correlation between these two variables was found to be significant at the 99% level, indicating that as surface roughness of a titanium substrate increases, a fibroblast population cultured on that substrate will possess significantly fewer numbers of vinculin markers per cell.

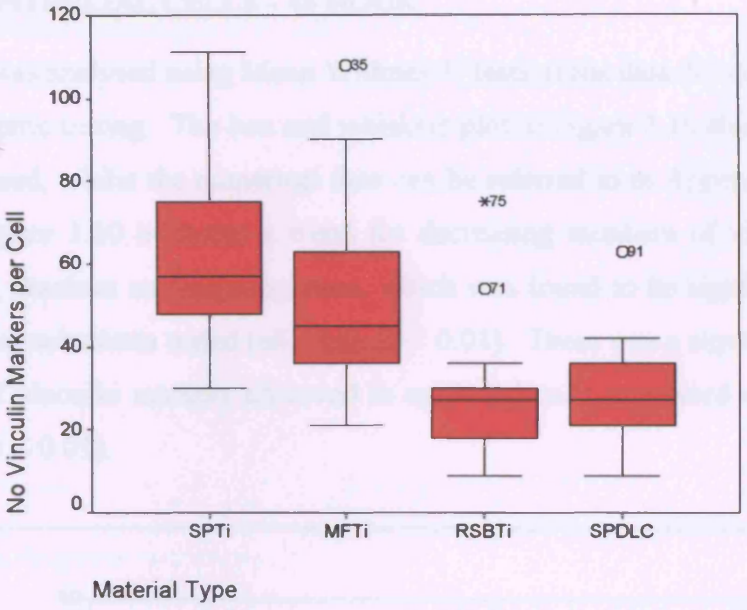

FIGURE 3.8 Box plot demonstrating the relative numbers of vinculin markers observed within fibroblasts cultured on the test substrates after a period of 48 hours.

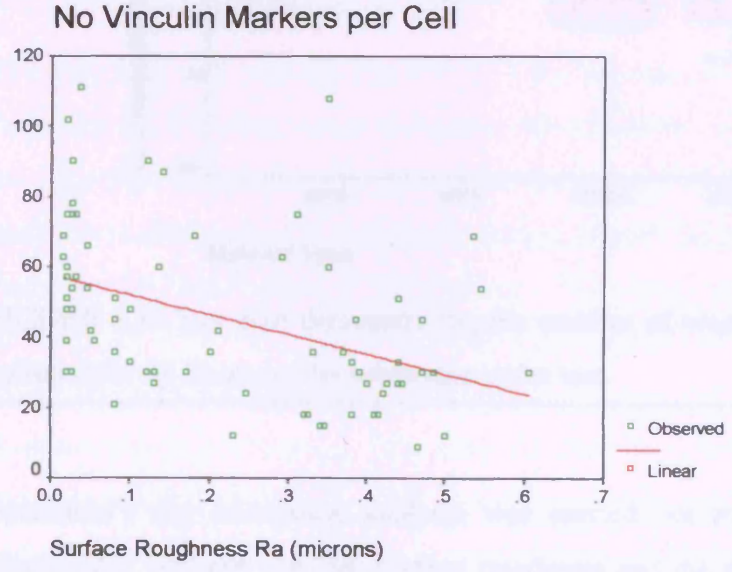

R squared = 0.184

Sig of R value = 4.06

Significant at 99.9% level

FIGURE 3.9 Spearman's rho correlation analysis demonstrating the nature of the relationship between titanium substrata surface roughness and the number of vinculin markers per fibroblast cultured thereon for a period of 48 hours.

3.3.4.2 EPITHELIAL CELLS - 48 HOUR

The data was analysed using Mann Whitney U tests as the data did not fit the assumptions for parametric testing. The box and whiskers plot in Figure 3.10 shows a summary of the data obtained, whilst the numerical data can be referred to in Appendix 2 (2.17, 2.18 and 2.19). Figure 3.10 indicates a trend for decreasing numbers of vinculin markers with increasing titanium surface roughness, which was found to be significant between all of the titanium substrates tested (all p values < 0.01). There was a significant decrease in the number of vinculin markers observed in epithelial cells supported on SPTi compared to SPDLC ($p < 0.01$).

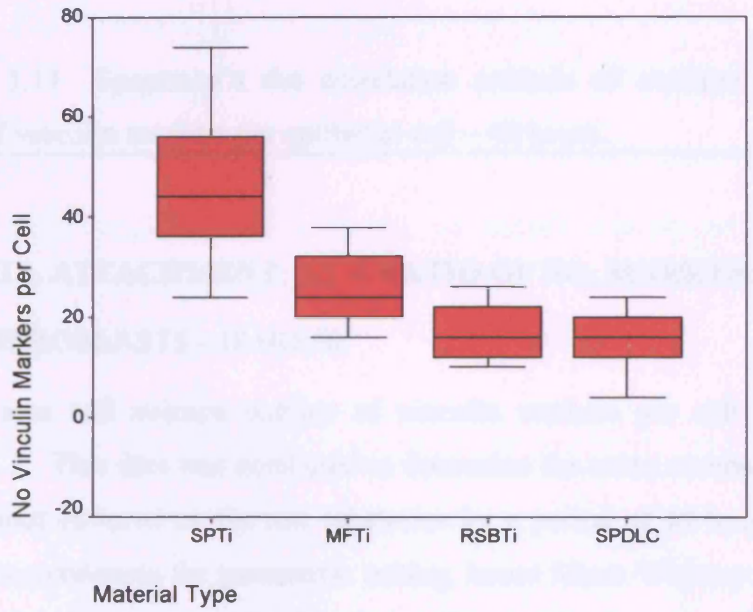

FIGURE 3.10 Box plot demonstrating the number of vinculin markers per epithelial cell cultured for 48 hours on the substrates under test.

Spearman's rho correlation analysis was carried out to determine the nature of the relationship between titanium surface roughness and the number of vinculin markers per epithelial cell cultured thereon for a period of 48 hours. Figure 3.11 displays the curve obtained for the analysis and demonstrates that the relationship is significant at the 99% level, indicating that as titanium surface roughness increases, the number of vinculin markers per epithelial cell decreases.

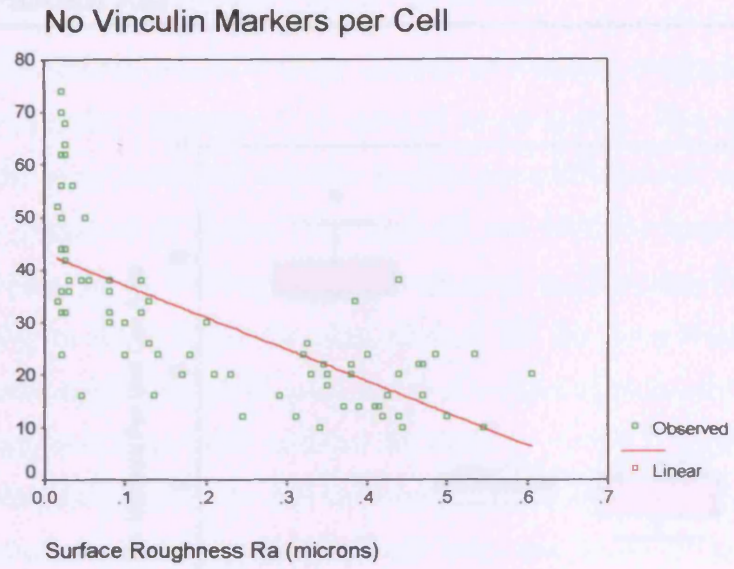

R sq = 0.493

Significance of R value = 8.308

Significant at the 99.9% level.

FIGURE 3.11 Spearman's rho correlation analysis of titanium surface roughness : number of vinculin markers per epithelial cell – 48 hours.

3.3.5 CELL ATTACHMENT: AS A RATIO OF NO. MARKERS:CELL AREA

3.3.5.1 FIBROBLASTS - 48 HOUR

The cell area and average number of vinculin markers per cell data can be seen in Appendix 3. This data was combined to determine the mean number of vinculin markers per fibroblast cultured on the test substrates for a period of 48 hours. The data did not meet the requirements for parametric testing, hence Mann Whitney U tests were used to determine the significance of the findings. The results show that fibroblasts cultured on SPTi for 48 hours have significantly greater numbers of vinculin markers per cell than those supported by MFTi or RSBTi (all p values < 0.02). The graph in Figure 3.12a demonstrates these findings. The data for fibroblasts cultured on SPDLC could not be compared statistically to all of the titanium materials tested, as both surface topography and material chemical composition are variables. As there was no significant difference observed for surface roughness between SPTi and SPDLC, the mean number of vinculin markers per unit fibroblast cell area cultured on each of these materials was compared statistically. The results of these findings are presented in Figure 3.12b, where it was established that the fibroblasts cultured on SPTi possessed significantly greater numbers of vinculin markers per unit cell area than those supported by SPDLC ($p < 0.05$).

FIGURE 3.12

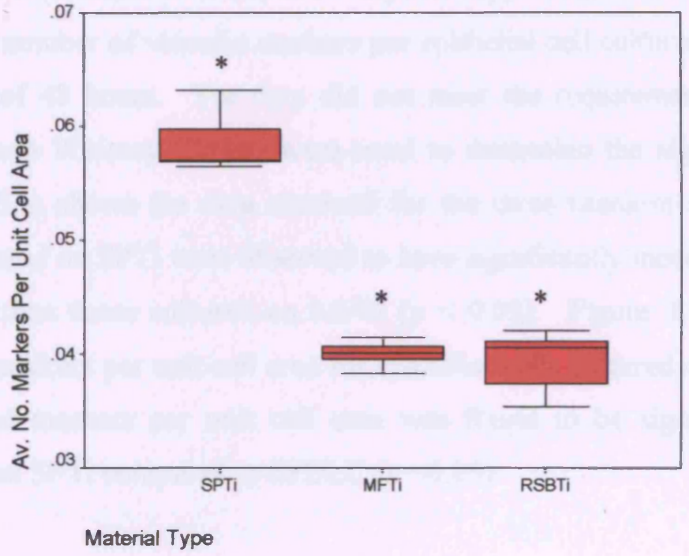

FIGURE 3.12a Graph of average number of vinculin markers per fibroblast cultured on the three titanium substrates under test.

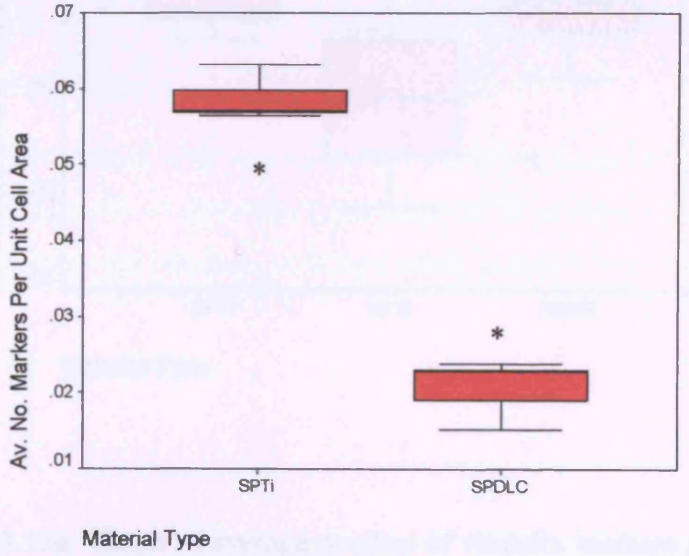

FIGURE 3.12b Graph of average number of vinculin markers per fibroblast cultured on SPTi and SPDLC.

3.3.5.2 EPITHELIAL CELLS - 48 HOUR

The cell area and average number of vinculin markers per cell data can be seen in Appendix 2 (sections 2.13 and 2.17 respectively). This data was combined to determine the mean number of vinculin markers per epithelial cell cultured on the test substrates for a period of 48 hours. The data did not meet the requirements for parametric testing; hence Mann Whitney U tests were used to determine the significance of the findings. Figure 3.13a shows the data obtained for the three titanium substrates. The epithelial cells cultured on SPTi were observed to have significantly more vinculin markers per unit cell area than those cultured on MFTi ($p < 0.02$). Figure 3.13b shows the number of vinculin markers per unit cell area for epithelial cells cultured on SPTi and SPDLC. The number of markers per unit cell area was found to be significantly greater for cells cultured on SPTi compared to SPDLC ($p < 0.05$).

FIGURE 3.13

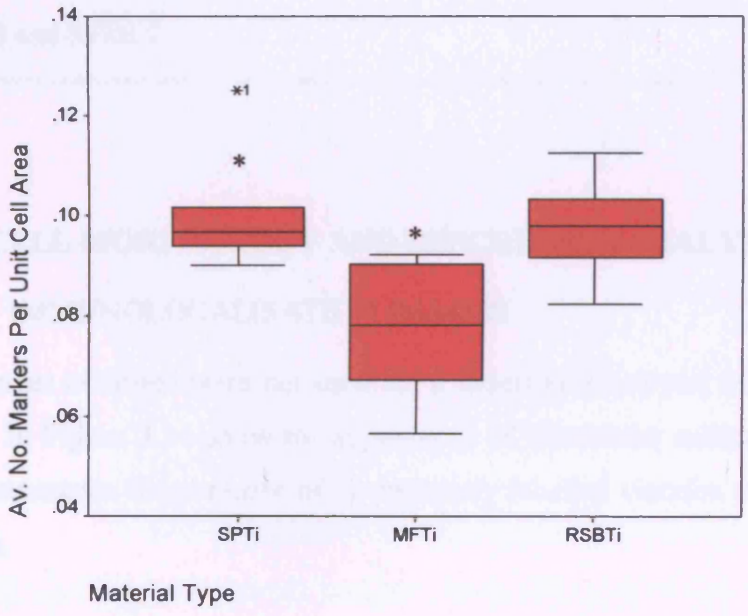

FIGURE 3.13a Graph of average number of vinculin markers per epithelial cell cultured on the three titanium substrates under test.

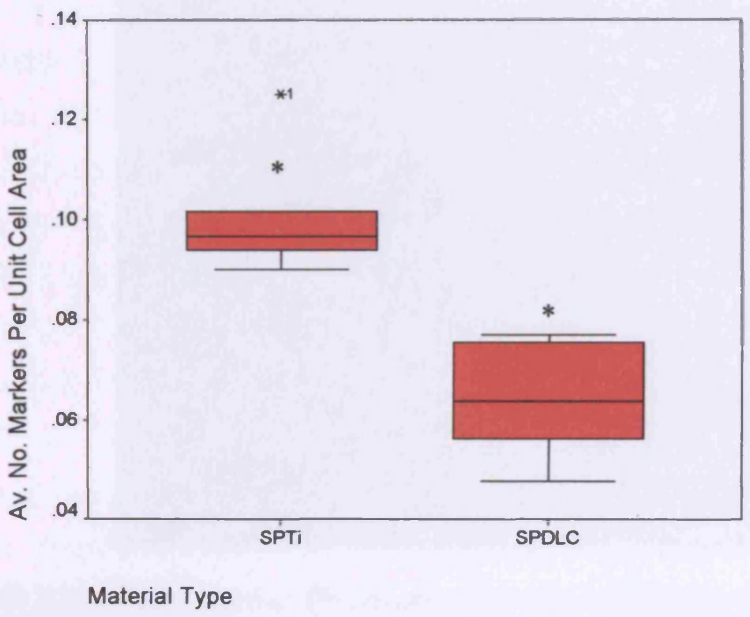

FIGURE 3.13b Graph of average number of vinculin markers per epithelial cell cultured on SPTi and SPDLC.

3.3.6 CELL MORPHOLOGY AND DESCRIPTIVE ANALYSIS

3.3.6.1 IMMUNOLOCALISATION IMAGES

The images obtained were not used for a descriptive analysis of cell morphology. The images in Figure 3.14 show the appearance of fibroblasts cultured on SPTi and RSBTi and demonstrate the presence of fluorescently labelled vinculin markers within adhesion plaques.

FIGURE 3.14

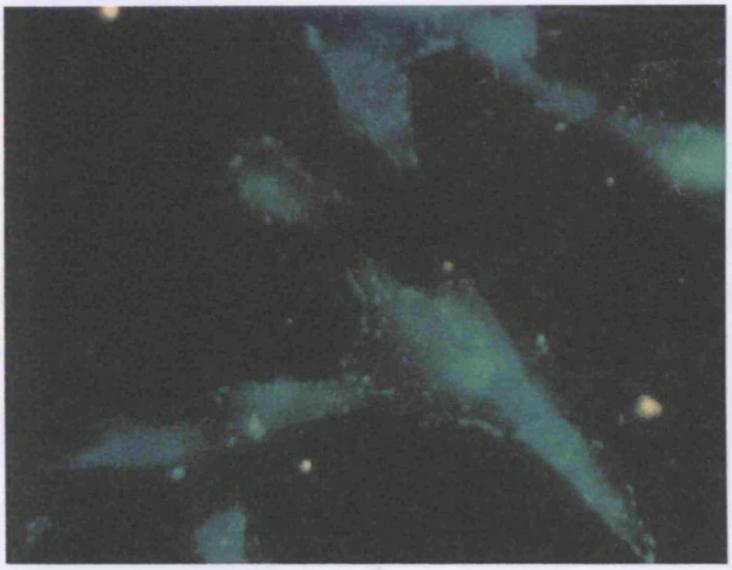

FIGURE 3.14a Appearance of fibroblasts under FM on SPTi for 48 hrs (x 50).

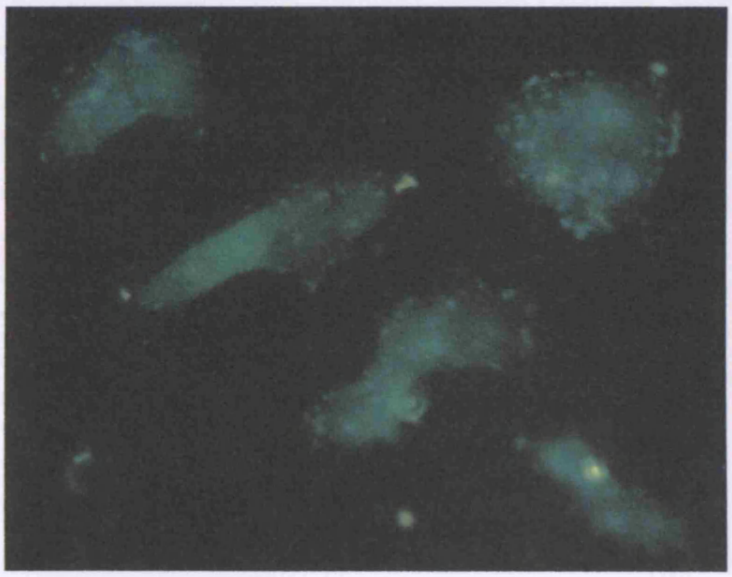

FIGURE 3.14b Appearance of fibroblasts under FM on RSBTi for 48 hrs (x 50).

3.3.6.2 SCANNING ELECTRON MICROSCOPY IMAGES

3.3.6.2.1 FIBROBLAST CELL CULTURE – 48 HOURS

Figures 3.15a-d demonstrate the appearance of fibroblasts cultured on the test substrates. Fibroblasts cultured on SPTi for 48 hours (Figure 3.15a) showed a definite polarity and appeared well spread out over the surface. They possessed numerous membrane projections indicating extensive cell-cell interaction, and an almost confluent monolayer of cells was observed over the entire material surface. After 48 hours, fibroblasts cultured on RSBTi (Figure 3.15b) were poorly spread and appeared to possess few membrane projections. The cells seemed to have maintained a polar nature, however they showed minimal cell-surface or cell-cell interaction. Fibroblasts supported by a MFTi substrate for 48 hours (Figure 3.15c) appeared flattened in morphology. The cells clearly displayed contact guidance as they were seen to be orientated parallel to the grooves of the titanium surface, whilst numerous membrane projections indicated a large degree of cell-cell communication. SPDLC supported a fibroblast population of considerably lower density than that of any of the titanium substrates tested (Figure 3.15d). The majority of the cells were observed to be adopting a more rounded morphology, indicating a lack of cell-substrate interaction. Large amounts of cell debris were observed, suggesting that a considerable number of cells had undergone programmed cell death. The fibroblasts were not seen to adopt any particular orientation pattern.

FIGURE 3.15

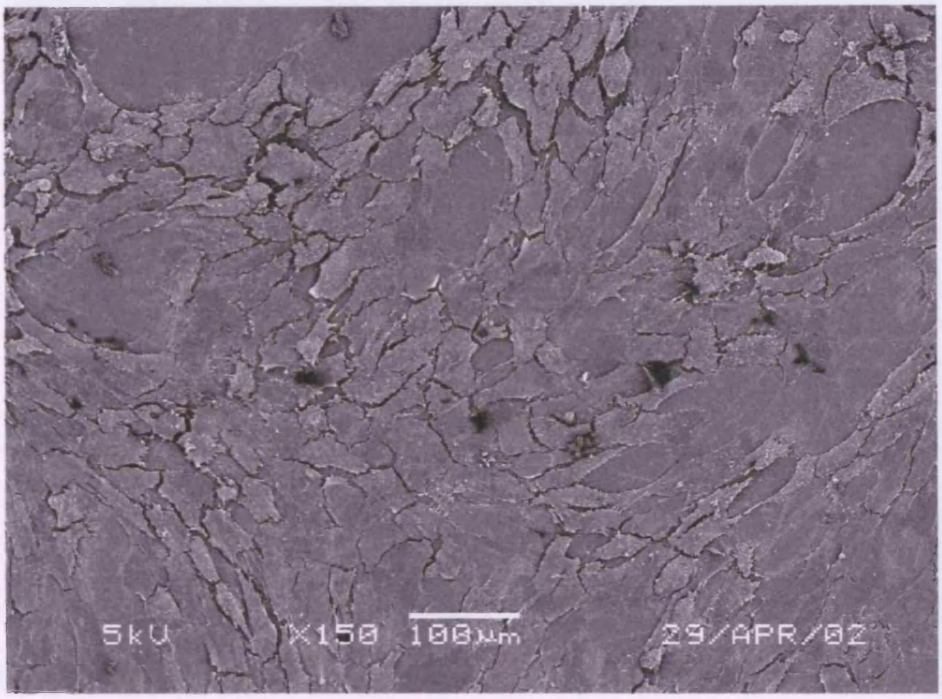

FIGURE 3.15a SEM image demonstrating the appearance of fibroblasts cultured for 48 hours on a SPTi substrate (x 150).

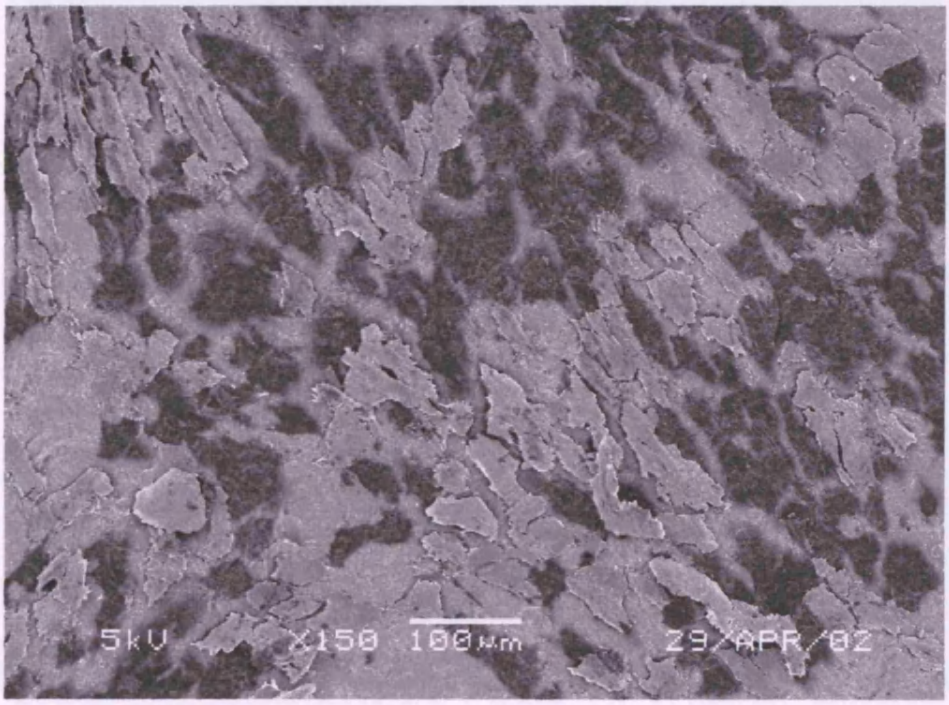

FIGURE 3.15b SEM image displaying the appearance of fibroblasts cultured on RSBTi for 48 hours (x 150).

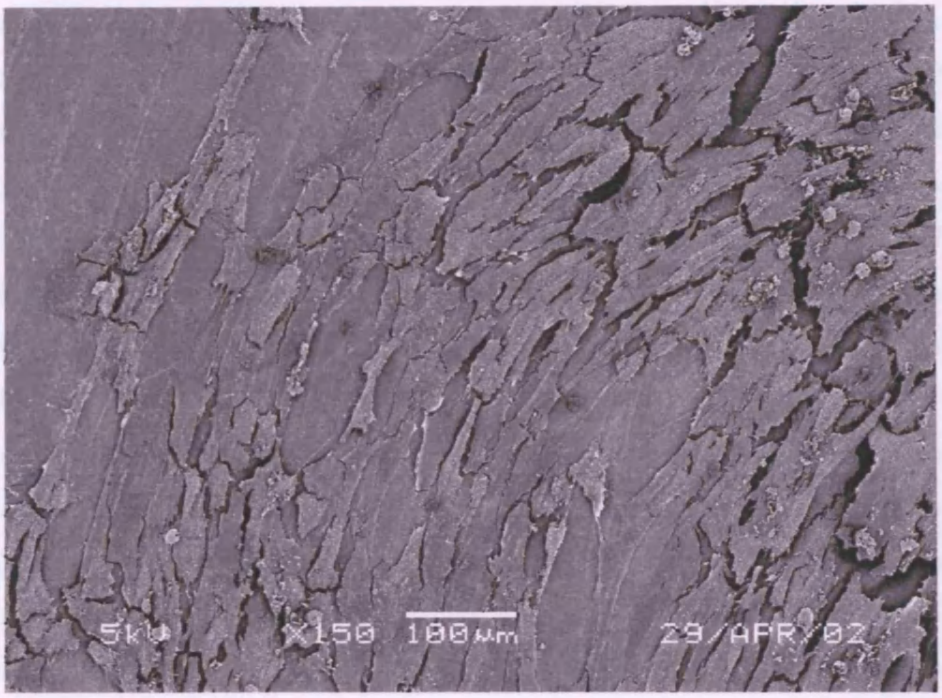

FIGURE 3.15c SEM image demonstrating the morphology of fibroblasts cultured on MFTi for 48 hours (x 150).

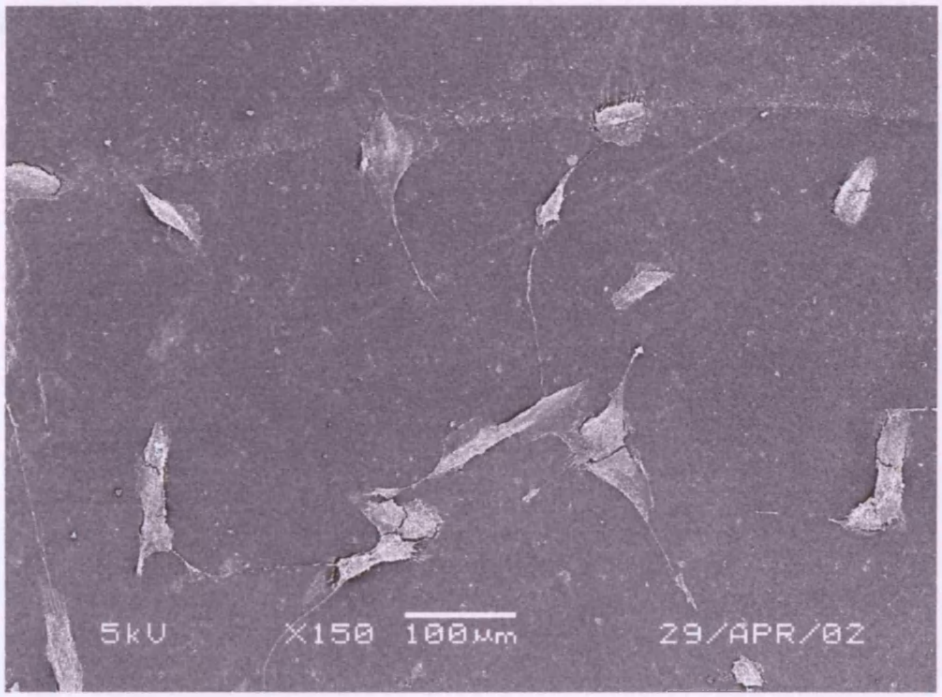

FIGURE 3.15d SEM image showing the appearance of fibroblasts cultured on a SPDLC substrate for 48 hours (x 150).

3.3.6.2.2 EPITHELIAL CELL CULTURE – 48 HOURS

Figures 3.16a-d demonstrate the appearance of epithelial cells cultured on the test substrates. Figure 3.16a shows the appearance of epithelial cells cultured on SPTi for 48 hours at a magnification of X150. The cells adopted a typical epithelial cell, cuboid morphology, clearly displaying the effects of contact inhibition – all cells were positioned immediately adjacent to the neighbouring cells on all sides. RSBTi supported an epithelial cell population (3.16b) of a much lower density than that observed on SPTi. The cells adopted a more rounded morphology and there was a considerable amount of cell debris observed across the substrate surface, indicating that a number of cells had undergone programmed cell death. Figure 3.16c demonstrates the appearance of epithelial cells cultured on MFTi for 48 hours. In contrast to fibroblasts cultured on MFTi for an equivalent time period (Figure 3.15c), the epithelial cells displayed contact inhibition overriding the effects of contact guidance, as no orientation to the grooved substratum is apparent. There was no visual difference in epithelial cell morphology between SPTi and MFTi. The epithelial cell population supported by the SPDLC substrate (Figure 3.16d) was of a markedly lower density than those sustained on any of the titanium surfaces tested. The cells displayed contact inhibition, whereby the cells adopting edge positions possessed increased numbers of projections and lamella podia, indicating migratatory behaviour as an attempt to establish continuity within the cell sheet.

FIGURE 3.16

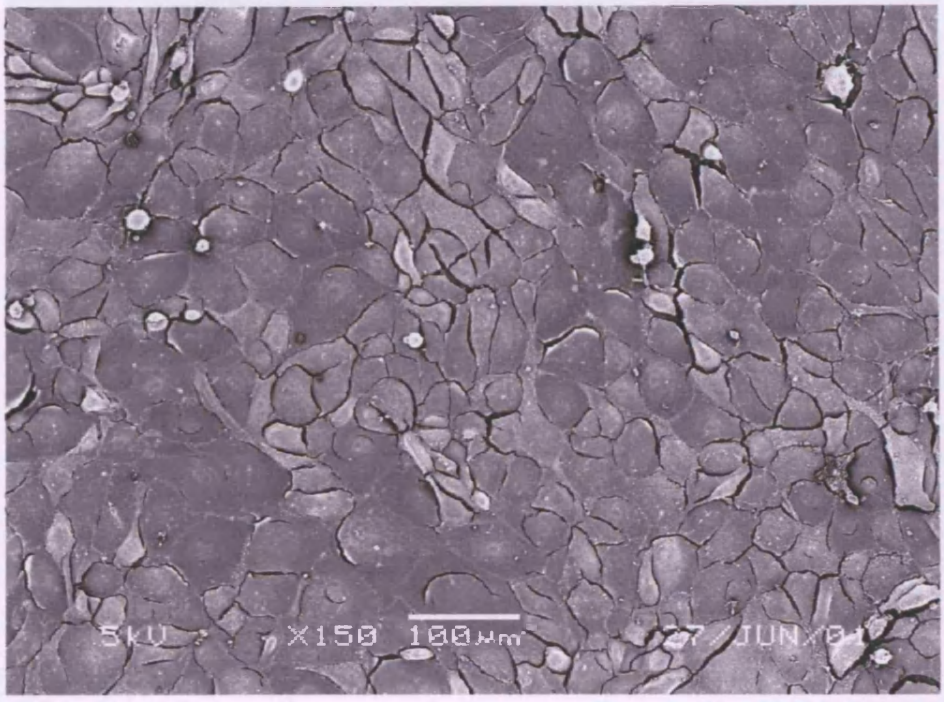

FIGURE 3.16a SEM image of epithelial cells cultured for 48 hours on SPTi (x150).

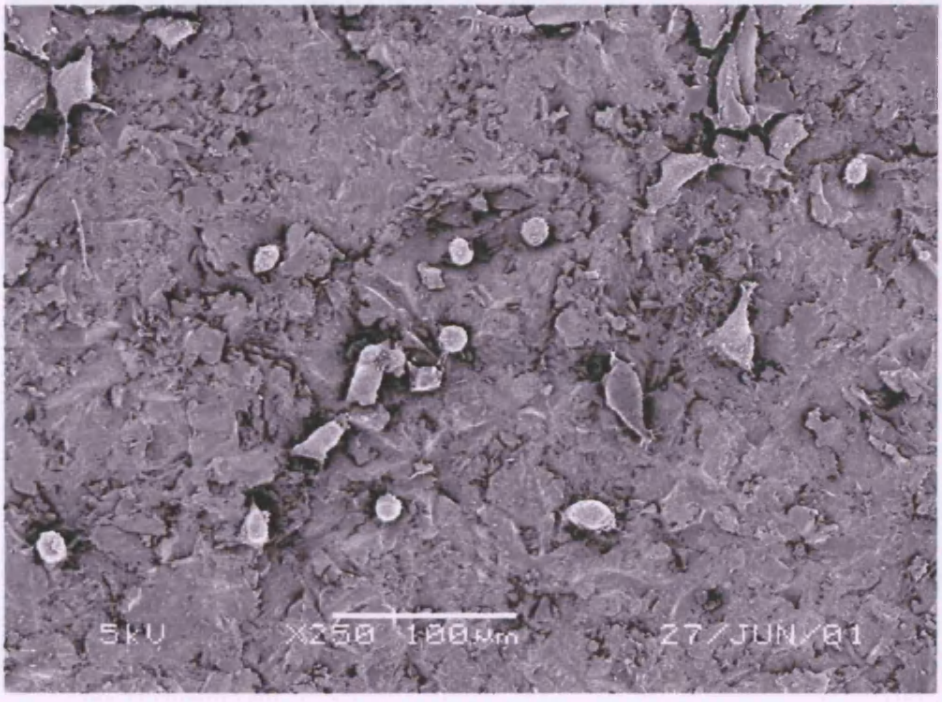

FIGURE 3.16b SEM image of epithelial cells cultured on RSBTi for 48 hours (x 250).

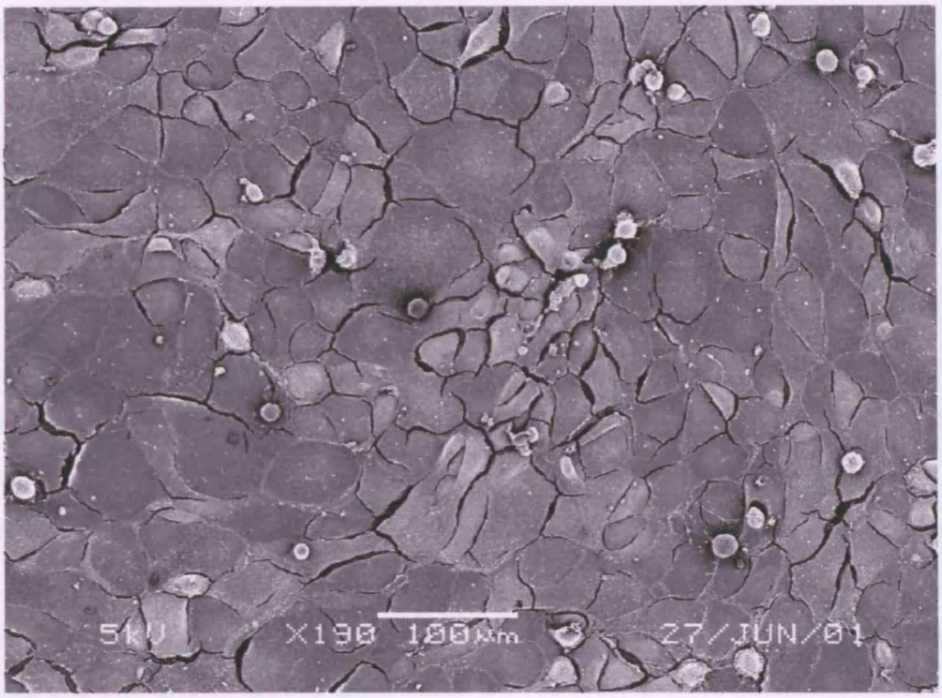

FIGURE 3.16c SEM image of an epithelial cell population supported by a MFTi substrate for 48 hours (x 190).

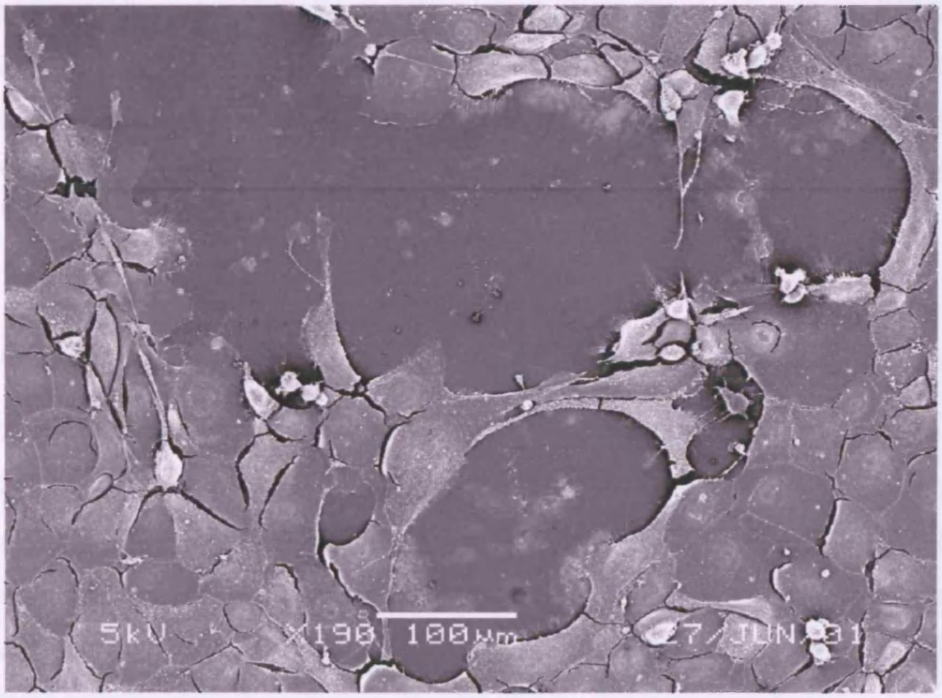

FIGURE 3.16d SEM image of epithelial cells cultured on SPDLC for 48 hours (x 190).

3.4 DISCUSSION

3.4.1 PROLIFERATION RATES – FIBROBLASTS 24/48 HOUR CULTURE

No significant differences were observed in proliferation rates of fibroblasts after 24 hours between titanium groups (smooth polished, rough shot blasted and machine finished). This finding is attributed to the short incubation duration because after 48 hours, significant differences were observed. This suggests that after 48 hours incubation, surface topography of titanium does affect proliferation rate of fibroblasts. Fibroblasts cultured on SPTi had significantly higher proliferation rates than those cultured on RSBTi and MFTi. In 1978, Folkman and Moscona demonstrated that cell morphology and shape have a regulatory effect on cell proliferation; well attached flattened cells have a higher proliferation rate than cells that are more rounded and loosely attached. These findings are observed to be true for this study where proliferation changes were observed, and further assays indicate an inverse correlation between surface roughness and cell attachment criteria.

Statistical analysis of SPTi and SPDLC materials showed no significant differences in surface roughness parameters. After 24 hours there was no significant difference in proliferation rates. However, after 48 hours the proliferation rate of fibroblasts on SPTi was significantly greater than the proliferation rate of those cultured on SPDLC. It is understood that the low surface energy of the DLC coating (40-50mN/m) and the lack of abundance of free electrons on its surface, should make it a substrate on which cells do not spread, attach and proliferate. This was found to be true after a 48 hour incubation period.

3.4.2 PROLIFERATION RATES – EPITHELIAL CELLS 24/48 HOUR CULTURE

After 24 hours incubation, no significant differences were observed in proliferation rate of epithelial cells cultured on any of the titanium materials tested. This implies that titanium topography does not influence epithelial cell proliferative capacity following a 24 hour incubation period. After 48 hours, a negative correlation between surface roughness and proliferation rate was observed within the titanium materials tested. Attachment criteria (cell spread and adhesion plaque density) were found to be influenced by surface roughness; hence these findings also complement those of Folkman and Moscona (1978) – implicating cell shape and attachment as controlling factors of proliferation rate.

In 1985, Jansen et al determined that properties of the substrate material are responsible for the nature and structure of epithelial cell – substratum contact sites. It was shown that attachment occurs on apatite and polystyrene materials, but not on metals (titanium or gold). The findings from this Chapter of my thesis have shown that epithelial cells proliferate, spread and attach to titanium *in vitro*. After 48 hours, epithelial cell proliferation was observed to be significantly higher on SPTi than on SPDLC. This finding must be attributed to the DLC coating, as the surface roughness values for these materials are not significantly different. In 1989 Jansen et al studied rat palatal epithelial cells cultured on various implant materials to determine the possible influence of surface free energy on cell growth rate. Their results demonstrated no significant relationship between the two parameters. The results of this study contradict these findings as it is clearly demonstrated that the DLC actively reduces epithelial cell proliferation.

3.4.3 CELL SURFACE AREA

No significant differences were observed between cell area data after 24 or 48 hours for fibroblasts or epithelial cells. These findings contradict those of Hormia et al 1991 who demonstrated that epithelial cells attach and spread more readily on smooth rather than rough sand blasted titanium. In this study, no significant change in epithelial cell spread was observed between any of the titanium groups at either time period tested.

Numerous reports provide explanations why increasing surface roughness should decrease cell surface area. The phenomenon may arise from the fact that cell spreading is an active process (Richards 1996, Brunette 1986). In 1996 Eisenbarth et al proposed that ridges and troughs form a physical barrier to the progression of migrating cells and this can be extrapolated to the migration of membranes in cell spreading. The results of this study show that fibroblast cell area is not influenced by the topography of the titanium groups tested. It is possible that the ridges and troughs of the sand blasted and machine finished substrata were not exaggerated enough to observe the results expected by Eisenbarth. It is postulated that the method employed to obtain cell area data is another factor influencing this study's findings. It should be noted that as the SEM observes cells from a plan view, it could only be used to record the cell area on the visible surface of the cells. A more accurate measure of cell spread would be a measure of the area of a cell's membrane that is in contact with a surface. On a smooth surface this area is clearly equivalent to the area measured by an SEM image. However, on a rough substratum the undulations may increase the surface area of the membrane contact underneath the cell

without increasing the area observed under a plan view. Unfortunately no assay could be carried out to measure the underside of the cells' membranes in contact with the biomaterials used.

3.4.4 NUMBER OF VINCULIN MARKERS PER UNIT CELL AREA

After 48 hours fibroblasts cultured on the three types of titanium finish tested showed a significant negative correlation between surface roughness and the number of adhesion plaques observed per cell. This finding opposes those of Richards (1996) who showed that surface finish had no effect on the measure of attachment for fibroblasts. However in 2000 Anselme et al demonstrated similar findings to those of this study using osteoblastic cells. The mean number of markers per cell cannot be taken as a measure of attachment alone, hence a ratio of mean number of markers : cell area was established. These results indicate that for fibroblasts cultured on titanium with three surface finishes, the extent of attachment decreases from SPTi to RSBTi to MFTi. It is thought that the cell membrane does not directly follow the undulations in surface topography of RSBTi and hence spaces are left between the cell membrane and the material surface. Close contacts are known to form in areas where the cell membrane is typically 10-15nm from the material surface (Burridge et al 1988). In areas where spaces exist between cell membranes and surface undulations, this distance may be greater than 10-15nm and thus they inhibit close contact formation, and hence decrease attachment. This theory holds for MFTi surfaces where the undulations in the surface exceed those observed on RSBTi in the grooved regions. It is accepted that cells align to grooves created on titanium surfaces, and the phenomenon is known as contact guidance (Chehroudi et al 1990). With contact guidance, if the cell membrane on the underside of the cell cannot follow the grooves in the substratum, large gaps exist between the two making adhesion plaque formation impossible and thus the cell is less well attached. This phenomenon is demonstrated by the graph presented in the Cell Attachment (48 Hour Fibroblasts) section of the results. A separate graph for cell attachment of fibroblasts is presented for SPTi and SPDLC. It is clear that DLC cannot be compared to all of the titanium groups, as both material type and surface topography are variables. It can however be evaluated against SPTi because the surface roughness values for these two materials are not significantly different, hence the only variation is chemical composition of the surface material. The graph demonstrates that fibroblasts cultured on SPDLC are less well attached than those on SPTi. The result was expected and is thought to be accreditable to the physical properties of the DLC coating. DLC has a very low surface energy and relatively few free electrons on its surface (www.bekart.com/dymonics/coatings/eng/E-deklagen.htm). Surface

energy, in the form of wetability, has been correlated to the strength of fibroblast attachment to metals and organic material types (Baier 1970). However, this relationship is seen to be a far more complex interaction between the substrate material, proteins and enzymes in the medium and ECM and the cell type used (Brunette 1986). Having taken these factors into consideration it is concluded that DLC coating is detrimental to fibroblast attachment due to its surface properties and chemical constitution.

Epithelial cell attachment results indicate a marked decrease in number of markers per unit cell area between SPTi and RSBTi and between SPTi and MFTi. Observation of SEM images demonstrate that, unlike fibroblasts, epithelial cells do not display contact guidance when cultured on MFTi surfaces. Moreover it appears that contact inhibition overrides the effect of contact guidance. This is determined from the fact that epithelial cells form a uniform layer with no alignment to the grooved substratum as observed with fibroblasts. Hence the majority of the epithelial cells are spread over smooth areas of the MFTi surfaces and not over the grooves like fibroblasts. Thus more epithelial cells have a greater proportion of their underlying membrane in contact with the substratum, hence covering areas that are well suited to adhesion plaque formation. Fibroblasts alignment to the grooves makes plaque formation impossible unless the membrane directly follows the surface undulations. This compliance with surface undulations is not observed, as a marked decrease was observed between RSBTi and MFTi indicating that gaps exist between the cell membrane and the material surface which are too to great for adhesion plaque formation to occur. This phenomenon can be explained using attachment ratios. The attachment ratios for epithelial cells and fibroblasts cultured for 48 hours on MFTi are 0.046 and 0.014 respectively. It is clear that the value for epithelial cells exceeds that for fibroblasts three fold. Thus, from these findings it is concluded that contact inhibition displayed by epithelial cells results in increased attachment to a MFTi substrate, in contrast to the actions of fibroblasts on an identical substrate and equivalent time period. In 1991, Hormia et al observed the attachment of gingival epithelial cells to different titanium surfaces and concluded that epithelial cells attach and spread more readily on smooth rather than rough finished titanium surfaces. These findings are complementary to those of this study. However, they also concluded that no vinculin containing focal adhesions were detected, suggesting that the cells attach by means of close contacts, ECM contacts and hemidesmosomes. This opposes the findings of this study, where vinculin containing focal adhesions were clearly labelled with indirect immunofluorescent techniques. Hormia concluded that smooth and finely grooved titanium surfaces could be

optimal in maintaining attachment of gingival epithelial cells and this is mirrored by my finding using epithelial cells derived from human skin.

The SPTi and DLC attachment data for epithelial cells mimicked that of fibroblasts and can also be contributed to the surface properties and chemical composition of DLC.

3.4.5 CELL MORPHOLOGY AND DESCRIPTIVE ANALYSIS

The SEM images show that fibroblasts adopt a typical morphology when cultured on SPTi and proliferate, spread and attach after an incubation period of 48 hours. The cells are seen to be migrating across the surface and cell-cell interaction is abundant. On RSBTi, the lack of cell processing and lamella podia suggests less cell-cell interaction and locomotion respectively. From qualitative data it is observed that cells proliferate on RSBTi. However a decrease in cell area and attachment compared to SPTi is observed.

Fibroblasts cultured on MFTi for 48 hours clearly exhibit contact guidance (Figure 3.15c). Figure 2.16c demonstrates the appearance of epithelial cells cultured on MFTi for the same duration and shows contact inhibition overriding contact guidance. This conclusion is presented because of the lack of epithelial cell alignment to the grooved substratum, whilst contact guidance is so clearly demonstrated by the fibroblast population.

Fibroblasts and epithelial cells cultured on DLC – Figures 3.15d and 3.16d respectively, have lower proliferation rates than those cultured on the other material types tested. All discs were seeded at the same initial rate, hence it is concluded that the DLC surface is not supporting growth and maintenance of either cell type population.

Epithelial cells form a complete monolayer on SPTi in which cells are seen to adopt typical epithelial cell morphology. This complements the findings of Hormia et al (1991). However RSBTi appears to be detrimental to epithelial cell populations. All cells observed on RSBTi appeared round in morphology and the overall cell density was far less than that observed on SPTi and DLC. This shows that epithelial cells are more sensitive to increasing surface roughness than fibroblasts. These findings contradict the proliferation results, which indicate no significant differences in proliferation rates between any of the material types. Conflict also exists between these findings and well-accepted theories of cell shape and attachment being strong influencing factors on the proliferative capacity of cells. It is thus concluded that the Alamar blue results are not

representative of the study as a whole and that a low sample number could be responsible for the lack of significant differences.

3.4.6 GENERAL CONCLUSIONS

It is concluded that smooth polished titanium is the optimal surface to support the growth and attachment of fibroblasts and epithelial cells *in vitro*. The findings of my study have demonstrated that the proliferative, morphological and attachment properties of fibroblasts and epithelial cells are greatly influenced by the surface topography of their titanium substrate. It has been clearly demonstrated that the effects of contact inhibition outweigh the phenomenon of contact guidance for epithelial cells and as such, a grooved substrate for the purpose of encouraging alignment and attachment of epithelial cells in ITAP is counterproductive. From the results of this chapter, it is conceivable that an innate property of a cell population can overcome the effects of substrate topography, with the emphasis being placed on contact inhibition and surface roughness respectively. My study has also shown that DLC is detrimental to the maintenance of fibroblastic and epithelial cell populations.

Based on the findings from this chapter, it is proposed that *in vivo*, grooved titanium alloy abutments for epithelial layer attachment will not reduce epithelial migration compared with smooth polished implants. However, they may direct attachment of dermal fibroblastic tissue layer attachment. It is postulated that epithelial cell attachment and migration may be prevented by DLC coating the external sections of ITAP implants. Implants with rough sand blasted, as apposed to a grooved topography, could enhance epithelial cell attachment *in vivo*, whereas a smooth topography could enhance attachment of tissues in which the predominant cell type is fibroblastic.

Hydroxyapatite has been shown to enhance attachment of soft tissues and their constituent cell types *in vivo* and *in vitro* (Butts et al 1989, Hardy et al 1991, Lindholm and Lindholm 1993). The main limitation of this chapter is that I was unable to examine the attachment of fibroblasts and epithelial cells to hydroxyapatite coated discs using immunolocalisation of vinculin. This is due to the fact that the coating absorbed the fluorescent dye, making it impossible to differentiate the cells from the disc surface. Preliminary work showed that fibroblasts cultured on hydroxyapatite coated discs, using the methods outlined in this chapter, have significantly greater proliferative capacity ($p<0.05$) compared to those cultured on titanium alloy discs with any of the surface topographies used in this chapter. Based on these observations it is postulated that

hydroxyapatite could enhance soft tissue attachment in both subcutaneous and percutaneous implants, and has been tested *in vivo* in Chapters five and six of my thesis.

It should be noted that the findings of this Chapter are limited to work *in vitro* and that *in vivo* analysis is required to test them in an environment where numerous other influencing factors present themselves to the relationship between cells and implant materials.

It is concluded that to achieve soft tissue attachment *in vivo*, the material properties of the implant should be tailored to the requirements of the predominant cell type within that specific tissue. Some of the findings from this Chapter have been tested *in vivo*, in Chapters five and six of my thesis.

CHAPTER FOUR

EFFECTS OF LAMININ AND FIBRONECTIN ON FIBROBLAST AND EPITHELIAL CELL ATTACHMENT, PROLIFERATION AND MORPHOLOGY

CHAPTER FOUR: EFFECTS OF LAMININ AND FIBRONECTIN ON FIBROBLAST AND EPITHELIAL CELL ATTACHMENT, PROLIFERATION AND MORPHOLOGY

4.1 INTRODUCTION AND HYPOTHESES

Intraosseous transcutaneous amputation prostheses (ITAP) are being developed in an attempt to solve the current problems associated with stump-socket design. It is essential that the final implant design maintains a strong and lasting integration within the internal and external environments that it will be subjected to on a daily basis. This criterion involves the stable integration of the implant into bone and a tight soft tissue attachment around the implant to form a biological seal. In past studies, emphasis has been placed on improving osseointegration (dental and maxillofacial), with little attention paid to soft tissue attachment. The formation and maintenance of a soft tissue biological seal is vital to protect the supporting bone from bacteria present in the external environment which could initiate an inflammatory response and thus threaten the integrity and long-term success of ITAP.

The first line of defence in the ITAP biological seal is attachment of the skin's epithelium to the body of the implant. In teeth, a natural example of epithelium-hard surface is presented. The interface consists of an epithelial attachment lamina interposed between the tooth enamel and the abutting junctional epithelial cells, as described in section 1.2.1.2 and Figure 1.2 in Chapter One of my thesis. Epithelial cells have also been shown to assemble hemidesmosomes on titanium and dental implants *in vivo* and *In Vitro* (James and Schultz 1974, Gould et al 1981, Karagianes et al 1982, Gould et al 1984, McKinney et al 1985).

It is thought that the use of a biological coating to enhance epithelial attachment may encourage the formation of a biological seal around the implant. Laminin-5 has been used previously, as it plays a crucial role in the assembly and maintenance of hemidesmosomes within the basement membrane. In 1997, Tamura et al reported the use of soluble laminin-5 as a coating for titanium alloy to promote the attachment of gingival epithelial cells (1HGK). It was shown that 1HGK cells formed hemidesmosomes within 24 hours of attachment to laminin-5 coated titanium alloy, but not to titanium alone. Thus it was concluded that soluble laminin-5 might be beneficial as a dental implant coating to promote a biological seal between epithelium and implant materials.

In 1985, Jansen et al cultured guinea pig epithelial cells on gold, titanium, carbon, hydroxyapatite, carbonate apatite and modified polystyrene substrates. They demonstrated that as attachment structures, focal contacts and hemidesmosome-like contacts could be distinguished. However, hemidesmosome-like contacts were observed only on polystyrene and apatite surfaces. It was concluded that a property of the substrata used to culture epithelial cells, determined the nature and structure of the contact sites.

In dentistry, hemidesmosomes are thought to play a mediating role in epithelial attachment. Since 1977 evidence suggests that titanium implants in jaws of edentulous (without teeth) patients have high long-term success rates (Branemark et al 1977, Adell et al 1981, Zarb and Symington 1983).

A principle factor in dental implant success is the attachment of oral epithelium to the implant in the same way that the epithelial cell attachment is applied to a tooth surface i.e.: sealing off the oral environment from the bone and surrounding tissues.

In 1984, Gould et al showed that after four weeks implantation, sections of titanium coated epon, placed into the gingival sulus-bone of a forty year old man, had numerous layers of epithelial cells formed against the titanium surface and demonstrated characteristic interdigitation of cell membranes and intercellular desmosomal attachment. At the titanium-epithelial interface there were also hemidesmosomes present and the appearance of basal lamina.

In 1976, Cohen stated that "Nowhere else in the body does so complex a relationship exist between soft and mineralised tissue, nowhere else is connective tissue separated from hostile environment by so tenuous an epithelial integument and in no other part of the skeleton is cancellous bone so ineffectively shielded from extraneous contamination". It is clearly important to strive to develop a firm epithelial-implant attachment so that the seal created separates the delicate endosseous from the bacteria-rife oral environments. The principle concern is the lack of ability to characterise the interface *in vivo*. Reports have implicated other parameters affecting fibroblast adhesion to biomaterials *In Vitro*, for example, the sterilisation process (Michaels et al 1991).

Biocompatibility and bio adhesiveness at an implant-soft tissue interface are essential in establishing the success of dental, auricular and amputation prostheses. Numerous investigations have concentrated efforts on the osseointegration of bone tissue adhesion to dental implants. However, limited studies have investigated the soft tissue-implant junction in detail. Owing to the fact that the biological junction is considered a predominant factor in the success of any transcutaneous implant, it is the soft tissue seal that will be examined here.

The soft tissue layers abutting a transcutaneous implant are presented in Chapter One of my thesis.

The biology and biochemistry of laminin has been extensively studied and it is thought that it may play a functional role in assisting epithelial cell adherence within the basal lamina (Tryggvason 1993, Martin 1987, Liotta et al 1985). Laminin is an important structural and regulatory molecule and has been shown to have diverse effects on cultured cells, influencing growth, survival, morphology, differentiation and motility (Kleinman et al 1985, Baker et al 1996, Gonzales et al 1999, Salo et al 1999). The effect of laminin on cells *In Vitro* is type dependent. In 1985, Hadley et al demonstrated that laminin affects sertoli cells by altering their morphology and in 1982, Baron Von Evercooren et al showed that neural cells produce axon-like processes in response to laminin. Laminin has also been shown to enhance gingival epithelial cell adhesion *in vivo* (El-Ghannam et al 1998). The molecular basis of the interaction between cells and laminin has been partially defined, including locating a major cellular receptor for laminin (Von der Mark et al 1984, Von de Mark and Kuhl 1985, Liotta et al 1985) and determining a major cell-attachment sequence on the laminin molecule (Graf et al 1987). Laminin resides in basement membranes (BM's) in combination with entactin, collagen IV and heparin sulphate proteoglycan, each of which may also possess cell binding capacities and/or modulate the cell binding activities of laminin. Hence it is conceivable that multiple interactions occur between cells and BM's. By isolating laminin and using it *in vitro* with single cell type populations, it is possible to investigate its effects without interactions with other BM components. This could be beneficial to ITAP. If laminin possesses properties that influence epithelial cell adhesion, proliferation and morphology, it could be used to enhance the epithelial layer – ITAP implant interface.

Fibronectin is an adhesive protein that helps cells adhere to the extracellular matrix (ECM) (Hynes 1986, Ruoslahti and Pierschbacher 1987). The ECM contains a number of non-collagenous adhesive proteins that have multiple domains, each with a specific binding site for other matrix macromolecules and for cell surface receptors. These proteins contribute to the organisation and cell adhesive properties of the ECM. One such protein is fibronectin (fn), which is a large glycoprotein found in all vertebrates. The biology and biochemistry of fibronectin is well understood, and its cell binding domain, the Arg-Gly-Asp or RGD sequence, has been identified (Hormia 1994, Zlatopolsky et al 1992, Culp et al 1979). The cell binding abilities of fibronectin *in vitro* and *in vivo* suggest that it could have a positive effect at the soft-tissue – ITAP interface (MacDonald et al 1998, Nuttleman et al 2001, Singer et al 1989, Dean et al 1995, Degasne et al 1999). If the RGD sequence of fibronectin can bind fibroblasts in the sub-epithelial soft tissue layers abutting transcutaneous implants, the interface could be stabilised and epithelial

layer migration could be retarded. Fibronectin's characteristic enhancement of blood clotting and wound healing may also prevent bacterial invasion of ITAP sites exposed to the external environment.

Cell adhesion to the ECM is essential in development, wound healing and tissue remodelling. In addition to anchoring cells to provide structural integrity, cell adhesion triggers signals that regulate survival, cell cycle progression and differentiation. Many pathological conditions, including blood clotting defects and tumour metastasis, involve abnormal adhesion processes. Cell attachment considerations are critical to biomedical and biotechnological applications, for example, biomaterials, tissue engineering and *in vitro* culture systems. In this study the understanding of cell attachment and the proteins laminin and FN, will be used in an attempt to enhance ITAP-soft tissue adhesion *in vitro*.

It is postulated that fibronectin and laminin will influence adhesion, proliferation and morphology of fibroblasts and epithelial cells cultured on biomaterials *In Vitro*. It is thought that fibronectin will increase the adhesion and proliferation of dermal fibroblasts cultured on biomaterials *In Vitro*, and that laminin will increase the adhesion and proliferation of dermal epithelial cells cultured on biomaterials *In Vitro*. It is also hypothesised that material topography will have a lesser effect on cellular behaviour compared to adhesion protein coating effects.

This Chapter examines the *in vitro* affects of fibronectin and laminin on fibroblast and epithelial cell attachment, proliferation and morphology, in association with the biomaterials used for the development soft tissue-implant interfaces. **It is hypothesised that fibronectin and laminin will increase fibroblast and epithelial cell attachment and proliferation respectively.**

4.2 MATERIALS AND METHODS

4.2.1 MATERIAL PREPARATION

The materials used for this study were smooth polished titanium (SPTi), rough sand blasted titanium (RSBTi) and diamond-like carbon coated smooth polished titanium (DLC). The titanium surfaces were prepared as stated in Chapter Two of my thesis. The DLC coating was applied at Diavac ACM^{LTD} at Brunel University. It was applied at a thickness of approximately 1-3 microns. DLC is a low surface energy coating, and was used in an attempt to deter cell adhesion.

4.2.2 CELL CULTURE TECHNIQUES

4.2.2.1 MATERIAL SET-UP

The following plates were set up for each cell line used:

PLATE 1: SEM Controls:

SPTi con	RSB con	DLC con
SPTi con	RSB con	DLC con

PLATE 2: Laminin Group SEM:

SPTi LN	RSBTi LN	DLC LN
SPTi LN	RSBTi LN	DLC LN

PLATE 3: Fibronectin Group SEM:

SPTi FN	RSBTi FN	DLC FN
SPTi FN	RSBTi FN	DLC FN

PLATE 4: FM Controls:

SPTi con	RSB con	DLC con
SPTi con	RSB con	DLC con
SPTi con	RSB con	DLC con

PLATE 5: Laminin Group FM:

SPTi LN	RSB LN	DLC LN
SPTi LN	RSB LN	DLC LN
SPTi LN	RSB LN	DLC LN

PLATE 6: Fibronectin Group FM:

SPTi FN	RSB FN	DLC FN
SPTi FN	RSB FN	DLC FN
SPTi FN	RSB FN	DLC FN

4.2.2.2 ADHESION PROTEINS AND PROTEIN ANALYSIS

Laminin (Human Placenta)(Sigma L6274) and Fibronectin (Human Plasma)(Sigma F2006) were applied to the surfaces of the test substrates at a rate of 10μg per disc.

To determine the amount of protein remaining on the discs after a series of incubation periods, a Bicinchoninic Acid Assay (Sigma BCA-1) was used. The assay determined the quantities of protein in the solution used to wash the discs, by reducing copper (II) to copper (I) in a concentration dependent manner. Bicinchoninic acid formed a complex with copper (I) resulting in a colour change, which was quantified using a BIO-RAD Micro-plate Manager 2.1 spectrophotometer. The readings were taken at a reference wavelength of 540nm. A calibration curve was established using a protein standard – bovine serum albumin (BSA). Concentrations of BSA from 0.5 to 10 μg/ml in sterile phosphate buffered saline (PBS) were added to 1ml of the protein determining reagent (one part copper II sulphate pentahydrate 4% solution to fifty parts bicinchoninic acid) and vortexed. The solutions were incubated for 30mins at room temperature, after which the absorbance of each solution was determined using the microplate reader.

The discs were spotted with 10μg of laminin or fibronectin dissolved in 5μl of sterile PBS, and placed to dry for durations of 30, 60, 90 and 120mins at 37°C, 5% CO_2.

The discs were then washed with 1ml of sterile PBS and the amount of protein in the wash solution was determined using the Bicinchoninic acid assay. The amount of protein remaining on each disc was calculated by subtracting the amount of protein in the wash, from the application amount of 10μg.

4.2.2.3 CELL LINES AND SEEDING TECHNIQUES

The cells used were obtained from the ECACC. The fibroblast line is a human skin fibroblast line derived from a biopsy of a radiosensitive female (84Br). The epithelial cell line was established by immortalisation of normal adult prostatic epithelial cells by transfection with a plasmid containing SV40 genome with a defective replication origin. The primary culture was obtained from a prostate of a 33-year-old male at post mortem.

The cells contain the SV40 genome and express large T protein and they possess a well-differentiated morphology (PNT-2). The cell lines were chosen as a representation of the cells abutting the materials chosen for implantation in ITAP. The fibroblasts are representative of the cell type found in the dermal layer of the skin, whilst the epithelial cells are typical of the epithelial layer.

The medium requirements for these cell lines are displayed in Chapter Three of my thesis.

The discs were incubated with the adhesion proteins for an optimal period and cells were then seeded onto all of the surfaces under test, at a rate of 30,000 cells per disc in 8µl medium. The cell spots were incubated for 1 hour to allow cell adhesion and the wells were then flooded with complete culture medium. The discs were incubated at 37°C, 5% CO_2 for 48 hours.

4.2.2.4 DETERMINATION OF PROLIFERATION RATES – ALAMAR BLUE

Alamar Blue is a redox indicator, which responds to oxidation and reduction of the surrounding medium. It changes colour in response to chemical reduction of culture medium, which results from cell growth and division.

Medium was made up using phenol red (PR) free medium. Alamar Blue was diluted 1:10 with PR free medium and added to the wells under test (1ml per well/disc). The discs were incubated for 3-4 hours at 37°C, 5% CO_2. Two 100µl aliquots were removed from each well and transferred to a 96 well plate. Absorbance was read at 570nm with a reference wavelength of 630nm on a Dynatech Plate Reader. Alamar Blue was washed from the discs with sterile PBS, and fresh medium was added.

4.2.2.5 INDIRECT IMMUNOFLUORESCENCE

The medium was removed from the wells containing discs to be processed for fluorescence microscopy (FM). Two, ten minute PBS washes were carried out prior to fixing the cells in 10% formal saline for 5 minutes. Four, 5 minute PBS washed were applied. The primary antibody – monoclonal anti-human clone HUV-1 (Sigma V9131 Anti-vinculin) was applied 0.2ml in 40ml PBS + 0.05ml Triton X-100 for 2 hours at room temperature. Three, 10 minute PBS washes preceded the secondary antibody stage – FITC (Fluoroscein isothiocyanate conjugate - Sigma F2883) 1 in 100 in PBS at room temperature for 1 hour. The discs were given three final PBS washes prior to examination under FM. Ten cells on each substrate type were randomly selected and the number of vinculin markers was determined.

4.2.2.6 CELL MORPHOLOGY - SCANNING ELECTRON MICROSCOPY

The discs to be processed for SEM were covered with fresh medium and placed in the fridge at 4°C for 20 minutes, after which the medium was removed and the cells on the discs were fixed using a solution of 1.5% glutaldehyde in 0.1M sodium cacocylate. After two hours this solution was replaced with 0.1M sodium cacocylate (stock buffer) and the plates were left at 4°C overnight. The buffer was removed and replaced with 1% osmium tetroxide in 0.1M stock buffer for 1 hour. Two 5 minute buffer washes were applied and a filtered solution of 1% tannic acid in 0.05M stock buffer was applied for a further hour. The discs were subjected to four 5 minute buffer washes prior to dehydration in an ascending alcohol series (2 x 5 minute in 20-70% ethyl alcohol). After the 70% alcohol wash, a solution of 0.5% uranyl acetate in 70% ethanol was applied and left for 30 minutes. This solution was removed, and the dehydration was continued (90, 96 and 100% @ 2 x 5 minute). The discs were air dried in HMDS and mounted. A small amount of conductive paint was applied between the mounting block and the discs. The discs were then sputter coated with a layer of gold and examined in a JEOL 35C scanning electron microscope. SEM images were taken and analysed with a Zeiss KS300 image analysis package to determine the average cell area of cells cultured on each of the test substrates.

4.2.3 STATISTICAL ANALYSIS

The degree of normality of all the data was determined using Kolmogorov-Smirnov tests and none of the data was observed to be normally distributed. Kruskal-Wallis H and Mann Whitney U tests were used to determine the significance of the findings. Mann Whitney U tests are significance tests for comparing two independent samples and can be used to determine whether a variable measured in each of the two samples can be assumed to be from the same underlying population. For multiple comparative analysis the p value obtained from Mann Whitney U tests can be reduced to avoid the Type I Error. However, for numerous comparisons this is impractical and an alternative analysis is the Kruskal-Wallis H test. For data to be analysed using this test, the samples must be taken randomly and independently from one another. The populations have to be approximately the same shapes (according to the box plots obtained) and the sample sizes have to be at least five. The Kruskal-Wallis H test is an extension of the Mann Whitney U test for multiple samples and is a nonparametric alternative to one-way analysis of variance. It tests the null hypothesis that samples do not differ in mean rank for the

criterion variable. Kruskal-Wallis H is calculated on the basis of sums of ranks for combined data. If the p value obtained from the Kruskal-Wallis H test is less than or equal to 0.05, then at the 0.05 level of significance it can be stated that enough evidence exists to conclude that there is a significant difference among the groups based on the test scores. The Kruskal-Wallis test cannot tell which of several groups stands out, but can show a significant variation across groups, after which a Mann Whitney U test can be used pair-wise.

4.3 RESULTS

4.3.1 ADHESION PROTEIN ANALYSIS – BICINCHONINIC ACID ASSAY

4.3.1.1 PROTEIN STANDARD CALIBRATION CURVE

Increasing amounts of protein standard BSA were added to 1ml of the protein reagent consisting of one part copper (II) pentahydrate solution (4%) in fifty parts bicinchoninic acid, and the absorbance of the resulting solutions was determined. The findings are presented in Figure 4.1 and demonstrate that increasing amounts of protein added to the assay reagents results in an increase in the absorbance observed. The curve was used to calculate the amounts of laminin and fibronectin remaining on the test substrates after different incubation periods.

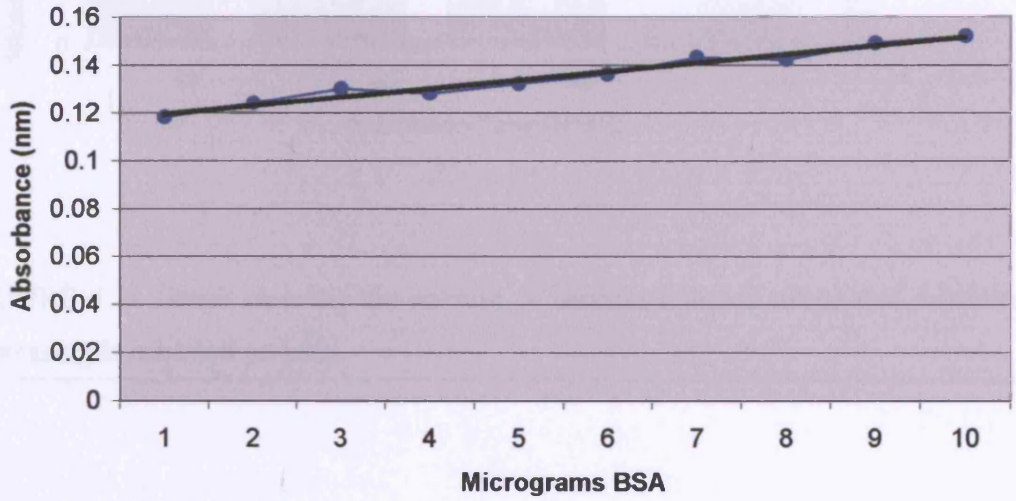

FIGURE 4.1 Graph showing absorbance values obtained using an increasing BSA protein standard solution and bicinchoninic acid assay.

4.3.1.2 DISC PROTEIN ANALYSIS

The bicinchoninic acid assay and calibration curve in Figure 4.1 was used to determine the amount of laminin and fibronectin in washes from the discs coated and incubated for increasing time periods. From this data the amount of laminin and fibronectin remaining on the discs after each incubation time was established and the data is presented in Figure 4.2. No significant differences were found between the amounts of laminin or fibronectin on any of the test substrates after 120 minutes (all p values <0.01). It was observed that with an incubation period of 120 minutes and an initial spotting concentration of 10μg, an average of 8.93μg of laminin and 8.87μg of fibronectin remain on all of the test substrates.

FIGURE 4.2

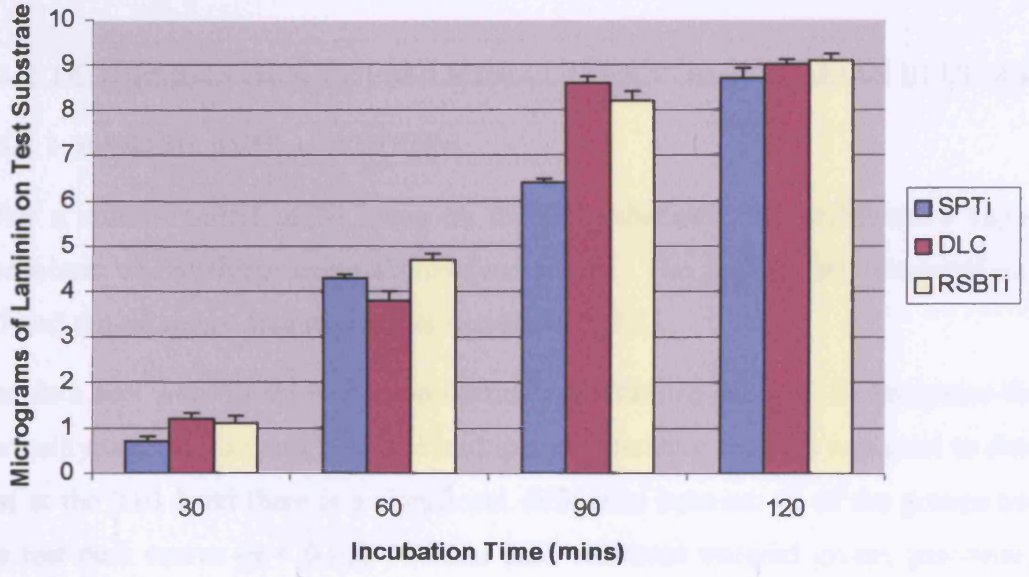

FIGURE 4.2a Graph showing the amount of laminin adhered to the test substrates after increasing incubation periods.

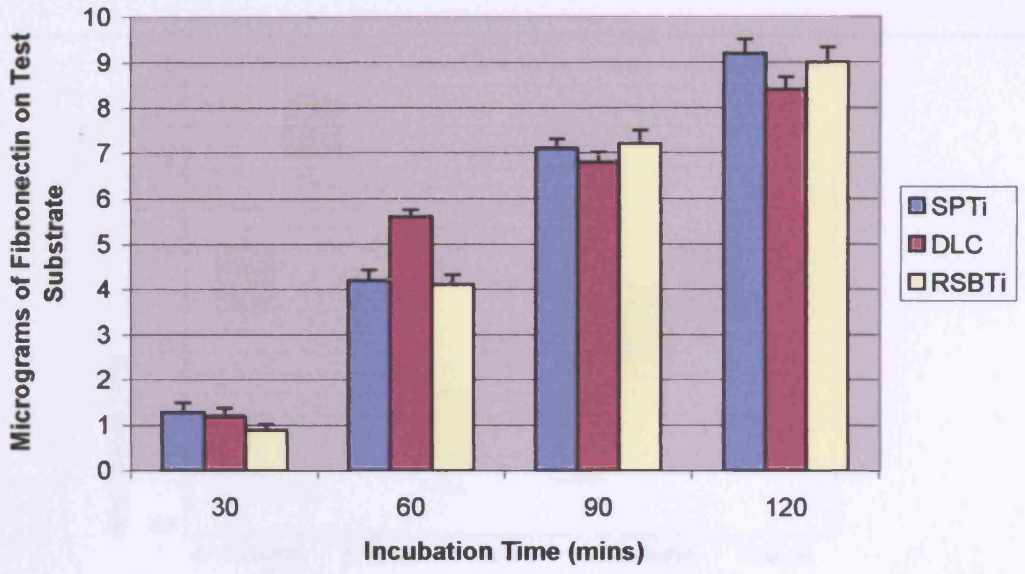

FIGURE 4.2b Graph showing the amount of fibronectin adhered to the test substrates after increasing incubation periods.

4.3.2 DETERMINATION OF PROLIFERATION RATES – ALAMAR BLUE ASSAY

4.3.2.1 FIBROBLASTS – 24 HOURS

After a culture peirod of 24 hours on the test substrates, the proliferative capacity of fibroblasts was analysed using alamar blue assays. The findings are presented in Figure 4.3 and the summary data is given in Appendix 3 (3.1).

The data sets were found to be non-normally distributed using a Kolmogorov-Smirnov normality test. A Kruskal-Wallis H multiple comparative analysis was used to determine that at the 0.01 level there is a significant difference between all of the groups based on the test rank scores ($p < 0.01$). Within each substrate material group, pair-wise Mann Whitney U tests determined a significantly higher proliferative capacity of fibroblasts cultured on fibronectin coated materials than on control or laminin coated substrates (all p values < 0.02).

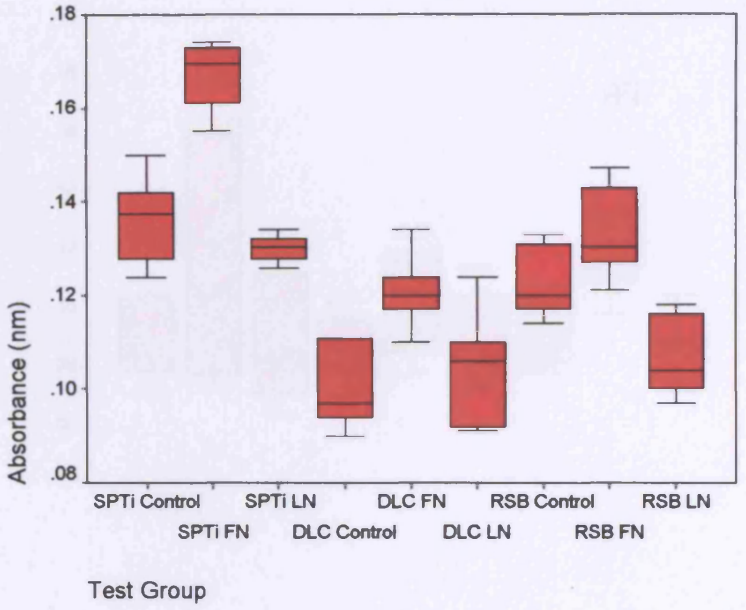

FIGURE 4.3 Box plot of data for fibroblast proliferation analysis after 24 hours on the test substrates.

4.3.2.2 FIBROBLASTS – 48 HOUR

After a culture peirod of 48 hours on the test substrates, the proliferative capacity of fibroblasts was analysed. The findings are presented in Figure 4.4 and the summary data is displayed in Appendix 3 (3.2).

The data sets were found to be non-normally distributed using a Kolmogorov-Smirnov normality test and a Kruskal-Wallis H multiple comparative analysis was used to determine that at the 0.02 level there is a significant difference between all of the groups based on the test rank scores ($p < 0.02$). Pair-wise Mann Whitney U tests determined a significantly higher proliferative capacity of fibroblasts cultured on fibronectin coated RBSTi than on control or laminin coated RSBTi (all p values < 0.01). Fibronectin coated RSBTi was also shown to support fibroblasts with significantly higher proliferative capacities than SPTi, SPTi LN, DLC and DLC LN substrates (all p values < 0.02). There were no significant differences observed between fibronectin coated SPTi, RSBTi or DLC, indicating that fibronectin overrides the material topography effect on fibroblast proliferation.

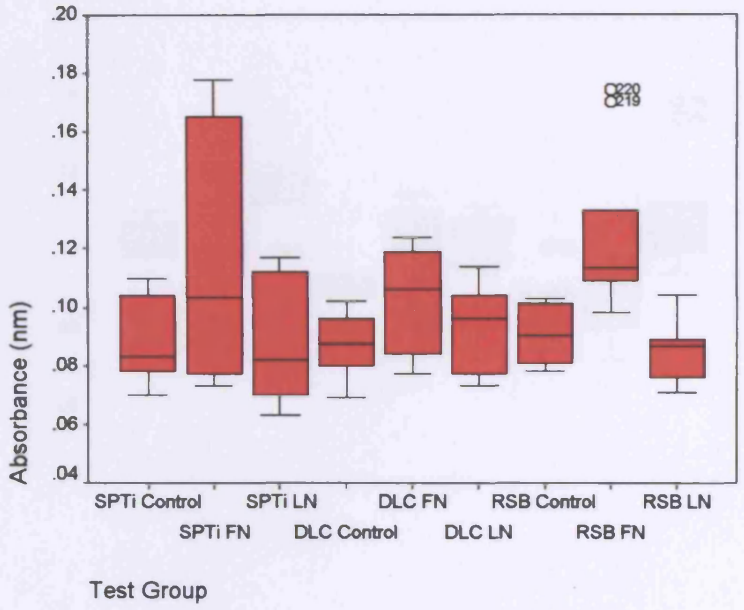

FIGURE 4.4 Box plot of data for fibroblast proliferation analysis after 48 hours on the test substrates.

4.3.2.3 EPITHELIAL CELLS – 24 HOUR

After a culture peirod of 24 hours on the test substrates, the proliferative capacity of epithelial cells was analysed. The findings are presented in Figure 4.5 and the summary data is displayed in Appendix 3 (3.3)

The data sets were found to be non-normally distributed using a Kolmogorov-Smirnov normality test and a Kruskal-Wallis H multiple comparative analysis was used to determine that at the 0.001 level there is a significant difference between all of the groups based on the test rank scores ($p < 0.001$). Pair-wise Mann Whitney U tests demonstrated the significantly greater proliferative capacity of epithelial cells cultured on laminin coated substrates of all material types tested compared to control and fibronectin coated discs (all p values < 0.002).

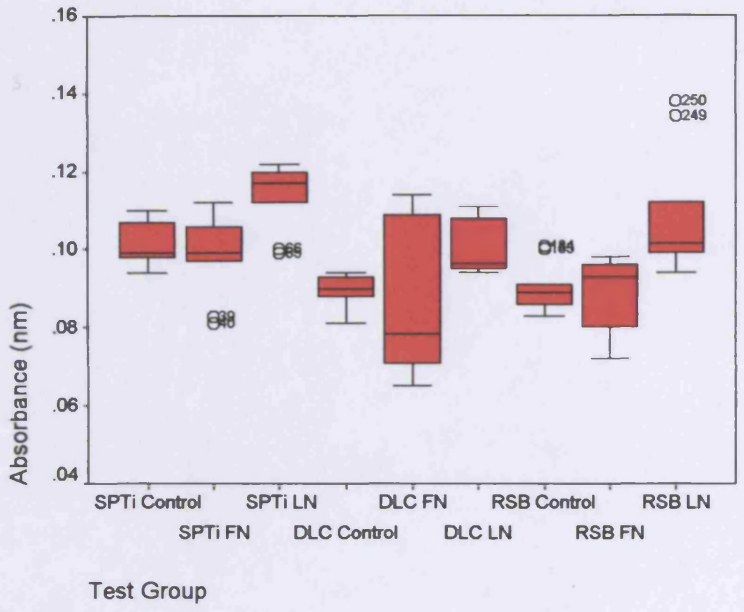

FIGURE 4.5 Box plot of data for epithelial cell proliferation analysis after 24 hours on the test substrates.

4.3.2.4 EPITHELIAL CELLS – 48 HOUR

After a culture peirod of 48 hours on the test substrates, the proliferative capacity of epithelial cells was analysed. The findings are presented in Figure 4.6 and the summary data is displayed in Appendix 3 (3.4). The data sets were found to be non-normally distributed using a Kolmogorov-Smirnov normality test and a Kruskal-Wallis H multiple comparative analysis was used to determine that at the 0.001 level there is a significant difference between all of the groups based on the test rank scores ($p < 0.001$). Pair-wise Mann Whitney U tests demonstrated that laminin coating substrates of all material types significantly increases the proliferative capacity of supported epithelial cell populations compared to fibronectin coated discs of the same type (all p values < 0.05). Laminin coated DLC discs supported epithelial cells with a significantly lower proliferative capacity than laminin coated SPTi or RSBTi (all p values < 0.01). This indicates that after 48 hours in culture the detrimental effect of DLC coating observed in Chapter two of my thesis is evident.

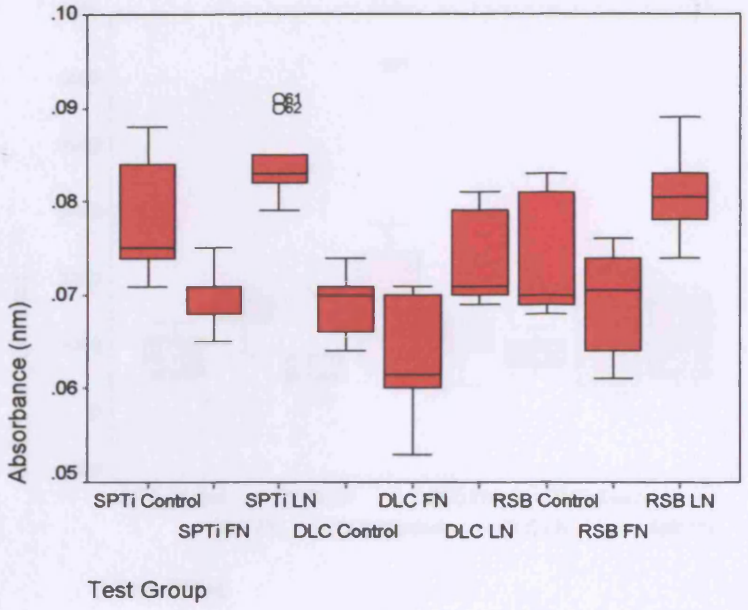

FIGURE 4.6 Box plot of data for epithelial cell proliferation analysis after 48 hours on the test substrates.

4.3.3 DETERMINATION OF CELL AREA – SEM AND IMAGE ANALYSIS

4.3.3.1 FIBROBLAST CELL AREA – 48 HOURS

Ten randomly selected cells from each substrate type were photographed under SEM and the cell areas were calculated using KS300 image analysis software. The laminin coated RSBTi discs did not support a fibroblast population large enough to obtain sufficient data for the statistical analysis. Figure 4.7 displays the data obtained and the summary data can be observed in Appendix 3 (3.5).

The data sets were found to be non-normally distributed using a Kolmogorov-Smirnov normality test and a Kruskal-Wallis H multiple comparative analysis was used to determine that at the 0.02 level there is a significant difference between all of the groups based on the test rank scores ($p < 0.02$). Pair-wise Mann Whitney U tests showed that fibroblasts cultured on fibronectin coated SPTi have significantly greater cell area than those cultured on SPTi ($p < 0.001$) and laminin coated SPTi ($p < 0.002$).

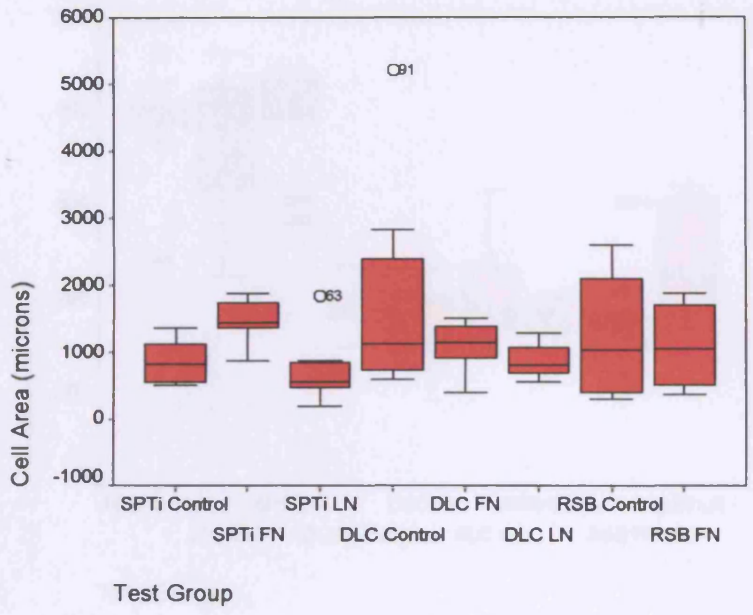

FIGURE 4.7 Box plot of fibroblasts cell area supported by the test substrates after 48 hours.

4.3.3.2 EPITHELIAL CELL AREA – 48 HOURS

The cell area of ten randomly selected epithelial cells cultured on each of the test substrates was analysed using KS300 image analysis software. Figure 4.8 displays the data obtained and the summary data can be observed in Appendix 3 (3.6). The data sets were found to be non-normally distributed using a Kolmogorov-Smirnov normality test. Kruskal-Wallis H multiple comparative analysis was used to determine that at the 0.01 level there is a significant difference between all of the groups based on the test rank scores ($p < 0.01$). Pair-wise Mann Whitney U tests showed that epithelial cells cultured on SPTi substrates, irrespective of protein coating, have significantly greater cell area than those on any of the surfaces tested. Epithelial cells cultured on laminin coated RSBTi display significantly greater cell areas than those on RSBTi control or fibronectin coated discs.

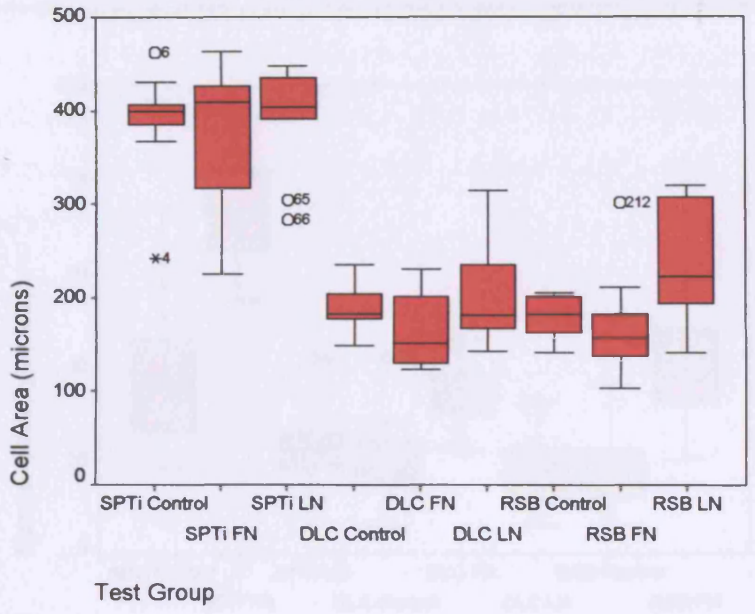

FIGURE 4.8 Box plot of average cell area of epithelial cells cultured on test substrates over a 48 hour peirod.

4.3.4 NUMBER OF VINCULIN MARKERS PER CELL – FLUORESCENCE

4.3.4.1 NUMBER OF VINCULIN MARKES PER FIBROBLAST – 48 HOUR

The number of vinculin markers in thirty randomly selected fibroblasts, from each substrate, was established using a Weiss Fluorescence Microscope. The data is presented in Figure 4.9 and the summary data is given in Appendix 3 (3.7). Fibroblasts cultured on laminin coated RSBTi had an insufficient cell population density to obtain the data required and has been omitted. The data sets obtained were found to be non-normally distributed using a Kolmogorov-Smirnov normality test. Kruskal-Wallis H multiple comparative analysis was used to determine that at the 0.01 level there is a significant difference between all of the groups based on the test rank scores ($p < 0.01$). Pair-wise Mann Whitney U tests showed that fibroblasts cultured on fibronectin coated SPTi possess significantly greater numbers of vinculin markers per cells than those supported by any of the other test substrates. This suggests that the surface topography and chemical composition are still affecting cell parameters despite the protein coating applied to the substrates. Within each substrate type group, SPTi, DLC and RSBTi, the fibronectin coated discs supported fibroblasts with significantly more vinculin markers per cell than the control or laminin coated discs.

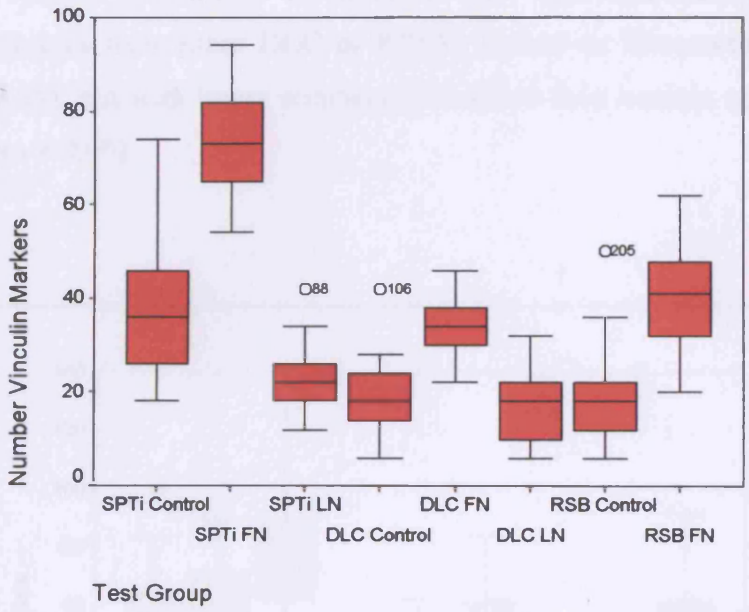

FIGURE 4.9 Box plot of the number of vinculin markers observed in fibroblasts cultured on test substrates for a 48 hour incubation period.

4.3.4.2 NUMBER OF VINCULIN MARKES PER EPITHELIAL CELL – 48 HOUR

The number of vinculin markers in thirty randomly selected epithelial cells, from each substrate, was established using a Weiss Fluorescence Microscope. The data is presented in Figure 4.10 and the summary data is given in Appendix 3 (3.8).

The data sets obtained were found to be non-normally distributed using a Kolmogorov-Smirnov normality test. Kruskal-Wallis H multiple comparative analysis was used to determine that at the 0.01 level there is a significant difference between all of the groups based on the test rank scores ($p < 0.01$). Pair-wise Mann Whitney U tests showed that within each material type group, SPTi, RSBTi and DLC, laminin coated discs supported epithelial cells with significantly greater numbers of vinculin markers per cell than control or fibronectin coated discs (all p values <0.01). Epithelial cells cultured on fibronectin coated substrates, within material type groups, show significantly higher numbers of vinculin markers per cell than those on control discs (all p values < 0.05). Laminin coated SPTi discs support epithelial cells with significantly greater numbers of vinculin markers per cell than either DLC or RSBTi laminin coated discs. This indicates that the surface roughness and chemical composition of material substrates still affect cell

population parameters, irrespective of the protein coating (all p values < 0.01). SPTi substrates support populations of epithelial cells with significantly higher numbers of vinculin markers than either DLC or RSBTi control or fibronectin coated discs (all p values < 0.01), but with lower numbers of markers than laminin coated DLC or RSBTi (all p values > 0.05).

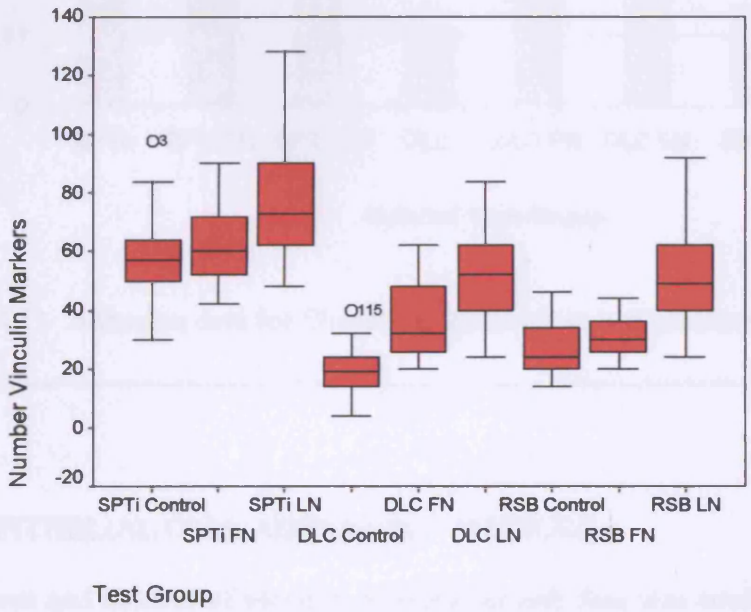

FIGURE 4.10 Box plot of the number of vinculin markers observed in epithelial cells cultured on test substrates for a 48 hour incubation period.

4.3.5 CELL ATTACHMENT: AS A RATIO OF NO. MARKERS:CELL AREA

4.3.5.1 FIBROBLAST CELL ADHESION – 48 HOURS

The cell area and number of vinculin markers per cell data was combined to establish the average number of vinculin markers per unit cell area for fibroblasts cultured on the test substrates for a 48 hour incubation period. The resulting data is presented in Figure 4.11 and the summary data is given in Appendix 3 (3.9). For each material type tested, the adhesion of fibroblasts to fibronectin coated discs is significantly greater than that for laminin coated or control discs (all p values < 0.05). In the case of DLC and RSBTi substrates the increase in fibroblast adhesion to fibronectin coated compared to control discs is threefold.

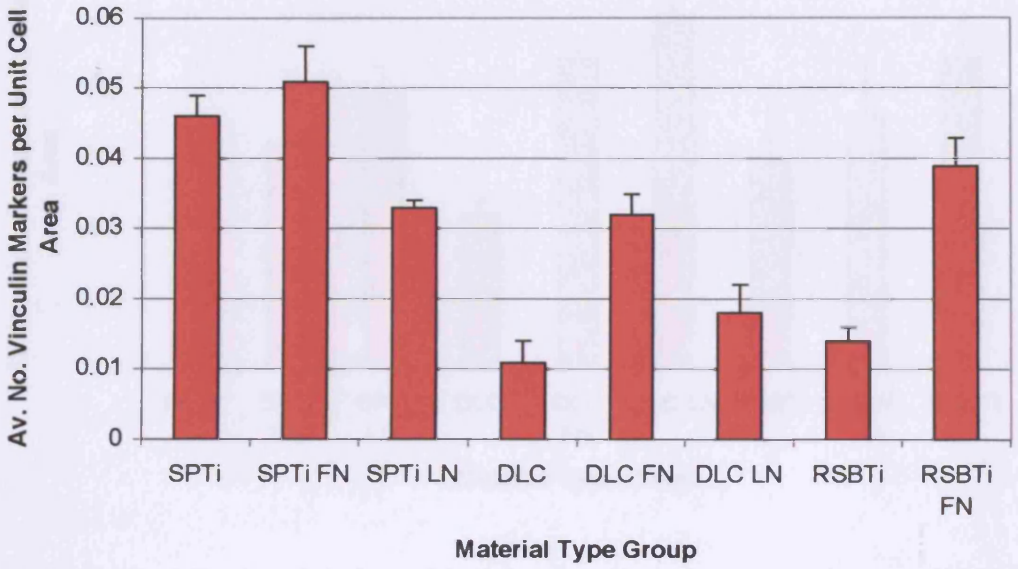

FIGURE 4.11 Adhesion data for fibroblasts cultured on test substrates for 48 hours.

4.3.5.2 EPITHELIAL CELL ADHESION – 48 HOURS

The cell area and number of vinculin markers per cell data was combined to establish the average number of vinculin markers per unit cell area for epithelial cells cultured on the test substrates for a 48 hour incubation period. The resulting data is presented in Figure 4.12 and the summary data is given in Appendix 3 (3.10). Laminin coated materials from each group support epithelial cells with a 1.5 to 2 fold increase in adhesion compared to the control substrates. For each group, SPTi, RSBTi and DLC, the laminin coating supports a population of epithelial cells that are significantly better adhered to the substrates than the control or fibronectin coated discs (all p values < 0.05).

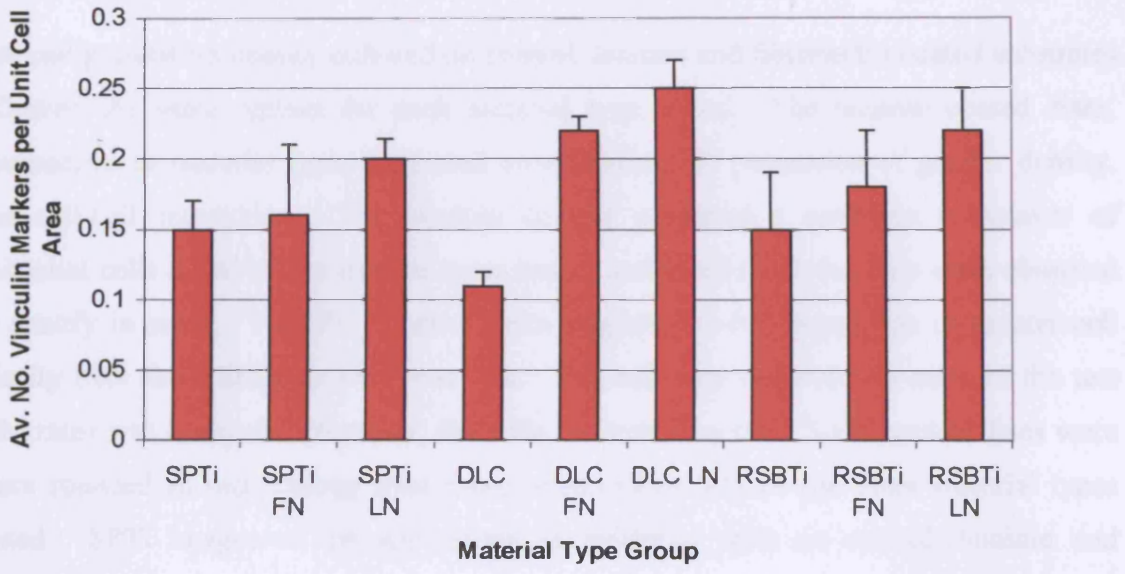

FIGURE 4.12 Adhesion data for epithelial cells cultured on test substrates for 48 hours.

4.3.6 MORPHOLOGICAL ANALYSIS – SCANNING ELECTRON MICROSCOPY

4.3.6.1 FIBROBLAST MORPHOLOGICAL ANALYSIS

The appearance of fibroblasts cultured for 48 hours on control, fibronectin and laminin coated DLC discs are presented in figure 4.13a – 4.13c. The morphology, density and general appearance of the fibroblast populations followed the same pattern for all of the material types tested. The cell density increased from control, laminin coated to fibronectin coated discs, the greatest cell density populations being observed on the latter. The fibronectin coating increased the extent of cell area / spreading on all of the substrate materials. The degree of cell-cell and cell-substrate communication and interaction were increased on the fibronectin coated materials compared to the control and laminin coated discs. The SPTi control discs supported the largest numbers of fibroblasts with greater cell areas and cell-cell interaction compared to the RSBTi control substrates, whilst the DLC control discs presented with a low density, low cell area and predominately rounded population. All fibronectin coated discs, irrespective of material type, supported a confluent monolayer of fibroblasts, with good cell spread, a large degree of cell-cell communication and a flattened morphology.

4.3.6.2 EPITHELIAL CELL MORPHOLOGICAL ANALYSIS

The cell population density cultured on control, laminin and fibronectin coated substrates followed the same pattern for each material type tested. The laminin coated discs, irrespective of material type, supported an epithelial cell population of greater density, and cell-cell interaction. The laminin coating produced a complete monolayer of epithelial cells on all of the surface types tested, and in all cases the cells were observed to stratify in areas. The SPTi control discs supported a cell population of greater cell density than the RSBTi or DLC controls. The cell area observed on each of the test substrates was constant. However, the cells examined on the RSBTi control discs were more rounded in morphology than those observed on any of the other material types tested. SPTi images of the appearance of epithelial cells on control, laminin and fibronectin coated discs are presented in figure 4.14.

FIGURE 4.13

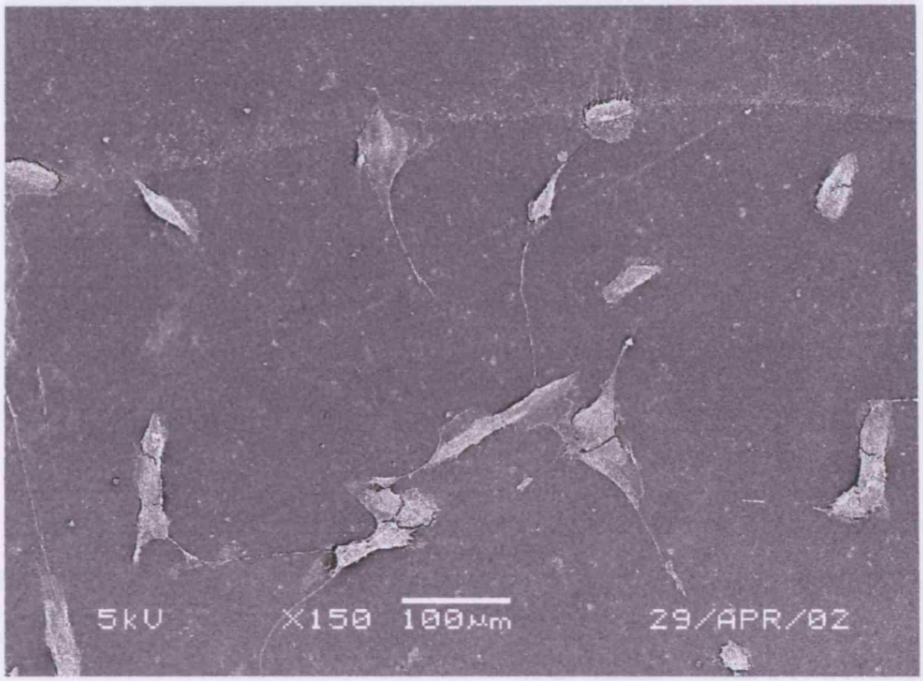

FIGURE 4.13a SEM of fibroblasts cultured on a DLC substrate for 48 hours at a magnification of x 150.

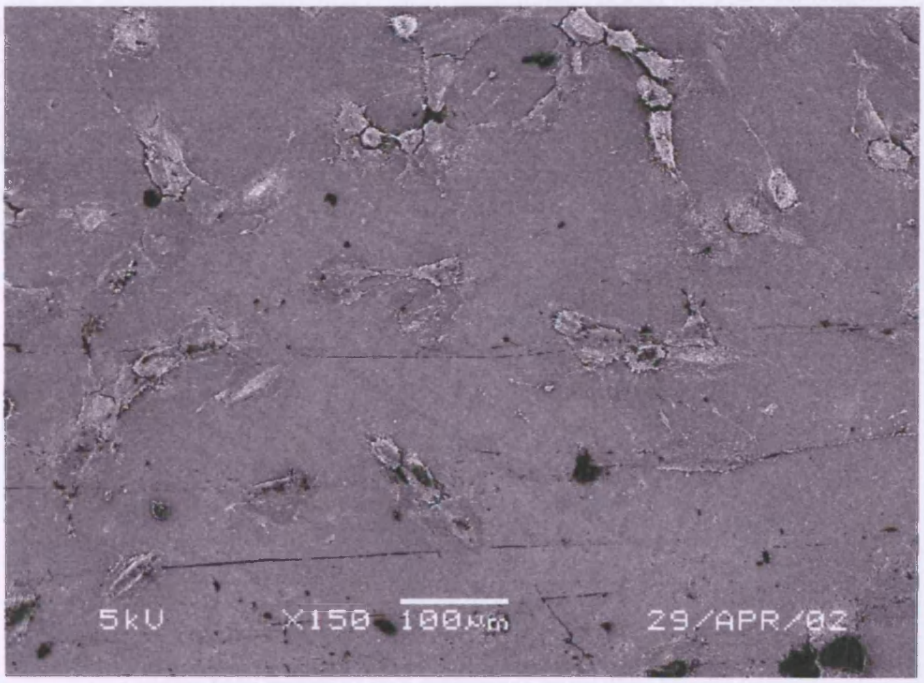

FIGURE 4.13b SEM of fibroblasts cultured on a DLC substrate coated with 10µg of laminin for 48 hours at a magnification of x 150.

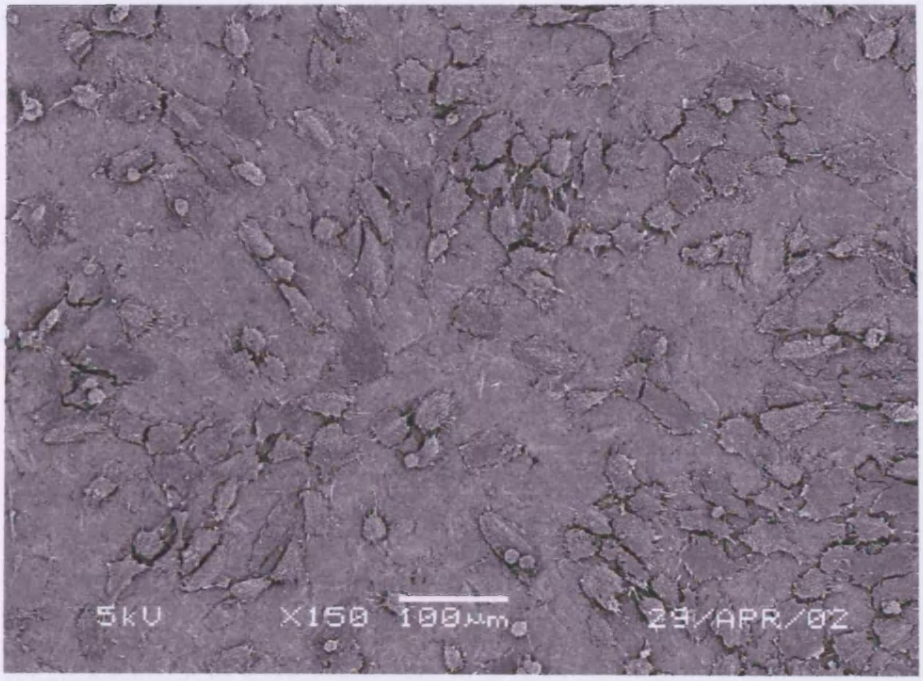

FIGURE 4.13c SEM of fibroblasts cultured on a DLC substrate coated with 10µg of fibronectin for 48 hours at a magnification of x 150.

FIGURE 4.14

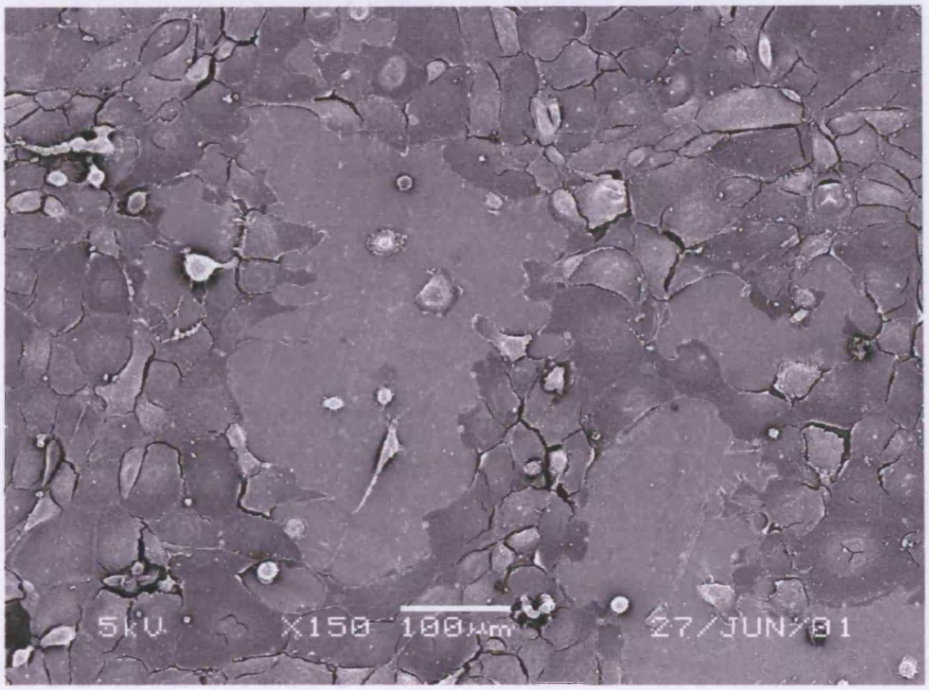

FIGURE 4.14a SEM of epithelial cells cultured on SPTi for 48 hours at magnification x 150.

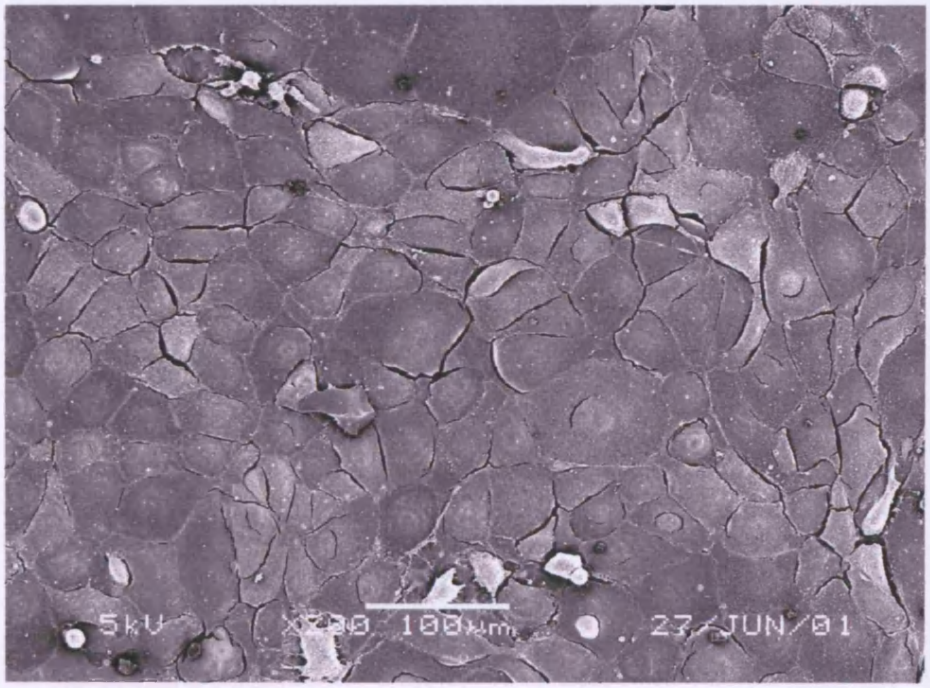

FIGURE 4.14b SEM of epithelial cells cultured on a SPTi substrate coated with 10µg of laminin for 48 hours at magnification x 200.

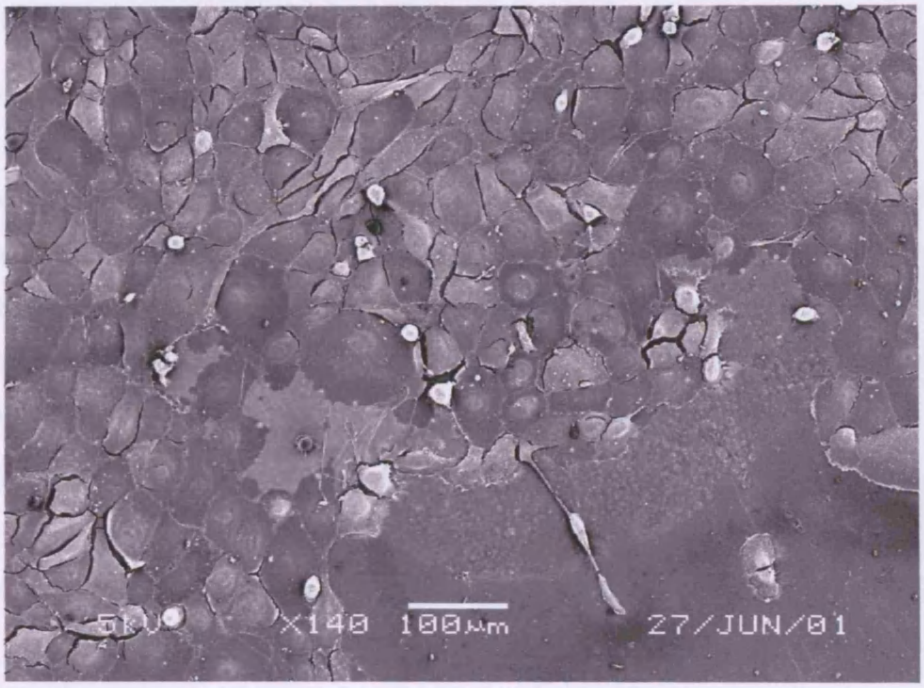

FIGURE 4.14c SEM of epithelial cells cultured on a SPTi substrate coated with 10µg fibronectin for 48 hours at magnification x 140.

4.4 DISCUSSION

4.4.1 FIBROBLAST PROLIFERATION

All materials coated with fibronectin were shown to support increased proliferative capacity of fibroblasts after 24 hours *in vitro*. This finding is supported by those of Nuttelman et al (2001) who looked at a modified poly (vinyl alcohol) (PVA) hydrogel, supporting NIH3T3 fibroblasts attachment. It was shown that by covalently attaching fibronectin to PVA hydrogel, the rate of fibroblast attachment and proliferation dramatically improved. In 1992, Zlatopolsky et al showed that heparin-binding fragments of fibronectin are capable of promoting fibroblast proliferation.

After 48 hours, the data obtained from proliferation analysis showed a significant difference between the groups, however the differences were less marked than those observed between the 24 hour data. Two reasons for these findings are proposed. Firstly, after 48 hours it is questionable whether any of the originally applied fibronectin or laminin remains present or active on the disc surfaces. Previous studies have examined the effects of fibronectin and laminin for periods ranging from 30 minutes (Tamura et al 1997), 1.5 hours (Dean et al 1995) to 24 hours (El-Ghannam et al 1998), and demonstrated significant differences in cell parameters. However, none have examined effects after a 48-hour duration. Secondly, it is postulated that even if the originally applied adhesion proteins still remain active or present, the effects could be reduced over time owing to the deposition of ECM by adherent cells.

4.4.2 EPITHELIAL CELL PROLIFERATION

After 24 hours *in vitro*, laminin coated discs were observed to support epithelial cell populations with increased proliferative capacity than control or fibronectin coated discs, irrespective of the substrate material. This finding is complemented by those of Gonzales et al, who in 1999 demonstrated that two distinct laminin-5 function-inhibitory antibodies inhibit proliferation of epithelial cells, and that proliferation inhibition by these function perturbing laminin-5 antibodies is reversed upon antibody removal (or by providing the antibody treated cells with exogenous laminin-5).

Following a 48 hour duration *in vitro*, there is still a significant difference among the test rank scores. Pair-wise analysis showed the pattern of proliferative capacity between the substrate types tested to be the same as that observed after 24 hours. This finding

demonstrates that the laminin coating is still affecting the proliferative function of epithelial cells after 48 hours in a culture system.

4.4.3 CELL ADHESION ANAYLSIS

The findings for both dermal epithelial and fibroblast cell adhesion, with and without laminin and fibronectin, complement those of Dean et al, whose 1995 study examined the effects of these protein coatings on gingival fibroblasts and epithelial cell adhesion in association with materials used in dental implantology. The study showed a 2/3 fold increase in fibroblast binding to fibronectin coated implants and a 3/4 fold increase for epithelial binding to laminin coated materials.

The findings of my study and those of Dean et al (1995), lead to the conclusion that both fibroblasts and epithelial cells of dermal and gingival origin present with distinct preferences for the different adhesion molecules tested. It is also proposed that surface roughness has some effect on adhesion of cells of this type.

Overall it is concluded that fibronectin coatings sustain fibroblast, and laminin coatings enhance epithelial cell populations compared with control discs. Cell spreading is an active process and cells rely on morphological changes associated with the cell cycle. Smaller cells membrane movement constraints, caused by topographical variations, would inevitably be more detrimental than those imposed on cells of a larger size.

4.4.4 GENERAL CONCLUSIONS

For application of the findings of this chapter for *in vivo* soft tissue adhesion promotion in transcutaneous or percutaneous environments, it is proposed that a fibronectin coating applied to implants abutting soft tissues with predominantly fibroblastic cell populations, could benefit from a fibronectin protein coating. The soft tissue-implant interface involving epithelial cell populations could be enhanced using a laminin protein coating. The effects of these proteins may be short-lived in an *in vivo* environment. However, it is concluded that if the coating can stabilise the interface between soft tissues and implant materials, even for a 24 hour period, then it could increase implant longevity.

There are limiting factors associated with the *in vitro* environment that have the potential to result in different findings in an *in vivo* system. Cells *in vitro* loose a degree of three-dimensional shape, adopting a flattened, spread morphology; they undergo a selection process for those that are best suited to the cell culture environment and are a uniform

population of cells. They are deprived of heterotypic cell interactions and can rapidly loose differentiated functions. As a result, the environment *in vitro* is significantly different from that which the cells would experience *in vivo*. These factors must be considered as limiting in terms of *in vivo* expectations.

CHAPTER FIVE

INTRAOSSEOUS TRANSCUTANEOUS AMPUTATION PROSTHESES – AN ALTERNATIVE TO CURRENT LIMB AMPUTATION MANAGEMENT

CHAPTER FIVE: INTRAOSSEOUS TRANSCUTANEOUS AMPUTATION PROSTHESES – AN ALTERNATIVE TO CURRENT LIMB AMPUTATION MANAGEMENT

5.1 INTRODUCTION AND HYPOTHESES

Skeletally anchored, transcutaneous amputation prostheses could be used to replace current stump-socket designs for amputees. To date, numerous problems associated with artificial limb design have been encountered. These include, mismanagement (Levy 1995), focal points of increased stress caused by non-uniform pressure distribution at stump-socket junctions (Lee et al 1997), skin related problems caused by sheer stresses leading to infection (Pritham 1990, Canale 1998) and the unnatural microbial environment at the stump-socket interface, to which the skin is unaccustomed, causing infection (Kohler et al 1989). The development aims of intraosseous transcutaneous amputation prostheses (ITAP) are to overcome these problems by attaching the external implant directly to the skeleton via a transcutaneous prosthesis. This method would transfer the detrimental loads currently applied to the stump-socket interface, directly to the skeleton.

Since the 1960's Branemark has been the pioneer of transcutaneous implant technology and research (Branemark et al 1969, Branemark et al 1977, Branemark and Albrektsson 1982, Branemark 1988, Branemark et al 1999, Branemark et al 2001). Branemark has demonstrated that skin penetrating implants in human epithelium, with restricted movement, show no inflammatory or other adverse skin reactions after 7-25 months, and that hearing aids anchored in temporal bone placed in a two stage surgical procedure will minimise trauma and remain functional after 38-50 months (Branemark and Albrektsson 1982). Dental and auricular implants using Branemark fixtures were originally placed in two stage surgical procedures. The first stage of the procedure introduced the bone anchored or subcutaneous section of the implant, after which the soft tissues were closed and allowed a healing time of between one and six months prior to a second stage operation to implant the transcutaneous section. In 1999 Branemark demonstrated encouraging results with single stage procedures in the lower jaw. In 1992, Chehroudi et al compared one and two stage procedures and demonstrated that placing implants in two stages improves the performance of transcutaneous devices, and that further improvement is observed by promoting connective tissue ingrowth.

Skin penetrating implants can be considered to be foreign bodies penetrating the skin through surgically created defects. Implant failure can occur as a direct result of marsupialisation, permigration, avulsion and infection (Heaney 1977, Von Recum 1984, Chehroudi et al 1989, Chehroudi et al 1992). In 2000, Holgers demonstrated that many inflammatory cells are present at tissue-implant interfaces of transcutaneous devices. T

and B-lymphocytes, macrophages, polymorphonuclear cells and plasma cells at the interface around transcutaneous devices indicate a chronic inflammatory state. Microbial adhesion is a prerequisite for infection. Immediately after implantation of a transcutaneous device, host proteins are adsorbed to the biomaterial surface. The proteins adsorbed depend on properties of the implant material, including hydrophobicity and surface charge, as well as the composition of the hosts proteinaceous fluid. Microbial adhesion can occur to these surface-adsorbed structures. Fibronectin has been shown to mediate adhesion of staphylococci to materials in the blood stream (Vaudaux et al 1993), whilst vitronectin could mediate adhesion of coagulase negative staphylococci to polymers in cerebrospinal fluid (Lundberg et al 1997). It has been shown that staph. epidermidis is the most common infectious agent in polymer related infections, whereas staph. aureus dominates infections surrounding metal implants (Gristina 1987). Decreasing bacterial adhesion to ITAP devices is vital to limit infection and increase implant longevity.

In 1999 Branemark presented data concerning the use of osseointegrated prostheses in lower limb amputation at the 10th International Symposium on Limb Salvage. The concept for this application was originally proposed by Winter in 1974, who stated that a new method for providing artificial limbs for amputees might be to attach the external prosthesis directly to the skeleton. In 1999 Branemark detailed 16 patients who had received bone anchored amputation prostheses. Most presented with superficial infections, treatable with peroral antibiotics and frequent re-dressing. However, four patients suffered deep infection and implant loosening and three required a new titanium fixture. One patient had stump shortening, whilst surgical intervention was needed for two patients with chronic fistulae, and improvement was observed following changes in surgical technique. These findings indicate a further need to develop the ITAP concept.

Numerous authors have published concerning design criteria for transcutaneous devices (Grosse-siestrup and Affeld 1994, Von Recum 1984, Tjellstrom 1985, Von Recum and Park 1981), as well as examining naturally permanent transcutaneous structures (Knabe et al 1999), and to date no truly successful artificial alternative is available for amputees. Studies have examined the attachment of human gingiva to teeth and dental implant materials to gain an insight into how the interface is formed (Gould et al 1984, McKinney et al 1985). It has been shown that epithelial cells attach to titanium *in vivo* in a similar manor to that observed *in vitro* and in the natural tooth, via formation of hemidesmosomes and basal lamina.

In 1981, Gould et al studied the attachment mechanism of epithelial cells to titanium *in vitro*, showing that hemidesmosome-like structure formation is key to epithelial cell attachment.

In dentistry and orthopaedics, hydroxyapatite (HA) has been utilised as the best biomaterial for bone prostheses as it bonds directly to hard tissues without forming a fibrous connective tissue layer at the implant-bone interface (Kato et al 1979, Jarcho 1981). Tissue reactions to various materials used for transcutaneous devices have been studied showing that HA has greater compatibility with skin tissue and imparts an increased resistance to bacterial infection (Shin and Akao 1997). Many devices and materials have been proposed to overcome the problems associated with transcutaneous implants, but as yet they remain unsolved, and a stable interface between living and artificial materials remains illusive. A totally stable junction between soft tissues and implants is essential for ITAP to function successfully. Nowicki et al (1990) have shown that porous materials can be used to promote tissue ingrowth and vascularisation and can provide an alternative to natural bonding, with pore size and structure being critical to success. However, transcutaneous devices composed of porous materials do not help prevent bacterial infection (Shin and Akao 1997) and are generally associated with a high risk of infection. Transcutaneous implants made from other porous materials, including fibermesh and velour for anchoring soft tissues into pores or among fibres, have also met with limited success (Paquay et al 1996).

In 1991 Tsuji et al demonstrated the use of HA transcutaneous devices implanted into the forearms of human volunteers that were successfully maintained for seven years with no special care. *In vivo* and *in vitro* studies of dental interfaces give a good insight into soft tissue and soft tissue cell interfaces with hard surfaces, and how surfaces and implants can be designed to maximise implant longevity (Listgarten 1966, Zachrisson and Schultz-Haudt 1968, Karring et al 1975, Mackenzie and Hill 1981, Mackenzie and Fusenig 1983, Meffert 1988, Seymour et al 1989, Kononen et al 1992). However, most literary evidence is conflicting and a totally successful implant design has not yet been developed for amputation prosthetics.

Epithelial downgrowth around transcutaneous implants is the principle reason for infection and ultimately implant failure. Winters' research in 1974 showed that the epidermis can migrate through damaged collagenous tissue, however epidermal cell migration is halted when confronted by healthy collagenous bundles. Downgrowth is a

result of epithelial cell proliferation one to two days post injury and the 'free edge effect' whereby the absence of neighbouring cells at a wound margin acts as a signal for migration and proliferation of wound edge epithelial cells, to re-establish epithelial cell layer continuity. Local release of growth factors has also been implicated as factors affecting epithelial proliferation and migration (Heimark et al 1986, Heimark and Schwartz 1985). In wound healing and response to transcutaneous implants, epithelial cells migrate over a provisional matrix of collagen I, collagen V, fibrin, vitronectin and fibronectin, which is deposited by wound fibroblasts, macrophages and migrating epithelial cells. A series of phenotypic alterations in epithelial cells results in their lateral mobility and they begin to migrate. In normal wound healing this migration serves to heal the wound defect, but in ITAP this leads to downgrowth. For ITAP to be successful it is necessary to prevent epithelial migration and downgrowth by utilising biomaterials and coatings to promote epithelial adherence, and to stabilise the sub-epithelial soft tissue seal by supplementing epithelial cell adherence with dermal attachment.

The research in this chapter aims to examine and enhance the reactions of the skin around titanium alloy transcutaneous implants, to eliminate downgrowth by incorporation of biomaterials and implant design and to promote sub-epithelial soft tissue adhesion, with the final aim being a tight soft tissue- implant interface for use in amputation prosthetics. Titanium alloy is the material of choice for the development of ITAP because it is stronger than commercially pure titanium (www.Matweb.com) and better suited to a weight bearing application such as amputation prosthetics.

Chapter Two of my thesis examined Deer antler as a model for the development of ITAP. The results showed that Deer antler are successful for a number of reasons. Thick collagen fibres anchor to the pedicle from the adjacent tissues, preventing epithelial downgrowth and providing a strong attachment at the interface. The highly porous pedicle provides an ideal surface for tissue ingrowth, whilst the ridges and grooves at the antler-pedicle interface mediate soft tissue adherence. In this chapter, these findings have been considered and applied to the development of ITAP to maximise efficiency and longevity. Chapter Two demonstrates that epithelial attachment to a transcutaneous structure is not a prerequisite for a stable interface between the soft tissues and the skin-penetrating device. **As a result of these findings it is hypothesised that for the development of ITAP, it is sub-epithelial/dermal fibroblastic, but not epithelial layer adhesion, that is directly responsible for the degree of downgrowth observed around ITAP implants. The development of the ITAP implant in this chapter is based on deer antler; biomimetic surfaces for the development of amputation prostheses. It is**

hypothesised that implants designed to mimic antler, providing ideal surface characteristics at different points along the length of the implant, will result in increased tissue attachment and reduced epithelial downgrowth. Also, that it is sub-epithelial/dermal fibroblastic, but not epithelial layer adhesion, that is directly responsible for the degree of downgrowth observed around ITAP implants.

5.2 MATERIALS AND METHODS

5.2.1 IMPLANT PREPARATION

Two implant designs were tested, straight and flanged, which were machined from a stock bar of medical grade titanium (Ti_6Al_4V)(BS7252 part 3). Both implant types were 40mm in length, of which 22mm comprised a self-tapping screw thread.

A minimum of six animals were used in each Group and the implants were tested with the surface finishes and coatings presented in table 5.1

Table 5.1 Implant surface finishes and coatings

Group 1	Group 2	Group 3	Group 4
MF	MF	MF	MF
RSB	SG + DLC	PTi	P Flange
SG	LG + DLC	PTi + HA	HA Flange
LG	RSB + DLC	PTi + DLC	100 FN Flange
HA	-	PTi + DLC + HA	200 FN Flange

(MF = Machine Finished, RSB = Rough Sand Blasted, SG = Small Grooved, LG = Large Grooved, HA = Hydroxyapatite, DLC = Diamond-like Carbon, P = Plain Machine Finished, FN = Fibronectin)

Following results from preliminary studies, Machine Finished (MF) (Ra 0.210μm, Ry 1.356μm, Rz 1.265μm), straight pins were used as a negative control in all animals. MF pins were rough sand blasted (sealed cabernet - 0.2mm aluminium oxide grit) to create the Rough Sand Blasted implants (RSB) (Ra 0.404μm, Ry 2.561μm, Rz 1.342μm). A 70 micron thick coating of dense hydroxyapatite was applied to MF implants to create Hydroxyapatite implants (HA) (Ra 2.375μm) using a plasma spray process (Plasma Biotal Ltd, UK). Small Grooved (SG) (groove depth = 0.3mm, groove width = 0.5mm), Large Grooved (LG) (groove depth = 0.6mm, groove width = 1.0mm) and RSB implants were coated with an externally applied 2-4 micron thick coating of diamond-like carbon (DLC) applied at Diavac ACM^{LTD} at Brunel University. DLC is a low surface energy coating used to deter bacterial adhesion to the external segments of the implants. MF

implants were plasma sprayed with porous titanium, at a thickness of 70-100 microns for the Porous Titanium implants (PTi). PTi implants were tested +/- HA and +/- DLC.

All of the coatings were applied to the surface region spanning the dermal and epidermal abutting region of the implants only, with the exception of the DLC coating which was only applied to the external portion of the implants.

The results obtained for the straight implant trials generated a change of design, which was tested in Group 4. A flange was incorporated into the straight implant design (Figure 5.1) to increase the surface area for soft tissue adhesion. The flange was positioned 2mm above the self-tapping screw thread, to be located immediately below the epithelial layer *in situ*. The flange diameter (including the central implant section) was 10mm, and a series of 24, 0.7mm diameter holes were drilled into the flange to simulate the porous nature of the pedicle structure observed in deer antler (see Chapter Two). The flanged implants were tested with and without a 70 micron thick HA coating, applied only to the flange section of the implants.

In Chapter Three of my thesis it was shown that a fibronectin coating, applied to titanium discs *in vitro*, results in a threefold increase in fibroblast adhesion. Owing to these findings, it was postulated that a fibronectin coating applied to the dermal abutting section of ITAP implants could increase the degree of dermal fibroblastic adhesion. Human plasma fibronectin (Sigma F2006) was dissolved in the minimum volume of sterile saline solution and applied to the flanged region of the implants at 100µg and 200µg. The coating was allowed to dry prior to implantation during the surgical procedure.

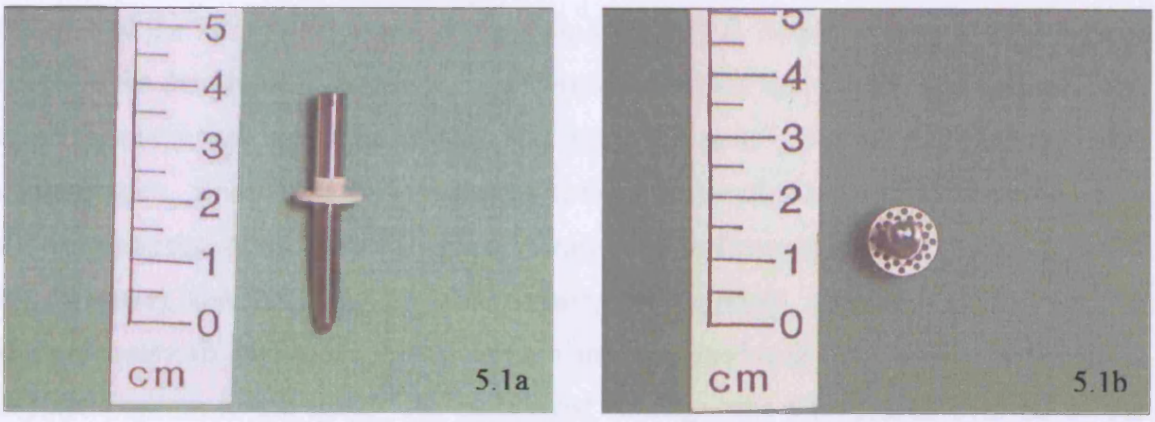

FIGURE 5.1 Appearance of the flanged pin design with a whole HA coating (5.1a) and from plan view (5.1b) showing the hole series.

5.2.2 OPERATIVE PROCEDURES

5.2.2.1 PIN IMPLANTATION

Four to five implants were surgically implanted into the medial aspect of the right tibia of adult female goats weighing between 60-90 Kg as specified in table 5.1. The animals were sedated pre-operatively with an intramuscular injection of Rompun at a dose rate of 0.005 ml/Kg body weight. Anaesthesia was induced with a Ketamine / Midazolam intravenous mix, at a dose rate of 0.2 and 0.5 ml/Kg respectively. The animals were intubated and anaesthesia was maintained with a 2% Oxygen Halothane mix. The animals were administered with analgesia 2 ml Fetagesic perioperatively and for two days post-operatively via intramuscular injection. Antibiotics (Ceporex) were administered perioperatively and for 5 days post-operatively in a 5 ml dose subcutaneous injection.

Once anaesthetised the right leg of the animal was shaved and cleaned using a dilute Pevidine solution, followed by a Hydrex wash and the medial aspect of the tibia was isolated in a sterile field (Figure 5.2). For each implant, a small incision was made in the skin over the site where the implant was to be placed and a periosteal elevator was used to expose and clear the tibial area. Care was taken to minimise the damage caused to the soft tissues. An electric drill was used to create a 4.2mm hole through both cortices of the tibia. The implants were sterilised in a steam autoclave at 135 degrees centigrade and then screwed into place using a hand held T-bar (Figure 5.3). The pins were inserted to the depth required for the appropriate section to be abutting the desired soft tissue layers, and at approximately 2cm intervals along the tibia. At each stage throughout the surgical technique, the operative site was well irrigated with saline solution.

Implantation of straight implants required no further surgical intervention. However, in the case of the flanged implants, one to two sutures (2.0 vicryl) were applied to tightly interface the dermis with the pin surface. Implant position was randomised and care was taken to ensure that each implant type was not in the same position relative to the other implant types. Once all of the implants had been positioned (Figure 5.4), the wound sites were cleaned and dressed with Opsite Moisture Vapour Permeable Spray dressing (Smith and Nephew), and a Sodium Fusidate dressing was applied. Cotton wool was used to apply pressure to the implant-skin interface and was bandaged from above the proximal implant position to the hock. An elasticated bandage was then placed over all of the dressings.

The animals were maintained under observation until they regained consciousness and were then transferred to individual pens where they were monitored at regular intervals for a four week duration (Figure 5.5).

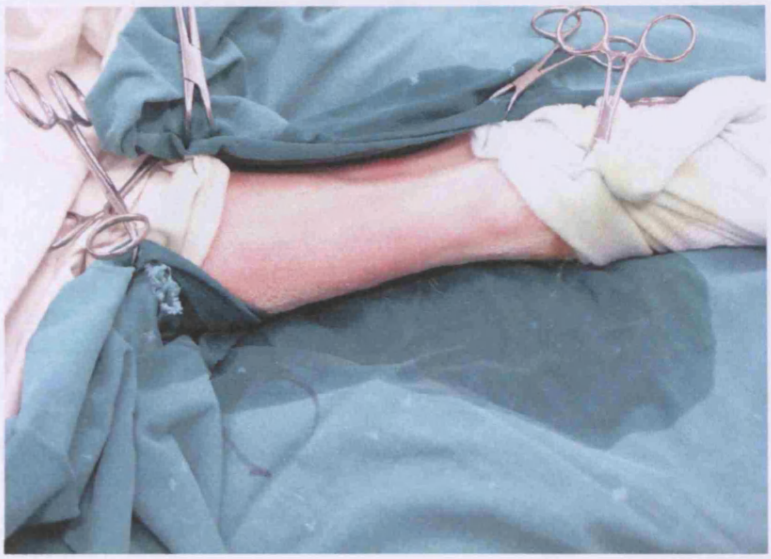

FIGURE 5.2 Medial aspect of the right tibia isolated in a sterile field – prepared for surgery.

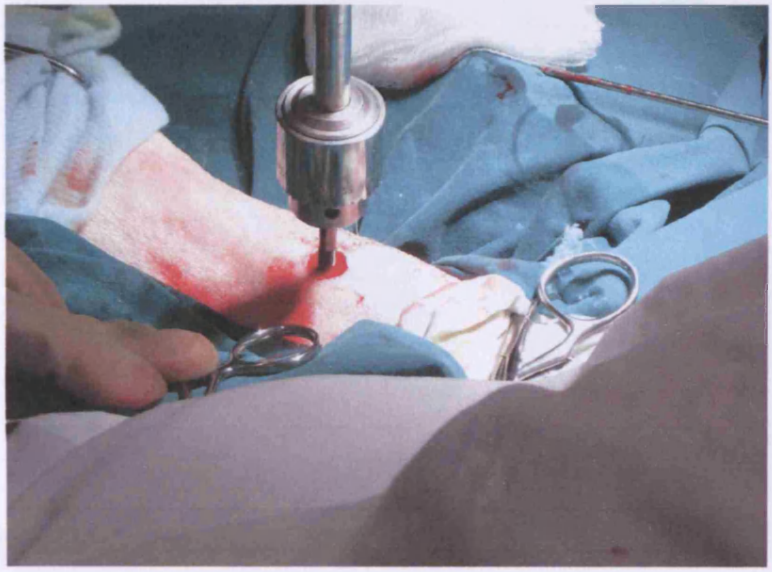

FIGURE 5.3 Central tibial implant being positioned with a hand held T-bar.

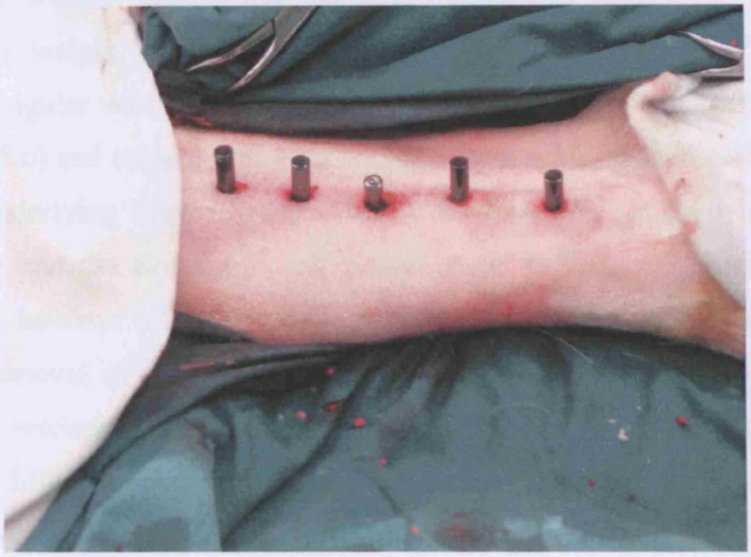

FIGURE 5.4 Appearance of the medial aspect of the tibia following implantation of five straight design transcutaneous implants.

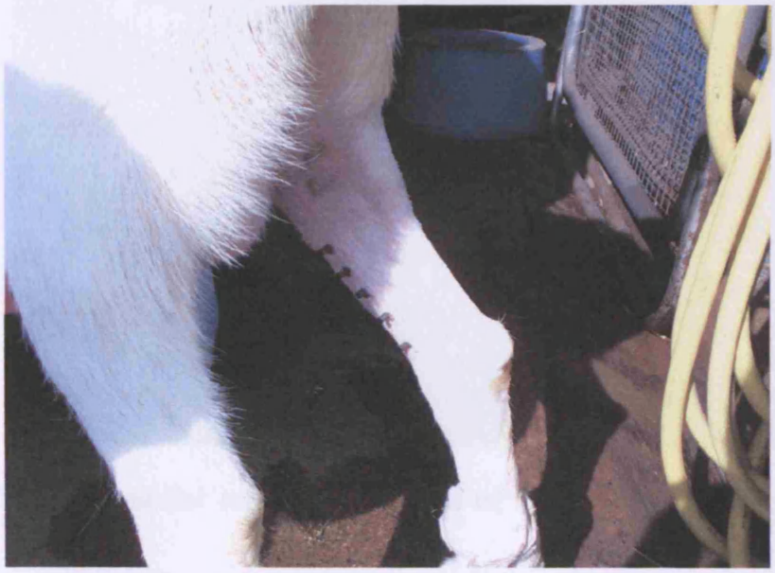

FIGURE 5.5 Monitoring of the implant site 3 weeks post operatively.

5.2.2.2 IMPLANT RETRIEVAL AND TISSUE HARVESTING

The animals were sedated with an intramuscular injection of Rompun at a dose rate of 0.005ml/Kg body weight, and were euthanised with an overdose of Pentobarbitone injected into the jugular vein. Once expired, the medial aspect of the animal's tibia was exposed (Figure 5.6) and using a scalpel, a square of soft tissue around each implant was incised to the underlying bone (Figure 5.7). The tibia was removed by amputation through the knee and the extraneous soft tissues were removed. Most implants were clinically normal, however a few had soft tissue overgrowing the transcutaneous section (Figure 5.8). Removal of all implants was carried out using a hand held saw to cut through the tibial sections surrounding each implant. The overgrown implants, however, required slightly different histological processing (see section 5.2.3). In all cases, care was taken not to disrupt the skin-implant interface during implant retrieval. Immediately after removal the tissue samples were fixed in 10% formal saline.

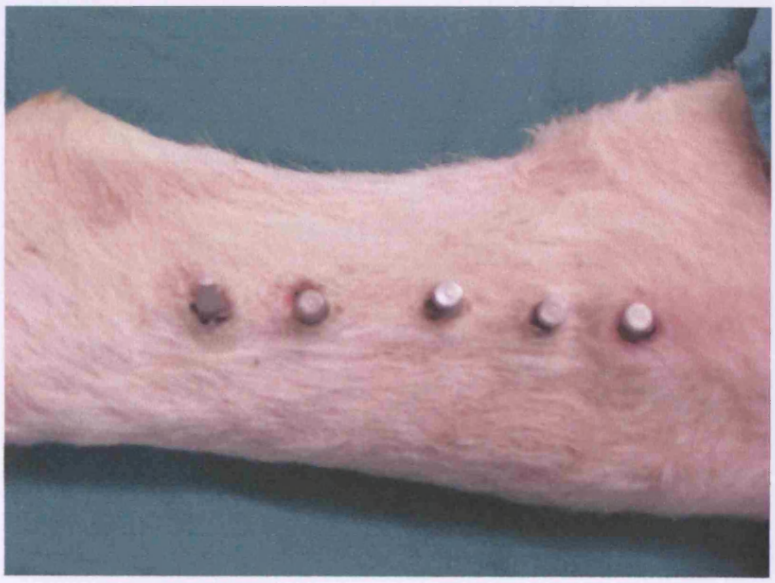

FIGURE 5.6 Exposed medial aspect of the tibia of the operated limb, 4 weeks post-operatively.

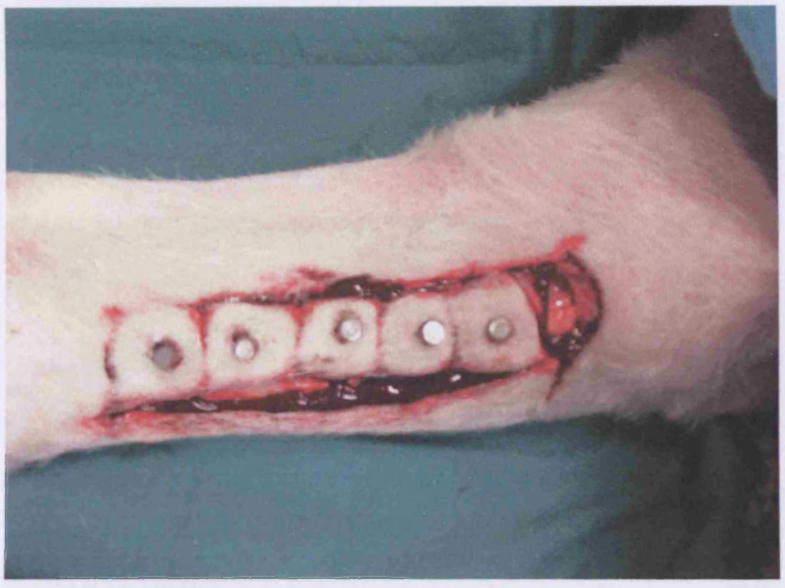

FIGURE 5.7 Appearance of the skin incised to the underlying bone around each of the transcutaneous implants.

FIGURE 5.8

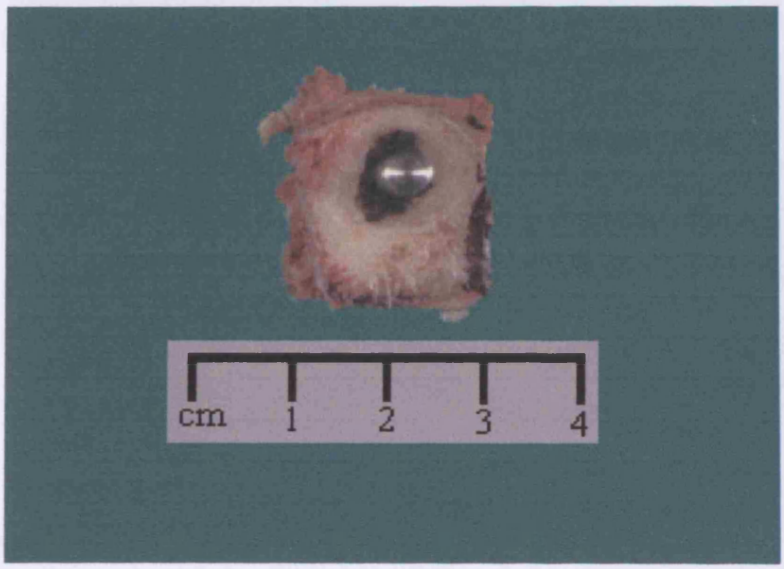

FIGURE 5.8a Appearance of a standard straight implant harvested from an unswollen site from a medial aspect.

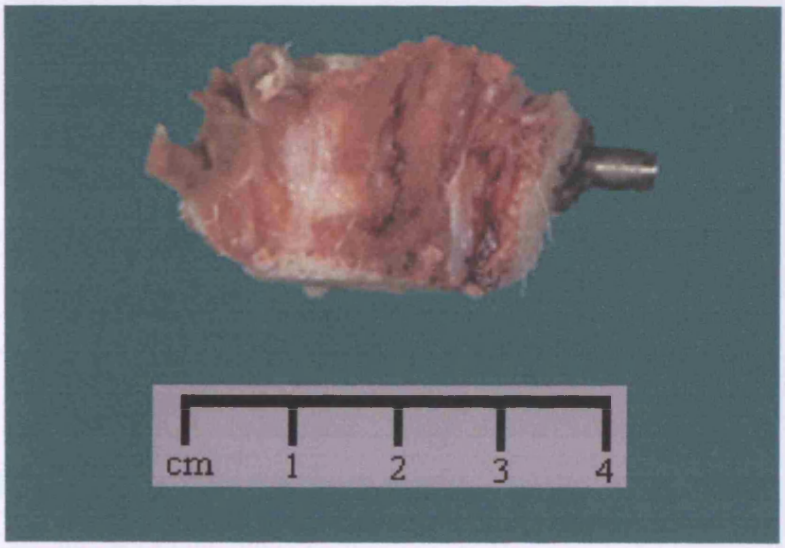

FIGURE 5.8b Shows a transverse section of the implant from 5.8a prior to removal of excess soft tissues.

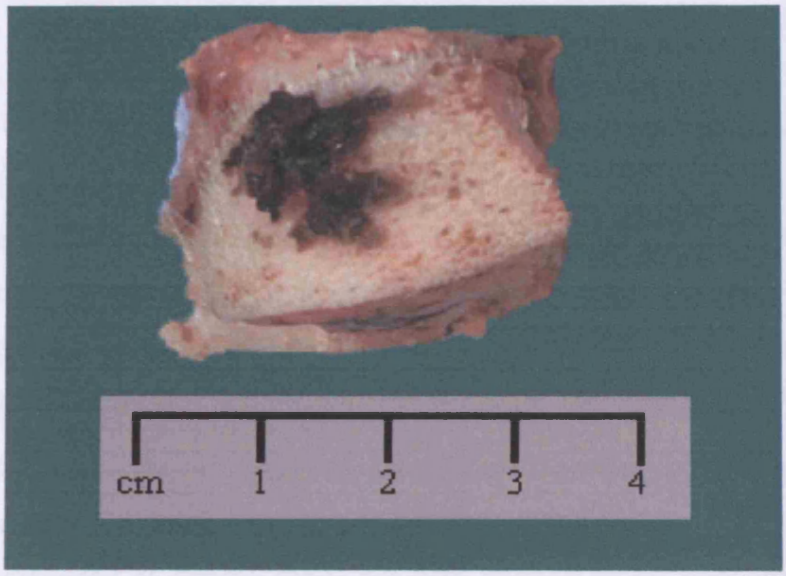

FIGURE 5.8c Appearance of an implant where the soft tissues have grown over the transcutaneous section, from a medial aspect.

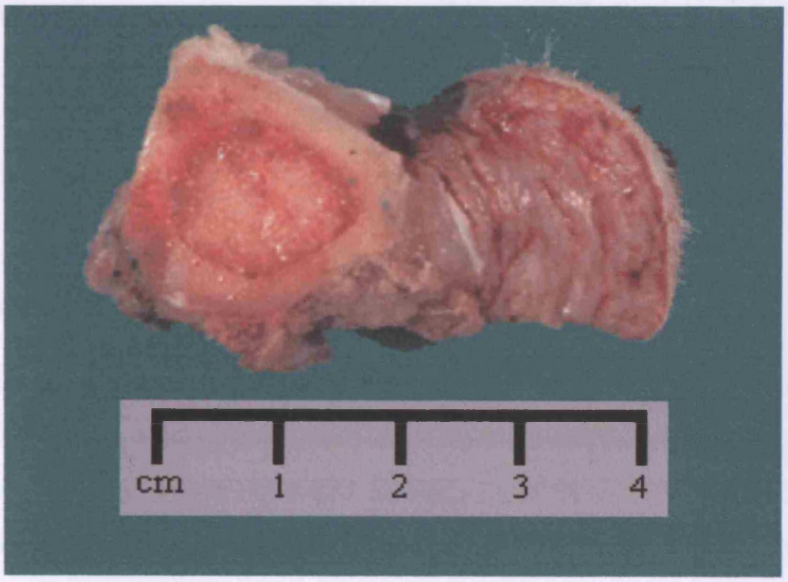

FIGURE 5.8d Tissue section form 5.8c in transverse section.

5.2.3 HISTOLOGY PROCESSING

For preparation of hard tissue sections, following 10% formal saline fixation for 8-10 days, the tissue samples were dehydrated in an ascending alcohol series (30, 50, 70, 90 and 100%) and washed in chloroform to achieve fat clearance, prior to impregnation and casting in LR White hard grade acrylic resin (Agar Scientific Ltd). The samples were then cut longitudinally through the centre of the implant and thin sections (70-100μ) were prepared from the cut surface, using an Exakt 310 band cutting system with a 0.2mm diamond cutting band, and an Exakt 400cs grinder and polisher. The sections obtained were stained with toluidine blue and paragon for soft tissue and bone respectively.

For tissue samples where the soft tissues had overgrown the transcutaneous section of the implant, the longitudinal centre pin cut position was established by x-raying the tissue samples once embedded in acrylic resin, for four minutes at 40 kilovolts and 5 mill amperes.

From the developed x-ray, the position of the pin within the tissue and resin block could be established and the central cut could be made without the ability to visualise the pin within the block itself.

Once stained, the sections were mounted and covered with glass cover slips prior to light microscopy and image analysis assessment. Light microscopy was used to qualitatively analyse the morphology of the transcutaneous interface, whilst image analysis was used for quantitative analysis.

5.2.4 IMAGE ANALYSIS

The Zeiss KS 300 Image Analysis System (Release 3.0) was used to measure values from each section for epithelial downgrowth, epithelial layer thickness and amount of epithelial layer attachment, soft tissue (sub-epithelial dermal) layer thickness and soft tissue layer attachment – see Figure 5.9. Drawing and measuring a line from the skin surface to the position at which the epithelium was observed to end at the epithelial layer – implant interface, was the method employed to measure epithelial downgrowth. A line was used to measure the thickness of the epithelial and sub-epithelial tissue layers, and the percentage of the layers contacting the implant surface was calculated using the line method. The values from both the left and right sides of each implant were taken, and the results were analysed statistically.

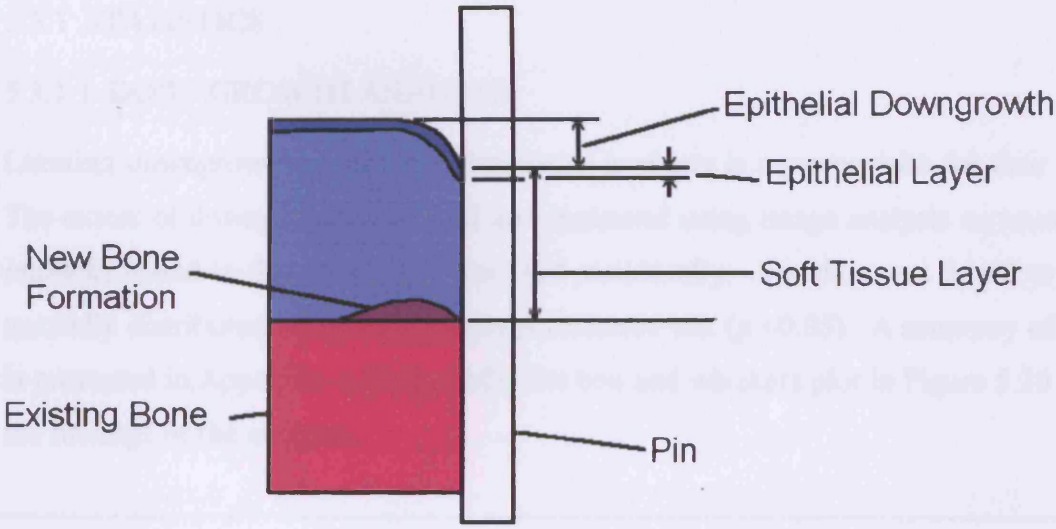

FIGURE 5.9 Schematic showing the values obtained from each transcutaneous pin using Image Analysis.

5.2.5 STATISTICAL ANALYSIS

The data obtained was analysed statistically using SPSS software. The values for downgrowth, percentage epithelial layer and percentage sub-epithelial soft tissue layer attachment were examined. The data was found to be non-normally distributed using Kolmogorov-Smirnov tests. For multiple comparative analysis of each pin type data set, a Kruskal-Wallis H test was used. If the p value obtained for the test was less than or equal to 0.05, then it was assumed that at the 0.05 level of significance there was enough evidence to conclude that there was a significant difference among the groups based on the test rank scores, showing a significant variation across groups. Pair-wise Mann Whitney U tests were used to further determine individual differences. Spearman R (nonparametric equivalent to standard correlation coefficient analysis) was used to determine the nature of relationships between downgrowth and percentage epithelial layer attachment, and between downgrowth and percentage sub-epithelial layer attachment.

5.3 RESULTS

5.3.1 STATISTICS

5.3.1.1 DOWNGROWTH ANALYSIS

Limiting downgrowth around transcutaneous implants is a prerequisite for their success. The extent of downgrowth observed and measured using image analysis surrounding the implants tested in this thesis was analysed statistically. The data was found to be non-normally distributed using a Kolmogorov-Smirnov test ($p < 0.05$). A summary of the data is presented in Appendix 4 (4.1), whilst the box and whiskers plot in Figure 5.10 presents the findings of the analysis.

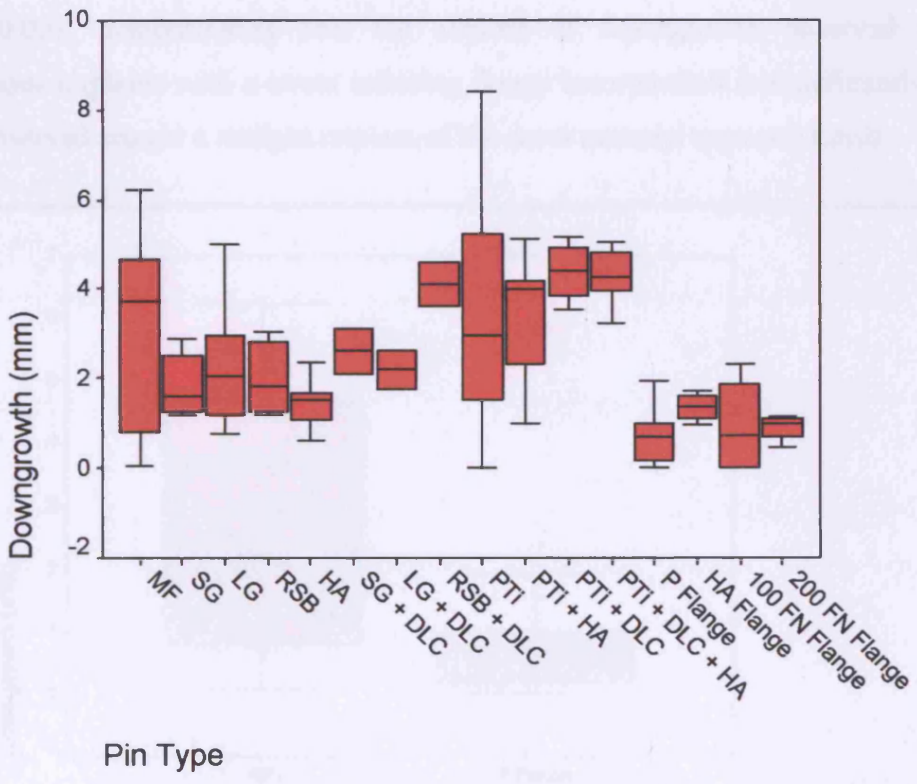

FIGURE 5.10 Box plot of data obtained for degree of downgrowth (mm) surrounding the transcutaneous pins tested. Key: MF = Machine Finished, SG = Small Grooved, LG = Large Grooved, RSB = Rough Shot Blasted, HA = Hydroxyapatite Coated, DLC = Diamond-like Carbon, PTi = Porous Titanium, P Flange = Plain Flange, 100 FN Flange = 100μg Fibronectin Coated Flange.

From the box plot, it is visually evident that the flanged implants present with lesser degrees of downgrowth than the straight pin design, irrespective of the coatings applied. A Kruskal-Wallis H test multiple comparative analysis was used to determine that at the 0.001 level there is a significant difference in downgrowth observed around all of the pin types tested based on the test rank scores ($p = 0.000$).

Pair-wise Mann Whitney U tests were then used to determine whether a difference in downgrowth is observed around straight and flanged implants of the same material type to determine the effect of the stress reducing flange in terms of limiting downgrowth. The data for the straight machine finished and the plain flanged implants were compared to determine the effect of altering implant design. Figure 5.11 shows a box and whiskers plot of the extent of downgrowth surrounding the two machine finished implant designs. The data was subjected to a pair-wise Mann Whitney U test which presented with a p value of 0.001, demonstrating that the amount of downgrowth observed around transcutaneous implants with a stress reducing flange incorporated is significantly lower than that observed around a straight implant of the same material type and finish.

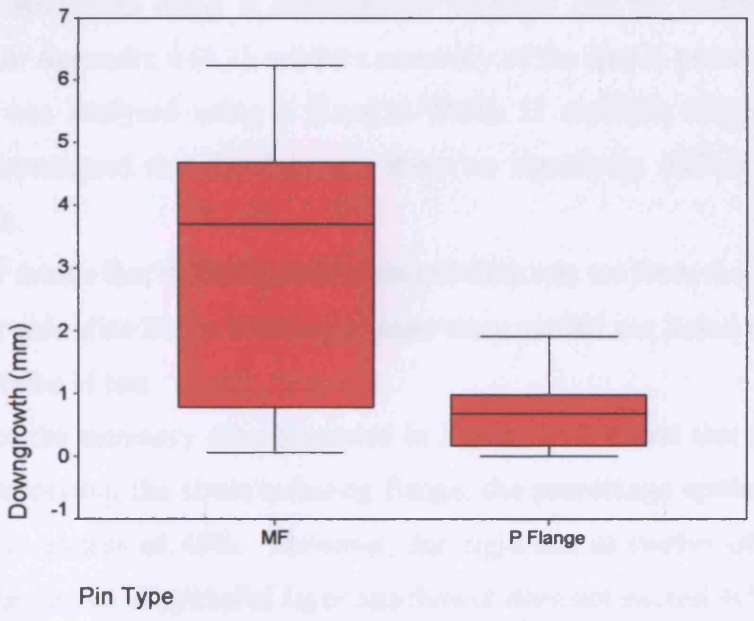

FIGURE 5.11 Box plot of the data obtained for the degree of downgrowth observed surrounding machine finished titanium transcutaneous pins of straight and flanged designs.

Pair-wise Mann Whitney U tests were used to determine that no significant differences in downgrowth are observed surrounding machine finished and straight implants of all other surface topographies and coatings ($p > 0.05$). For the straight porous pins, an HA coating with or without an external DLC coating did not significantly alter the extent of downgrowth observed ($p > 0.05$). However the incorporation of a flange into the implant design resulted in a significant decrease in the degree of downgrowth surrounding the transcutaneous implants ($p < 0.01$). Plain flanged implants evoke significantly less downgrowth than all straight pin designs ($p < 0.01$), irrespective of surface finish or coating. However no significant difference between plain and fibronectin coated flanged implants is observed ($p > 0.05$).

5.3.1.2 ANALYSIS OF % EPITHELIAL LAYER ATTACHMENT

The percentage of the epithelial layer attached to the transcutaneous implants was calculated as the amount of epithelial layer immediately abutting the implant surface divided by the thickness of the epithelial layer, multiplied by one hundred. The data for percentage epithelial layer attachment did not fit the assumptions required for parametric testing - established using a Kolmogorov-Smirnov test ($p < 0.05$). The raw data is presented in Appendix 4 (4.2), whilst a summary of the data is presented in Figure 5.12.

The data was analysed using a Kruskal-Wallis H multiple comparative analysis test, which demonstrated that the data sets show no significant difference based on the test rank scores.

This result means that the independent sample data sets are from the same population.

No further pair-wise Mann Whitney U tests were carried out based on the findings of the Kruskal-Wallis H test.

The plot of the summary data presented in Figure 5.12 shows that for all of the implant types incorporating the stress reducing flange, the percentage epithelial layer attachment is always in excess of 40%. However, for eight out of twelve of the straight implant designs, the degree of epithelial layer attachment does not exceed 40%.

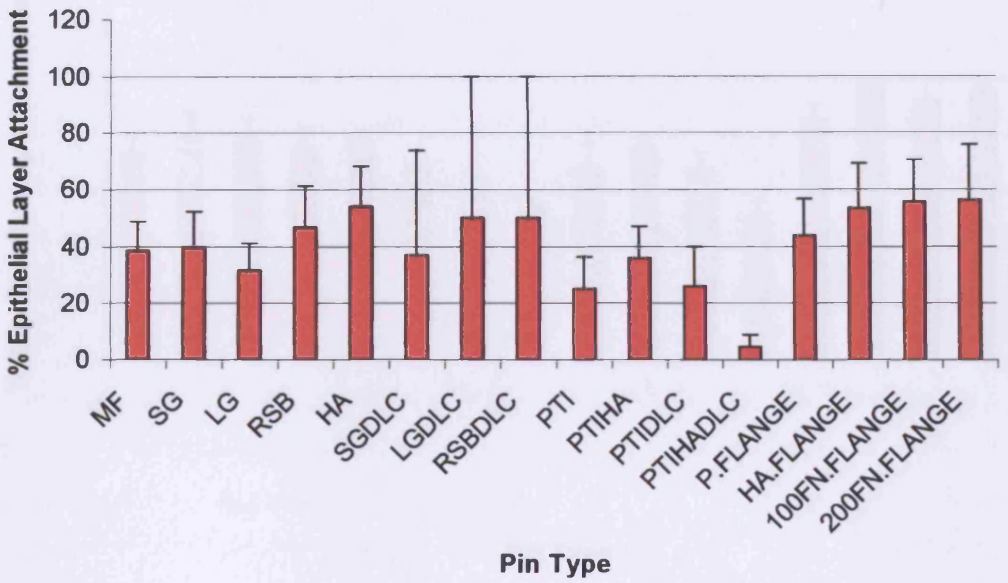

FIGURE 5.12 Graph demonstrating the % epithelial layer attachment observed surrounding the transcutaneous implants tested.

5.3.1.3 ANALYSIS OF % SUB – EPITHELIAL SOFT TISSUE LAYER ATTACHMENT

The data was found to be non-normally distributed using a Kolmogorov-Smirnov test ($p < 0.05$), and a Kruskal-Wallis H multiple comparative analysis showed that the individual sample data sets are from significantly different populations ($p = 0.004$). Appendix 4 (4.3) presents the raw data, and Figure 5.13 displays a summary of the findings.

Pair-wise Mann Whitney U tests show that flanged pins support a significantly greater degree of sub-epithelial soft tissue attachment than straight implants, irrespective of surface topographies and coatings ($p < 0.05$). No significant differences in the extent of sub-epithelial soft tissue attachment were observed between any of the straight implants tested ($p > 0.05$), nor between any of the flanged pin designs ($p > 0.05$).

The summary data for the HA coated straight and flanged implants was compared statistically, using a Mann Whitney U test, as the data did not fit the assumption required for parametric testing (Kolmogorov-Smirnov $p < 0.05$). It was found that the HA coated flanged pins supported significantly greater degrees of sub-epithelial attachment than the HA coated straight implants ($p < 0.001$). A box and whiskers plot of the data is shown in figure 5.14.

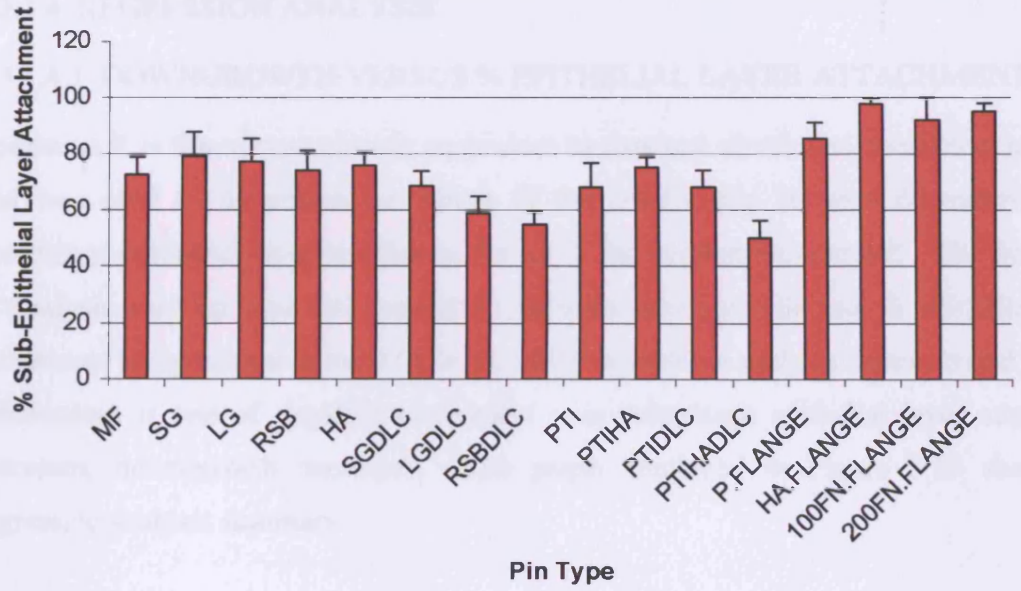

FIGURE 5.13 Graph showing the % sub-epithelial, soft tissue layer attachment surrounding transcutaneous implants.

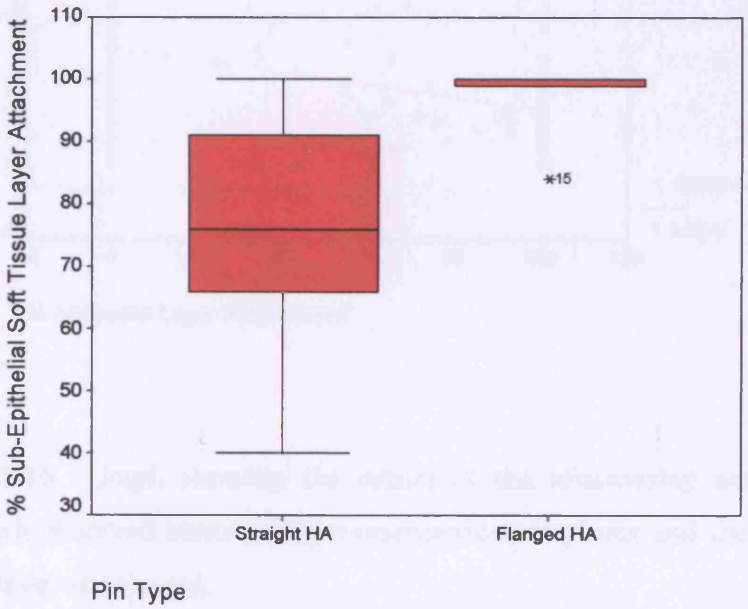

FIGURE 5.14 Box plot demonstrating the extent of sub-epithelial soft tissue layer attachment to HA coated straight and flanged implant designs.

5.3.1.4 REGRESSION ANALYSIS

5.3.1.4.1 DOWNGROWTH VERSUS % EPITHELIAL LAYER ATTACHMENT

Spearman R is the non-parametric equivalent to standard correlation coefficient analysis, and was used to determine the nature of the relationship between downgrowth and percentage epithelial layer attachment for all of the implant types tested. The Spearman R analysis showed that the correlation between downgrowth and % epithelial layer attachment is significant at the 0.01 level, whilst regression analysis demonstrated that the relationship is one of negative correlation – as percentage epithelial layer attachment increases, downgrowth decreases. The graph displayed in Figure 5.15 shows the regression analysis summary.

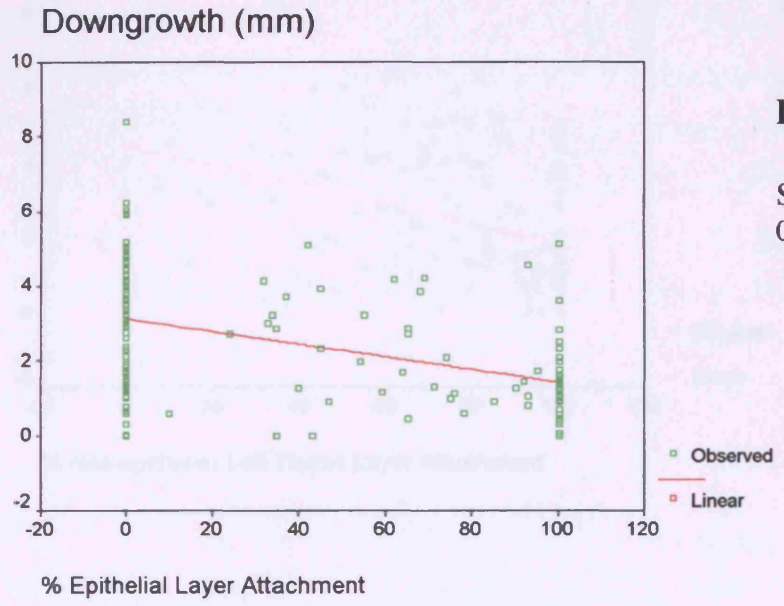

FIGURE 5.15 Graph showing the nature of the relationship between the degree of downgrowth observed surrounding transcutaneous implants and the associated extent of epithelial layer attachment.

5.3.1.4.2 DOWNGROWTH VERSUS % SUB - EPITHELIAL LAYER ATTACHMENT

Spearman R standard correlation coefficient analysis, and was used to determine the nature of the relationship between downgrowth and percentage sub-epithelial layer attachment. A significant negative correlation between the extent of downgrowth observed surrounding transcutaneous implants and the degree of sub-epithelial dermal fibroblastic layer attachment was established and was found to be significant at the 0.01 level. Figure 5.16 demonstrates the nature of the relationship.

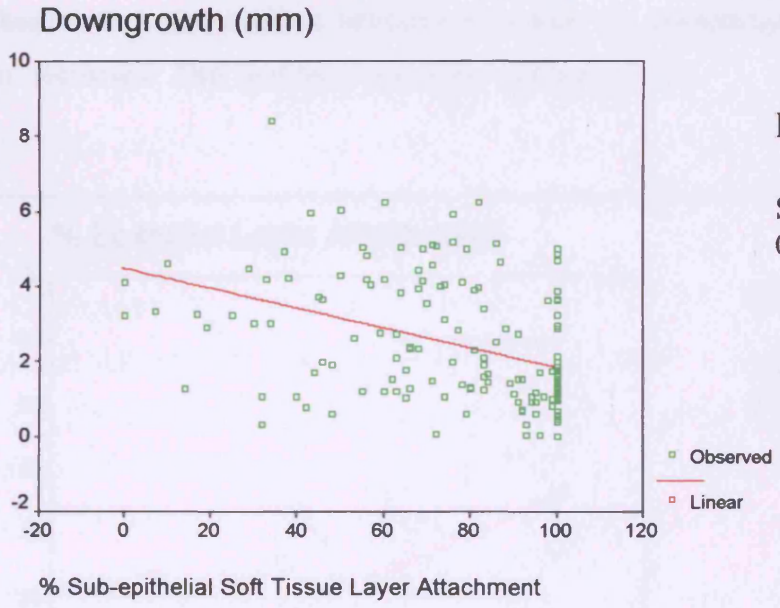

FIGURE 5.16 Graph demonstrating the relationship between downgrowth and percentage sub-epithelial soft tissue attachment observed around transcutaneous implants.

5.3.1.4.3 % EPITHELIAL LAYER ATTACHMENT VERSUS % SUB-EPITHELIAL LAYER ATTACHMENT

It has been observed that the extent of adhesion of both soft tissue layers abutting transcutaneous implants significantly influences the degree of downgrowth observed. It was hypothesised that the degree of sub-epithelial dermal fibroblastic tissue adhesion ultimately determines the amount of downgrowth and epithelial layer attachment. To test this hypothesis, the relationship between the amount of adhesion of the epithelial and sub-epithelial layer was tested using Spearmans R and regression correlation analysis. It was established that there is a significant positive correlation between the two variables at the 0.01 level. This demonstrates that as the percentage of sub-epithelial dermal fibroblastic tissue adhesion to transcutaneous implants increases, the percentage of epithelial layer attachment increases. This finding is presented in Figure 5.17.

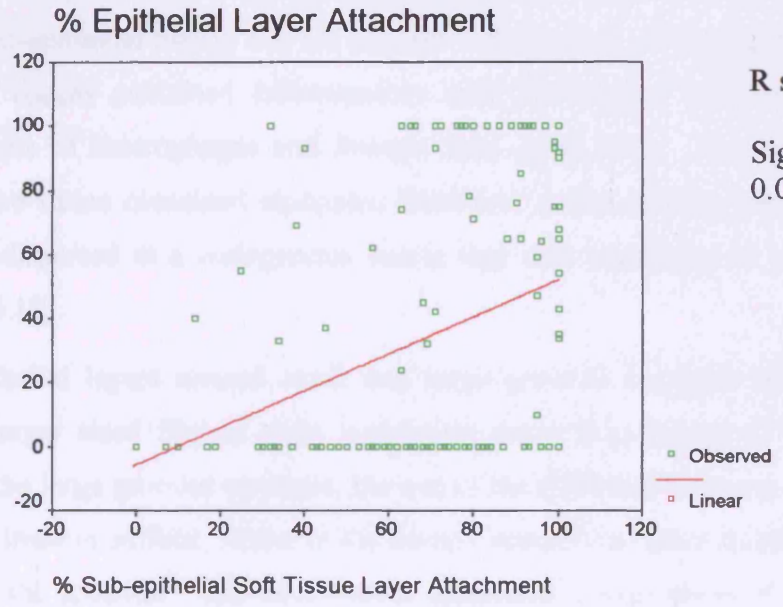

FIGURE 5.17 Graph demonstrating the nature of the relationship that exists between the amount of sub-epithelial dermal fibroblastic tissue and epithelial layer attachment to transcutaneous implants.

5.3.2 HISTOLOGICAL ANALYSIS

Host tissues surrounding straight implants with standard orthopaedic finishes (machine finished, small and large grooved, shot blasted and HA coated), displayed no signs, which could result in total implant failure. In most cases the epidermis was observed to migrate from the cut edges beneath the resulting blood clot and fibrinous exudate, vertically down between the cut dermal surface and the implant. The epidermal layer migration into the dermis was of varying depth, but was greatest surrounding machine finished implants. A contact between the dermis and the implant surface was observed at some point for every implant examined, hence a tract directly from the external environment to the host bone was avoided in all cases.

Downgrowth around machine-finished implants was observed in all cases. The epithelial layer was seen to stop within the host sub-epithelial tissues, and was never found to be in close association with the implant surface. A dense non-fibrous clot was observed between the epithelial downgrowth and the implant, which dispersed when an attachment of the sub-epithelial tissues and the implant was formed. At the three-phase junction, the adjacent tissues contained inflammatory cells, principally lymphocytes, with smaller populations of macrophages and foreign body giant cells. The matrix of the dermal connective tissue contained elongated fibroblast nuclei running parallel to the implant surface, dispersed in a collagenous matrix that was organising in a similar orientation (Figure 5.18).

The epithelial layers around small and large grooved implants were seen to migrate around larger sized fibrous clots, supporting dense populations of inflammatory cells. Around the large grooved implants, the end of the epithelial layer was in close apposition with the implant surface, whilst in the dermal connective tissue attachment was sporadic between the grooves. The host tissues supported a population of inflammatory cells mainly concentrating around the three-phase junction. However, the density was lower than that observed within the external fibrous exudate (Figure 5.19). The small grooved implants did not support attachment of the host epithelial or dermal tissues. The end of the epithelial layer was free from the pin surface and generally obscured by the fibrous exudate. The connective tissue of the dermis was rarely observed to attach to the groove troughs, but generally contacted the peak regions of the implant surface over small areas (Figure 5.20). The tissues contained a high density population of lymphocytes, macrophages, foreign body giant and other multi-nucleated cells.

A DLC coating applied to the small and large grooved implant appeared to increase the degree of downgrowth observed around the pins. However, it did not alter the morphology of the tissue contact regions. When poorly positioned, the DLC surface was immediately abutting the epithelial and sub-epithelial tissues resulting in further migration of the epithelial cut surface. In these cases even the large grooved implants demonstrated a lack of epithelial layer attachment, with the end of the basement membrane observed within the exudate. In one slide, a small section of ectopic bone was observed immediately adjacent to the exudate-implant interface. The epithelial layer was seen to cease in this region and intimately associate with the bone surface (Figure 5.21).

HA coating of straight implants supported improved dermal connective tissue integration. A layer of dense connective tissue was observed immediately adjacent to the HA coating, which was clearly different from the surrounding layers of the dermis (Figure 5.22). The layer abutting the implant surface was more darkly stained and supported a large population of lymphocytes and macrophages. However, elongated and oval fibroblast nuclei were well organised within a collagenous matrix that was observed to run perpendicular to the HA coating. The surrounding layers possessed defined zones of tissue containing mainly rounded fibroblast nuclei with randomly orientated collagen matrices and fewer inflammatory cells, interspersed with occasional adipocytes and fluid filled vacuole-like regions.

Shot blasted implants generated a degree of downgrowth similar to that observed for other straight pin types. The amount of dermal tissue contacting the pin was reduced and in most cases the collagenous fibres were adopting a parallel orientation to the pin surface. An exudate was observed at the skin – implant interface and the tissue close to the implant surface was rich in inflammatory cells, including lymphocytes, macrophages and foreign body giant cells. Pockets of high density lymphocytic populations became more prominent towards the epithelial-implant interface. Application of an external DLC coating produced an increase in downgrowth and a decrease in sub-epithelial layer attachment when the DLC segment of the implant was positioned abutting the host tissues.

The degree of downgrowth associated with porous titanium coated implants was greater than that observed surrounding straight implants with standard orthopaedic finishes. The tissue immediately below the keratinised epithelial layers contained numerous vacuoles,

epithelialised pockets and small reservoirs of lymphocytes. Debris was observed to be encapsulated within epithelial invaginations and were surrounded by densely populated

lymphocytes. The cut surface of the epithelial layer was found to be in association with the exudate rather than the surface of the implant and the surrounding tissue contained a large number of lymphocytes and macrophages and a small number of foreign body giant cells. Below the epithelial layer, large empty spaces were observed between the surface of the porous titanium and the dermal tissue, which were interrupted by dermal tissue in intimate contact with the implant surface. The tissue immediately abutting the implant surface contained numerous lymphocytes, macrophages and foreign body giant cells, whilst the collagenous ground substance was disorganised with round, oval and elongated fibroblast nuclei interspersed in no definable orientation (Figure 5.23).

The epidermal and dermal layers approaching hydroxyapatite coated porous titanium implant are vacuolated and contain reservoirs of lymphocytes immediately below the basement membrane. Clotting obscured the epithelial – implant interface of some implants. However, the soft tissue of the dermis was found to be closely adhered to the HA surface and a small number of inflammatory cells were observed within the poorly organised collagenous matrix. In other sections, the epithelial layer was found to be in complete contact with the implant after a degree of downgrowth, and beneath this attachment a more organised collagenous dermal ground substance was seen, supporting more oval and elongated fibroblast nuclei (Figure 5.24). An externally applied DLC coating appeared to have the same effect as that observed on previous implant types. The positioning of the DLC in relation to the surrounding tissues determined the degree to which downgrowth and attachment parameters were affected. Where the DLC coating had been implanted abutting the host tissues, an increased degree of downgrowth was seen and the dermal tissues contained a large population of inflammatory cells, including lymphocytes, macrophages and foreign body giant cells. The cut surface of the epithelial layer was not attached to the implant surface and the underlying dermal tissues were more fatty in nature with large pockets of inflammatory cells and infiltrate (Figure 5.25).

The plain flanged implants produced a clear reduction in epithelial downgrowth, which was either eliminated by epithelial layer attachment to the implant surface, or where the epithelial layers cut surface was free within an exudate which had been invaded by fibrous tissue, and was actively remodelling a new tissue-implant interface (Figure 5.26). The dermal tissues were found to be in complete contact with the implant surface, including the flange portion, for almost all implant sections examined. The sub-epithelial layers were not vacuolated and did not contain pockets of large numbers of lymphocytes. Instead a few inflammatory cells were dispersed within the matrix of organising collagenous ground substance (Figure 5.26). The findings for HA coated flanged

implants were comparable to those of the plain flanged pins. The epithelial layers were found to be intimately associated with the pin surface, and the dermal tissues with the HA coating. Some macrophages and lymphocytes were present in the tissues surrounding the epithelial layer-implant interface, but were not as evident in the surrounding dermal tissues (Figure 5.27). The fibronectin coated flanged implants produced an interface similar to those observed for the other flanged implants tested. The epithelial layer was in contact with the pin surface, and the tissue immediately adjacent supported a population of inflammatory cells. Dermal tissues were usually in complete contact with the implant surface and contained fewer inflammatory cells than the epithelium immediately abutting the attachment site (Figures 5.28 and 5.29).

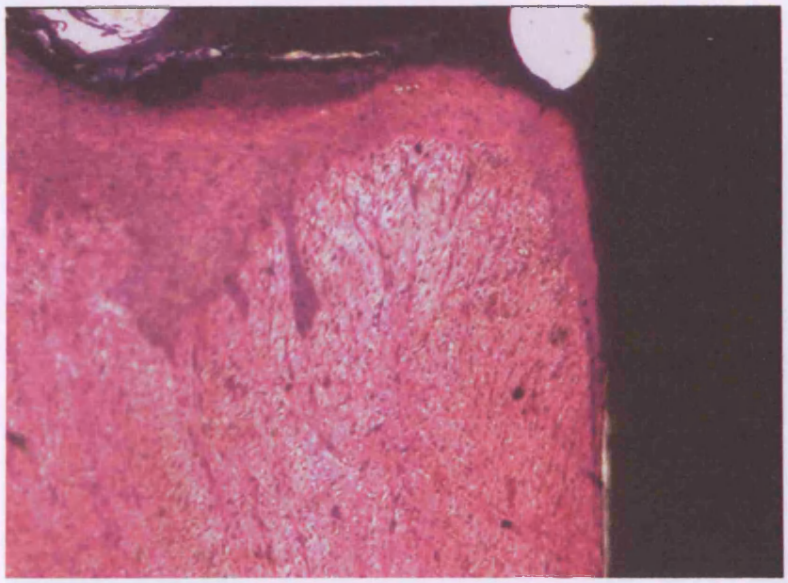

FIGURE 5.18c Downgrowth around clot and free end of epithelial layer between dermal tissues and implant surface at a magnification of x40.

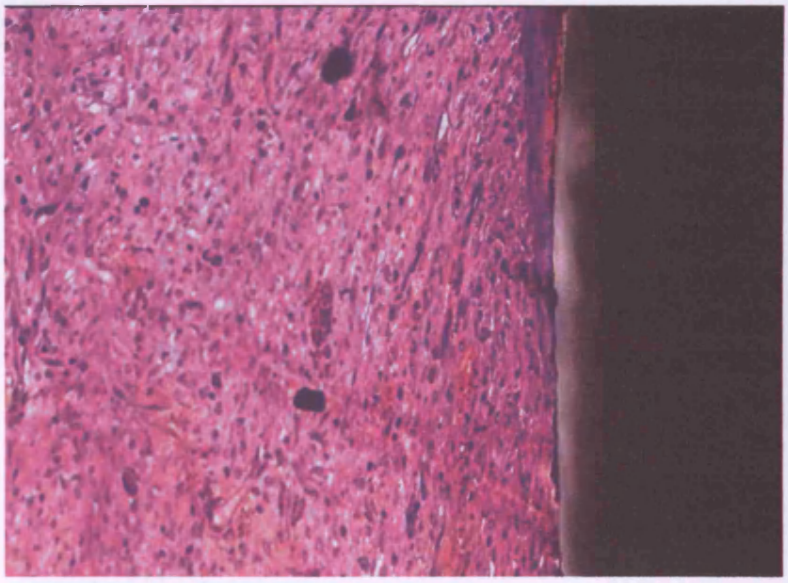

FIGURE 5.18d The free end of the epithelial layer seen in 5.18c at a magnification of x100. The epithelial cell layer has not been arrested by sub-epithelial dermal tissue adhesion.

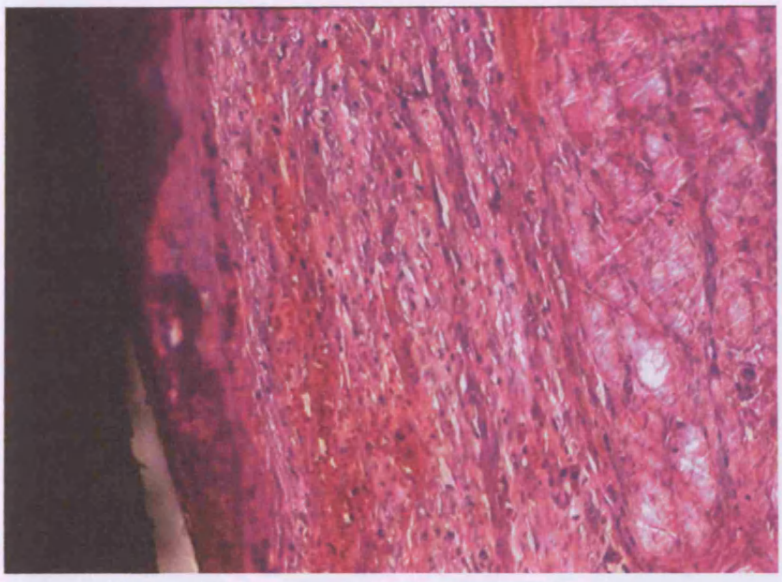

FIGURE 5.18e Dermal tissues adjacent to the end of the epithelial layer harbouring a small reservoir of inflammatory cells, predominately lymphocytes and macrophages, at a magnification of x100.

FIGURE 5.19

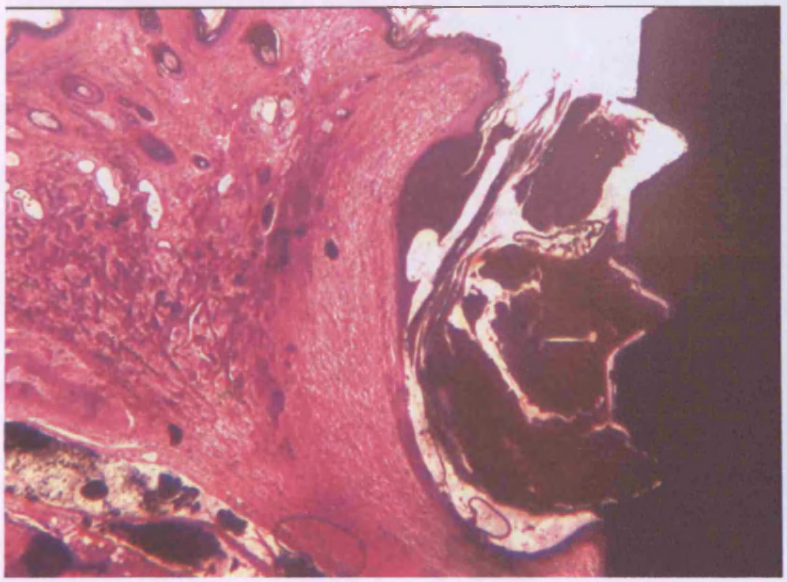

FIGURE 5.19a Downgrowth around clot associated with large grooved implant , at a magnification of x10.

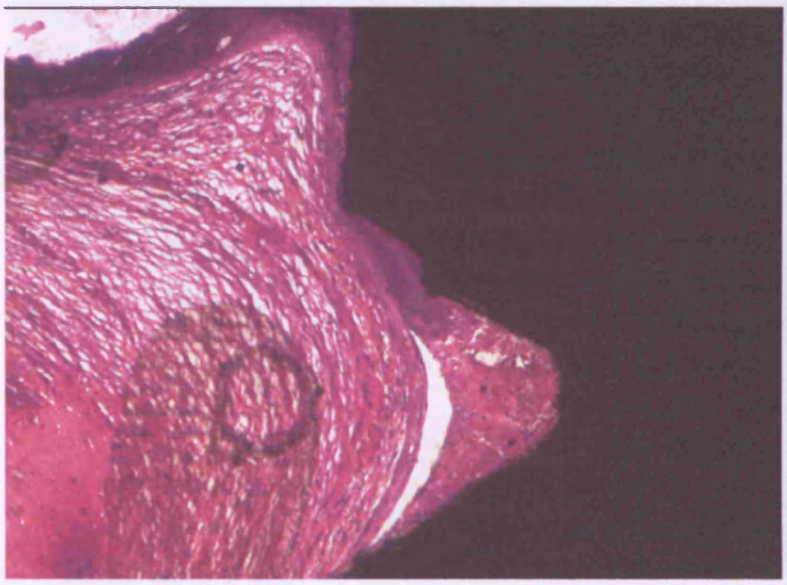

FIGURE 5.19b Displays the appearance of the end of the epithelial layer in close apposition with the implant surface, at a magnification of x40.

FIGURE 5.20

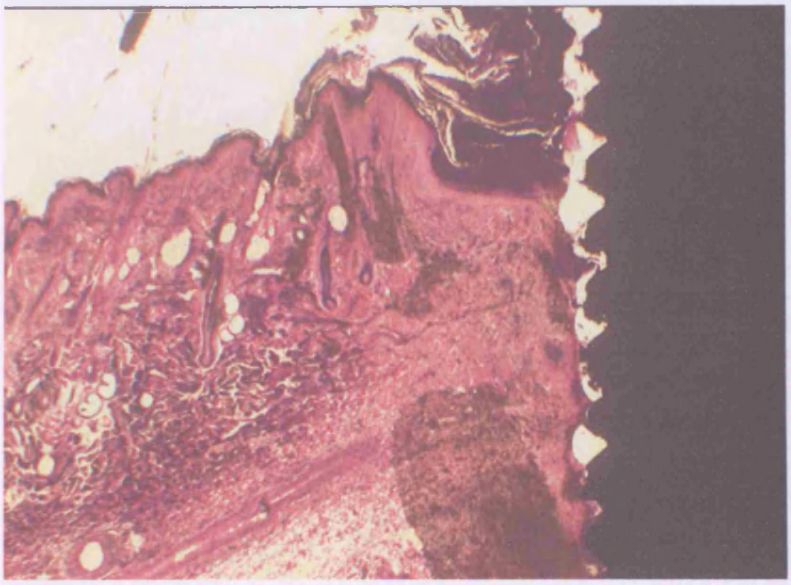

FIGURE 5.20a Demonstrates the appearance of the interface between the host soft tissues and the small grooved implant; the epithelial layer being remote from the implant surface, at a magnification of x10.

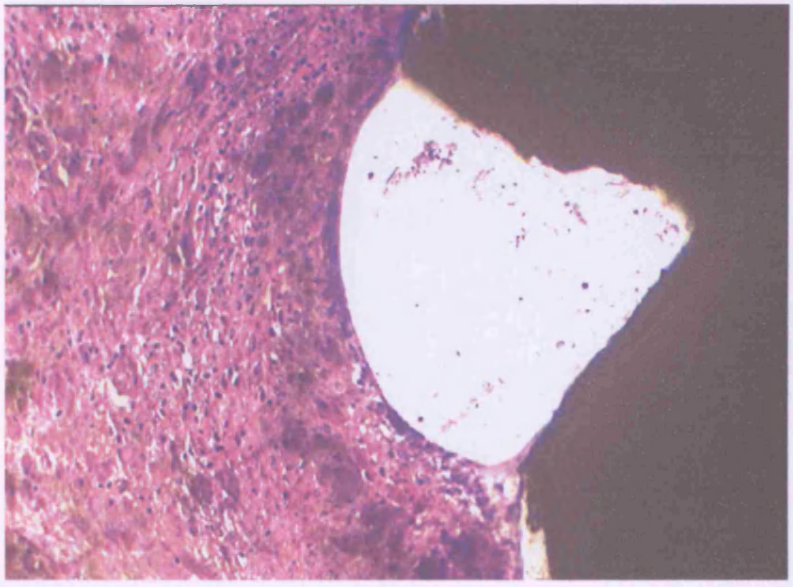

FIGURE 5.20b Shows the dermal tissues attaching to the peaks of the small grooved implants, but lacking attachment in the trough regions x100.

FIGURE 5.21

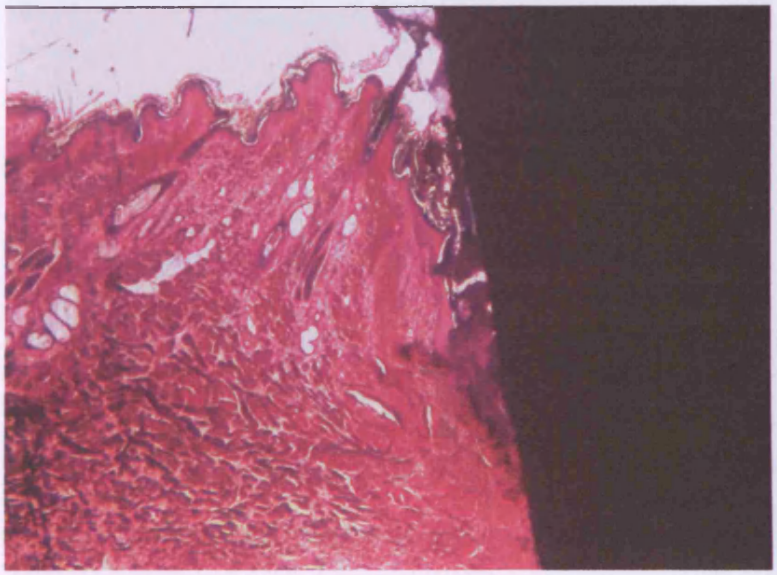

FIGURE 5.21a Demonstrates the appearance of skin layers abutting DLC coating, resulting in increased migration of the epithelial layers around exudate, at a magnification of x10.

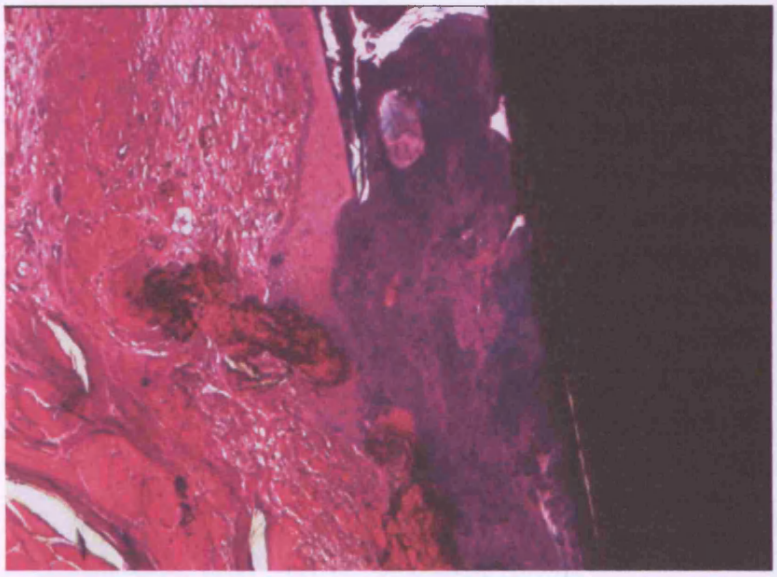

FIGURE 5.21b Shows the presence of a small amount of ectopic bone at the epithelium-exudate-implant interface, at a magnification of x40.

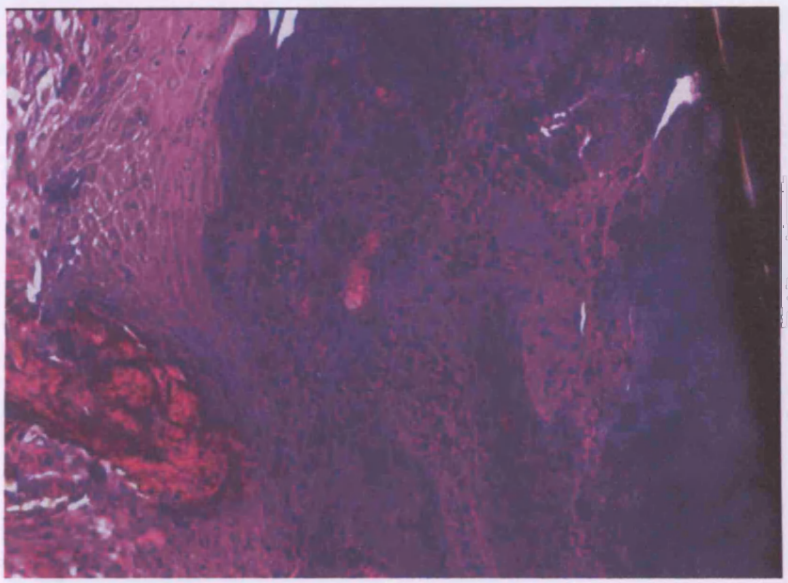

FIGURE 5.21c The end of the epithelial layer is not associated with the implant surface, however it appears to terminate at an interface with the ectopic bone segment. The adjacent exudate is rich in inflammatory cells, predominately lymphocytes, and has been invaded by fibrous tissue, resulting in a new host tissue-implant interface which does not involve the epithelial layer. Magnification x100.

FIGURE 5.22

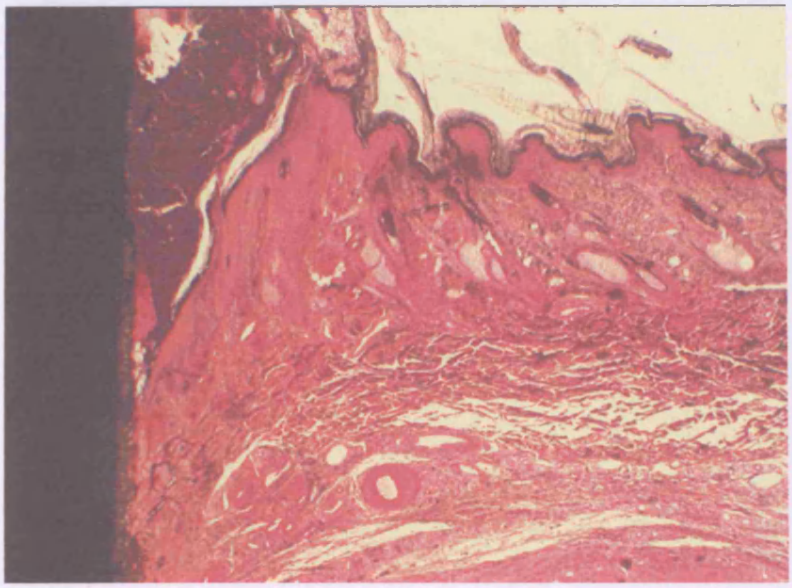

FIGURE 5.22a Demonstrates the appearance of downgrowth around an HA coated implant at a magnification of x10.

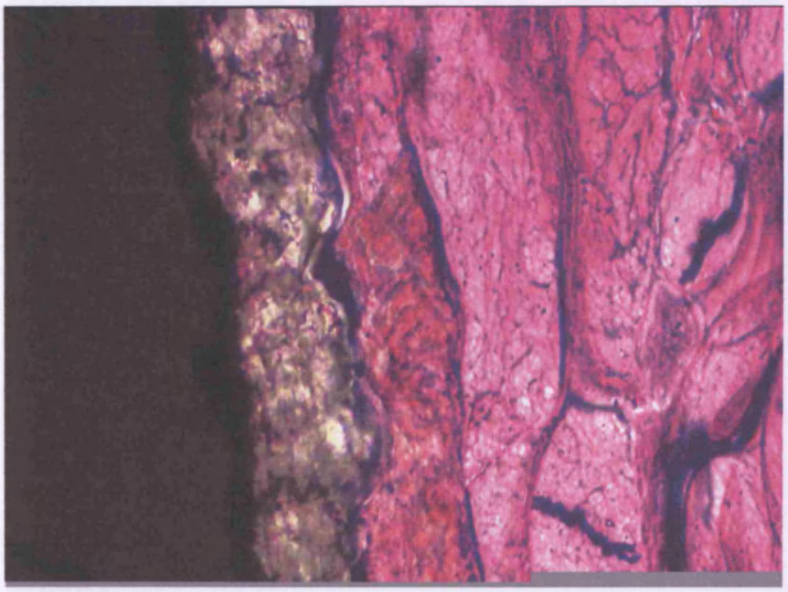

FIGURE 5.22b Shows the presence of a layer of dense connective tissue immediately adjacent to the HA coating, containing regions of calcification, at a magnification of x100.

FIGURE 5.23

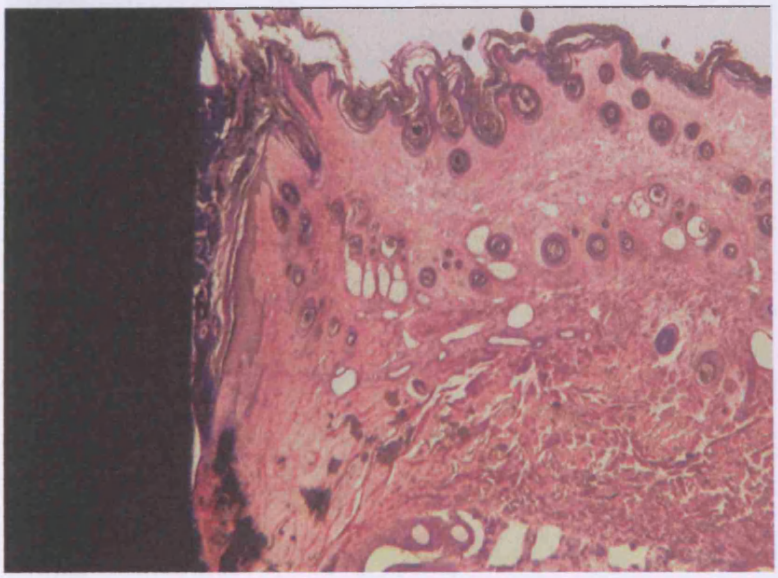

FIGURE 5.23a Demonstrates the appearance of downgrowth surrounding porous titanium implants, at a magnification of x10.

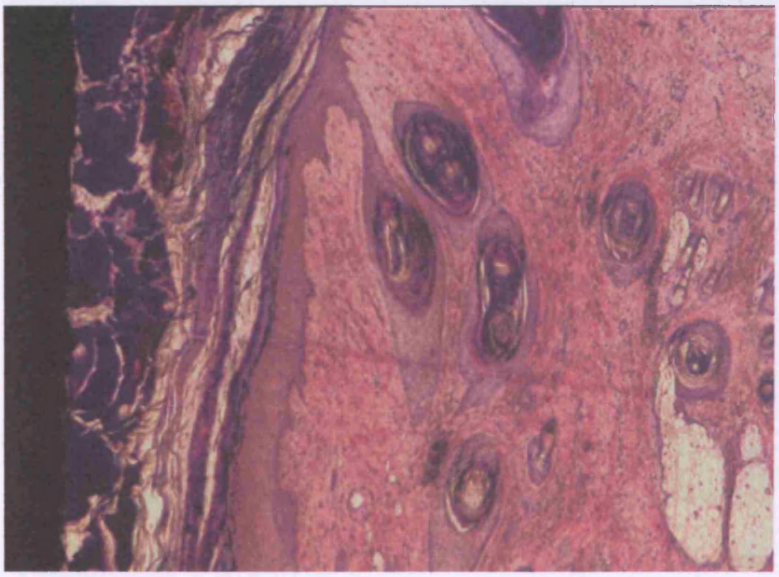

FIGURE 5.23b Shows the tissue below the epithelial layer, containing numerous vacuoles, epithelialised pockets and invagniations and small reservoirs of lymphocytes, at a magnification of x40.

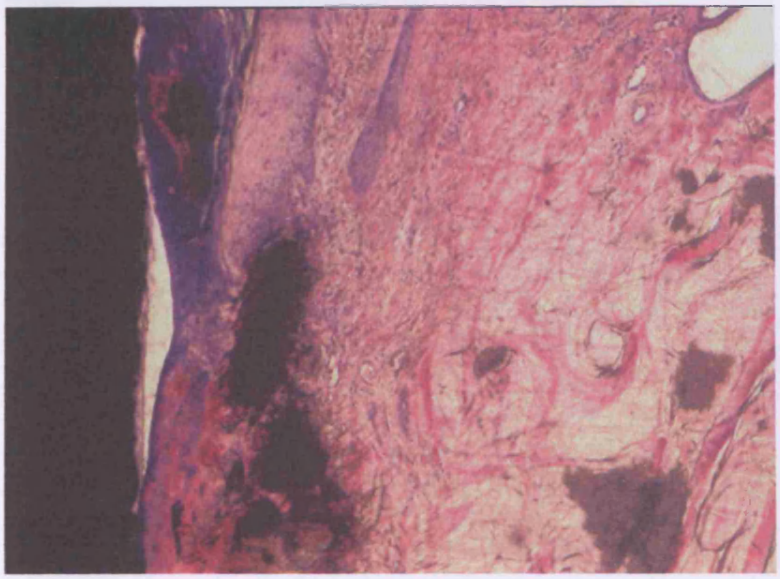

FIGURE 5.23c Displays the cut surface of the epithelial layer in association with the exudate, and not the implant surface. Magnification x40.

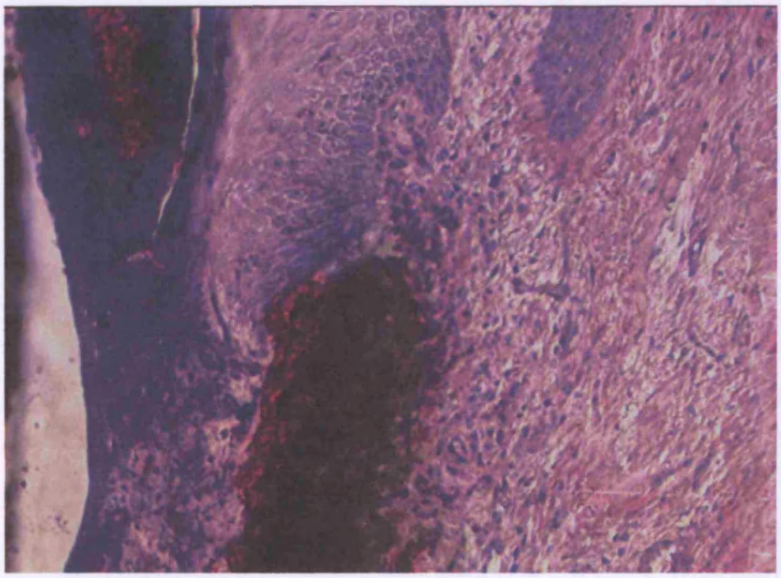

FIGURE 5.23d Shows the end of the epithelial layer from Figure 5.23c at a magnification of x100. The cut surface is free from any association with the implant surface, and terminates within a fibrous exudate, rich in inflammatory cells, principally lymphocytes and macrophages.

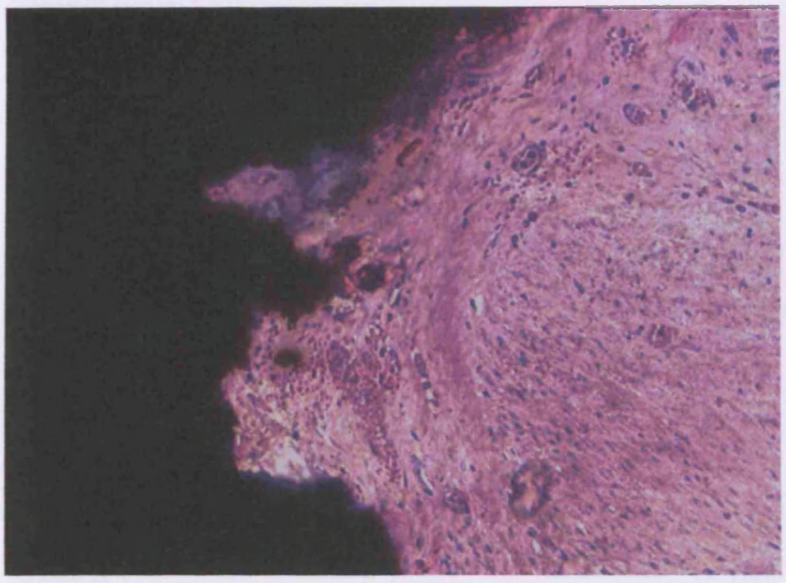

FIGURE 5.23e Shows a region of dermal tissue in intimate contact with the porous titanium coating, rich in lymphocytes and macrophages, with a lesser population of foreign body giant cells. Magnification x100.

FIGURE 5.24

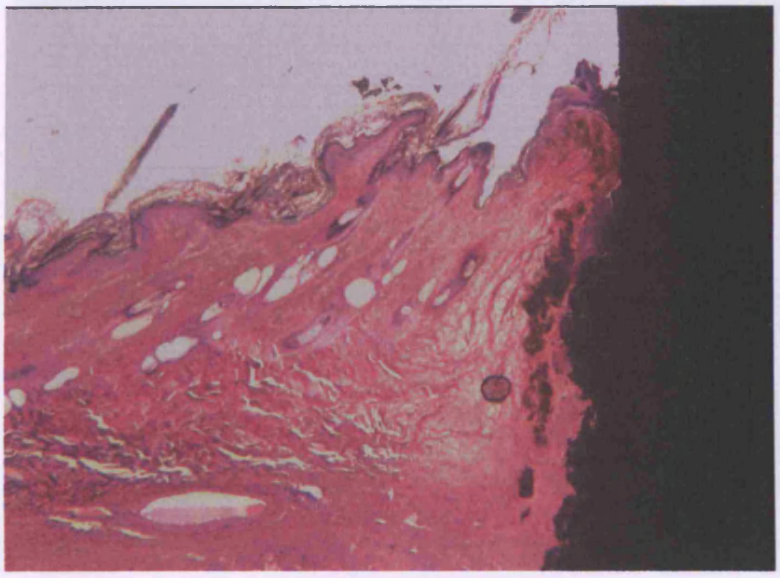

FIGURE 5.24a Demonstrates the appearance of the soft tissue – implant interface around HA coated porous titanium implants, at a magnification of x10.

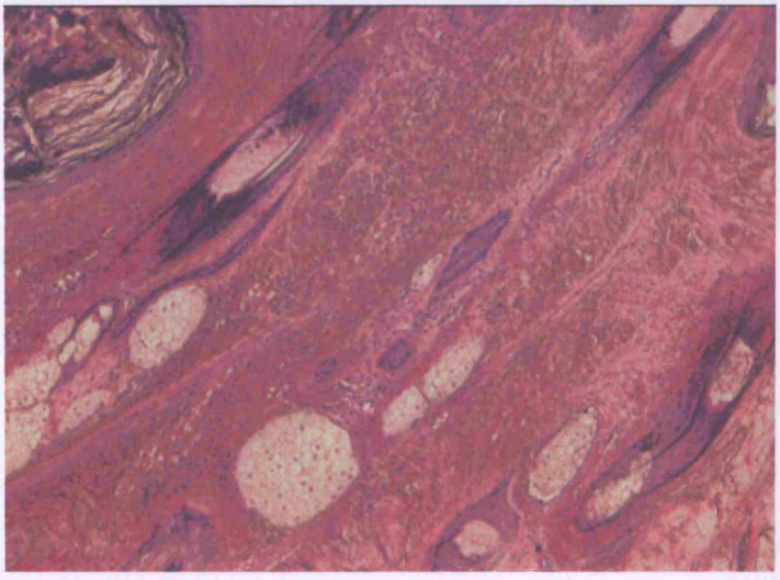

FIGURE 5.24b Shows the vacuolated tissue immediately below the epithelial layer at a magnification of x40.

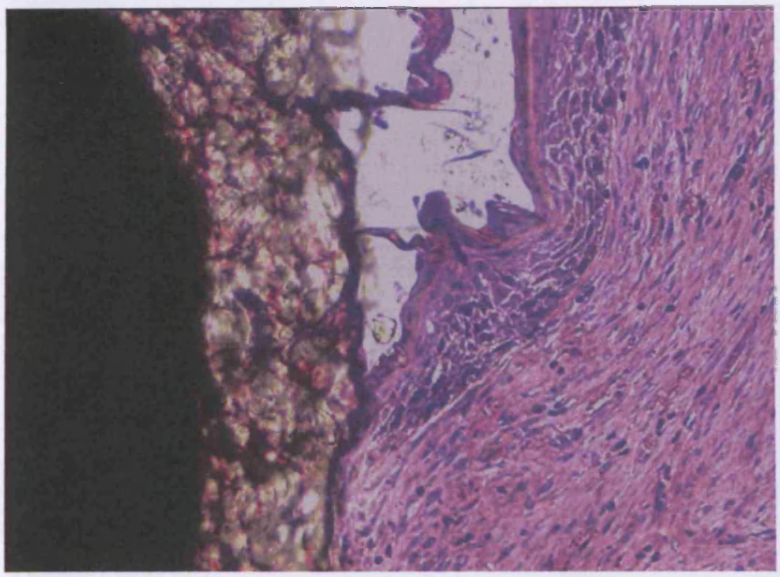

FIGURE 5.24c The epithelial layer is seen to be in complete contact with the HA porous titanium surface, below a small downgrowth with no exudate. Magnification x 40.

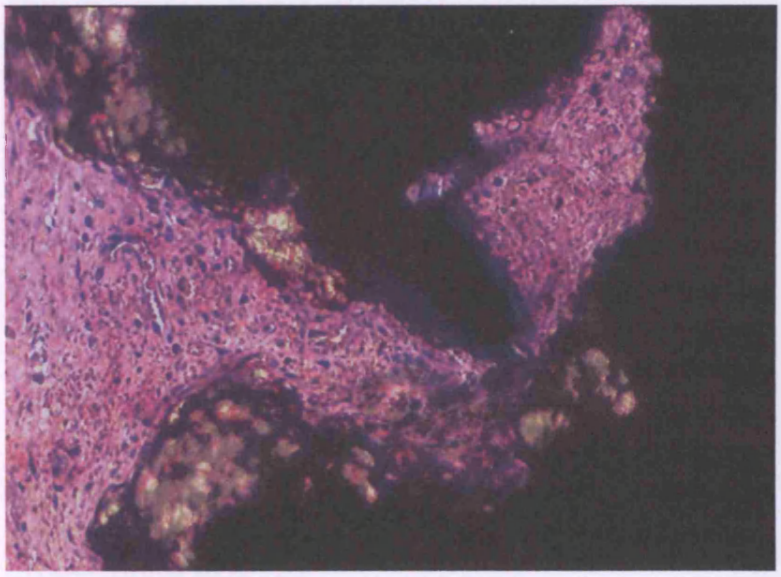

FIGURE 5.24d Shows the complete ingrowth of dermal tissues into a pore within the HA porous titanium coating, at a magnification of x100.

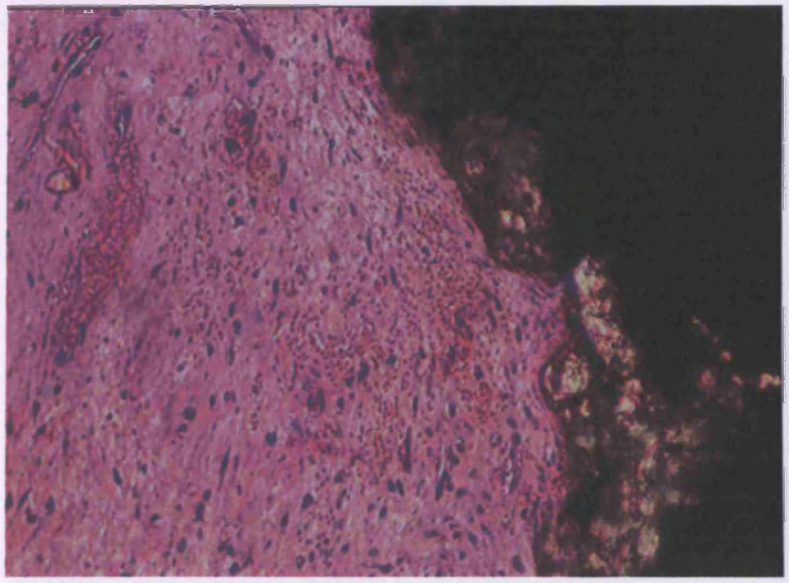

FIGURE 5.24e The dermal layers abutting the HA coated porous titanium - rich in macrophages, lymphocytes and foreign body giant cells, whose population density was observed to decrease with distance from the implant surface. Magnification x100.

FIGURE 5.25

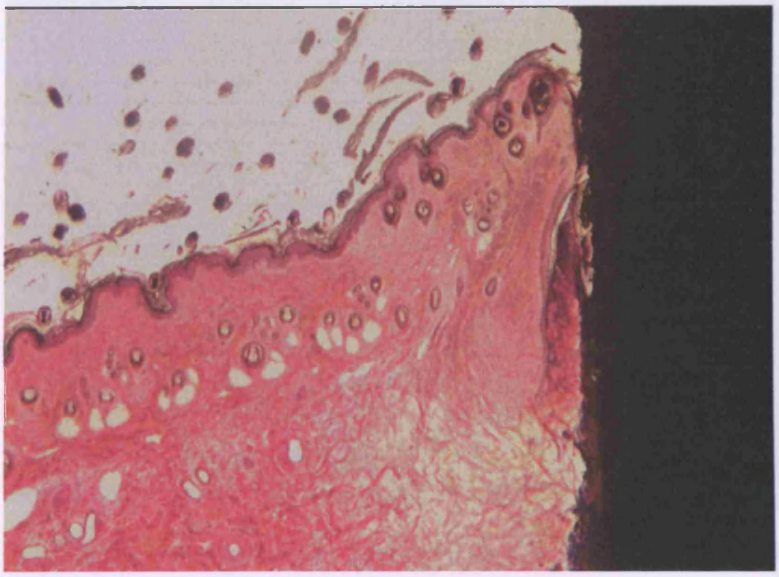

FIGURE 5.25a Demonstrates the epithelial downgrowth and dermal tissue adhesion to externally DLC coated, HA coated porous titanium implants, at a magnification of x10.

FIGURE 5.25b Shows the downgrowth path of the cut epithelial surface adjacent to the fibrous exudate and implant. The exudate contains a high density population of lymphocytes, interspersed with macrophages. Magnification x100.

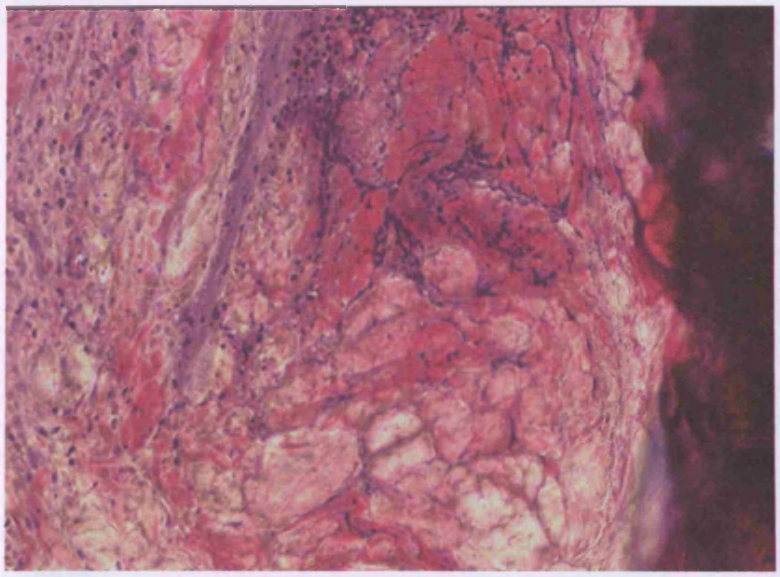

FIGURE 5.25c The end of the epithelial layer, immediately distal to 5.25b, terminates between the dermal fibroblastic tissue and the fibrous exudate – no relation to the implant surface. All tissues immediately adjacent to the implant are rich in inflammatory cells, which reduce in number with distance from the pin surface. Magnification x100.

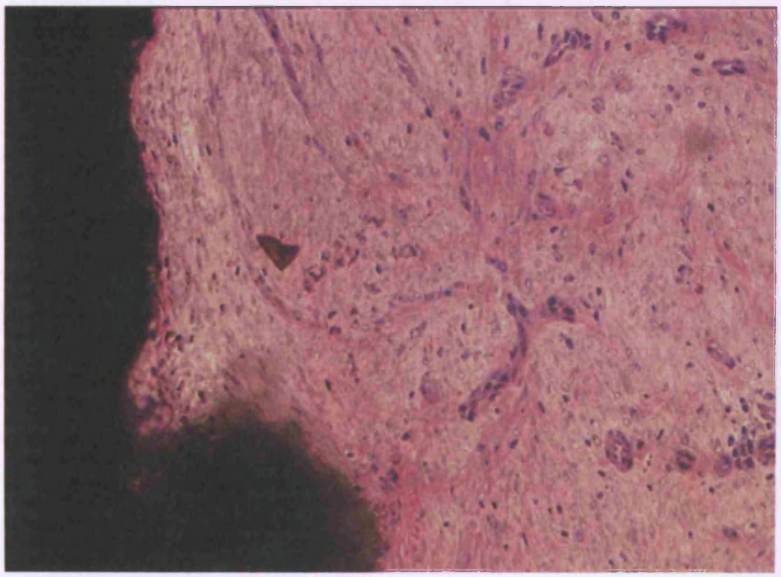

FIGURE 5.25d Demonstrates the appearance of the dermal tissues in association with the implant surface at a magnification of x100. The dermal tissues are completely in contact with the implant surface and host a large population of macrophages, lymphocytes and foreign body giant cells. The concentration of inflammatory cells reduces with distance from the implant surface.

FIGURE 5.26

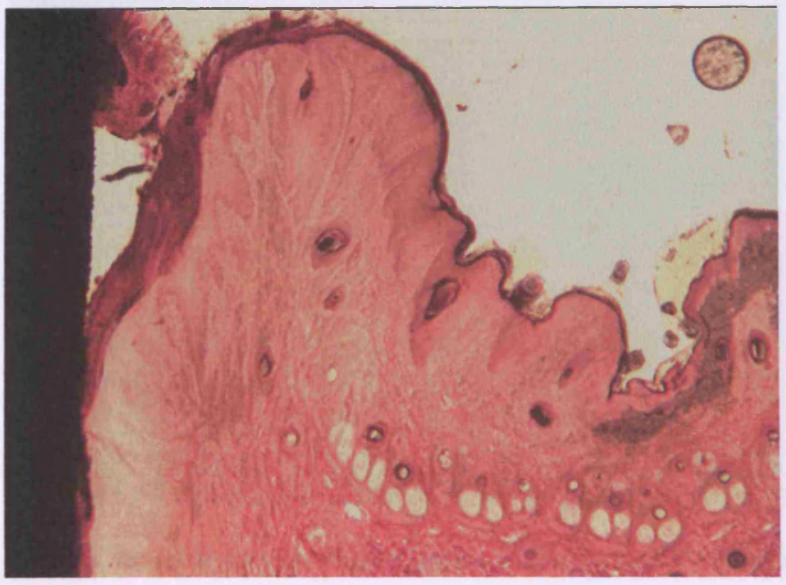

FIGURE 5.26a Demonstrates the appearance of downgrowth around a plain flanged implant. The epithelial layer migrates towards the surface of the implant, as it approaches the surface, and the downgrowth terminates at the level of the epithelial layer to the left of the image. Magnification x10.

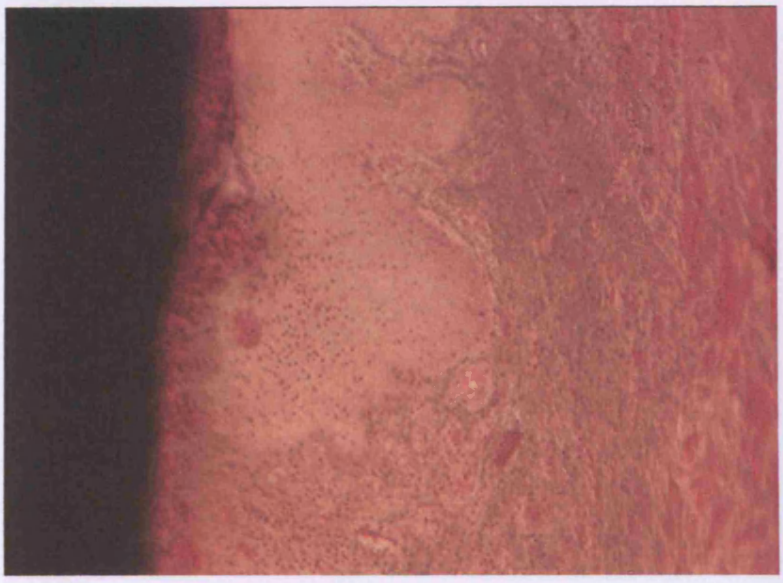

FIGURE 5.26b The epithelial layer terminates between the dermal layers and the fibrous exudate. The exudate is located immediately adjacent to the implant surface. The inflammatory infiltrate reduces in density with distance from the implant surface, but is mostly localised within the fibrous exudate, which forms a biological seal with the transcutaneous implant. Magnification x40.

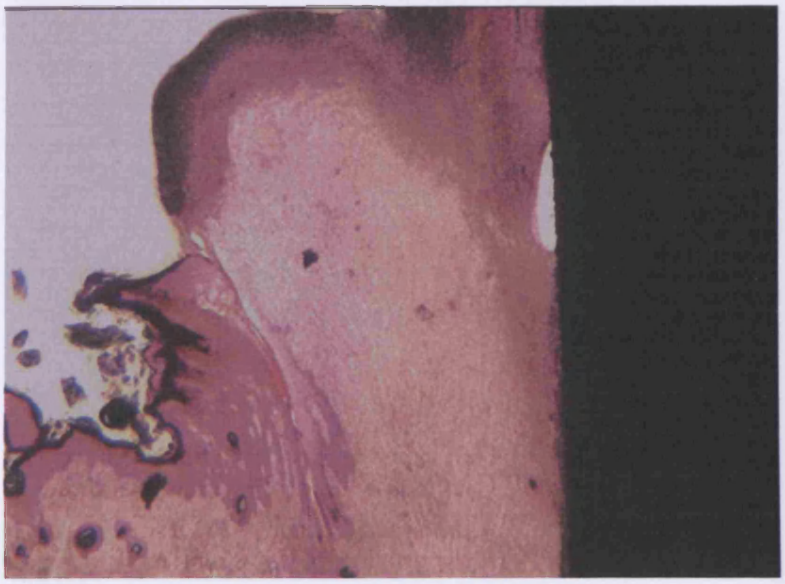

FIGURE 5.26c Displays a second example of the fibrous exudate produced immediately adjacent to the implant surface of plain flanged pins. Once again, the epithelial layer terminates within the exudate, and the area abutting the implant contains a high density population of inflammatory cells, which decrease with distance from the surface. Magnification x10.

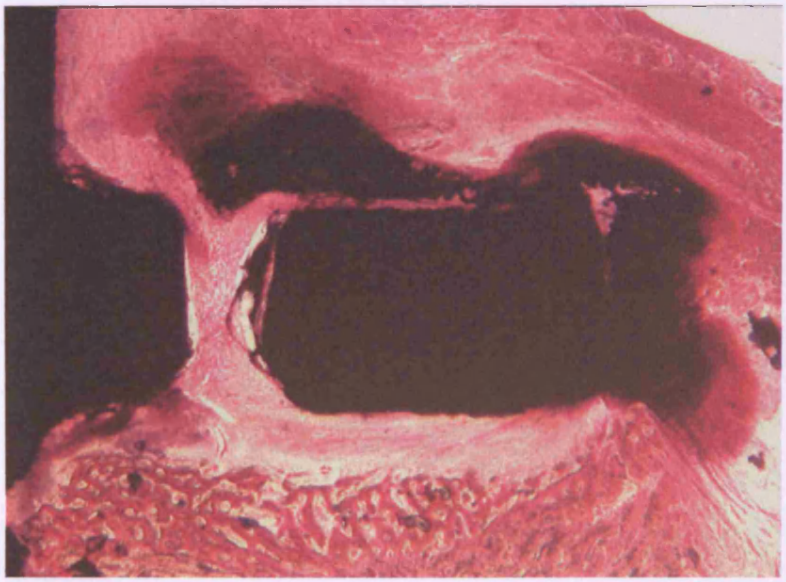

FIGURE 5.26d The dermal layers were observed to be in intimate contact with the flanged implant surface to the level of the underlying bone. Magnification x10.

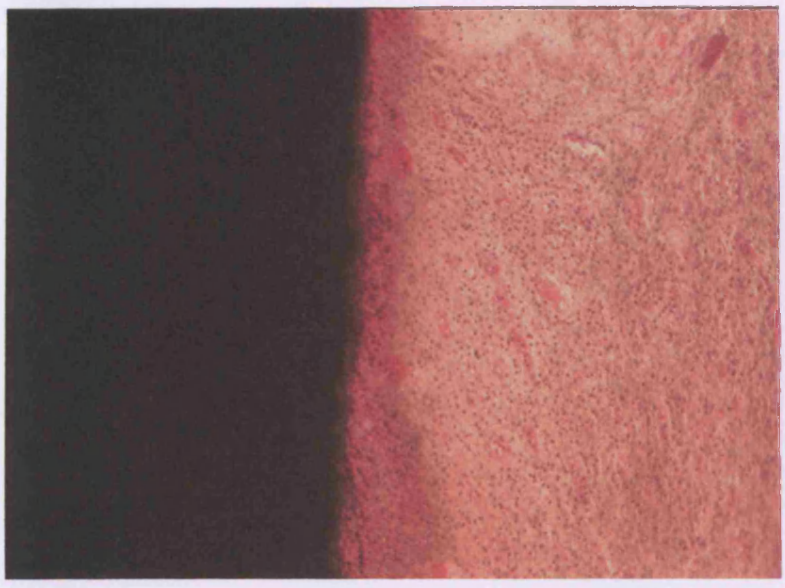

FIGURE 5.26e Beneath the end of the epithelial layer, the dermal tissues are abutting the implant surface. There is a large population of inflammatory cells, including lymphocytes, macrophages and foreign body giant cells, observed immediately adjacent to the pin surface. This layer clearly differs from the surrounding dermal tissues. Magnification x40.

FIGURE 5.27

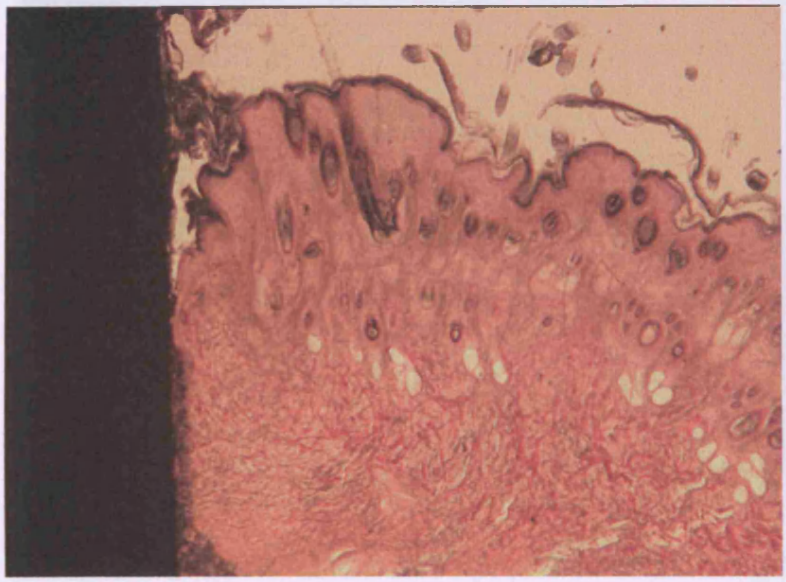

FIGURE 5.27a Demonstrates the degree of downgrowth surrounding HA coated flanged implants, at a magnification of x10.

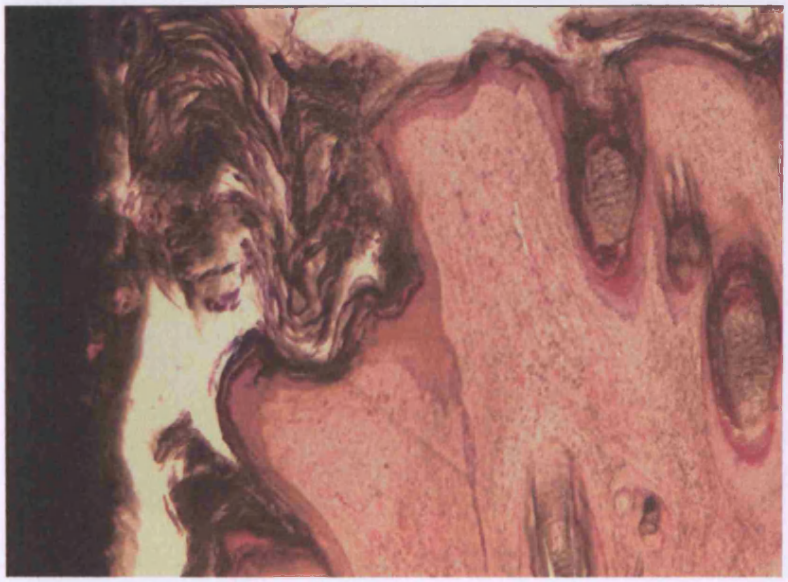

FIGURE 5.27b Shows the absence of fibrous exudate adjacent to the implant surface at a magnification of x40.

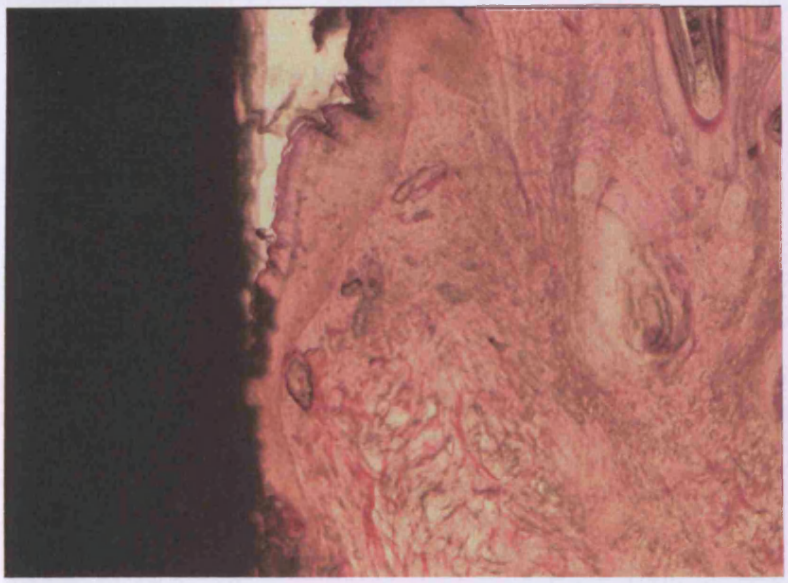

FIGURE 5.27c Shows the epithelial layer intimately associated with the pin surface, at a magnification of x40.

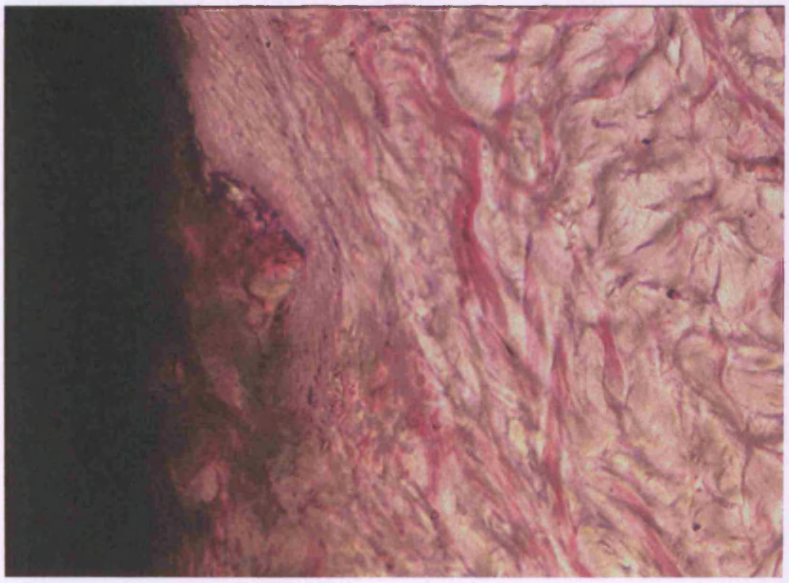

FIGURE 5.27d Demonstrates the termination of the epithelial layer at the HA surface. The underlying tissues of the dermis are in close association with the HA. Magnification x100.

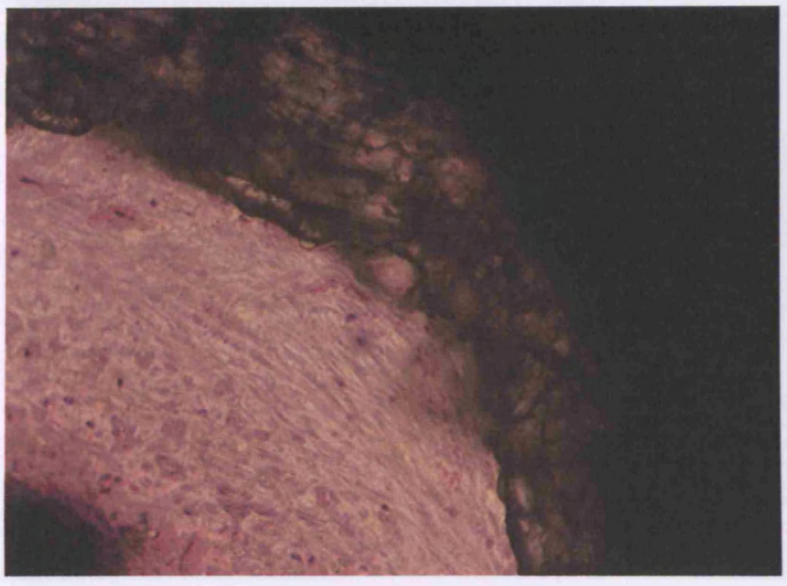

FIGURE 5.27e Shows the HA – dermal interaction on the underside of the flange, with complete tissue attachment, at a magnification of x100.

FIGURE 5.28

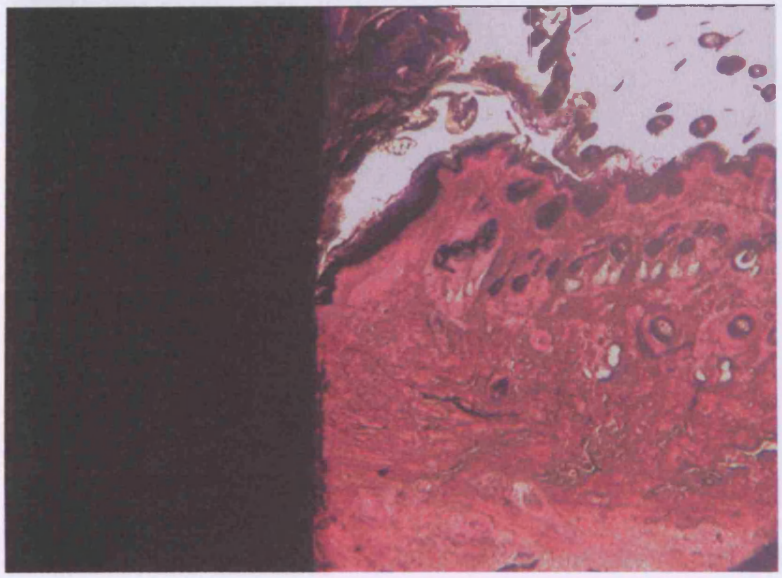

FIGURE 5.28a Displays the minimal downgrowth associated with fibronectin (100 μg) coated flanged implants, at a magnification of x10.

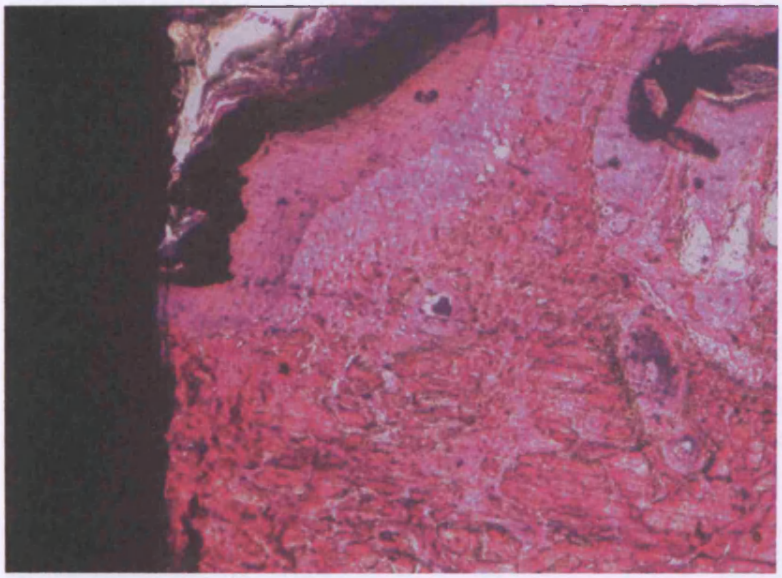

FIGURE 5.28b Shows the epithelial layer in intimate contact with the implant surface, at a magnification of x40. The underlying dermal layers are in immediate association with the pin, and contain a low density population of inflammatory cells.

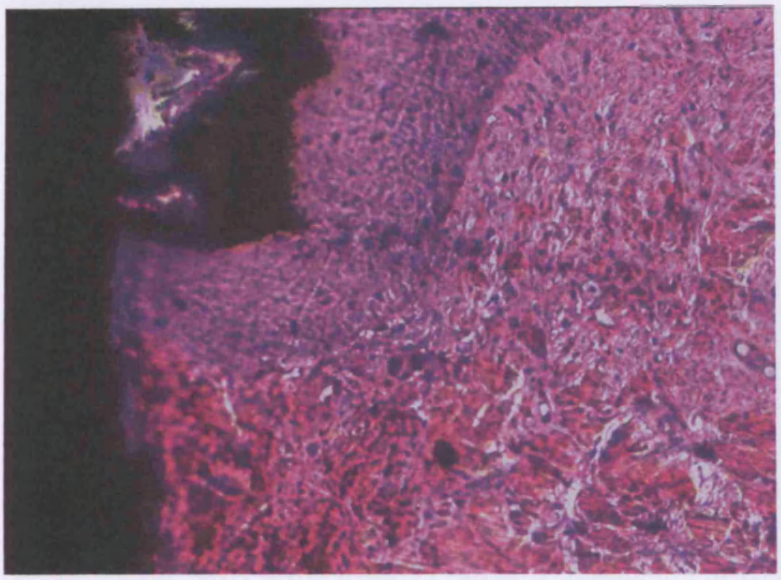

FIGURE 5.28c At a magnification of x100, this is a higher power image of the epithelial – implant interface seen in Figure 5.28b. The end of the epithelial layer is clearly attached to the implant surface, and the dense population of inflammatory cells observed surrounding other implant types is absent.

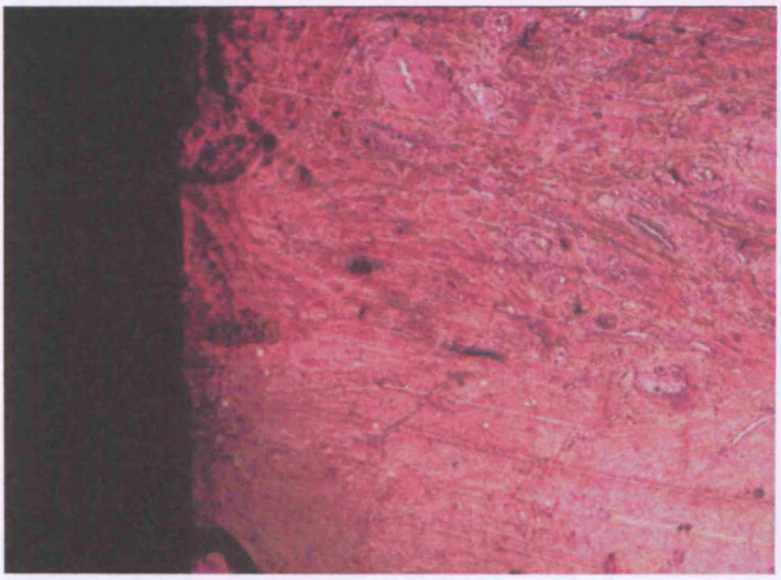

FIGURE 5.28d Displays the 100% dermal attachment observed around the 100 μg fibronectin coated flanged implants, at a magnification of x40.

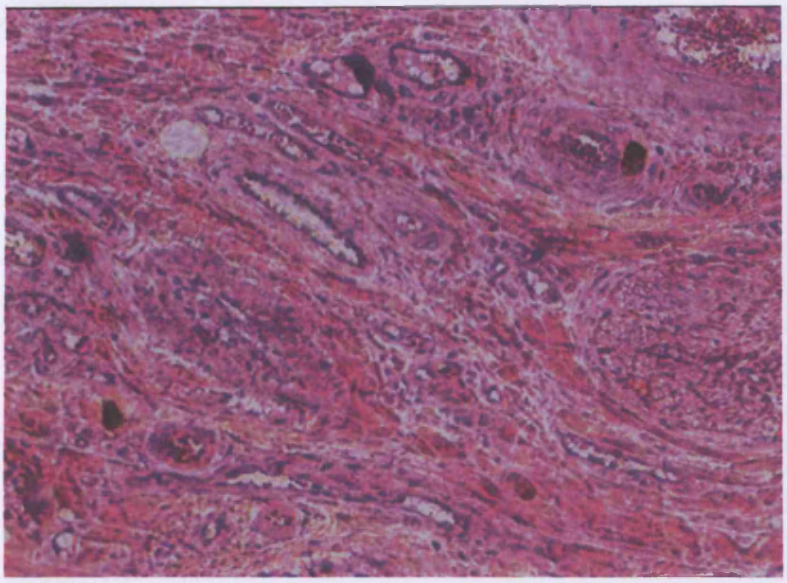

FIGURE 5.28e Shows the normal morphology of the dermal tissues adjacent to the implant surface, containing small blood vessels, capillaries and low density population of lymphocytes and macrophages. Magnification x100.

FIGURE 5.29

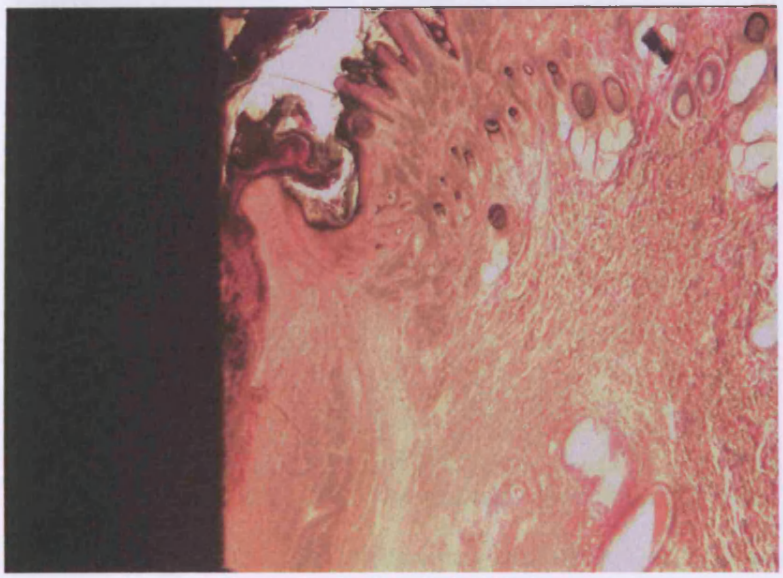

Figure 5.29a Shows the low degree of downgrowth associated with 200µg fibronectin coated flanged implants. There is a small amount of fibrous exudate at the epithelial layer – implant interface. Magnification x10.

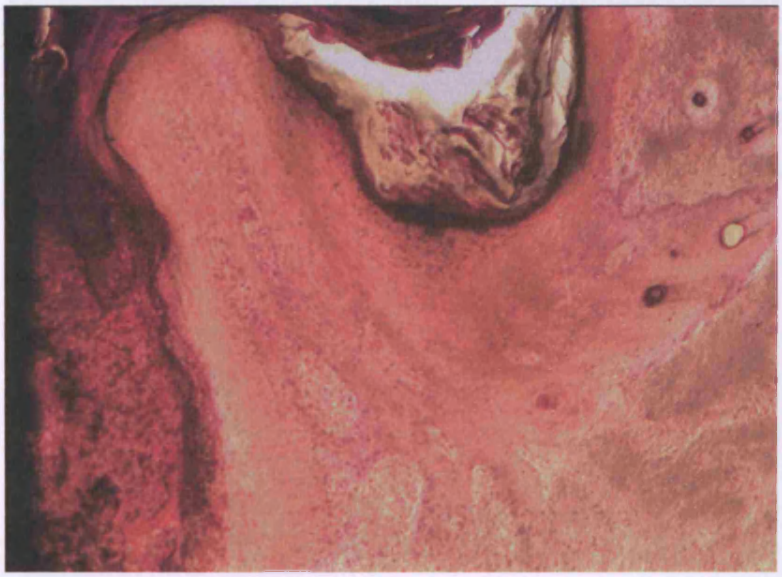

FIGURE 5.29b Displays the epithelial layer – implant interface from figure 5.29a at a magnification of x40.

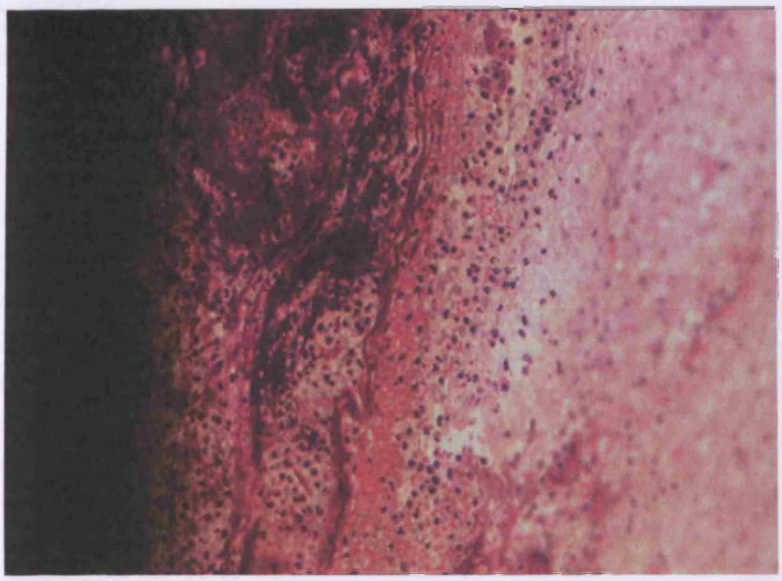

FIGURE 5.29c A x100 image of the fibrous exudate immediately adjacent to the implant surface from Figure 5.29b. The exudate contains a high density population of lymphocytes and macrophages, interspersed with foreign body giant cells and red blood cells.

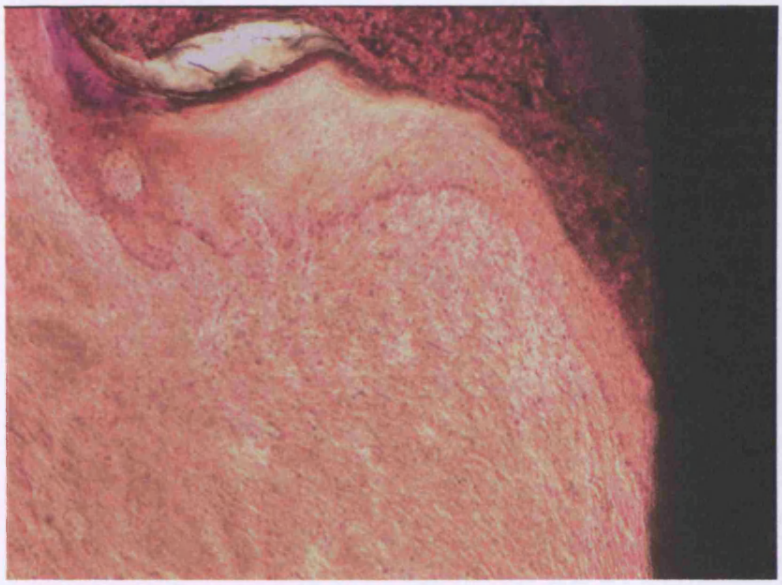

FIGURE 5.29d Demonstrates the appearance of another 200μg fibronectin coated flanged implant – host tissue interface, at a magnification of x40. Here the epithelial layer is intimately associated with the implant surface.

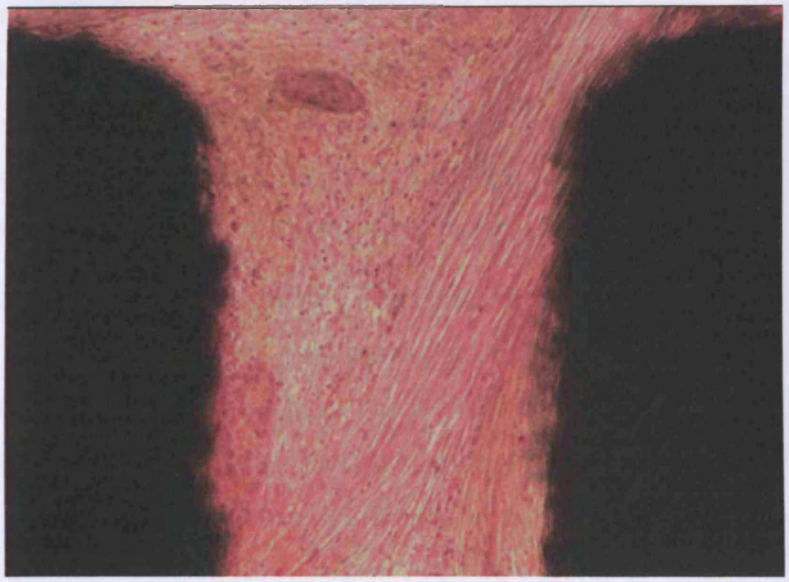

FIGURE 5.29e Shows the dermal tissue in 100% contact with the flange section of the implant. The image centres on a stress reducing hole within the flange, which has been completely invaded by the fibrous tissue of the dermis. Magnification x40.

5.4 DISCUSSION

The transcutaneous implants used in this study demonstrated no adverse soft tissue reactions and in most cases, generated a biological seal around the implant surface that prevented infection. Branemark et al (1969, 1975) have shown that there are no detrimental effects on the skin surrounding mandibular maxillary implants penetrating the gingiva, inserted with care to minimise surgical trauma. These findings suggest that the care taken during implantation of ITAP assists in the successful seal formation process.

It is proposed that for gingival implants, the surgical technique is not the only factor responsible for favourable outcome. Comparing transcutaneous implant passage through the tissues to those observed surrounding natural transepithelial passages of the tooth, it is observed that in the natural analogue, the soft tissues are firmly attached at the epithelial-penetration site and the abutting tissue movement is restricted by this attachment. It is thus postulated that no transcutaneous implant can be successful without elimination of the relative movement between the soft tissues and the implant. The significant decrease in downgrowth and increase in sub-epithelial layer attachment surrounding flanged implants is thought to be due to decreasing the relative movement between the host tissues and the implant surface, via the stress reducing segment. Hence it is proposed that the flange is responsible for the significant improvement in attachment parameters.

In 1983, Squier and Kammeyer stated that for clinical applications, reduction of the subcutaneous tissue is essential in maintaining a reaction-free interface around transcutaneous implants. Removing subcutaneous tissues could reduce mobility of the skin hence assist healing and attachment to the abutment surface. It could also minimise the contact area between host and implant materials, thus reducing the possibility of detrimental metal/implant influence on the biological tissues. The sub-epithelial tissue may contain factors that stimulate growth and migration of epithelial cells, hence its reduction could be advantageous. The subcutaneous tissues surrounding the transcutaneous implants examined in my thesis were not reduced, as there was minimal soft tissue coverage over the tibial implantation sites. Implants located in the proximal tibia were seen to interface with a greater amount of subcutaneous tissues than those in distal sites. This did not cause any adverse effects on the development of the skin - implant interface. It is possible that given an increased amount of subcutaneous tissue with which to interface, the implants would be subject to larger amounts of interfacial movement and at greater risk of failure due to downgrowth and marsupilisation. This was not observed in my research.

It is without doubt that surgical technique and implant design are principle criteria in determining the success of transcutaneous implants. However, other limiting factors are observed. Patient hygiene is paramount if transcutaneous implants are to be functional and remain uninfected. It is also possible that hair in the skin surrounding transcutaneous implants could cause adverse reactions, whilst hairless skin is easier to keep clean.

Contact dermatitis is an immune-mediated inflammatory skin rash that results from an allergy to a substance that is elicited by metals, and is characterised by infiltration and presence of mononuclear cells. Plasma cells and polymorphonuclear cells are indications of bacterial infection (Welbourn et al 1976). Any presence of polymorphonuclear cells, B-lymphocytes and plasma cells suggests that the response is due to presence of exogenous agents rather than an allergic skin response. The cellular presence surrounding the skin – penetrating implants used in my thesis indicates that the response observed was totally independent of the implant material. It can be stated that the integrity of the implant-soft tissue interface as a barrier to exogenous agents is vital to the success of an implant. It is thought that if the epithelium is attached to the implant surface, then this attachment provides the barrier function. However if not, the subcutaneous connective tissue layer attachment supplemented by an inflammatory infiltrate, provides a secondary barrier ready to eliminate any extrogenous agents attempting to invade the transcutaneous site. This was found to be the case for all implants examined in this research. Implants with total attachment to the host epithelium demonstrated lower density populations of lymphocytes, macrophages and foreign body giant cells than those lacking attachment. In implants lacking epithelial layer adhesion, the sub-epithelial attachment appeared to arrest downgrowth, and a high density population of inflammatory cells was present at the interface zone immediately below the cut end of the epithelial layer. In some cases, where the epithelial layer ended further from the implant surface, a considerable amount of fibrous exudate containing numerous inflammatory cells was observed. It appears from these findings, that epithelial layer attachment to the implant surface is not essential for the short-term success of skin penetrating implants. However, it is felt that for long term viability, the integrity of the implant - soft tissue seal could only benefit from this additional protective adhesion.

In 1990, Chehroudi et al, examined smooth transcutanous implants and those incorporating grooves of different dimensions (30μm pitch with depths of 22, 10 and 3μm. 10μm and 3μm deep grooves with pitches of 39 and 7μm respectively). Clinical observations included the advantage of placing the pins in a parietal area, which provided support beneath the implants reducing the chance of dislocation, as well as providing a

good reference surface so that depth of implantation could be maintained. The degree of healing was excellent and uneventful judged by tissue texture and colour, as well as the absence of bleeding or exudates. Histological observations included a clear outline of cell nuclei with both epithelium and connective tissue found snugly attached to the grooved and smooth implant surfaces. Differences in cell arrangement, orientation and location on grooved and smooth coated implants were observed. Epithelial cells were closely attached to all surfaces. On smooth surfaces epithelial cells were arranged in multilayer fashion with elongated nuclei. In contrast, fibroblasts were found to be inserting obliquely into implants with 22μm deep grooves and nuclei were round and elongated in nature. Inflammatory cells were observed in some sections. They found no noticeable differences between smooth and grooved implants. It was concluded that groove depth is an important factor in controlling epithelial migration on horizontally orientated grooves, shallow grooves being least effective. My research has produced a high success rate with few clinical complications and a fast healing time. However, it has produced a number of results which contrast with those of Chehroudi et al (1990). The groove dimensions of even the small grooved implants used in my thesis are far larger than those utilised by Chehroudi et al. However, they did not support an epithelial or sub-epithelial – implant interface akin to that described in 1990. The sub-epithelial layer tissues were unable to invade the troughs of the small grooved implants. However, by increasing the depth of the grooves to 600μm and the width to 1000μm, a dermal fibroblastic seal was observed. In comparison to the research by Chehroudi et al (1990), the bone anchor system did similarly reduce the relative interfacial movement between the implant and the host tissues, and the finding regarding groove depth is maintained. However, due to the significant differences observed between straight and flanged implant types, it is concluded that to optimise ITAP success, a stress reducing flange, as apposed to a grooved substrate, is more beneficial.

My research has shown that where sub-epithelial dermal fibroblastic layer attachment is observed, even with a lack of attachment of the epithelial layer, downgrowth is effectively inhibited or retarded, hence the underlying organisation and attachment of the connective layer is contributing, at least in part, to the prevention of epithelial layer migration. In 1981, Squier and Collins reported inhibition of epithelial downgrowth by connective tissue attachment and ingrowth on millipore filters with pores of greater than 3 μm implanted percutaneuosly in pigskin. In my study, where connective tissue was not organised in such a way as to inhibit epithelial downgrowth, contact guidance and the free edge effect lead to migration of the layer. This was eliminated by increasing the surface

area for tissue attachment and reducing micromotion between the implant and the host tissues. Further research with porous implant material in a flanged pin design could optimise the interface further. Surface topographies of dental and percutnaeous implants have been varied, but the need is to optimise the extent of tissue attachment to the implant surface. Some designs have presented differing surfaces to bone and soft tissues. However, it is uncommon that a distinction is made between the layers of the soft tissues. The optimal surface for epithelial and sub-epithelial tissues may not be the same, hence the perfect implant would be one where the surface topography of the implant is optimal for the attachment of the specific tissue type it contacts.

To avoid marsupilisation, a number of transcutaneous studies have incorporated porous implant surfaces. It is thought that a porous surface will allow for growth and migration of dermal components as well as epithelial cells into the superficial pores, forming a bacteria and fluid-tight seal. In 1974, Winter demonstrated that connective tissue infiltrates pores greater than 40 μm, and when pores are between 10 and 40 μm only individual cells and collagen can migrate in. In 1980 Daly stated that after migrating into such pores, fibroblasts do not survive owing to lack of nutrients and the pores finally become filled with cell debris. When the pores are in excess of 40μm, connective tissue soon fills them in a manor similar to normal wound healing, except that they are in competition for space between fibroblasts, macrophages and giant cells. Epidermal basal cells are seen to follow the connective tissue ingrowth into the pores. In rabbits, dogs and pigs, epidermal basal cells migrate through dacron velour and porous materials in 10-20 days (Winter 1974, Hall 1975).

There are four principle reasons for transcutaneous implant failure; infection, avulsion (mechanically induced failure), permigration and marsupilisation (downgrowth and pocket formation causing transcutaneous implant to become extracutaneous). To reduce infection, low surface energy coatings such as diamond-like carbon can be incorporated. In 1995, Tang et al, demonstrated that diamond-like carbon is as biocompatible as Ti and stainless steel, but *in vivo* and *in vitro* shows reduced cellular adhesion (polymorphonuclear leucocytes) and activation. In this thesis, the application of diamond-like carbon was not found to have any significant effects on downgrowth, epithelial or sub-epithelial layer attachment. As a means of preventing infection, the soft tissue seal surrounding all implants tested in my research proved sufficient to prevent failure due to infection, and the application of DLC did not significantly alter the results obtained. The reasons for this could be two fold. First, the titanium material used for implant manufacture could elicit an adequate soft tissue attachment that prevented

infection, without the need for any external coatings. Alternatively, the diamond-like carbon coating was not presented to the correct area of the interface. If the pin was screwed too far into the tibia, and the DLC coating was found to be abutting the soft tissues, the coating would minimise the extent of epithelial attachment and lead to downgrowth, which would halt when faced with the healthy collagenous dermal-implant interface. If the DLC coating was not implanted, interfacing with the three-phase junction, the area of the pin immediately external to the skin would not have been coated, hence the effect would be the same as that observed surrounding non-DLC coated implants. It is thought that a combination of screwing the implants in too far, and not far enough, resulted in a lack of significant differences in DLC coated and uncoated implants. Further research would be required to develop an implantation system whereby precise positioning of the implant surface is possible. This system could be used to position sections of the implant with surface properties that would optimise tissue attachment immediately adjacent to specific layers of tissues.

Overall, the implants developed in my thesis have been successful in that none have failed due to infection, avulsion, permigration or marsuplilsation. The degree of downgrowth associated with transcutaneous implants was shown to be directly related to the condition and extent of attachment of the dermal fibroblastic tissue layers. It has been shown that over a four week duration, downgrowth has been retarded and in some cases prevented by the establishment of a healthy collagenous tissue – implant interface at the dermal level. The degree of downgrowth has been significantly reduced and the extent of sub-epithelial soft tissue attachment has been significantly increased, by the incorporation of a flange positioned immediately below the epithelial layer. It is thought that the flanged implants are more successful because they not only reduce the radial stresses at the skin-implant interface and the relative interfacial movement between the implant and host materials, but they also provide an increased surface area for sub-epithelial, dermal fibroblastic tissue adhesion. Further work will be carried out, evaluating the effect of increasing the surface area of the flanged implants by incorporating porous titanium flanges. A long-term follow up study is required to test the stability and integrity of the soft tissue – implant seal over a greater period of time.

CHAPTER SIX

TENDON ATTACHMENT TO A METAL PROSTHESIS : A FUNCTIONAL AND HISTOLOGICAL STUDY OF THE RECONSTRUCTION OF EXTENSOR MECHANISM

CHAPTER SIX: TENDON ATTACHMENT TO A METAL PROSTHESIS : A FUNCTIONAL AND HISTOLOGICAL STUDY OF THE RECONSTRUCTION OF EXTENSOR MECHANISM

6.1 INTRODUCTION AND HYPOTHESES

The function of a tendon is to transmit the forces generated in the muscles to the skeletal system resulting in the movement of the body. The use of segmental massive endoprostheses to replace bone tumours often involves resection of the tendon-bone interface. Recovery of normal limb function following this type of surgical intervention depends on the re-attachment of the connective tissues to the metal implant. The method of re-attachment must provide sufficient mechanical strength to allow force transmission.

Resection of the proximal tibia is a limb sparing operative procedure for bony sarcomas. Several problems have hindered the success of limb sparing surgery for tumours at this site, including anatomical constraints, awkward surgical approach, vascular complications, lack of soft tissue coverage and the need to recover the patellar or extensor mechanism (Cannon 1997). The proximal tibia is one of the most common sites for primary bone sarcomas (Sim et al 1987, Yaw and Wurtz 1991, Malawer and McHale 1989, Horowitz et al 1991). There are complications associated with the replacement of the proximal tibia that include failure of the extensor mechanism following reconstruction resulting in altered gait (Cannon 1997), extension lag, *patella alta* (high-riding patella), altered biomechanics and quadriceps atrophy (Jeon et al 1999).

Several methods have been employed to re-attach the patellar tendon to proximal tibial replacement. However, no technique is universally accepted due to inconsistencies in functional outcome (Cannon 1997). Methods of patellar tendon re-attachment have included suture to Dacron tape anchored to a metal loop on the anterior surface of the implant that is reinforced with a gastrocnemius flap (Malawer and McHale 1989, Eckardt et al 1991) or overlying a porous coated extra-medullary implant surface (Bickels et al 2001), direct anchorage with twisted polyester sutures to drill holes (Jensen 1983), tendon autograft reinforcement using gracilis or sartorius tendons (Jeon et al 1999), allograft replacement of the proximal tibia (Brien et al 1994), anchoring of muscle flaps and tendon sections to polyethylene terephalate tubes (Gosheger et al 2001), the use of non-resorbable mesh to augment fixation strength (Ozaki et al 1999) and the use of allograft to re-establish continuity between the tendon and the proximal tibia following total knee arthroplasty (Emerson et al 1990, 1994). With extra reticular resection of tumours around the knee, excision margins can be extended to include the patellar tendon and the patella. In these instances an augmentation process is required, for example using polytetrafluoroethylene (PTFE) and a gastrocnemius flap to bridge the defect (Jeon et al

1999). However, where adequate amounts of soft tissue have been preserved, augmentation processes can be avoided.

This chapter of my thesis explores novel methods of soft tissue attachment to prostheses, using extensor mechanism reconstruction in sheep. Extensive research has been carried out to describe the interface that exists at the normal tendon – bone interface, and its functional and morphological characteristics are well understood (see Introduction section 1.2.2.1.2). A number of research groups have attempted to re-attach tendons to the body of a metallic prosthesis with varying results. In 1994 Gottsauner-Wolf et al analysed the mechanical strength of a tendon attachment to metal, with and without a bone block. They tested a number of different attachment devices, including a custom-made enhanced tendon anchor consisting of a base plate with sintered titanium wire mesh with ten protruding spikes, and a bridging plate housing three angled interlocking spikes. The initial attachment strength of the enhanced tendon anchor was found to be greater than that of other commercially available devices, with or without a bone block. The same group published data of an *in vivo* canine model (1994), reporting improved forelimb function, using force-plate analysis, following supraspinatus tendon attachment to their enhanced tendon anchor and bone block compared with a direct tendon attachment. Histological analysis showed that in the bone block group, a mature interface had developed between the bone and the sintered mesh of the base plate. However, in the direct tendon group, a fibrous tissue was found penetrating the mesh with no evidence of a re-modelling enthesis after sixteen weeks. Two out of twelve of the specimens were found to contain necrotic tissue with no attachment of any form. Chao et al (1997) and Inoue et al (1996, 1999) have further investigated the custom tendon anchor with incorporation of an autogenous cancellous bone graft. A sixteen week *in vivo* study demonstrated that the graft material was absorbed and replaced with collagen fibres, which underwent a significant, random to parallel, orientation change (Inoue et al 1996). In a similar model where bone marrow supplement was used, areas of ectopic calcification were observed. An improved mechanical and functional outcome was demonstrated in the marrow supplement group compared with tendon or bone graft alone. Histological analysis of the marrow supplemented group showed the formation of new bone, mineralised and unmineralised fibrocartilage and a mature direct-like enthesis after fifteen weeks *in vivo*. It was proposed that these findings were a direct result of osseoinduction, initiated by the bone marrow in the graft material (Chao et al 1997).

Tendon healing within a bone tunnel has been shown to occur by a front of advancing mineralisation into a collar of soft tissue callus surrounding the tendon (see Introduction

section 1.2.2.1.4). This phenomenon could be applied to the attachment of a tendon to the body of a metal implant, via generation of an *in situ* bone block on the implant surface, into which the tendon could integrate. Fixation may be augmented via established mechanisms known to promote osteogenesis and osseointegration, or those that accelerate healing of tendon to bone. This technique would avoid the problems associated with attaching a connective tissue to a biocompatible, but inert metal implant.

Accepted techniques in orthopaedic surgery to increase bone stock for filling bone defects, aiding fracture healing and fixation of uncemented implants, include autologous bone grafting, bone allograft, demineralised bone matrix, cytokines, including bone morphogenic proteins in carrier systems such as collagen I, and bioactive ceramic incorporation (Grey and Elves 1982, Lewis et al 1997, Oikarinen and Korhonen 1979). Bone marrow has been identified as a source of pluripotent cells which can differentiate into many different connective tissue cell types (Haynesworth et al 1992). Engineered constructs containing growth factors or mesenchymal stem cells extracted from marrow or periosteum, have been shown to elicit calcification responses *in vivo* and *in vitro* (Oreffo et al 1998, Goshima et al 1991, Ohgushi et al 1989, Salama et al 1973, Caplan 1991, Burwell 1985, Majors et al 1997, Beresford et al 1989, Ashton et al 1980, Sakou 1998, Uludag 1998, Nakahara et al 1990). Other work on tendon re-attachment to bone has included biological augmentation with periosteum (Ohtera et al 2000), bone morphogenic proteins (Rodeo et al 1999) and bone growth factors (Anderson et al 2001). Augmentation using these methods produced a mature enthesis containing regions of fibrocartilage. A recent study of tendon reattachment to a metal prosthesis used a similar implant and study design to those used in my thesis (Inoue et al 2002). The supraspinatus tendon was re-attached to a porous titanium prosthesis in a canine model. At 16 weeks the interface demonstrated four zones, tendon with no crimp pattern, rounded chondrocyte-like cells arranged in rows corresponding to unmineralised fibrocartilage, newly formed bone with large rounded cells arranged in rows corresponding to mineralised fibrocartilage, and bone. The patellar tendon model used in my thesis, is a more testing model of tendon re-attachment compared to the supraspinatus, which "while it undoubtedly plays an important role in shoulder function it is sometimes difficult to demonstrate its necessity" (www.ortho-u.net/05/187.htm). It has been shown that total experimental paralysis of supraspinatus will simply reduce the force of abduction with no other loss of function (www.ortho-u.net/05/187.htm). The patellar tendon is vital to the extensor mechanism and no other structures can compensate for its loss. It is a model in which relevant functional assessments in the form of kinematic gait, and force plate

analysis can be applied. As the supraspinatus is one of four muscles of the rotator cuff, the *in vivo* forces do not directly correspond to the measurable values from force plate data. Re-attachment of the patellar tendon is more representative of the clinical model of extensor mechanism recovery following proximal tibial replacement, compared to the canine supraspinatus as a model for proximal humeral replacement adopted by Inoue et al (2002).

My study has used HA as an intermediate between the cut surface of the tendon, the autologous cancellous bone graft and the implant surface, as mesenchymal stem cells have been shown to differentiate along an osteoblast lineage on an HA scaffold (Rust et al 2003).

In my thesis, it is postulated that a tendon-implant neo-enthesis can be engineered using a hydroxyapatite coated implant, augmented with a suitable bioactive material; autogenous cancellous bone graft and marrow. It is hypothesised that a tendon-implant neo-enthesis with similar functional and morphological properties to that of a normal tendon-bone interface, can be engineered *in situ* (See Figure 6.1).

FIGURE 6.1 Hypothesis Schematic

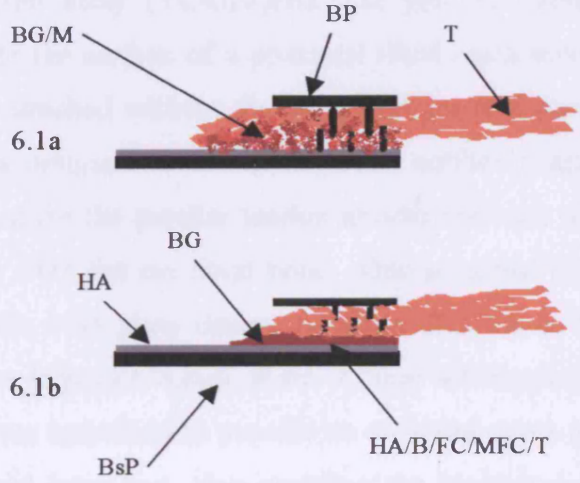

FIGURE 6.1a Perioperative construct with the tendon (T) clamped onto the hydroxyapatite coated (HA) base plate (BsP) using the bridging plate (BP), augmented with bone graft and marrow (BG/M).

FIGURE 6.1b Post-operatively the hypothetical remodelling and integration of bone graft (BG) on the hydroxyapatite coated (HA) base plate (BsP), resulting in the formation of a hydroxyapatite–bone–fibrocartilage–mineralised fibrocartilage–tendon (HA/B/FC/MFC/T) neo-enthesis.

6.2 MATERIALS AND METHODS

6.2.1 THE CLAMP DEVICE

Cadaveric and radiographic analyses of the ovine proximal tibia were used to design a custom-made titanium alloy (Ti_6Al_4V)(BS7252 part 3) implant. A base plate was designed to simulate the surface of a proximal tibial replacement, to which the patellar tendon could be re-attached without the complications of a proximal tibial replacement. The base plate was designed to fit the cut bone surface resulting from tibial tubercle osteotomy and to isolate the patellar tendon attachment site, which involves preventing bone cell migration from the cut tibial bone. One proximal and three distal holes were incorporated into the base plate design to allow fixation to the proximal tibia using cortical bone screws (Synthes cortex screw 2.7mm self-tapping L 14mm ref: 402.814). The clamp design was optimised to provide an enclosed space to isolate the tendon from the surrounding tibial bone bed, thus enabling the biological processes at the tendon-implant interface to take place as if the whole of the proximal tibia had been replaced. The solid bridging plate was clamped to the base plate via screws through the lid sides. A series of nine interlocking spikes, 1mm in diameter and 4mm in length, which were press-fit into the clamp plates, were designed to secure the cut end of the tendon.

Following cadaveric and pilot clamp testing studies (outlined in section 6.2.2), the bridging plate was modified to create a more open environment on the extra-medullary surface. The upper bridging plate was reduced to an open H-shaped segment containing a series of 1mm drill holes (Figure 6.2). The upper surface of the base plate was plasma sprayed with a seventy to one hundred micrometer thick coating of CAPTAL® Hydroxyapatite (Plasma Biotal Limited, UK). The implants were cleaned ultrasonically and sterilised in an autoclave (Instaclave 230, 136°C, 2.2 bar, 3.5 minutes, total cycle length 15 minutes) pre-operatively.

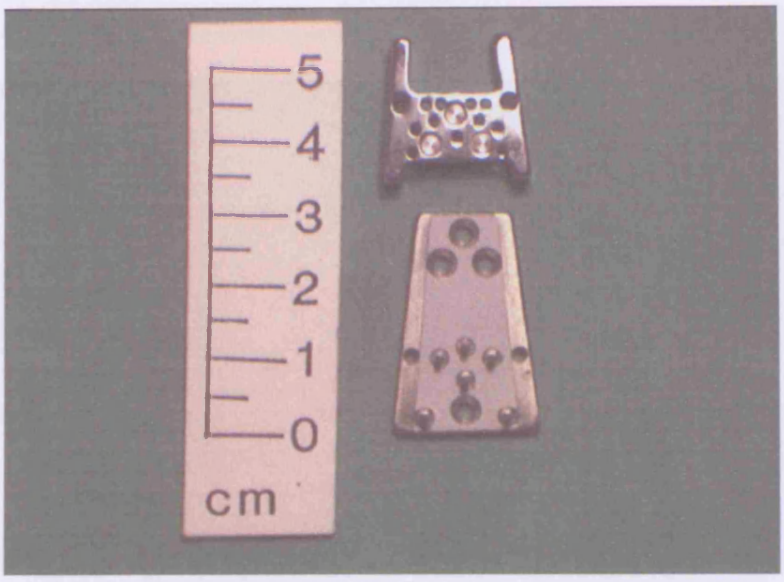

FIGURE 6.2 Final clamp design in plan view showing base plate (BsP) with spikes (S) and redesigned open H-shaped bridging plate(BP).

6.2.2 CADAVERIC AND PILOT STUDIES

6.2.2.1 ANIMAL MODEL SELECTION

The ovine patellar tendon was selected for this model since sheep have a single true patellar tendon, whose most significant attachment is to the tibial tuberosity with medial and lateral retinacular expansions, as in the human knee (Allen et al 1998). Cadaveric dissection of the ovine hind limb stifle joint (knee) revealed this to be an accurate description (Figure 6.3). The lateral retinacular expansion formed a tough fibrous band that enclosed a tunnel for the Long Digital Extensor tendon. It was decided that interruption of this might compromise the distal function and stability of the joint. The medial retinacular expansion comprised a thin broad retinacular expansion blending with the antero-medial soft tissues. Other ruminants possess three discrete patellar ligaments (Dyce et al 1996). The sheep was selected as a model for study because of its patellar tendon morphology, which is analogous to the single tendon found in humans. The size of the ovine patellar tendon is of a similar magnitude to that of a human and during normal gait, it is anticipated that a comparable physiological loading of the tendon – implant interface would occur.

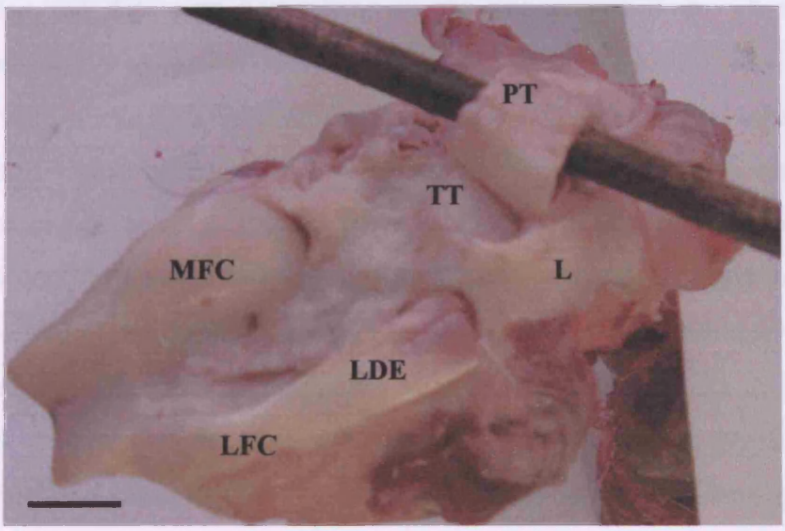

FIGURE 6.3 Dissection of the ovine stifle joint revealing central patellar tendon (PT) inserting into the tibial tuberosity (TT). The lateral retinacular expansion (L) enveloping the tunnel for the Long Digital Extensor Tendon (LDE), and the Medial/Lateral Femoral condyles (MFC/LFC). Bar = 15mm.

6.2.2.2 CLAMP DESIGN PILOTS

The operative protocol outlined in section 6.2.5 of my thesis was carried out in an ovine model *in vivo*, using the original prototype, solid bridging plate / clamp design, and remained in situ for two weeks. This was carried out to determine whether the implant could provide sufficient mechanical fixation of the tendon to the base plate, whilst allowing revascularisation and repopulation of the tendon. A second two week, *in vivo* pilot study was run in parallel, using the modified open H-shaped clamp lid with perforated drill holes. This was carried out to determine whether a more open environment, introduced by the modifications to the clamp lid, would reduce the periods of necrosis, revascularisation and repopulation, whilst still providing sufficient mechanical fixation.

6.2.2.3 CONTROL PILOT

Pre-operative force plate measurements served as positive control data, whilst for analysis of joint function the data was normalised to the unoperated limb. A single *in vivo* negative control pilot was carried out, in which the operative protocol from section 6.2.5 of my thesis was performed without clamping the patellar tendon within the clamp device. The soft tissue fascia was closed over the top of the clamp, and the patellar tendon was sutured into the subcutaneous soft tissue layers with 2.0 Vicryl ®. The animal was allowed free mobilisation on return to an individual pen, and for a further six weeks post-operation. Force plate assessment was carried out at six weeks as stated in 6.2.4.2 to determine functional outcome without tendon-tibia re-attachment. No further animals were operated on as negative controls due to the severity of the effects observed in this case. With the exception of the re-attachment of the patellar tendon, the surgical procedures carried out on the negative control animal were identical to those performed on the test Groups. Hence the poor functional outcome could not be attributed to the surgical intervention, but only a result of the lack of extensor mechanism function resulting from the free tendon suture. It was thus considered unethical to continue with a group of negative control animals.

6.2.3 *IN VIVO* ANIMAL STUDY

6.2.3.1 STUDY OVERVIEW

Twenty-four skeletally mature Friesland ewes, weighing fifty five to ninety kilograms were used for this study. Pre-operatively the animals were subjected to two-dimensional optical kinematic gait analysis of the right hind limb (6.2.4.1). For each of these animals, the surgical procedures described in section 6.2.5 were employed, to clamp the patellar tendon into the custom made implant (6.2.1). Twelve animals were randomly selected to constitute the Autograft Group, in which the tendon-implant interface was augmented with fresh autogenous cancellous bone and marrow graft. The remaining twelve animals served as non-augmented controls and were assigned to the Hydroxyapatite (HA) Group.

6.2.3.2 ANIMALS

6.2.3.2.1 SIX WEEK ANIMALS

Six weeks post-operatively, all animals were subject to force-plate analysis of both hind limbs. Twelve animals, six from each of the study groups (Autograft and HA), were assigned to the Six-Week Group (by time), and underwent two-dimensional optical

kinematic gait analysis of the right hind limb, followed by euthanasia (under Schedule I method of the Animals (Scientific Procedures) Act 1986) by lethal injection of 20% Pentobarbital Solution. A radiograph of the right proximal tibia was taken for each animal, prior to harvest and standardised dissection of both proximal tibiae and patellar tendons. The removed specimens were processed as outlined in section 6.2.6.

6.2.3.2.2 TWELVE WEEK ANIMALS

Twelve weeks post-operatively, the remaining twelve animals, six from each study group, assigned to the Twelve-Week Group (by time), were subject to further force plate and two-dimensional optical kinematic gait analyses. Measures were taken to ensure that functional results were not compromised, by allowing each animal twenty four hours rest between kinematic gait analysis and force-plate assessment. The Twelve-Week animals then underwent euthanasia, harvest and processing procedures (6.2.6).

6.2.3.3 OPERATIVE PROCEDURES

All animals were starved of solid foods for at least twelve hours prior to surgery. Peri-operatively the animals received a 1mg/kg antibiotic dose of Excenel RTU (Ceftiofur) (Pharmacia & Upjohn, UK) subcutaneously, and an intra-muscular 10-20μg/kg dose of Vetergesic (Buprenorphine hydrochloride, Reckitt & Coleman Products Ltd, UK). The animals were returned to individual pens post-operatively once vital signs were stabilised, and positioned with the operated limb extended at the knee in a position of sternal recumbency. Regular checks were carried out until the animals were fully awake, after which they were allowed free mobilisation and were returned to solid food access. Vetagesic was administered at the previously stated dose rate, one day post-operatively, whilst subcutaneous doses of Excenel RTU antibiotic were administered for a further five days. The animals remained individually housed for a period of between five and seven days, after which they were placed in larger pens in small groups of three to four animals. During the first two weeks post-operatively the animals were checked regularly. The wounds were assessed frequently, with local wound hygiene being administered in the form of topical cleaning with Pevidine (aqueous Povidone Iodine 0.75% W/V). The wound dressings were removed one week post-operatively.

All procedures were carried out under a project licence protocol accepted under the Home Office Animals (Scientific Procedures) Act 1986. Each animal was sedated pre-operatively with a subcutaneous injection of Rompun (Bayer plc, Germany) (Xylazine Hydrochloride solution 2%) at 0.2mg/kg. Anaesthesia was induced with Hypnovel® (Midazolam, Roche Products Ltd, UK) 2.5mg dose, and Ketaset® (Ketamine Hydrochloride, Fort Dodge Animal Health Ltd, UK) at 2.5mg/kg intravenously. The animals were intubated and anaesthesia was maintained with Halothane (Merial Animal Health Ltd, UK) 3% and 100% oxygen (flowing at four litres per minute). A stomach tube was placed on free drainage and intra-operative vital signs were monitored using a pulse oximeter. The hindquarter was shaved and cleaned with dilute Pevidine prior to transfer to theatre. Operative procedures were carried out with the animal in the left lateral position. The operative site was prepared with Hydrex® solution (Blue Chlorhexidine Glucuronate 0.5% w/v in 70% v/v Industrial Methylated Spirit, Adams Healthcare, UK) and isolated in a sterile field with drapes.

A midline incision, approximately eight centimetres long was made over the anterior aspect of the right stifle joint, with the tibial tuberosity located centrally to the incision. The subcutaneous tissues were divided to enable isolation of the patellar tendon. The lateral margin was defined, and the tendon was isolated by passing small artery forceps, lateral to medial, through the infra-patellar tendon space (Figure 6.4). The tendon was released from its insertion into the tibial tuberosity by sharp dissection. The deep infra-patellar fat pad was removed, and the soft tissues over the proximal tibia were cleared with a periosteal elevator. An osteotomy of the tibial tuberosity was performed with an oscillating power saw (Howmedica), from proximal to distal, creating a flat bone bed to accommodate the base plate. The base plate was located onto the tibial osteotomy site and three holes were drilled through the proximal and two of the distal holes, using a 2mm drill bit. The plate was fixed to the bone bed with three 14mm long, Ø 2.7mm self-tapping cortical bone screws (SYNTHES®, STRATEC Medical Ltd, UK)(Figure 6.5).

The tendon was pressed onto the spikes within the clamp lid in an inverted position, and the clamp was assembled by screwing the bridging plate to the base plate with custom made screws whilst the leg was held in extension (Figure 6.6). The wound was irrigated with one litre of normal saline (Aquapgarm NaCl Ph. Eur. 0.9% w/v), and haemostasis was secured with bipolar diathermy. The wound was closed in three layers with absorbable Coated Vicryl® (Ethicon®, Johnson & Johnson Intl, Belgium). Skin closure was carried out with sub-cuticular sutures. The wound was sprayed with OpSite (Smith & Nephew Medical Limited, UK) moisture vapour permeable spray dressing and a gauze

dressing was applied, followed by a cotton wool layer, crepe bandage and 'Tubigrip' elastic stocking.

Bone graft was harvested intra-operatively from the ipsilateral iliac crest, for animals in the Autograft Group. A skin incision approximately 40mm in length was made over the right iliac crest and the subcutaneous tissues were divided. A hole was drilled into the iliac crest through a protective sleeve (Dynamic Hip Screw 5-hole plate) using a 6mm auger drill-bit. The reamings were collected. A curette was used to collect cancellous bone from the site, whilst a 16-gauge needle with syringe was used to draw the fluid contents of the iliac crest drill hole and aspirate bone marrow from the bone substance. The wound was closed in two layers with Vicryl®, with sub-cuticular sutures for the skin closure. The skin was sprayed with OpSite.

The cancellous bone and marrow (wet weight approximately 1.5g) was packed into the central portion of the base plate to the height of the spikes, prior to assembly of the clamp. Remaining graft material was packed around the distal section of the tendon protruding distally from the lid of the clamp (Figure 6.8).

Professor Gordon Blunn and myself (Centre for Biomedical Engineering, Institute of Orthopaedics, University College London) performed the first three operations. Mr Michael Oddy (MSc Student – Centre for Biomedical Engineering) and I performed the remaining operations.

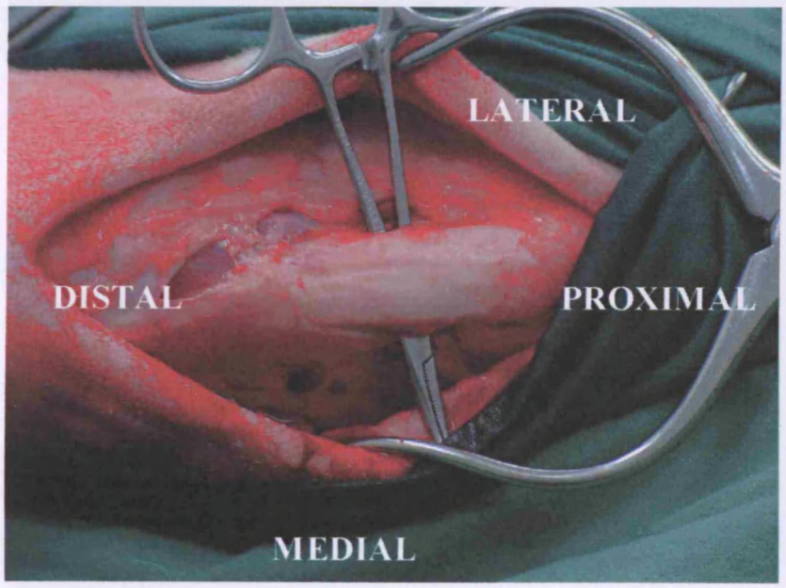

FIGURE 6.4 Image showing the appearance of the Patella Tendon isolated with small artery forceps.

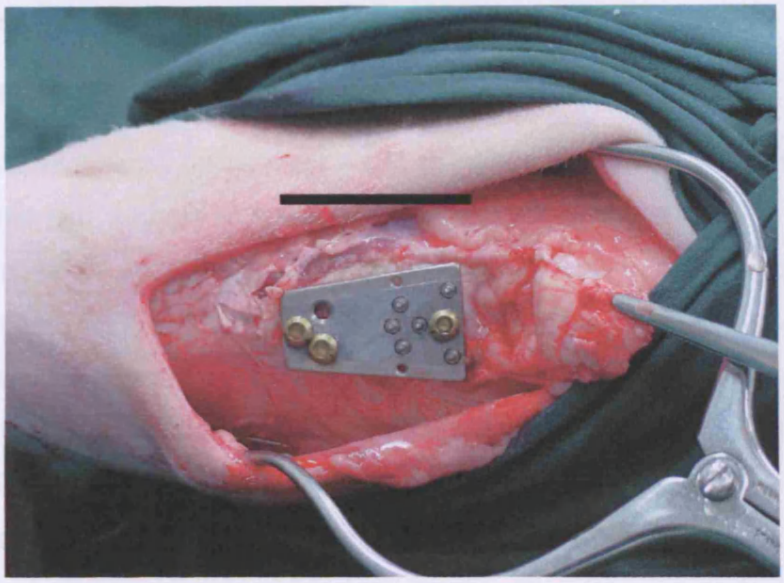

FIGURE 6.5 Shows the base plate screwed to the tibial osteotomy with three cortical bone screws. Bar = 30mm.

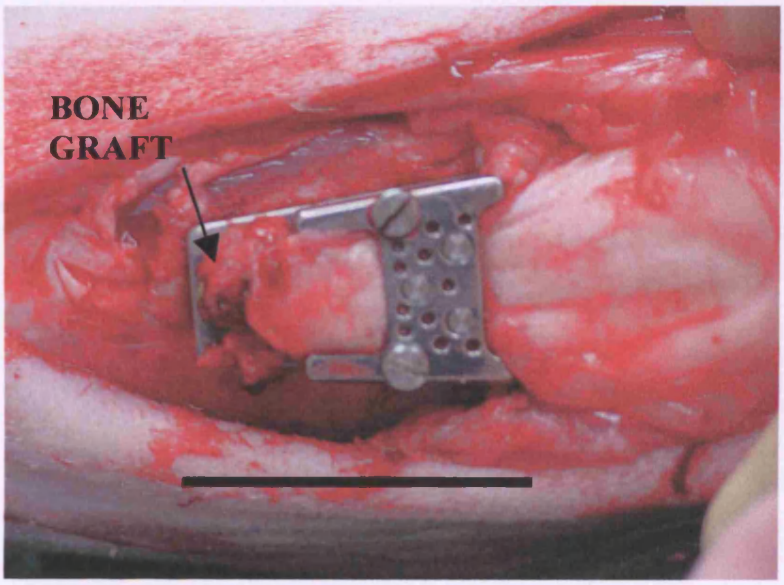

FIGURE 6.6 Demonstrates the clamp fully assembled prior to closure of the wound. The bone graft taken from the ipsilateral iliac crest is visible beneath the tendon. Bar = 30mm.

6.2.3.4 GAIT ASSESSMENT TECHNIQUES

6.2.3.4.1 TWO-DIMENSIONAL KINEMATIC GAIT ANALYSIS

6.2.3.4.1.1 CADAVERIC STUDY – ASSESSMENT OF SKIN DISPLACEMENT

It was postulated that skin displacement could affect the data for *in vivo* two-dimensional optical kinematic gait analysis (6.3.4.1.1). To determine the extent of skin displacement in the chosen model of study, radiographs of the hind limbs of ovine cadavers were taken, with markers positioned and glued to the skin, with metal-backed cross-hair wires at different degrees of flexion (Figure 6.7) and extension (Figure 6.8) to assess skin displacement. The markers were positioned using a two person assessment of surface anatomy, on the skin overlying the greater trochanter, distal femur, proximal tibia and distal tibia, and the extent of marker migration from the centre of each anatomical landmark was measured on the resulting radiographs. The data was analysed using SPSS (version 10.1 for Windows). The Kolmogorov-Smirnov test was used to test for normality of the data and analysis was carried out using the Mann-Whitney U non-parametric test.

FIGURE 6.7

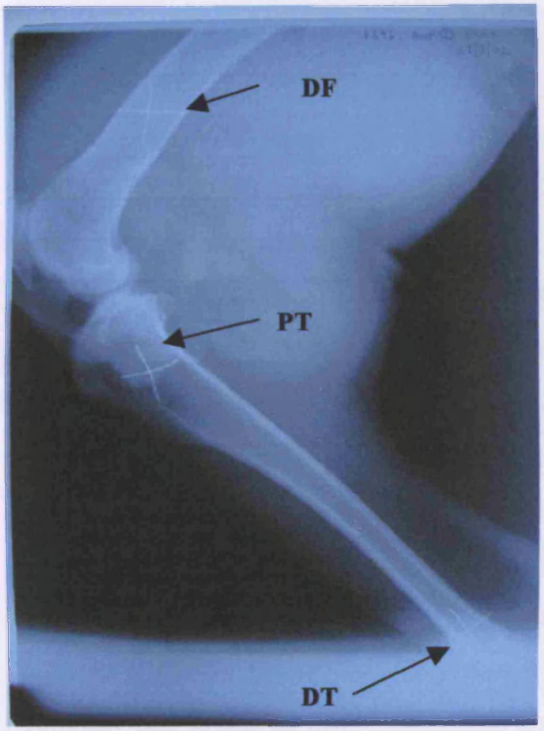

6.7 A radiograph of a cadaveric ovine hind limb in full flexion, with markers positioned on the distal femur (DF), the proximal tibia (PT) and the distal tibia (DT) – arrows demonstrate the positions of the cross-hairs of the wires fixed to the back of the polystyrene skin markers.

FIGURE 6.8

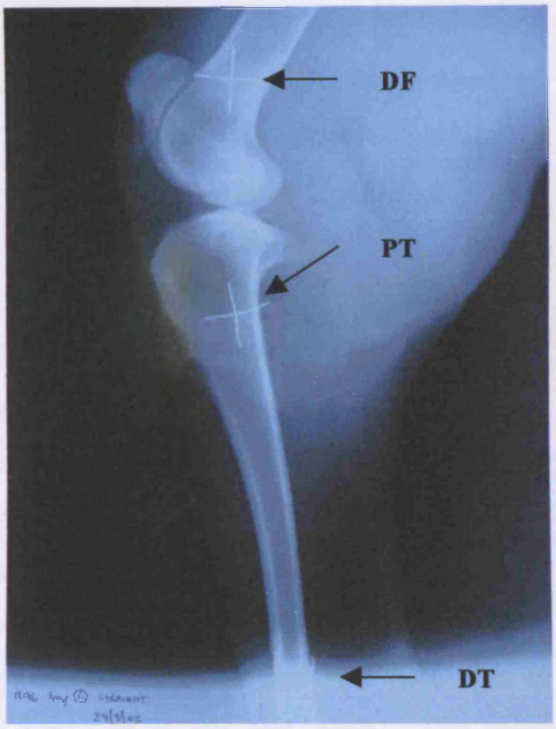

6.8 A radiograph of a cadaveric ovine hind limb in extension, with markers positioned on DF, PT and DT as above, arrows demonstrate the cross-hairs fixed to the skin markers. The distal femoral marker shows slight displacement from its position in flexion (above).

6.4.4.1.2 *IN VIVO* TWO-DIMENSIONAL KINEMATIC GAIT ANALYSIS

The animals were allowed to acclimatise to the gait laboratory prior to any functional assessment. The right hind quarter of each animal was shaved to enable more accurate positioning of the skin markers. Careful assessment of surface anatomy was used to locate landmarks for four markers (25mm diameter, hemispherical polystyrene covered with retro-reflective tape) which were positioned on the right hind limb, on the skin surface overlying the greater trochanter, lateral distal femoral condyle, lateral proximal tibial condyle and lateral distal tibial condyle. The animals were trained to walk in a straight line, along a twelve meter runway and once a routine had been established, their gait was recorded with an infra-red light emitting diode camera system (Qualisys ProReflex Version 6.42, Qualisys AB, Sweden). One camera was used at 240 Hertz (one still image recorded every 1/240 of a second) to record the two-dimensional positional

change of the reflective markers in the sagittal plane over a ten second time period. The camera was set with a field of view angle of 43.8 degrees and was positioned 2.16 meters from the centre of the runway. Using trigonometry, the field of gait recorded was calculated to be 1.7 meters. Up to fifteen voluntary walks were recorded for each animal and the data from each file generated (one file per walk) was processed using the Qualisys Qtrac software (version 2.56). Each file consisted of at least two full gait cycles over the 1.7 meter distance recorded. The files were exported from the Qtrac software into readable Microsoft Excel files, expressing the sagittal plane x-y coordinates in millimetres, for the position of each marker over time. The speed of each walk was independently calculated using the x-coordinate displacement of the greater trochanter marker, and dividing it by the duration of the walk (Appendix 6.1). Only walks which did not significantly differ in terms of speed (determined using SPSS version 10.1) were used for further analysis of gait. A custom-written programme, designed and written by Andy McPherson (The Centre for Biomedical Engineering, Institute of Orthopaedics, University College London, UK) was applied to the tracked Excel raw data files to calculate the angle at the stifle joint at the extremes of the gait cycle. The angle calculated was the bisecting angle between two lines drawn between the two femoral markers and the two tibial markers (Figure 6.9). The calculated difference between the angle at extremes of flexion and extension was defined as the Range of Movement, in degrees. A second derived angle was calculated by subtracting the post-operative angle of the knee in the extended position, from the equivalent pre-operative value (Figure 6.9 – difference in pre- and post-operative angle B), and was used as a measure of extensor mechanism competence following reconstruction. This derived angle was termed Lag if it was a negative value, or Hyperextension if positive.

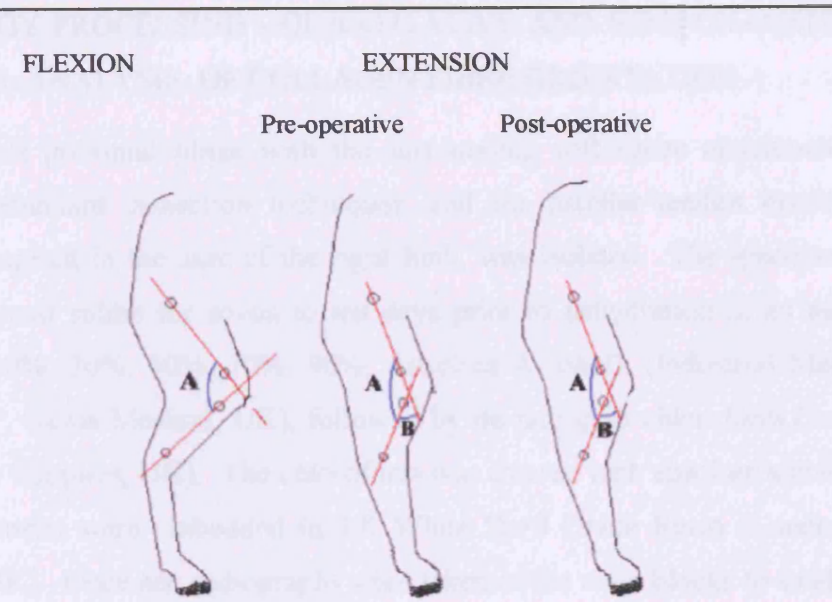

FIGURE 6.9 Schematic demonstrating the right hind limb marker positions for gait analysis. The difference in angle A between full flexion and full extension positions corresponds to the Range of Movement. The difference in angle B between pre- and post-operation corresponds to the Lag or Hyperextension.

6.2.3.4.2 FORCE PLATE ANALYSIS

In the gait laboratory, animals were trained to walk across a force plate (Kistler Biomechanics Ltd, UK) that had been incorporated at ground level and was indistinguishable from the remainder of the floor surface. A walk was only recorded when one or other of the animal's hind limbs had contacted the centre of the force plate without any contact with other limbs, in a normal walking cycle. Twelve readings were performed for each hind limb. The data were collected as x, y and z coordinates of the Ground Reaction Force (GRF) in Newtons, and the force plate software calculated the mean peak vertical component (z co-ordinate) normalised for the weight of the animal for each limb (Fmax/weight), and the mean right hind limb peak vertical (Fz) GRF as a percentage of the mean left hind limb peak vertical (Fz) GRF (operated/control expressed as a percentage) for all twenty four walks.

6.2.4 HISTOLOGY PROCESSING - QUANTITATIVE AND SEMI-QUANTITATIVE HISTOLOGICAL ANALYSIS OF COLLAGEN FIBRE ORIENTATION

The right and left proximal tibiae with the surrounding soft tissue attachments were removed using standard dissection techniques, and the patellar tendon insertion site containing the implant in the case of the right limb, was isolated. The specimens were fixed in 10% formal saline for seven to ten days prior to dehydration in an ascending alcohol series (10%, 30%, 50%, 70%, 90%, Absolute Alcohol), (Industrial Methylated Spirit 99%, 74°P, Genta Medical, UK), followed by de-fatting in chloroform (AnalaR®, BDH Laboratory Supplies, UK). The chloroform was cleared with absolute alcohol, after which the specimens were embedded in LR White Hard Grade Resin (London Resin Company Ltd, UK). Once set, radiographs were taken of the resin blocks to establish the specimens orientation. An EXAKT 310CP (supplied by MEDEREX, UK) was employed to rough cut sections of between 150-200μm in thickness. The resulting sections were ground using P500/P1200 grade paper on an EXAKT-Micro-Grinding System (MEDEREX, UK) to a thickness of approximately 100μm, prior to polishing with a Motopol 2000 using Mastertex® polishing cloth and Silico-Colloidal liquid (Buehler, UK). The slides were stained with Toluidine Blue and counter stained with Paragon (approximately twenty minutes each), air dried and then covered with a cover slip and Pertex Mounting Medium. The slides were viewed with an Olympus BH2 microscope linked to Zeiss KS300 3.0 computer image software.

Three sections at regular width intervals across the clamp were prepared for each animal. For each section, five fields of view along the length of the base plate were observed at a magnification of x100. A double-blind, quantitative analysis of collagen fibre orientation at the implant surface was performed by measuring the angles of elevation of the collagen fibres per field of view, with respect to the HA-coated base plate which was taken as a point of zero reference, using Adobe® Photoshop® version 6.0.1. The collagen fibre orientation in the normal patellar tendon – bone enthesis was measured similarly, using the tangent to the surface of the tibial tuberosity as a point of zero reference. Comparisons were made between the HA and Autograft Groups, and normal patellar tendon – bone insertion using a Mann-Whitney U test (SPSS version 10.1 for Windows). A double-blind analysis of the bone – tendon interface was carried out for all sections where bone graft was observed within the clamp, whether associated with the HA coating or not. The tissue was described as either fibrous or fibrocartilaginous on the basis of the histological appearance at six and twelve weeks, and was expressed as a percentage. The

independent assessments were carried out by Siva Sundar (BSc student – Centre for Biomedical Engineering). The results were tested for significance using a Mann-Whitney U test.

6.2.5 STATISTICAL ANALYSIS

The raw data was entered into SPSS version 10.1 for Windows statistical analysis software. The distribution of the data was analysed for normality using the Kolmogorov-Smirnov test. The data sets were examined for statistical differences between groups at a single time period and within each group between the two time periods. Non-normally distributed data sets were analysed using the Mann-Whitney U test, with results of $p<0.05$ being considered to be significantly different.

6.3 RESULTS

6.3.1 CLAMP DESIGN PILOTS

Results from hard grade resin histology of the prototype clamp device with a solid bridging plate (Figure 6.10a) demonstrated that a more enclosed environment lead to significant tissue necrosis (Figure 6.10b). The modified H-shaped clamp lid with perforating drill holes allowed ingrowth of the overlying tissues and vascular infiltration that was sufficient to prevent tissue necrosis, whilst providing sufficient mechanical fixation to hold the tendon within the clamp.

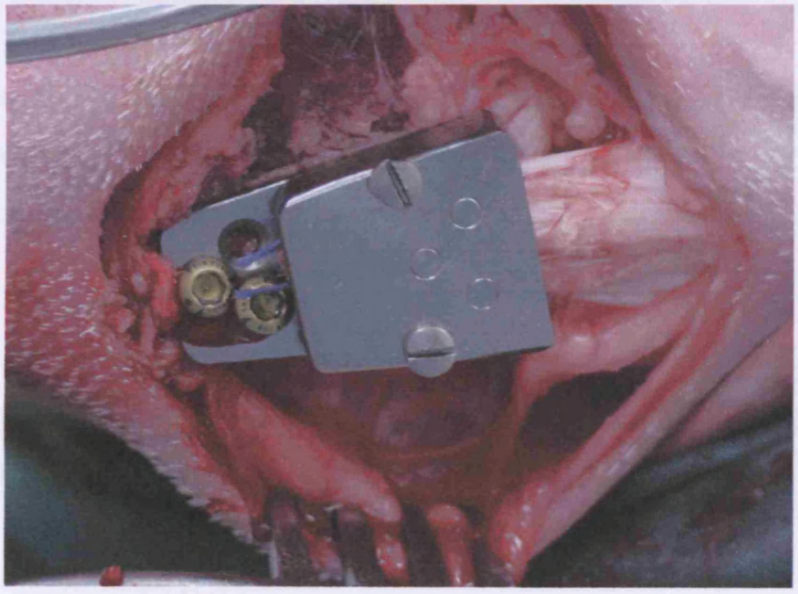

FIGURE 6.10 a Shows the prototype clamp device used in pilot study with solid lid

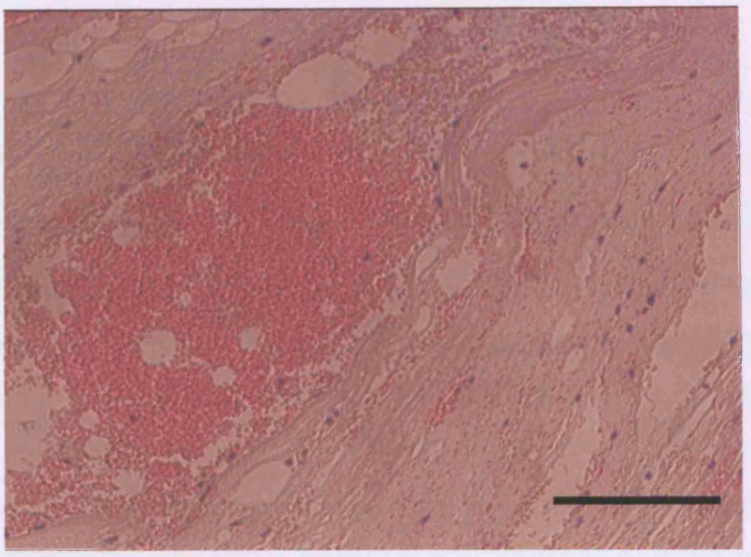

FIGURE 6.10b Shows the necrotic tendon at autopsy processed in paraffin wax and stained with haematoxylin and eosin. Bar = 100 μm.

6.3.2 NEGATIVE CONTROL PILOT

The negative control animal was found to be lame at six weeks post-operation, and it was considered unethical to force the ewe to walk.

6.3.3 SURGERY

All animals recovered from the surgical procedures and were observed to be standing within twenty-four hours. One animal (#1382) developed a deep suppurative infection - *Actinomyces pyogenes* and coagulase-negative *Staphylococcus*, which became apparent after thirteen days. A Veterinary Surgeon incised the wound whilst the animal was under general anaesthesia. The tendon-attachment site was found to be necrotic, hence the animal underwent terminal anaesthesia. This animal was replaced with another animal selected at random from the same stock (#1652). One animal (#1399) developed a superficial wound infection approximately twenty-one days post-operation. The animal was examined by a Veterinary Surgeon who prescribed an intra-muscular course of Ceftiofur antibiotic and local wound cleaning with Pevidine, which cleared the infection.

Some animals in the Autograft Group were lethargic in the early post-operative period, however this appeared to resolve itself within three weeks post-operative date.

6.3.4 GAIT ASSESSMENT RESULTS

6.3.4.1 TWO-DIMENSIONAL KINEMATIC GAIT ANALYSIS RESULTS

The gait laboratory provided an unrestrained path for the animals to walk at their own speed and direction. Generally, the animals maintained a straight gait pattern and were assisted by guided strips of flooring. The speed at which the animals walked was found to vary and in some cases the animals would stop directly in front of the camera. Owing to these problems, a large number of walks were discarded, either because the walk was flawed, as determined by a two person subjective assessment, or if the optical system did not correctly track the position of the markers for at least one entire gait cycle per walk. All animals were walked pre-operatively and pre-euthanasia. Animals in the Twelve-week Group did not undergo assessment at six weeks post-operation due to a computer-software problem.

6.3.4.1.1 CADAVERIC STUDY – ASSESSMENT OF SKIN DISPLACMENT

The data did not fit the requirements for parametric testing; hence a Mann-Whitney U test was used. No significant differences were observed between the position of the markers on their original anatomical landmarks and their respective positions with the limb orientated in full flexion or full extension (p values > 0.05).

6.3.4.1.2 GAIT SPEED

It was assumed that the speed at which an animal walked would affect the range of movement at the stifle joint. The nature of the correlation between pre-operative gait speed and the range of movement of the stifle joint was determined using Spearman's rho analysis. The relationship was found to be significant at the 99.9% level (R squared = 0.264, $p<0.001$), hence the range of movement at the stifle joint is observed to increase with increasing walking speed. Figure 6.11 displays a regression curve of the results obtained.

In order to study the effect of the operative procedure on the gait kinematics, the speed of the animals had to be eliminated as a variable from the pre- and post-operative data. For each animal, the data sets of up to fifteen accepted walks were analysed. At least six walks were taken for each animal, both pre- and post-operatively, where the speed was not significantly different between the time periods. The speed data sets were found to be non-normally distributed, hence Mann Whitney U tests were carried out on all of the pre- and post-operative raw speed data, for each animal individually. The mean, +/- standard error, median and p values for pre- and post-operative speeds are presented in Appendix 5 (5.1).

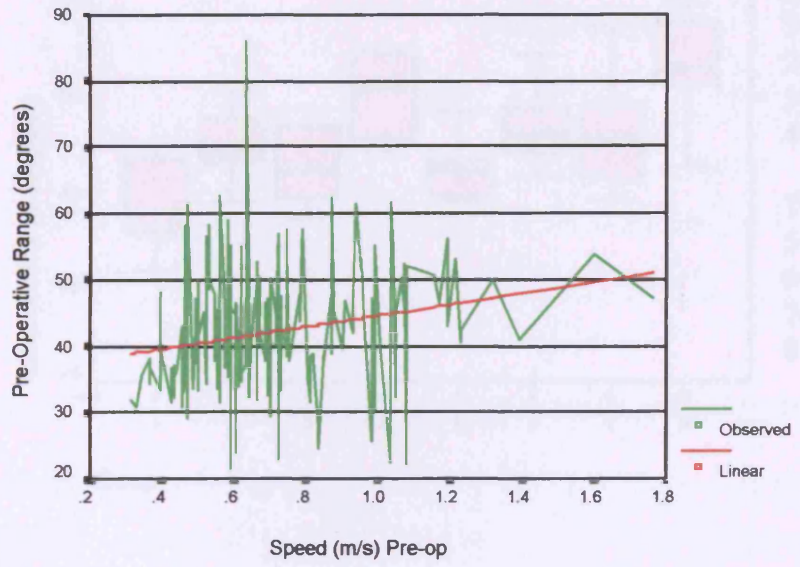

FIGURE 6.11 Demonstrates the relationship observed between pre-operative speed and stifle joint range, obtained using two-dimensional optical kinematic gait analysis.

6.3.4.1.3 RANGE OF MOVEMENT

The data obtained for range of movement at the stifle joint (normalised for speed pre- and post-operatively) for the groups by intervention and time and are presented in Figure 6.12. The summary and individual animal data is presented in full in Appendix 5 (5.2).

The results were analysed statistically using the Mann –Whitney U test to establish any significant differences between the stifle joint range pre- and post-operatively, within each of the four groups by intervention or time. No significant differences were observed (p values > 0.05). A summary of these findings is presented in Appendix 5 (5.2). There were no significant differences between data sets for pre- and post- operative stifle joint range in the HA or Autograft Group animals in both the Six- and Twelve-Week groups (all p values >0.05).

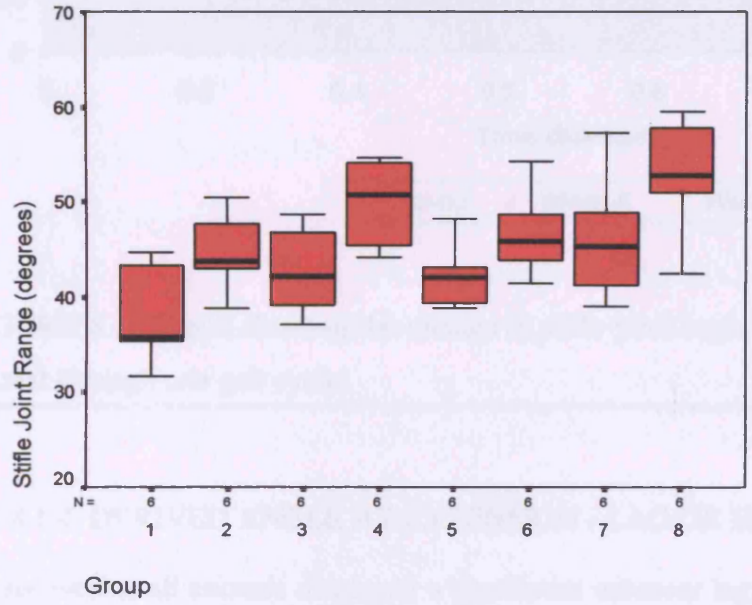

Groups (x-axis):

Six-Week groups
1= HA Group pre-op
2= HA Group 6 weeks
3= Autograft Group pre-op
4= Autograft Group 6 weeks

Twelve-Week groups
5= HA Group pre-op
6= HA Group 12 weeks
7= Autograft Group pre-op
8= Autograft Group 12 weeks

FIGURE 6.12 Displays a box and whiskers plot of the stifle joint range data, displaying the median, interquartile range and extreme values of stifle joint range in degrees, for the grouped data listed in the table above, which presents a summary of stifle joint range statistics for HA and Autograft (Auto) groups pre- and post-operatively.

Stifle joint range data was plotted on a graph as shown in Figure 6.13. The graph demonstrates that the surgical procedure did not compromise the stifle joint range at either six or twelve weeks post-operation, and that the morphology of the range of movement of the joint through one gait cycle was not altered by the re-attachment of the patellar tendon using the methods described.

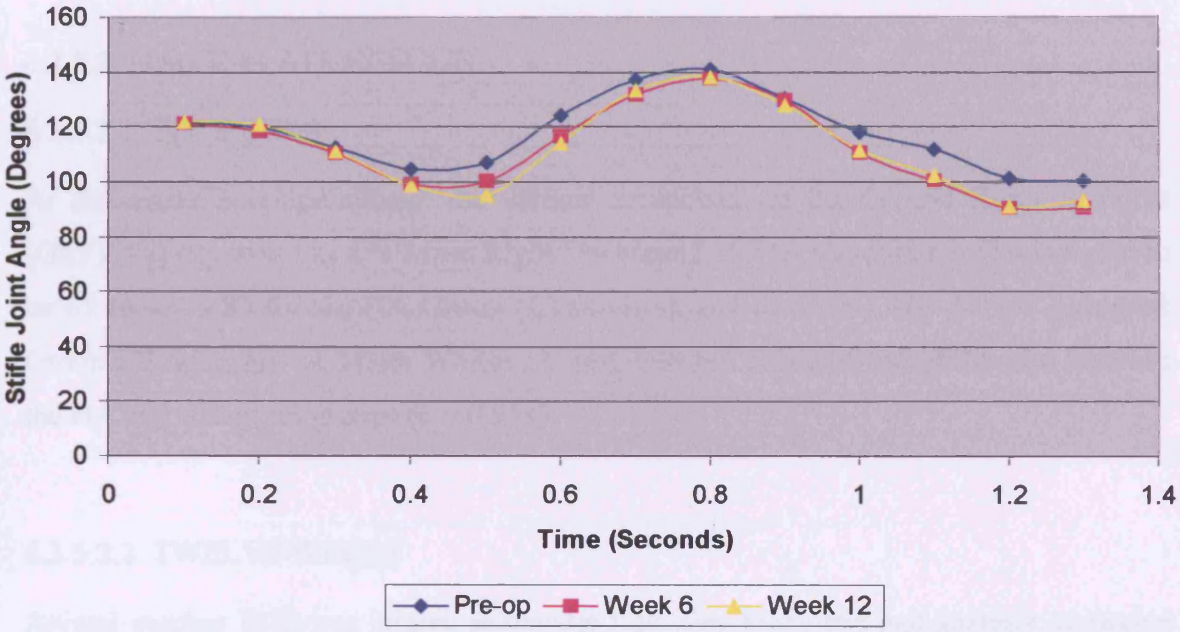

FIGURE 6.13 Graph showing the change in stifle joint angle with time for an individual animal through one gait cycle.

6.3.4.1.4 DERIVED ANGLE AT EXTENSION - LAG OR HYPEREXTENSION

At six weeks, all animals displayed a significant extensor lag; the position of the knee at extension was in a more flexed position than the same limb pre-operatively ($p < 0.05$). The mean (+/- standard error) lag for the HA and Autograft groups were found to be –14.75 +/-3.71 degrees and –18.34 +/- 4.75 degrees respectively. A Mann Whitney U test showed that there was no significant difference in the extent of lag measured between the HA and Autograft groups ($p = 0.631$). The individual animal data is presented in Appendix 5 (5.3).

At twelve weeks, a number of animals displayed hyperextension of the stifle joint during the gait cycle, as compared with their joint position at extension pre-operatively (Appendix 5 (5.3)). The mean angles (+/- standard error) for the HA and Autograft groups were found to be 2.73 +/-6.13 degrees and 0.97 +/- 7.31 degrees respectively, and the data is presented in a box and whiskers plot in Figure 6.11b (individual animal data is presented in Appendix 5 (5.3)). A Mann Whitney U showed that no significant difference

in mean extension angle was observed between the HA and Autograft groups at twelve weeks ($p = 0.749$).

6.3.5.2 FORCE PLATE RESULTS

6.3.5.2.1 SIX WEEKS

At six weeks post-operatively, the vertical component of the Ground Reaction Force (GRF) (Fz) expressed as a % Mean Right / % Mean Left (+/- standard error) was found to be 65.16 +/- 3.83 for the HA Group (12 animals), and 65.51 +/- 3.05 for the Autograft Group (12 animals). A Mann Whitney U test detected no significant difference between the HA and Autograft groups ($p = 0.954$).

6.3.5.2.2 TWELVE WEEKS

Animal number 1386 was injured in transfer following kinematic gait analysis, at twelve weeks post-operation. When tested over the force plate the following day, she displayed a noticeably altered gait pattern and a decrease in the GRF (Fz) compared with the value recorded at six weeks was noted. The animal was considered lame on grounds unrelated to the surgery; hence force plate data were not included at twelve weeks.

At twelve weeks post-operatively, the GRF (Fz) expressed as % Mean Right / Mean Left (+/- standard error) for the HA Group (6 animals) was found to be 78.97 +/-3.71, and for the Autograft Group (5 animals) was 80.21 +/- 7.65. A Mann Whitney U test showed no significant difference between the HA and Autograft Groups ($p = 0.465$).

6.3.5.2.3 BETWEEN SIX AND TWELVE WEEKS

The data obtained for the Twelve-Week Group animals was examined to determine whether there was a change in functional weight bearing between six and twelve weeks post-operatively. To allow the data to be compared between the six and twelve week time points, the differences in Fmax/weight (data normalised for weight of each animal – Methods Section 6.2.4.2) between the two time points was calculated for both right (operated) and left (non-operated control) hind-limbs for animals in the Autograft (five animals) and HA (six animals) groups. The mean increase in Fmax/weight (+/- standard error) for the operated limb was 0.81 +/- 0.80 for the HA Group and 5.31 +/- 0.86 for the Autograft Group. A Mann Whitney U test detected a significant difference between the

change in Fmax/weight for the Autograft Group compared with the HA Group between six and twelve weeks ($p = 0.018$). The increase in force (normalised for weight) put through the operated limb between six and twelve weeks, was significantly greater in the Autograft Group compared to the HA Group ($p < 0.05$). In comparison, for the non-operated limb (control), the mean change in Fmax/weight was –3.99 +/- 1.76 for the HA Group and –1.71 +/- 2.08 for the Autograft Group. No significant difference was detected between the group changes in Fmax/weight for the Autograft Group compared with the HA Group using a Mann Whitney U test ($p = 0.715$). These findings are presented in Figure 6.14.

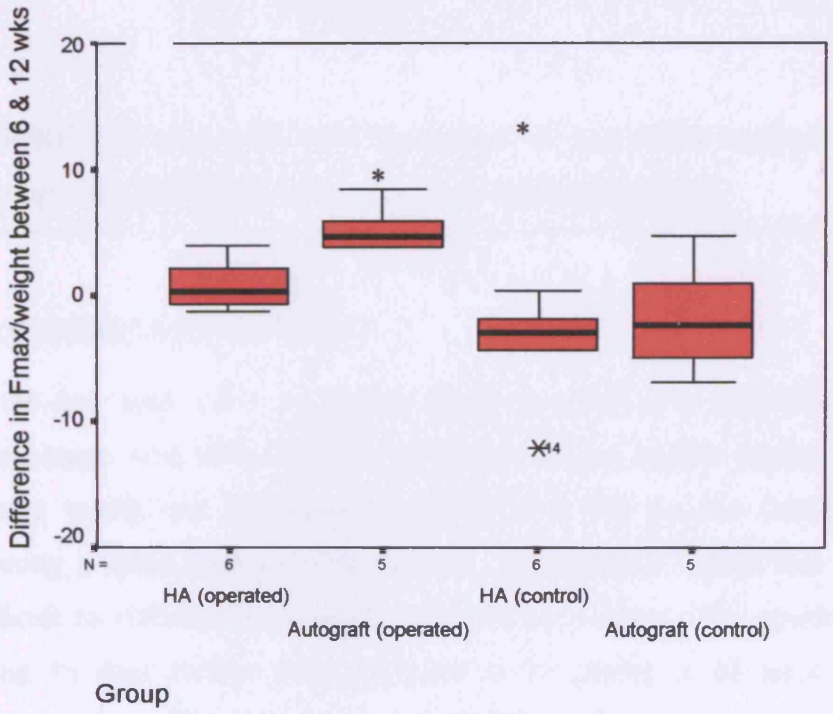

FIGURE 6.14 Presents the Box and Whiskers plot of the data obtained for differences in Fmax/weight between six and twelve weeks for the HA vs. Autograft operated limb data ($p = 0.018$*) and HA vs. Autograft control limb data ($p = 0.715$).

Force plate assessment of early functional response to the operative procedure at six weeks varied noticeably between individual animals in both the Autograft and the HA Group. Twelve weeks post operatively, some individuals were observed to have recovered a GRF (Fz) for the operated limb, with a magnitude and morphology approaching that of the control limb – Figure 6.15.

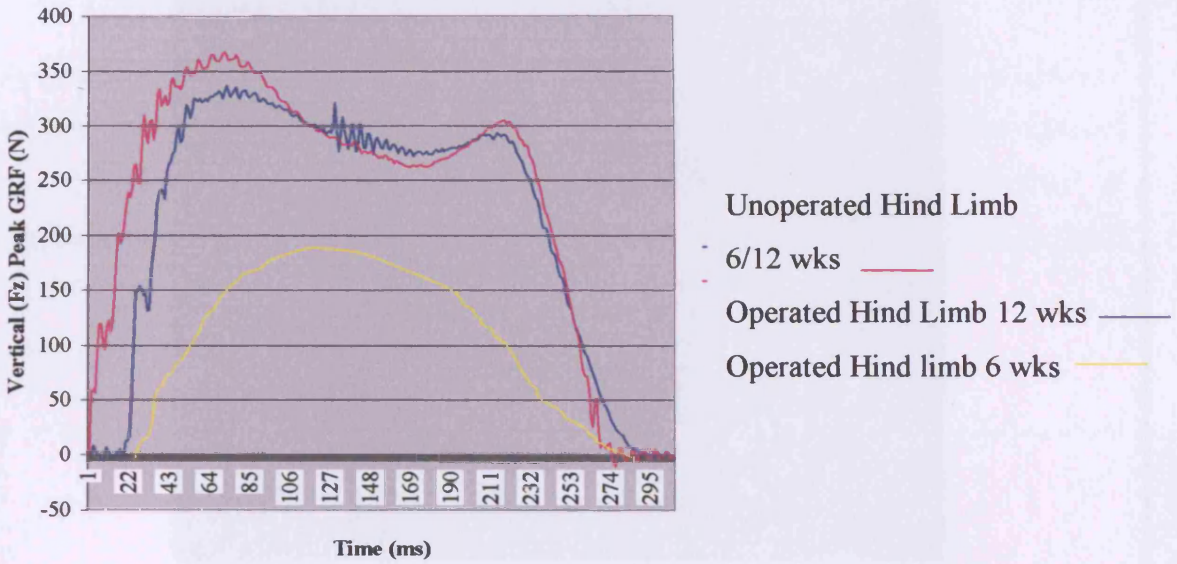

FIGURE 6.15 Shows the GRF (Fz) plot at six and twelve weeks for operated (right) and non-operated (left) hind limbs with the traces superimposed.

6.3.6 GROSS MORPHOLOGY

In the two week pilot, the tendon tissue appeared as a soft, brittle, brown degenerate tissue mass, with little similarity to that of normal healthy tendon material. At six and twelve weeks, the subcutaneous tissues over the patellar tendon-clamp had healed, forming a dense connective tissue scar. The patellar tendon had thickened and it was difficult to differentiate it from the overlying tissues. The patellar tendon was traced along the deep surface from proximal, at the patella, to its entry into the clamp. The clamp was enveloped in a mass of thickened, hard white scar tissue, whilst moderate vascularity in the surrounding tissues was noted. Disruption to the tissue-clamp construct was avoided. The specimens for histology were maintained intact to prevent damage to the developing interface (Figure 6.16).

FIGURE 6.16

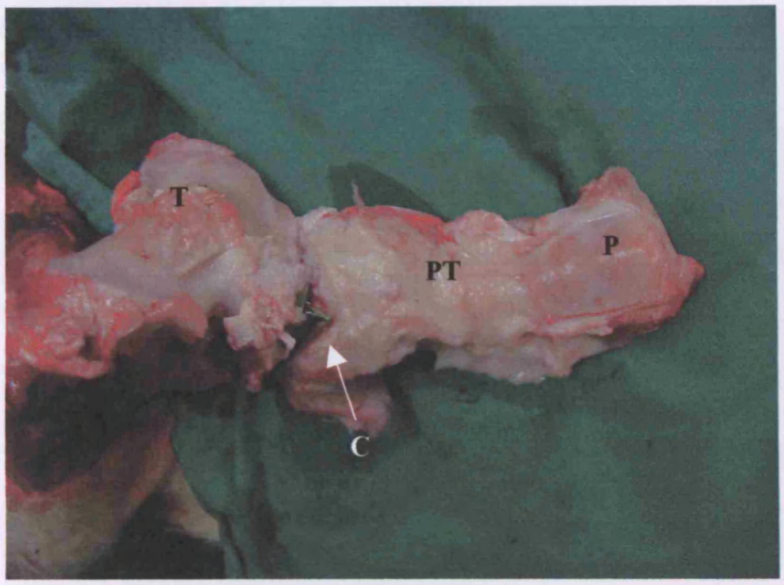

FIGURE 6.16a Shows the deep surface of the patellar tendon (PT) as dissected out, with the patella (P) and clamp (C) in a six week specimen.

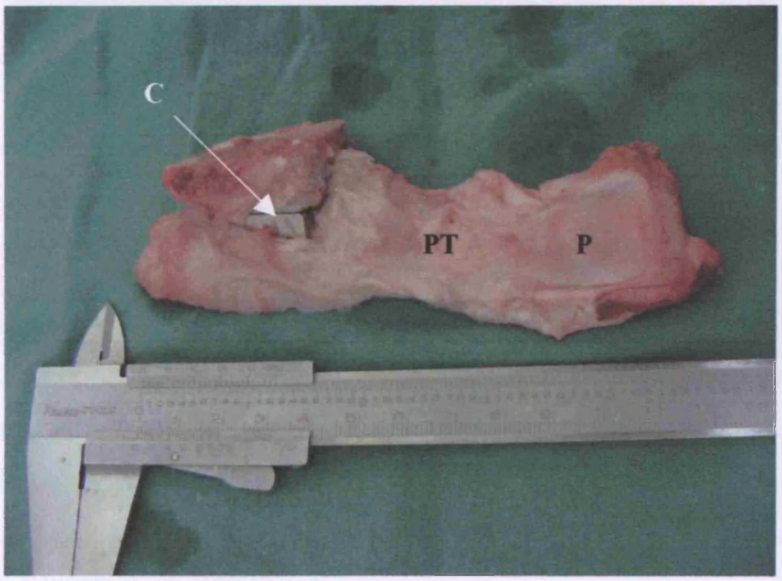

FIGURE 6.16b Shows the superficial surface of the patella (P) – Patellar Tendon (PT) – Clamp (C) dissection of a six week specimen.

6.3.7 HISTOLOGY RESULTS

6.3.7.1 NORMAL TENDON-BONE INTERFACE HISTOLOGY

The left hind control, stifle joint patellar tendon-bone interface site is a direct-type insertion comprising a four-layered enthesis as seen in Figure 6.17. A clear layer of rounded cells lying in lacunae was observed between the tendon and the bone. A tidemark of differential staining was seen, separating the unmineralised and mineralised fibrocartilage regions.

FIGURE 6.17

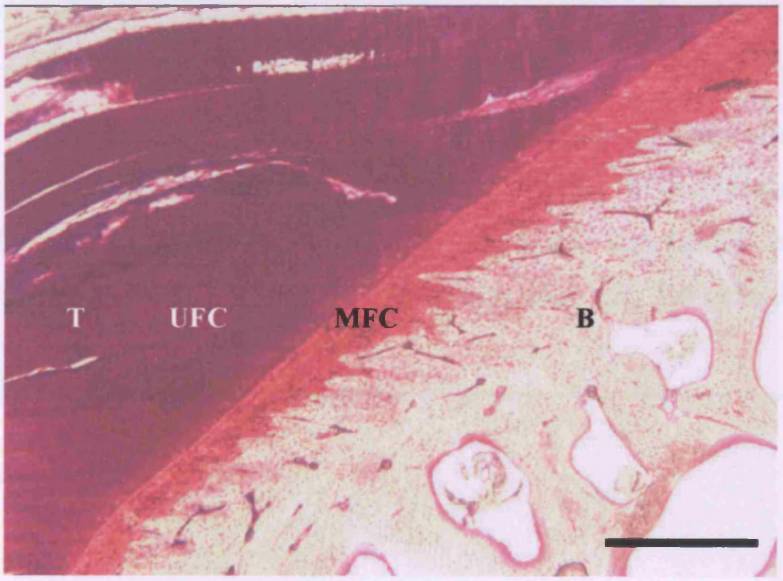

FIGURE 6.17 a Shows the appearance of a normal patellar tendon insertion in the sheep stifle joint. Tendon (T) and bone (B) are clearly separated by a fibrocartilage region, where a tidemark of stain is seen between unmineralised (UFC) and mineralised (MFC) zones. Toluidine blue and Paragon X10. Bar = 1mm.

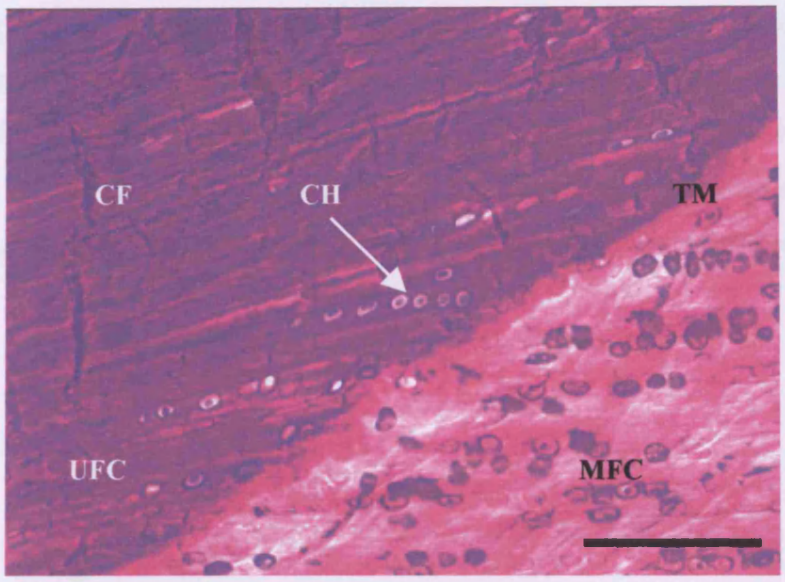

FIGURE 6.17 bThe tidemark (TM) from 6.17 a at a higher magnification, separating regions of unmineralised (UFC) and mineralised (MFC) fibrocartilage. Rounded chondrocyte-like cells (CH) are visable within lacunae, surrounded by a parallel-orientated collagenous fibre (CF) matrix. Toluidine blue and Paragon X100. Bar = 100μm.

6.3.7.2 CLAMP DESIGN PILOTS

The clamped portion of the tendon from the two week pilot study, appeared to have lost all normal parallel-orientated crimped collagenous fibre morphology. It possessed regions of vacuolar and fatty degeneration surrounded by a sparse network of collagen-fibre remains, interspersed with disorganised areas containing amorphous cells in a pale stained matrix, the remnants of a resolving blood clot and an acute inflammatory infiltrate – Figure 6.18.

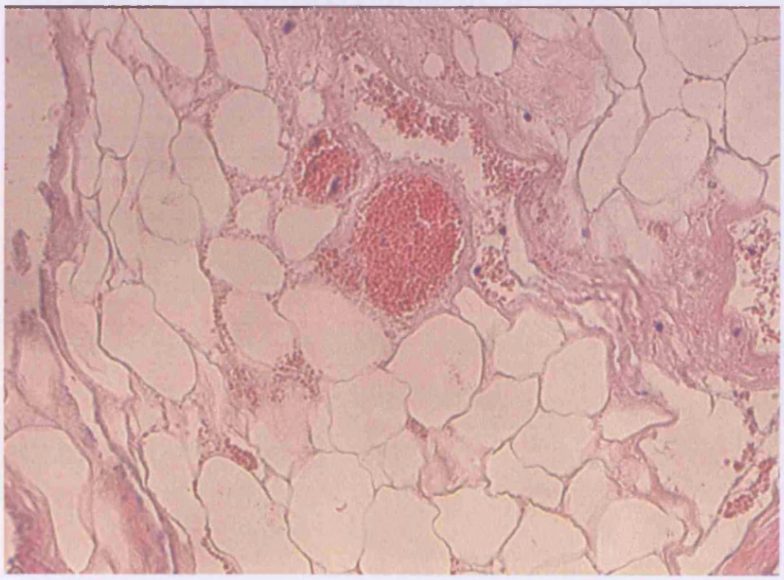

FIGURE 6.18 Demonstrates the appearance of the degenerate clamped tendon two weeks post-operatively. The sparce strands of collagen fibres border areas of vacuolar degeneration and adypocytes. Haematoxylin and Eosin x40.

6.3.7.3 SIX AND TWELVE WEEK HA AND AUTOGRAFT GROUP HISTOLOGY

For ease of analysis, the low power sections were divided into regions, which were considered separately, as shown in Figure 6.19.

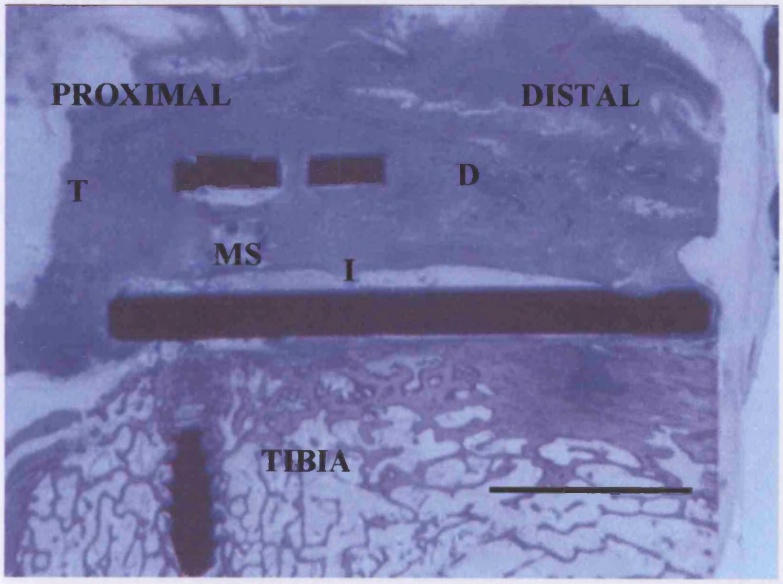

FIGURE 6.19 Low power section of clamped tendon six weeks post-operatively. T – Normal tendon region. MS – Mid-substance tendon. I – Interface region. D – Down-growth. Toluidine blue and Paragon. Bar = 10mm.

6.3.7.3.1 NORMAL TENDON REGION

Analysis of the normal tendon region in all sections revealed the morphology to be similar to that of an unoperated tendon running into the clamp, consisting of dense connective tissue with parallel orientated collagen fibres adopting a crimped pattern (Figure 6.20). In some sections this region was easily differentiated from that of the mid-substance (MS), defined by a clear boundary between the two tissue types with differing morphologies, whilst in others a gradual transition was evident between the two zones. Ectopic calcification was observed within the normal tendon region of some specimens from both the HA and Autograft Groups at six and twelve weeks.

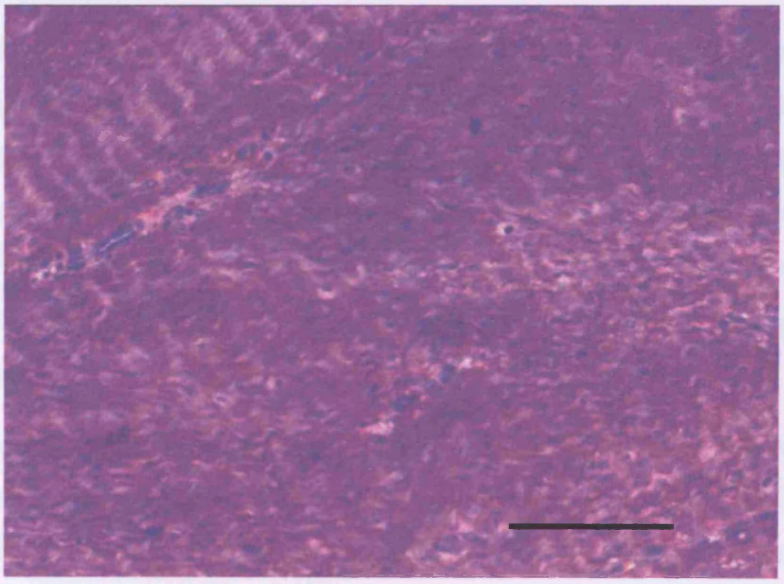

FIGURE 6.20 Shows the dense crimped collagenous connective tissue observed in the normal tendon region of all sections, six weeks post-operatively. Toluidine blue and Paragon x100. Bar = 100 μm.

6.3.7.3.2 MID-SUBSTANCE REGION

The clamped tissue was found to be morphologically distinct from that of normal tendon. At six weeks, the connective tissue showed extensive loss of normal collagen fibre density and orientation. In some areas, collagen fibres appeared randomly organised and interspersed with a moderately high population density of fibroblast-like cells with rounded, plump nuclei, whilst in others they maintained a degree of parallel alignment and contained oval/spindle shaped fibroblast nuclei. Some sections contained areas of vacuolar degeneration (Figure 6.21a), which were located centrally within the mid-substance tissue, whose peripheral morphology consisted of a denser collagenous connective tissue with a higher cell population density. A number of sections from both groups displayed a mixture of chronic inflammatory cells, with pools of lymphocytes and macrophages, and occasional foreign-body giant cells.

At twelve weeks, the mid-substance region in both groups had significantly re-organised. Collagen fibre density had increased, with a higher proportion of tissue displaying a parallel orientation to the long axis of the tendon. Some areas had adopted a 'wavy' pattern (Figure 6.21b). Fewer inflammatory cells were present compared with the six week sections and numerous fibroblasts were observed with both oval and spindle shaped nuclei. No noticeable differences were observed between the HA and Autograft groups at six or twelve weeks.

At six and twelve weeks, the Autograft group sections contained islands of actively remodelling bone graft material which had become incorporated into the mid-substance tissue. Osteoblasts and osteoclasts were visible within the bone graft regions (Figure 6.21c). At six weeks (6.21d), collagenous fibres were seen running in a perpendicular orientation into the remodelling bone graft material. By twelve weeks, areas of the bone graft material were found to be surrounded by fibrocartilagenous regions, in which cells adopting a rounded morphology were observed, set in lacunae within a darkly stained ground substance (6.21e).

FIGURE 6.21

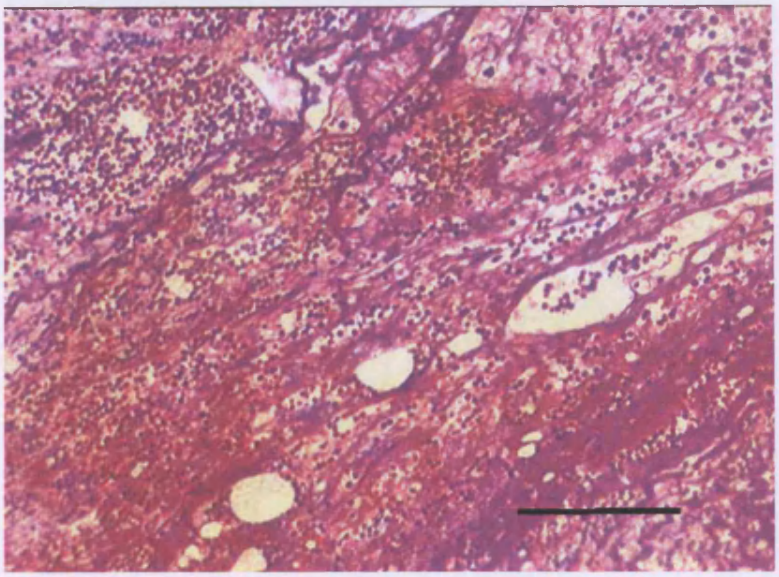

FIGURE 6.21a Demonstrates the appearance of a degenerative clamped tendon at six weeks with a considerable inflammatory infiltrate and vacuole density. Toluidine blue and Paragon x100. Bar = 100 μm.

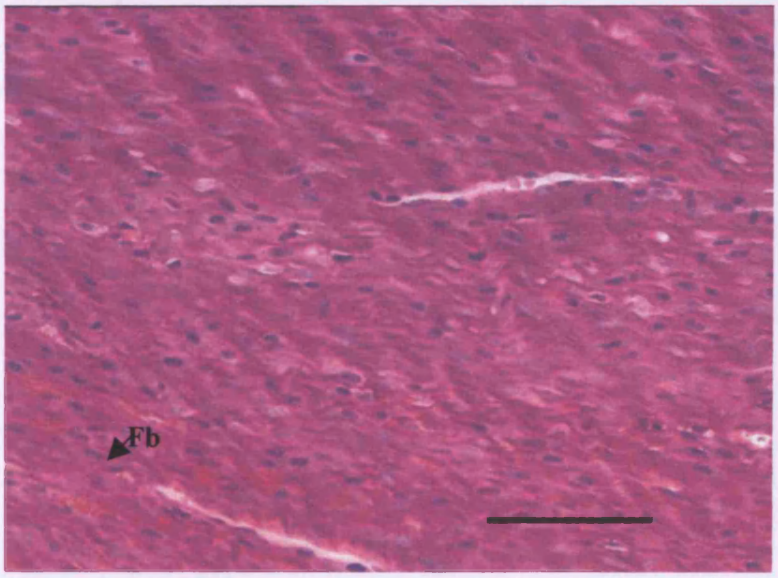

FIGURE 6.21b Shows the dense crimped collagenous connective tissue observed within the mid-substance clamped tissue at twelve weeks, containing fibroblasts with oval, plump nuclei (Fb). Toluidine blue and Paragon x100. Bar = 100 μm.

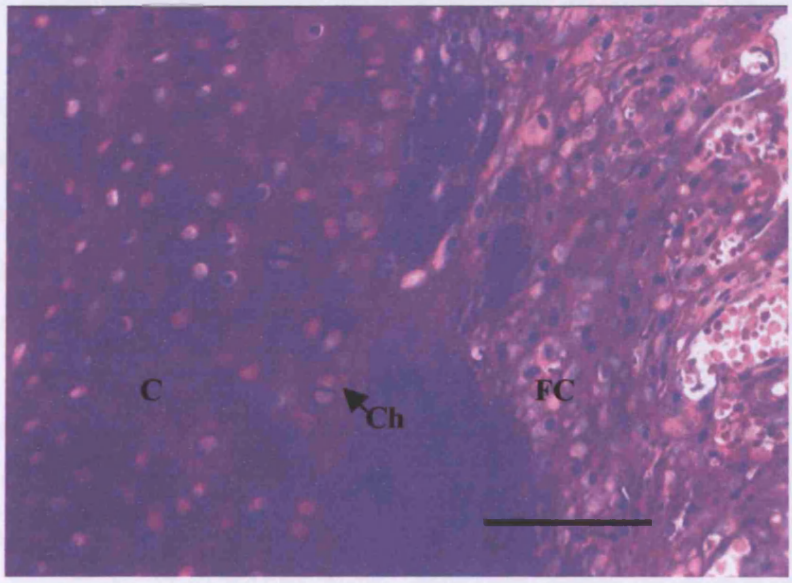

FIGURE 6.21e Shows the zonal organisation observed at the periphery of the bone graft material at twelve weeks. The cartilage layer (C) showed a uniformally stained amorphous ground substance with chondrocyte-like cells (Ch) seen singly or grouped in lacunae. The neighbouring fibrocartilage (FC) region, with a mixed morphology was easily differentiated from the cartilagenous tissue. Toluidine blue and Paragon x100. Bar = 100 μm.

6.3.7.3.3 INTERFACE REGION

In the Autograft Group specimens in regions where the bone graft was retained on the HA surface, the interface was found to be different from the HA Group interface. Tissue processing and preparation resulted in the loss of tissue in intimate apposition with the HA surface in a number of samples. However, a sufficient number retained the tissue-implant interface to enable a descriptive analysis of the resulting attachment. In the HA group at six and twelve weeks, the implant surface was enveloped by a connective tissue layer in which the collagen fibres were observed to run parallel to the orientation of the base plate (Figure 6.22a). In the Autograft group, the fate of the bone graft varied between specimens. In some samples, the graft material became incorporated into the mid-substance connective tissue without an attachment to the HA surface. In others, where the bone graft remained in intimate contact with the HA layer, the graft material was seen to undergo significant resorption, leaving faint impressions of trabecular structures with a considerable inflammatory infiltrate. In the six week specimens, some areas contained actively remodelling bone graft and newly formed bone in intimate contact with the HA layer of the base plate. In some of these sections, a developing soft tissue-bone interface with the adjacent tendon material in the clamp centre was also observed. The early (six week) soft tissue-bone interface was composed of collagenous Sharpey's-like fibres, originating from new bone, and spanning the soft tissue-bone interface in a perpendicular orientation (Figures 6.22b and 6.22c). By twelve weeks, insufficient bone graft material remained in intimate contact with the HA surface to accurately describe the soft tissue-bone-implant interface. However, it is speculated that had the interface been preserved and continued to develop from the morphology of the interface observed at six weeks, a layered soft tissue-fibrocartilage-bone interface, similar to that observed between the mid-substance soft tissue and dislodged bone graft islands, may have developed (Figure 6.22e).

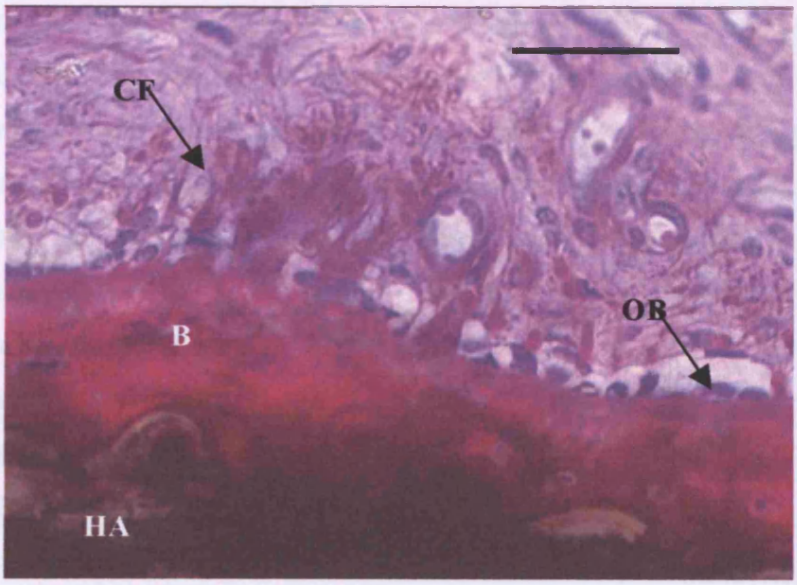

FIGURE 6.22c High power image of the interface observed in 6.22b. Bone (B) is seen in intimate association with the HA surface, with clearly visible ostoeblasts (OB) and perpendicular Sharpey's-like, collagen fibres (CF) spanning between the new woven bone and soft tissue in a perpendicular maner. Toluidine blue and Paragon x200. Bar = 50 μm.

6.3.7.4 QUANTITATIVE AND SEMI-QUANTITATIVE HISTOLOGICAL ANALYSIS OF COLLAGEN FIBRE ORIENTATION

Quantitative analysis showed the collagen fibre orientation to the implant surface in both the HA and Autograft Group to be significantly lower than the fibre insertion angle at a normal patellar tendon enthesis ($p < 0.05$) (Table 6.1). However, there was significantly less difference in collagen fibre orientation angle between the Autograft Group and the normal patellar tendon enthesis (14.13 +/- 1.77 degrees) than between the HA Group and normal patellar tendon enthesis (27.18 +/- 3.54 degrees) ($p < 0.01$).

In the Autograft Group the nature of the tendon – bone graft interface, increased significantly with respect to percentage fibrocartilagenous nature, between six and twelve weeks ($p < 0.01$). The bone graft – tendon interfaces in the Autograft Group were significantly more fibrocartilaginous in nature at twelve weeks compared to those at six weeks ($p < 0.01$). In the HA Group no bone was found within the clamp and hence no semi-quantitative analysis of tendon – bone interface was performed.

	HA GP		AUTOGRAFT GP		INTACT
	6 Wks	12 Wks	6 Wks	12 Wks	
Collagen fibre orientation (Degrees +/- Standard Error)	- +/- 0.86	13.68	- +/- 1.02	19.73	34.96 +/- 2.55
Fibrocartilagenous % Interface	-	-	16 +/- 1.4 +/- 3.4	76	100
Fibrous % Interface	-	-	84 +/- 5.7 +/- 1.6	24	0

TABLE 6.1 Shows collagen fibre orientation and interface characterisation data for HA, Autograft and Intact Groups

6.4 DISCUSSION

This Chapter was carried out in an attempt to re-attach a major load-bearing tendon to a metal implant with sufficient mechanical strength to enable early limb use, whilst incorporating elements to develop a biological interface that would, over time, resemble the structure of the normal enthesis.

6.4.1 THE CLAMP DEVICE – EFFECTS ON TENDON ATTACHMENT

In current clinical practice, tendons are physically clamped to the body of the implant via specialised design features (Cannon 1997). Biologic responses of tendons subjected to compressive loads are often overlooked in an attempt to re-establish the biological continuity between muscle and bone units (Meriam et al 1995). In 2001, Rempel and Abrahamsson examined the effects of local ischaemia, a low oxygen state usually caused by the obstruction of the blood supply, on tendon explants *in vitro*, finding it significantly reduced collagen synthesis, whilst having no effect on tendon cell proliferation, proteoglycan and non-collagenous protein production or synthesis. Gottsauner-Wolf et al (1994) postulated that perforation of a tendon under compression results in less tissue damage. The clamp tested in my thesis provided mechanical fixation, which enabled immediate unprotected weight bearing, with no evidence for attachment failure. Functional assessment by direct biomechanical testing would provide useful objective data to supplement my results. However, this has not been presented here. The clamp compresses the tendon, hence the internal environment will be relatively avascular. Degenerative changes were only observed in the two-week studies. Tissue necrosis was not observed as a consistent finding in either Group, which concurs with other work in this field (Gottsauner-Wolf et al 1994). The prototype design tested in the pilot studies showed that a more enclosed environment lead to tendon necrosis. The modified H-shaped lid was a compromise to optimise ingrowth and allow vascular infiltration, whilst maintaining mechanical fixation. A time course assessment of the compressive forces encountered by the tendon *in vivo* may be valuable in determining whether degenerative changes are directly associated with mechanical clamping. Degenerative changes may also be a result of tendon detachment (Skoog and Persson 1954, Whiston and Walmsley 1960, Forward and Cowan 1963).

6.4.2 GAIT ASSESSMENT

Kinematic gait analysis has been utilised in numerous clinical and *in vivo* experimental models (van Best et al 1984, Chen et al 1991, Laassel et al 1992, Gage et al 1996). Reflective markers are fixed to the skin over skeletal prominences to define body segments. However, skin displacement and inconsistencies in surface anatomy definition are considered the principle drawbacks. In my study, surface anatomy assessment and marker attachment was carried out by two independent assessors to reduce error in marker positioning, whilst skin displacement was considered negligible based on radiograph analysis (Figures 6.4 and 6.5). More advanced gait laboratories can perform three-dimensional assessments. Two-dimensional analysis is limited by the fact that a surgical procedure on an isolated joint will undoubtedly affect the total gait patterns of the subject, and that limb segments both proximal and distal to the site of intervention should be evaluated (van Best at el 1984). However, more advanced software would be required. Despite these drawbacks, it is considered a more objective measure of extensor mechanism competency than some of the previously reported subjective scales of function (Gottsauner-Wolf et al 1999). No previous study of tendon re-attachment has reported the use of kinematic gait analysis with force-plate assessment of weight bearing. For all animals in my study, there were no significant differences in gait cycle speed. Force-plate analysis is widely used to assess limb function. It can be used independently or in association with gait analysis (Otis et al 1985, Ghosh et al 1993, Jevens et al 1996, Muir et al 1996). Using data recorded from an implanted transducer in a goat model, it has been shown that the forces transmitted through the patellar tendon during normal gait increase in relation to the GRF (Fz) in a non-linear manner (Korvick et al 1996). For my study, the data obtained using force-plate analyses were thought to be directly related to the *in vivo* forces encountered by the tendon-implant construct. The speed of the animals over the force-plate was maintained using two-person subjective assessment to avoid possible error associated with speed effects on GRF (Fz). Force plate data obtained from twelve equivalent Friesland ewes showed that pre-operatively there was no significant difference between the right and left hind-limb GRF (Fz) (Appendix 6.5). Thus, differences observed in GRF (Fz) data post-operatively were considered to be a direct result of the surgical intervention and an accurate representation of the function of the extensor mechanism reconstruction. No significant differences were observed in weight bearing, determined using force plate data, between the groups at six or twelve weeks post-operatively. The increase in Fmax/weight between six and twelve weeks was significantly greater for the Autograft group compared to the HA group for the operated

limb, whilst no significant differences were observed for the non-operated limb of either group. In the Autograft group, both surgical procedures (the tendon re-attachment and the bone graft harvest) were carried out on the right hindquarter. It is possible that at six weeks the animals were affected by the dual interventions. However, by twelve weeks the animals showed a significant increase in functional weight bearing through the operated limb. It is appreciated that this increase may be the result of recovery from the operative procedures as apposed to a true reflection of the effects of the bone and marrow graft augmentation. At six weeks, the non-operated limb may be compensating for the weakened operated limb, thus resulting in a higher GRF (Fz) during the normal walking gait cycle. As the operated limb function improves with time, the GRF (Fz) of the non-operated limb would be expected to decrease. This was observed to be true where a negative value for the difference in Fmax/weight between six and twelve weeks for the non-operated limb is presented. Quadrepedal locomotion may enable the forelimbs to compensate for reduced operated limb function. In retrospect, it is thought that the GRF (Fz) should have been measured in all four limbs to quantify any compensatory gait variations. The operated limb of all animals demonstrated no significant variation from pre-operative range of movement at the stifle joint at six and twelve weeks. This is thought to reflect the successful mechanical fixation of the clamp device. At six weeks, the lag demonstrated by all animals indicated there was extensor mechanism dysfunction. By twelve weeks, an improvement in extensor mechanism was observed, where mean angles at extension for both groups indicated hyperextension. At twelve weeks, the near normal extension angle achieved, with the range of movement being not significantly different from that observed pre-operatively, is proposed evidence for a kinematic functional result equivalent to that seen in the normal stifle joint. The degree of extensor mechanism recovery here is greater than that reported (Jeon et al 1999, Bickles 2001). However, it is appreciated that the use of a quadrupedal model may mean that the *in vivo* patellar tendon forces are less than those encountered in a biped.

6.4.3 DEVELOPMENT OF THE TENDON-IMPLANT INTERFACE

Tendon and ligament insertions are characterised according to differences in morphology, into direct and indirect (Benjamin et al 1986, Rufai et al 1995, Clark and Stechschulte 1998). The normal ovine patellar tendon insertion is a direct enthesis. In studies of tendon – bone tunnel healing, collagen fibres are seen to span the developing interface (Jones et al 1987, Liu et al 1997). Although the clamp environment is unlike that seen

within a bone tunnel, it is proposed that augmentation with autogenous bone and marrow graft applied to the HA-coated implant can create an environment capable of supporting the development of a tendon – implant attachment. In the Autograft Group at six weeks, the presence of perforating collagen fibres between the tendon and bone is consistent with development of a direct enthesis. In the Autograft Group fibrous, tissue encapsulation was observed adjacent to the HA in areas not covered in bone graft material. Values for collagen fibre orientation at the interface showed no significance between the HA and Autograft Groups. In the Autograft Group, the interface contained regions with both tendon – HA and Tendon – bone attachment. The collagen fibre angles in both these regions contributed to the overall results and were responsible for the apparent lack of statistical significance, despite obvious qualitative morphological differences between regions on the same base plate. Better bone graft retention at the HA surface in the Autograft Group would reflect the different interface characteristics between the two groups. The differences in interface morphology between the Groups are thought to be due to biological augmentation with marrow and bone, since both Groups were exposed to similar local mechanical environments. It is appreciated that the presence of additional bone graft volume may have influenced the degree of tendon compression, and thus affect the resulting morphology. Collagen fibre insertion angle in a normal enthesis varies with respect to the position along the tuberosity and hence I have presented mean values in this Chapter. Variation in fibre orientation with respect to bone and implant surfaces has been shown to reflect the nature and integrity of the resulting attachment (Donley and Gillette 1991). The flat implant surface and angle of the osteotomy may have contributed to the shallow insertion angles observed in the Groups, and hence the mechanical environment may have influenced our findings. Tissue within the mid-substance region showed a progressive change with time for both groups. The morphology of the tissue through the integration phases was found to be consistent with other studies of tendon and ligament scarring (Liu et al 1997; Frank et al 1999). The process of tissue integration encompasses phases of tissue necrosis, revascularisation, cell re-population and collagenisation. Early regenerative processes associated with tendon and ligament healing have been reported to be 'disorganised' and the tissue is observed to be populated with numerous inflammatory cells and plump fibroblasts, which are seen to remove debris and produce new, but disorganised collagenous matrix (Frank et al 1985). Maturation and remodelling of tendon has previously been seen to occur from six weeks (Woo et al 1998) and was also observed in my study. Fibroblast shape has been studied under a number of mechanical conditions (Shrive et al 1993; Giori et al 1993) and the fibroblasts observed in the twelve

week specimens adopting a spindle-shaped / elongated morphology are consistent with that expected of cells in tensile load-bearing tissue. The tissue-implant interface in the HA group specimens did not form a similar attachment to a direct or indirect enthesis, and in all samples the HA layer was enveloped in a dense collagenous tissue with collagen fibres running parallel to the surface and the axis of tensile load. Reports demonstrating the osteoinductive potential of HA *in vivo* have always incorporated mineralised tissue, for example, in bone tunnel models (Ishikawa et al 2001) or injected into bone marrow sites (Katumura et al 1998; Sato et al 1998). Studies of soft tissue-implant interfaces have demonstrated that cell morphology and collagen fibre orientation to the implant surface are found to direct towards fibrous encapsulation rather than attachment (Donley and Gillette 1991; Chehroudi et al 1992; Steflik et al 1993). In the Autograft group at six weeks, the interface was similar in morphology to those observed previously in bone tunnel studies in which, at six weeks no layered enthesis with fibrocartilagenous regions were observed. However, the attachment consisted of anchoring collagen fibres originating from the new woven bone lining the tunnel (Jones et al 1987; Rodeo et al 1993; Panni et al 1997; Liu et al 1997; Shaieb et al 2000; Oguma et al 2001). The augmentation of bone and marrow graft used in my study assisted the successful development of a neo-enthesis, with the trabeculae of the cancellous bone providing an osteoconductive scaffold and the marrow providing a source of pluripotent cells, which are thought to induce osteogenesis (Gray and Elves 1982; Burwell 1985; Ohgushi et al 1989a and 1989b; Caplan 1991; Goshima et al 1991). By twelve weeks the morphology was similar to that seen in direct entheses. The maturation phase of bone tunnel-tendon healing interfaces has been reported to be considerably variable. Development of direct-like entheses up to six months post-operatively in tendon-bone tunnel healing studies have been shown (Rodeo et al 1993, Panni et al 1997, Aoki et al 1998). However, conflicting reports have described the presence of a less mature indirect-type entheses after twenty weeks (Jones et al 1987). Previous studies of tendon-implant attachment have used cancellous bone blocks and marrow augmentation; however they have not described the morphology of the bone block-implant interface or the extent of bone graft retention. In their 1995 and 1996 studies, Inoue et al observed the absorption of supplemented autogenous bone graft and replacement with a 'thick collagen bundle'. Inoue et al (1996) and Chao et al (1997) proposed that marrow supplement was responsible for osseoinduction and limited bone resorption. However, in my research the principle drawback with marrow augmentation was reliable retention within the clamp device. Since the clamp used in my thesis is a more closed system than the Enhanced

Tendon Anchor used by Inoue et al (1996) and Chao et al (1997), it is considered that their assumptions concerning the role of marrow supplement in osseoinduction and bone resorption processes are questionable. They showed a four-layered interface after sixteen weeks with bone integration through the titanium wire mesh-base plate construct. Successful attachment of bone graft to the HA coated implant used in my study would provide a superior attachment, mechanically and biologically, than that observed via solely mechanical fixation of bone to a wire mesh as presented by Chao et al (1997). Increased duration *in vivo* may allow further characterisation of the developing enthesis whilst implant design modification could improve graft retention. The interlocking spike mechanism within the clamp was shown to provide adequate mechanical stability. However, alternative means of fixation, including the development of a purely biological attachment using a resorbable mesh, are being examined further (Appendix 6.6). The bone and marrow graft may affect all of the layers of the developing interface. The marrow provided a source of pluripotent cells with osteogenic potential (Beresford 1989, Caplan 1991), whilst the trabeculae of the cancellous bone provided an osteoconductive scaffold for subsequent remodelling. HA has been shown to induce differentiation of pluripotent cells along an osteoblast linage (Rust et al 2003), provide a bioactive surface that can support mineralisation (Cook et al 1988, Ohgushi et al 1989, Meffert 1997) and induce collagen synthesis (Soballe et al 1990). I have shown that integration is observed with bone in intimate apposition with an HA-coated base plate. At twelve weeks, fibrocartilagenous regions between the tendon and bone trabeculae in the Autograft Group differentiated the interface from that observed in the Autograft group at six weeks and the HA Group at both time points. Semi-quantitative analysis of the amount of fibrocartilagenous tissue present at the bone graft – tendon interface showed an increase of 60% between six and twelve weeks. This was consistent with observations in longer-term tendon-bone tunnel healing studies (Rodeo et al 1993, Panni et al 1997). Other studies have shown lack of interface maturation (Jones et al 1987, Hausman et al 1989), however the type of model and study duration may have contributed to these findings. It is appreciated that the fibrocartilagenous tissue could represent progression of endochondrial ossification rather than a four zone direct interface and it is postulated that a longer term follow-up would help to determine the fate of the tissue. This study was limited by poor graft retention. However, the analysis of the tendon – bone interface was performed regardless of whether the bone was attached to the HA surface and hence, reflects the nature of the interface rather than the problem of bone – HA association that was experienced in the methodology.

6.4.4 SUMMARY

- The mechanical fixation provided by the interlocking-spike mechanism enabled unprotected weight bearing, with no evidence of attachment failure.
- In contrast to a negative control, extensor mechanism function with an attachment implant has been shown to recover fully by twelve weeks post operation and was not significantly compromised by the surgical procedures used here.
- Tendon reconstruction to a metal implant, augmented with autogenous cancellous bone and marrow, has been shown to result in the development of a neo-enthesis with similar morphological features to those observed in time-course studies of tendon re-attachment to bone.

CHAPTER SEVEN

GENERAL DISCUSSION

The aim of my study was to investigate the concept that soft-tissue implant interfaces can be engineered *in vivo*, using surface texturing, coatings and biological augmentation. The materials were chosen from *in vitro* studies and research into natural analogues, and were used to enhance the attachment and function of the soft tissues abutting implants used for proximal tibial implants and transcutaneous amputation prostheses.

In this thesis, Chapter One presented a background into soft tissue biology, naturally occurring and artificially engineered transcutaneous and subcutaneous soft-hard tissue interfaces, and an overview of implant integration into connective tissue. Based on this review and on the aims of the project, a number of hypotheses were constructed and investigated. Subsequently, each practical chapter investigated a hypothesis.

Chapter Two examined the histology of deer antlers, in which the skin forms an interface with the pedicle at the antler-pedicle junction that maintains a stable transcutaneous interface (Chapman 1975, Goss 1985, Banks and Newbrey 1982, Li and Suttie 1994). It was hypothesised that as different soft tissue types interface with the antler and pedicle structure as it traverses the skin layers, the surface morphology of those regions would be significantly different from one another, thus optimising attachment of each specific tissue. The results proved the hypothesis, demonstrating that there is a significant difference in surface structure and morphology of the antler compared to the pedicle surface to which the sub-epithelial soft tissues attach. Numerous thick collagen fibres were observed connecting the pedicle with the soft tissues. The pedicle bone is highly specialised to maximise sub-epithelial tissue attachment and maintain the tight seal between the internal and external environments. The chapter determined the histological morphology of a non-gingival transcutaneous structure, which was compared with the periontal ligament in the gingival environment. The findings were used in Chapter Five of my thesis to develop an analogue for use in limb replacement prostheses.

Chapter Three determined the effects of substrate topography on fibroblast and epithelial cell proliferation, morphology and attachment. It was hypothesised that low surface energy coating of implant materials is detrimental to fibroblast and epithelial cell population maintenance *in vitro*, and that inherent properties of cell populations, for example contact inhibition displayed by epithelial cells, can outweigh the properties instigated by surface topography. The findings demonstrated that significant differences in fibroblast and epithelial cell proliferation, morphology and attachment are brought about by implant topography. This Chapter showed that low surface energy coatings reduce attachment of both fibroblasts and epithelial cells *in vitro*. Contact inhibition,

which is an inherent property of epithelial cells, was seen to outweigh the effects of material topography, which normally results in contact guidance and thus, cell alignment. The Chapter demonstrated that different types of connective tissue cells are influenced to differing degrees by surface topography and that cell properties can overcome the potential influence of implant surface characteristics. Hence, in terms of 'soft tissue attachment' to implants in any field, it is proposed that each cell population in tissue types abutting an implant should be considered separately, and that the implant surface must be engineered to take account of specific connective tissue cell requirements.

Chapter Four of my thesis was carried out to determine the influence of bio-adhesive factors, namely fibronectin and laminin, on the attachment, proliferation and morphology of fibroblasts and epithelial cells cultured on biomaterials *in vitro*. Fibronectin was shown to significantly increase the attachment and proliferation of dermal fibroblasts, whilst laminin was seen to have a similar influence on epithelial cells. Implant topography was observed to have a lesser effect on cell behaviour in the presence of bio-adhesive factors. Once again, a clear difference was observed between the distinct connective tissue cell populations used in this Chapter. This indicates that for successful connective tissue attachment to orthopeadic implant materials, it is necessary to consider the precise cellular composition of the interfacing tissue and tailor the implant surface appropriately to maximise attachment for each specific tissue type. *In vivo*, there may be more than one cell type to consider, for example, in transcutaneous devices which interface with a fibroblastic population in the sub-epithelium, as well as epithelial cells in the epidermis.

Chapter Five of my thesis examines soft tissue attachment to, and development of intraosseous transcutaneous amputation prostheses (ITAP). In this Chapter, biomimetic surfaces whose designs were based on information from Chapter Two, were developed and the hypotheses tested were that it is the sub-epithelium, but not epithelial layer attachment, that is responsible for the degree of downgrowth observed around ITAP. In this Chapter, the degree of downgrowth was shown to be governed by the condition and extent of the attachment of the sub-epithelium and was reduced with implant biomaterials and coatings designed to mimic the surfaces of the deer antlers.

Chapter Six tested the hypothesis that a tendon-implant neo-enthesis could be engineered using a hydroxyapatite coated implant, augmented with autogenous cancellous bone and marrow graft. It was proposed that a tendon-implant interface, with similar functional and morphological properties to that of a normal tendon-bone enthesis, could be engineered *in situ*. Tendon attachment to bone in a normal direct type enthesis occurs via

progressive calcification through regions of fibrocartilage, mineralised fibrocartilage and bone (Cooper et al 1970, Benjamin et al 1986, Evans et al 1990, Kumagai et al 1994, Rufai 1995, Clark et al 1998, Waggett et al 1998, Benjamin et al 1998). Hence, it was considered necessary to introduce an intermediate tissue rather than attach the soft tissue of the tendon directly to an implant biomaterial. The attachment of tendon (soft tissue) was thus not a direct attachment as observed in ITAP, but one that introduced morcelised autogenous cancellous bone, marrow and HA, to mimic those of fibrocartilage and mineralised fibrocartilage, as observed in a normal enthesis. The findings showed that by supplying appropriate bio-active and biological augmentation, namely HA and autogenous cancellous bone and marrow, a functional tendon – bone – HA – implant interface develops, whose function and morphology are similar to that of a normal direct-type enthesis.

Overall, my thesis was designed to determine the optimal material types, biological augmentation factors and implant designs required for the artificial development of successful soft tissue – implant interfaces in both transcutaneous and subcutaneous environments. Natural examples of such interfaces overcome the problems of insufficient soft tissue attachment strength, as demonstrated by natural analogues such as deer antler, teeth and normal tendon-bone entheses. Both deer antlers and tendon-bone entheses encompass soft – hard tissue interfaces that are of sufficient strength to prevent epithelial migration and infection, and provide successful muscle attachment and function respectively. This thesis has aimed to mimic some of the aspects of these natural analogues in an attempt to improve the quality of life for patients requiring proximal tibial replacement and amputation.

Natural analogues of the soft-hard tissue interfaces examined in my thesis include deer antlers, teeth and normal tendon insertions. I have shown that thick collagen fibres span the interface and maintain the tight soft tissue seal around deer antlers. Fine filaments span the interposing lamina between gingival marginal tissues and tooth enamel in normal dental morphology, combining them to form a stable structural unit (Listgarten 1966, Schroeder 1969, Kobayashi et al 1976, Marks et al 1994, Hormia et al 2001). Finally, in tendon insertions, the soft-hard tissue interface occurs either via perpendicularly orientated perforating fibres (indirect type enthesis), or via progressive calcification through intermediate tissue layers (direct type enthesis) (Benjamin et al 1986, Evans et al 1990). Knese and Bierman (1958) proposed that the entheses have evolved to balance the differing elastic (Young's) moduli of tendon and skeletal tissue so that peaks in tension

are avoided. It is also proposed that tendons splay out at their attachment sites, in order to to distribute force over a greater area.

It is accepted that stress will concentrate at interfaces between structures with different mechanical properties, namely soft-hard tissue interfaces, and thus the tendon entheses, deer antlers and teeth have all adapted and evolved to dissipate stress away from the interface to the surrounding tissues.

The analogues examined here involve perforating fibres or tissues to mediate the interfaces. As nature appears to solve all of the problems associated with artificially engineering the soft-hard tissue interface, both transcutaneously and subcutaneously, the aim of this thesis was to attempt to mimic some of these evolutionary adaptations for use in orthopaedic implant development.

It is documented that parallel alignment of fibres adjacent to implant biomaterials will lead to encapsulation, and that connective tissue cells will deposit their collagen matrix with respect to their orientation (Donley and Gilette 1991). It is concluded that for artificially engineered soft-hard tissue interfaces to be successful, both functionally and morphologically, fibres or tissues are required to mediate at the attachment site. To enable perforating collagen fibres to develop within the soft tissue seal around transcutaneous implants, or within tendon re-attachment sites, the formation of connective tissue matrix must be perpendicular to the implant surface. These cells will deposit extracellular matrix and hence collagenous fibres, in a similar orientation, which can act as an intermediary between the soft connective tissues and the hard implant material. The implant surface must be adequately porous to enable ingrowth of the perforating fibres, as well as to increase the surface area for soft tissue attachment. Providing there are suitable biomaterials, bioactive augmentation factors and healthy collagenous tissues, the resulting interface has the potential to develop and encompass at least some of the aspects of normal soft – hard tissue interfaces. It is appreciated that there are numerous other factors that dictate the success or failure of soft tissue attachments, namely micromotion at the soft tissue – implant interface, infection, encapsulation and pull out. However, it is proposed that provided adequate mechanical fixation is avaliable, biological integration will occur over time.

My thesis has shown that soft – hard tissue interfaces can be engineered *in vivo*, both transcutaneously (Chapter Five) and subcutaneously (Chapter Six), by drawing on findings of *in vitro* studies of cell – implant interactions as described in Chapters Three and Four, and mimicking aspects of natural analogues like deer antler and normal tendon

insertions (Chapters Two and Six respectively). In this thesis I have demonstrated that the resulting artificial interfaces are both morphologically and functionally similar to those of their natural counterparts.

It is concluded that research designed to further mimic natural analogues may eliminate the problems that persist in this field, and that the resulting implant technology could have a huge impact on the quality of life experienced by patients requiring any surgical intervention that disrupts the soft – hard tissue interfaces of the body.

CONTRIBUTION TO SCIENTIFIC RESEARCH AND FURTHER WORK

In my thesis, I have developed new methods of soft tissue integration and attachment to orthopaedic implants for two types of implant, subcutaneous and transcutaneous, both of which rely on the integrity of the soft tissue-implant interface for success.

For the re-attachment of tendon soft tissues (subcutaneous) to implant materials, my thesis has concentrated on the re-attachment of the patellar tendon to proximal tibial replacements. The findings can be tailored to suit a number of clinical applications, including re-attachment of tendons or ligaments inserting into or around any part of the skeleton, which may require replacement with a massive endoprosthesis e.g., rotator cuff during shoulder replacement, abductors during hip replacement. The successful re-attachment of tendons and ligaments in this way provides an interface between the body and the implant material that is both functionally and morphologically similar to the natural entheses observed. Attachment of tendons in this way re-establishes continuity within the musculoskeletal system that is lacking with current methods of tendon-implant fixation. A successful method for tendon re-attachment in the form of a viable biological-artificial material interface has been presented here. Further work in this field is ongoing to determine the long-term outcome of tendon-implant fixation using this method and examine the progressive maturation of the tendon-bone-HA-implant interface. A study examining the effects of a more open environment on the maturation of the tendon-bone-HA-implant interface has begun, in which the patellar tendon has been attached to a customised implant base plate with a sleeve of resorbable undyed Vicryl® knitted mesh. The interface has been augmented with autogenous cancellous bone and marrow graft and will be compared using the same techniques to the closed system presented in Chapter six of my thesis. Following endoprosthetic replacement for tumour surgery, the surgeon is often required to remove a large amount of the surrounding soft tissues to remain within safe surgical parameters. When this happens, some of the length of the tendon is sacrificed, and hence no longer reaches its insertion site on the body of the prosthesis.

Further work is being carried out to develop ways of augmenting tendon length, with the use of autograft, allograft and tissue engineered constructs.

The development of a successful seal around transcutaneous prostheses has also been presented in my thesis, from cell-implant material interactions *in vitro*, to tissue layer attachment to transcutaneous abutments *in vivo*. The findings of this research can be applied to any implant that penetrates the skin for a prolonged period of time, but are principally aimed at the development of amputation prostheses. The attachment of an external implant directly to the skeleton via a transcutaneous abutment will totally eliminate stump-socket interface complications, which are the principle limiting factors for lower limb amputees wanting to return to an active lifestyle. The requirements outlined here, for a successful soft-tissue – implant seal, have been incorporated into a prototype implant design and a clinical trial of an intraosseous transcutaneous amputation prosthesis has begun. Research into methods to further stabilise the interface is ongoing and further work aims to assess the skin-implant interface in clinical trial subjects.

Current methods of re-establishing soft tissue attachments to implants are insufficient and result in abnormal gait and altered limb function. It is my hope that the findings of my thesis will be incorporated into orthopaedic implant design to improve the quality of life of individuals who have undergone surgery which results in disruption of the soft tissue attachments that we normally rely on for basic locomotion.

APPENDIX 1

APPENDIX 1 : CHAPTER TWO

1.1 STATISTICAL ANALYSIS OF PORE NUMBER

Case Processing Summary

		Cases					
		Valid		Missing		Total	
	SAMPLE	N	Percent	N	Percent	N	Percent
Number of pores	Pedicle	41	100.0%	0	.0%	41	100.0%
	Antler	40	100.0%	0	.0%	40	100.0%

Descriptives

	SAMPLE			Statistic	Std. Error
Number of pores	Pedicle	Mean		18.8049	1.0135
		95% Confidence Interval for Mean	Lower Bound	16.7566	
			Upper Bound	20.8532	
		5% Trimmed Mean		18.5921	
		Median		18.0000	
		Variance		42.111	
		Std. Deviation		6.4893	
		Minimum		7.00	
		Maximum		38.00	
		Range		31.00	
		Interquartile Range		10.0000	
		Skewness		.523	.369
		Kurtosis		.480	.724
	Antler	Mean		11.8000	.6672
		95% Confidence Interval for Mean	Lower Bound	10.4505	
			Upper Bound	13.1495	
		5% Trimmed Mean		11.6944	
		Median		12.0000	
		Variance		17.805	
		Std. Deviation		4.2196	
		Minimum		4.00	
		Maximum		23.00	
		Range		19.00	
		Interquartile Range		6.0000	
		Skewness		.153	.374
		Kurtosis		.017	.733

1.2 STATISTICAL ANALYSIS OF PORE SIZE

Case Processing Summary

		Cases					
		Valid		Missing		Total	
	Sample	N	Percent	N	Percent	N	Percent
Pore size	Pedicle	72	100.0%	0	.0%	72	100.0%
	Antler	71	100.0%	0	.0%	71	100.0%

Descriptives

	SAMPLE			Statistic	Std. Error
Pore size	Pedicle	Mean		217.2222	19.0710
		95% Confidence Interval for Mean	Lower Bound	179.1958	
			Upper Bound	255.2487	
		5% Trimmed Mean		197.2531	
		Median		160.0000	
		Variance		26186.54	
		Std. Deviation		161.8226	
		Minimum		50.00	
		Maximum		800.00	
		Range		750.00	
		Interquartile Range		190.0000	
		Skewness		1.975	.283
		Kurtosis		3.855	.559
	Antler	Mean		40.1408	3.1749
		95% Confidence Interval for Mean	Lower Bound	33.8086	
			Upper Bound	46.4730	
		5% Trimmed Mean		37.8638	
		Median		40.0000	
		Variance		715.694	
		Std. Deviation		26.7525	
		Minimum		10.00	
		Maximum		120.00	
		Range		110.00	
		Interquartile Range		40.0000	
		Skewness		1.109	.285
		Kurtosis		1.115	.563

APPENDIX 2

APPENDIX 3

3.9 FIBROBLAST CELL ADHESION – 48 HOURS

	Mean Cell Area (μm)	Mean No Markers/Cell	Ratio
SPTi	828	38	4.6×10^{-2}
SPTi FN	1464	74	5.1×10^{-2}
SPTi LN	672	22	3.3×10^{-2}
DLC	1733	19	1.1×10^{-2}
DLC FN	1078	34	3.2×10^{-2}
DLC LN	875	16	1.8×10^{-2}
RSBTi	1263	18	1.4×10^{-2}
RSBTi FN	1055	41	3.9×10^{-2}
RSBTi LN	-	-	-

3.10 EPITHELIAL CELL ADHESION – 48 HOURS

	Mean Cell Area (μm)	Mean No Markers/Cell	Ratio
SPTi	389	59	0.15
SPTi FN	376	62	0.16
SPTi LN	392	77	0.20
DLC	187	20	0.11
DLC FN	165	37	0.22
DLC LN	207	51	0.25
RSBTi	179	27	0.15
RSBTi FN	168	31	0.18
RSBTi LN	241	52	0.22

APPENDIX 4

APPENDIX 4 : CHAPTER FIVE

4.1 DOWNGROWTH SUMMARY STATISTICS

PIN TYPE	MEAN DOWNGROWTH (mm):	ST. ERROR:	ST. DEVIATION:	MEDIAN:
MF	3.12	0.46	2.12	3.70
SG	1.83	0.21	0.66	1.61
LG	2.21	0.36	1.24	2.04
RSB	1.96	0.23	0.74	1.84
HA	1.49	0.13	0.L47	1.52
SG + DLC	2.60	0.50	0.71	2.60
LG + DLC	2.19	0.44	0.62	2.19
RSB + DLC	4.10	0.49	0.69	4.10
PTi	3.36	0.59	2.36	2.97
PTi + HA	3.48	0.38	1.42	4.00
PTi + DLC	4.16	0.37	1.16	4.39
PTi + DLC + HA	4.28	0.19	0.59	4.24
P. FLANGE	0.69	0.15	0.58	0.68
HA FLANGE	1.36	0.10	0.29	1.37
100 FN FLANGE	0.94	0.57	1.14	0.72
200 FN FLANGE	0.89	0.15	0.09	0.99

Tests of Normality

		Kolmogorov-Smirnov		
	Pin Type	Statistic	df	Sig.
Downgrowth (mm)	MF	.197	21	.033
	SG	.187	10	.200
	LG	.136	12	.200
	RSB	.216	10	.200
	HA	.194	13	.193
	SG + DLC	.260	2	.
	LG + DLC	.260	2	.
	RSB + DLC	.260	2	.
	PTi	.148	16	.200
	PTi + HA	.248	14	.019
	PTi + DLC	.194	10	.200
	PTi + DLC + HA	.142	10	.200
	P Flange	.149	16	.200
	HA Flange	.156	8	.200
	100 FN Flange	.295	4	.
	200 FN Flange	.286	4	.

4.2 % EPITHELIAL LAYER ATTACHMENT SUMMARY STATISTICS

PIN TYPE	MEAN % EPITHELIAL ATT :	ST. ERROR:	ST. DEVIATION:	MEDIAN:
MF	38.48	10.35	47.41	37.20
SG	39.80	12.70	40.22	37.50
LG	31.58	9.59	33.22	29.00
RSB	46.90	14.28	45.17	49.00
HA	54.08	14.04	50.61	54.53
SG + DLC	37.00	37.00	52.33	37.00
LG + DLC	50.00	50.00	70.71	50.00
RSB + DLC	50.00	50.00	70.71	50.00
PTi	25.00	11.18	44.72	22.22
PTi + HA	36.00	11.27	42.17	16.00
PTi + DLC	26.20	13.56	42.88	23.56
PTi + DLC + HA	4.50	4.50	14.23	2.50
P. FLANGE	43.75	12.81	51.24	43.06
HA FLANGE	53.38	15.84	44.80	75.00
100 FN FLANGE	55.75	14.91	29.82	44.00
200 FN FLANGE	56.50	19.27	38.54	70.50

Tests of Normality

		Kolmogorov-Smirnov		
	Pin Type	Statistic	df	Sig.
% Epithelial Layer Attachment	MF	.363	21	.000
	SG	.239	10	.111
	LG	.246	12	.044
	RSB	.250	10	.075
	HA	.318	13	.001
	SG + DLC	.260	2	.
	LG + DLC	.260	2	.
	RSB + DLC	.260	2	.
	PTi	.462	16	.000
	PTi + HA	.303	14	.001
	PTi + DLC	.429	10	.000
	PTi + DLC + HA	.524	10	.000
	P Flange	.366	16	.000
	HA Flange	.310	8	.022
	100 FN Flange	.391	4	.
	200 FN Flange	.337	4	.

4.3 % SUB - EPITHELIAL LAYER ATTACHMENT SUMMARY STATISTICS

PIN TYPE	MEAN % SUB - EPITHELIAL ATT :	ST. ERROR:	ST. DEVIATION:	MEDIAN:
MF	72.71	6.23	28.56	78.00
SG	79.10	8.65	27.35	90.50
LG	77.25	8.40	29.11	93.00
RSB	74.30	6.93	21.89	80.00
HA	75.77	5.21	18.79	76.00
SG + DLC	68.50	5.50	7.78	68.50
LG + DLC	59.00	6.00	8.49	59.00
RSB + DLC	55.00	45.00	63.64	55.00
PTi	68.44	8.48	33.94	82.50
PTi + HA	75.36	3.61	13.49	72.50
PTi + DLC	68.20	6.09	19.27	70.50
PTi + DLC + HA	50.00	6.51	20.58	55.50
P. FLANGE	85.56	5.65	22.61	94.00
HA FLANGE	97.75	1.97	5.57	100.00
100 FN FLANGE	92.00	8.00	16.00	100.00
200 FN FLANGE	95.25	2.75	5.50	95.50

Tests of Normality

		Kolmogorov-Smirnov		
	Pin Type	Statistic	df	Sig.
% Sub-epithelial Soft Tissue Layer Attachment	MF	.170	21	.117
	SG	.300	10	.011
	LG	.265	12	.020
	RSB	.249	10	.079
	HA	.111	13	.200
	SG + DLC	.260	2	.
	LG + DLC	.260	2	.
	RSB + DLC	.260	2	.
	PTi	.246	16	.011
	PTi + HA	.143	14	.200
	PTi + DLC	.214	10	.200
	PTi + DLC + HA	.223	10	.173
	P Flange	.362	16	.000
	HA Flange	.464	8	.000
	100 FN Flange	.441	4	.
	200 FN Flange	.306	4	.

APPENDIX 5

APPENDIX 5: CHAPTER SIX

5.1 SPEED ANALYSIS DATA

SIX-WEEK Animal No.	Pre-op Speed (Mean +/- std error)	Post-op Speed (Mean+/-std error)	Post-op Speed (Mean+/-std error)	Post-op Median	Mann-Whitney U p value
1379 (HA)	0.86 +/- 0.09	0.86 +/- 0.05	0.79	0.89	0.625
1395 (HA)	0.67 +/- 0.07	0.57 +/- 0.01	0.60	0.56	0.295
1398 (HA)	0.55+/- 0.06	0.77 +/- 0.22	0.45	0.48	0.538
1380 (HA)	0.72+/- 0.05	0.72 +/- 0.08	0.66	0.64	0.593
1399 (HA)	0.40+/- 0.02	0.47+/- 0.03	0.42	0.48	0.061
1393 (HA)	0.58+/- 0.04	0.60+/- 0.04	0.56	0.62	0.662
1649(A)	0.56+/- 0.01	0.58+/- 0.04	0.54	0.62	0.099
1384 (A)	0.77+/- 0.04	0.82 +/- 0.04	0.76	0.87	0.264
1381 (A)	0.78 +/- 0.06	0.67+/- 0.04	0.73	0.72	0.236
1394 (A)	0.86+/- 0.08	0.85 +/- 0.05	0.88	0.82	0.931
1396 (A)	0.66+/- 0.04	0.67 +/- 0.03	0.59	0.68	0.772
1652 (A)	0.53+/- 0.02	0.49+/- 0.02	0.52	0.50	0.315

TWELVE-WEEK Animal No.	Pre-op Speed (Mean +/- std error)	Post-op Speed (Mean+/-std error)	Post-op Speed (Mean+/-std error)	Post-op Median	Mann-Whitney U p value
1378 (HA)	0.83 +/- 0.12	0.79 +/- 0.05	0.69	0.77	0.298
1391 (HA)	1.02+/- 0.07	0.92+/- 0.04	1.04	0.89	0.210
1383 (HA)	0.63+/- 0.02	0.65+/- 0.04	0.62	0.67	0.583
1390 (HA)	0.60+/- 0.03	0.66+/- 0.03	0.56	0.68	0.163
1397 (HA)	0.63+/- 0.04	0.68+/- 0.02	0.63	0.68	0.335
1642 (HA)	0.54+/- 0.05	0.49+/- 0.03	0.50	0.45	0.213
1386 (A)	0.64+/- 0.03	0.57 +/- 0.04	0.69	0.55	0.157
1389 (A)	0.85+/- 0.07	0.71+/- 0.05	0.74	0.72	0.254
1387 (A)	0.59+/- 0.01	0.66+/- 0.03	0.58	0.68	0.045
1392 (A)	0.47+/- 0.05	0.60 +/- 0.02	0.43	0.62	0.087
1647 (A)	0.72+/- 0.03	0.77+/- 0.07	0.70	0.78	0.805
1646 (A)	0.91+/- 0.09	0.83+/- 0.07	0.87	0.83	0.703

5.2 SUMMARY AND INDIVIDUAL ANIMAL RANGE DATA

SUMMARY DATA

Group Number From Box Plot Above	Group	Mean (degrees)	Standard Error	Standard Deviation	Median	Normality p-value
1	HA Gp Pre-op (6 Wk Gp)	37.80	2.07	5.07	35.82	0.0087
2	HA Gp 6 Wks (6 Wk Gp)	44.61	1.65	4.05	43.84	0.200
3	Auto Gp Pre-op (6 Wk Gp)	42.73	1.92	4.71	42.28	0.200
4	Auto Gp 6 Wks (6 Wk Gp)	50.01	1.90	4.66	50.83	0.200
5	HA Gp Pre-op (12 Wk Gp)	42.27	1.38	3.39	42.03	0.200
6	HA Gp 12 Wks (12 Wk Gp)	46.65	1.82	4.45	45.87	0.200
7	Auto Gp Pre-op (12 Wk Gp)	46.17	2.63	6.44	45.29	0.200
8	Auto Gp 12 Wks (12 Wk Gp)	52.78	2.46	6.03	52.85	0.200

SIX-WEEK GROUP – Stifle joint range (degrees) - Kinematic Gait Analysis

SIX-WEEK Animal No.	Pre-op Range (Mean +/-std error)	Post-op Range (Mean+/-std error)	Pre-op Normality test	Post-op Normality test	Mann Whitney U p value
1379 (HA)	44.67 +/- 1.87	43.60 +/- 1.99	0.170	0.172	0.792
1395 (HA)	43.35 +/- 0.98	50.53 +/- 0.78	0.200	0.200	0.004
1398 (HA)	34.38 +/- 1.60	44.05 +/- 3.78	0.001	0.148	0.049
1380 (HA)	36.01 +/- 2.35	42.98 +/- 1.19	0.200	0.065	0.028
1399 (HA)	35.63 +/- 0.51	47.67 +/- 3.49	0.199	0.008	0.045
1393 (HA)	31.73 +/- 0.89	38.81 +/- 1.72	0.200	0.002	0.002
1649(A)	46.78 +/- 2.22	44.16 +/- 1.92	0.200	0.199	0.668
1384 (A)	37.15 +/- 2.16	48.27 +/- 0.87	0.000	0.200	0.000
1381 (A)	39.57 +/- 1.91	45.44 +/- 1.69	0.200	0.010	0.073
1394 (A)	44.98 +/- 1.27	54.22 +/- 4.26	0.200	0.200	0.065
1396 (A)	39.17 +/- 1.11	53.39 +/- 2.34	0.200	0.200	0.003
1652 (A)	48.17 +/- 2.69	54.60 +/- 1.20	0.200	0.143	0.109

5.3 LAG / HYPEREXTENSION DATA

SIX-WEEK GROUP – Pre and Post-Operative Stifle Joint Extension Angle, and Derived Lag or Hyperextension Angle (degrees) for Individual Animals in the Six-Week Group.

SIX-WEEKS Animal No:	Mean Ext^n angle pre-op (degrees)	Mean Ext^n angle post-op (degrees)	Lag (-) or Hyper-extension (+) Angle (degrees)
1379 (HA)	119.57	116.42	-3.15
1395 (HA)	155.99	135.80	- 20.19
1398 (HA)	134.07	121.27	-12.80
1380 (HA)	152.84	124.33	-28.51
1399 (HA)	138.09	130.67	- 7.42
1393 (HA)	150.73	134.28	-16.45
1649(A)	136.86	122.13	- 14.73
1384 (A)	151.76	136.94	-14.82
1381 (A)	154.44	127.43	-27.01
1394 (A)	146.56	126.97	-19.59
1396 (A)	165.77	131.94	- 33.83
1652 (A)	128.45	128.39	- 0.06

TWELVE-WEEK GROUP – Pre- and Post-Operative Stifle Joint Angle, Derived Lag or Hyperextension Angle (degrees) for Individual Animals in the Twelve-Week Group.

TWELVE-WEEKS Animal No:	Mean Ext^n angle pre-op (degrees)	Mean Ext^n angle post-op (degrees)	Lag (-) or Hyper-extension (+) Angle (degrees)
1378 (HA)	142.81	140.90	-1.91
1391 (HA)	136.77	149.13	12.36
1383 (HA)	141.10	145.51	4.41
1390 (HA)	157.37	146.57	- 10.80
1397 (HA)	150.29	136.42	- 13.87
1642 (HA)	125.25	151.45	26.20
1386 (A)	129.12	150.84	21.72
1389 (A)	145.08	154.55	9.47
1387 (A)	155.97	143.29	- 12.68
1392 (A)	158.45	138.48	- 19.97
1647 (A)	130.35	149.15	18.80
1646 (A)	154.76	143.26	-11.50

5.5 MESH STUDY SUMMARY

A mesh pilot was used to evaluate an attachment model that did not use the clamp lid, thus providing an open environment for the patellar tendon – base plate construct. The surgical procedures were followed from the previous HA and Autograft Groups. However, instead of clamping the tendon onto the base plate with the clamp lid, absorbable undyed Vicryl ® Mesh (VM 95 from Ethicon Ltd, UK) was used to create a sleeve to house the tendon and was sutured to the base plate which was augmented with autogenous cancellous bone and marrow graft material. The pilot ran for six-weeks, after which time the GRF (Fz) expressed as % Mean Right / Mean Left was 79.85%. This value was found to be 14.34% greater than the mean value for the Autograft Group six weeks post-operatively.

Histologically, the specimen demonstrated a similar loss of bone graft material at the HA-coated interface of the clamp. The absence of the bridging plate meant that the specimen was more accessible to the surrounding tissues, allowing earlier revascularisation, fibroblast infiltration and collagen matrix production. It also meant that the tendon tissue was harder to define from the surrounding tissues. The tissue in the central region above the base plate was observed to be a more organised, dense collagenous tissue compared to that observed in the Six –Week HA or Autograft Groups. The tendon tissue was completely integrated with the remaining visible mesh fibres and there was a vigorous inflammatory response observed, immediately associated with the mesh zones. This reaction was characterised by the presence of lymphocytes, macrophages and foreign body giant cells.

BIBLIOGRAPHY

Abercrombie M, Ambrose EJ. Interference microscope studies of cell contacts in tissue culture. Exp Cell Res 1958; 15: 332-345.

Abercrombie M, Heaysman JEM, Pegrum SM. The locomotion of fibroblasts in culture IV. EM of the leading edge. Exp Cell Res 1971; 67: 359-67.

Abrahamsson SO. Matrix metabolism and healing in the flexor tendon. Scan J Plast Reconstr & Hand Surg Suppl 1991; 23: 1-39.

Abrahamsson SO, Lundborg G, Lohmander LS. Segmental variation in microstructure, matrix synthesis and cell proliferation in rabbit flexor tendon. Scand J Plast Reconstr & Hand Surg 1989; 23: 191-198.

Abudu A, Carter SR, Grimer RJ. The outcome and functional results of diaphyseal endoprostheses after tumour excision. J Bone Joint Surg 1996; 78B(4): 652-657.

Adell R. Long-term treatment results. In Bränemarks/Zarb/Albrektsson (eds), Tissue Integrated Prostheses. Chicago, Quintessence. 1985; pp: 175-186.

Adell R, Lekholm U, Rockler B, Branemark PI. A 15-year study of osseointegrated implants in the treatment of the edentulous jaw. Int J Oral Surg 1981; 10(6): 387-416.

Agins HJ, Alcock NW, bansal M, Salvati EA, Wilson PD Jr, Pellicci PM, Bullough PG. Metallic wear in failed titanium alloy total hip replacements; A histologic and quantitative analysis. J Bone Joint Surg 1988; 70A: 347-356.

Alberts B, Bray D, Lewis J, Raff M, Roberts K, Watson JD. In: Molecular Biology of the Cell. 1994 Ed.

Albrektsson T, Branemark PI, Hansson HA, Lindstrom J. Osseointegrated titanium implants; requirements for ensuring a long-lasting direct bone-to-implant anchorage in man. Acta Orthop Scand 1981; 52: 155.

Allen MJ, Houlton JEF, Addams SB, Rushton N. The surgical anatomy of the stifle joint in sheep. Veterinary surgery 1998; 27: 596-605.

Allen M, Myer B, Rushton N. *In Vitro* and *in vivo* investigations into biocompatibility of diamond-like carbon (DLC) coatings for orthopaedic applications. J Biomed Mater Res 2000; 58(3): 319-328.

Amiel D, Frank C, Harwood F, Fronek J, Akeson W. Tendons and ligaments: a morphological and biochemical comparison. J Orthop Res 1984; 1: 257-265.

Amstutz HC, Coulson WF, David E. Reconstruction of the canine Achilles and patellar tendons using dacron mesh silicone prosthesis. I. Clinical and biocompatibility evaluation J Biomed Mater Res 1976; 10(1): 47-59.

Amundson DC, McArthur W, Mosharrafa M. The porous endocardial electrode Pacing Clin Electrophysiol 1979; 2(1): 40-50.

Anderson K, Seneviratne AM, Izawa K, Atkinson BL, Potter HG, Rodeo SA. Augmentation of tendon healing in intraarticular bone tunnel with use of a bone growth factor. Am J Sports Med 2001; 29: 689-698.

Anselme K, Linez P, Bigerelle M, Le Maguer D, Le Maguer A, Hardouin P, Hildebrand HF, Iost A, Leroy JM. The relative influence of the topography and chemistry of TiAl6V4 surfaces on osteoblastic cell behaviour. Biomaterials 2000; 21(15): 1567-1577.

Aoki M, Isogai S, Okamura K, Fukeshima S, Ishii S. Healing of the rotator cuff at tendon insertion to bone: a study using canine infraspinatus. Trans Orthop Res Soc 1998; 23: 627.

Appoldt FA, Bennett L, Contini R. Stump-socket pressure in lower extremity prostheses. J Biomech 1968; 1(4): 247-257.

Ashton BA, Allen TD, Howlett CR, Eaglesom CC, Hattori A, Owen M. Formation of bone and cartilage by marrow stromal cells in diffusion chambers *in vivo*. Clin Orthop 1980; 151: 294-307.

Bacci G, Pagani PA, Donati U. Adjuvant chemotherapy associated with surgery in the treatment of osteosarcoma. Preliminary results. Ital J Orthop Traumatol 1976; 2(3): 363-374.

Badylak S, Arnoczky S, Plouhar P, Haut R, Mendenhall V, Clarke R and Horvath C. Naturally occuring extracellular matrix as a scaffold for musculoskeletal repair. Clin Orthop 1999; 367 Suppl: S333-S343.

Baier RE, Mayer AE. Future directions in surface preparation of dental implants. J Dent Educ 1988; 52: 788-791.

Baier RE. Surface properties influencing biological adhesion. In; Adhesion in Biological Systems. Manly RS Ed Academic press NY 1970; pp: 55.

Baker SE, DiPasquale AP, Stock EL, Quaranta V, Fitchmun M, Jones JC. Morphogenic effects of soluble laminin-5 on cultured epithelial cells and tissue explants. Exp Cell Res 1996; 228: 262-270.

Banks WJ, Newbrey JW. Antler development as a unique modification of mammalian endochondrial ossification. Antler development in Cervidae. RD Brown, ed. Caesar Kleberg Wild Res Inst Kingsville 1982; 279-306.

Bannister LH, Berry MM, Collins P, Dyson M, Dussek JE, Ferguson MWJ. In: Greys Anatomy. 1995 Edition; pp: 1699-1720.

Banwart JC, Asher MA, Hassanein RS. Iliac crest bone graft harvest donor site morbidity. A statistical evaluation. Spine 1995; 20(9): 1055-1060.

Baron van Evercooren A, Kleinman HK, Ohno S, Marangos P, Schwartz JP, Dubois-Dalcq ME. Nerve growth factor laminin and fibronectin promote neurite growth in human fetal sensory ganglia cultures. J Neurosci Res 1982; 8: 179-194.

Bauer TW, Geesink RCT, Zimmermann R, McMahon JT. Hydroxyapatite-coated femoral stems, histological analysis of componants, retrieval at autopsy. J Bone Joint Surg 1991; 73A: 1439-1452.

Belvins FT. Structure, function and adaption of tendon. Curr Op Orthop 1996; 7(VI): 57-61.

Benjamin M, Evans EJ. Fibrocartilage: A Review. J Anat 1990; 171: 1-15.

Benjamin M, Evans EJ, Copp L. The histology of tendon attachments to bone in man. J Anat 1986; 149: 89-100.

Benjamin M, Ralphs JR. Fibrocartilage in tendons and ligaments – an adaption to compressive load. J Anat 1998; 193(4): 481-494.

Beresford JN. Osteogenic stem cells and the stromal system of bone and marrow. Clin Orthop 1989; 240: 270-280.

Berglundh T, Lindhe J, Ericsson I, Marinello CP, Liljenberg B, Thomsen P. The soft tissue barrier at implants and teeth. Clin Oral Implants Res 1991; 2: 81-90.

Bickels J, Wittig JC, Kollender Y, Neff RS, Kellar-Graney K, Meller I, Malawer MM. Reconstruction of extensor mechanism after proximal tibia endoprosthetic replacement. J Arthroplasty 2001; 16: 856-862.

Black J. Biological performance of materials: fundamentals of biocompatibility 2nd ed. New York, dekker. 1992; 110: 184-275.

Bobyn JD, Pilliar RM, Cameron HU, Weatherly GC, Kent GM. The effect of porous surface configuration on the tensile strength of fixation of implants by bone ingrowth. Clin Orthop 1980; 149: 291-298.

Bobyn JD, Pilliar RM, Cameron HU, Weatherly GC. The optimum pore size for the fixation of porous-surfaced metal implants by the ingrowth of bone. Clin Orthop 1980; 150: 263-270.

Bobyn JD, Stackpool GJ, Hacking SA, Tanzer M, Krygier JJ. Characteristics of bone ingrowth and interface mechanics of a new porous tantalum biomaterial. J Bone Joint Surg Br 1999; 81: 907-914.

Bobyn JD, Toh KK, Hacking SA, Tanzer M, Krygier JJ. Tissue response to porous tantalum acetabular cups: a canine model. J Arthroplasty 1999; 14: 347-354.

Bobyn JD, Wilson GJ, MacGregor DC, Pilliar RM, Weatherly GC. Effect of pore size on the peel strength of attachment of fibrous tissue to porous-surfaced implants. J Biomed Mater Res 1982; 16: 571-584.

Bodner L. Effect of parotid submandibular and sublingual saliva on wound healing in rats Comp Biochem.Physiol A 1991; 100(4): 887-890.

Branemark PI, Albrektsson T. Titanium implants permanently penetrating human skin. Scand J Plast Reconstr Surg 1982; 16(1): 17-21.

Branemark PI, Branemark R, Bergh P, Rydevik B, Gunterberg B. Osseointegrated prosthesis in lower limb amputation; the development of a new concept. 1999 10th International symposium on limb salvage conference proceedings 11-14th April, Cairns Australia.

Branemark PI, Breine U, Adell R, Hansson BO, Lindstroem J, Olsson A. Intra-osseous anchorage of dental prostheses. Scand J Plast Recon Surg 1969; 3(2): 81-100.

Branemark PI, Engstrand P, Ohrnell LO, Grondahl K, Nilsson P, Hagberg K, Darle C, Lekholm U. Branemark Novum: a new treatment concept for rehabilitation of the edentulous mandible. Preliminary results from a prospective clinical follow-up study. Clin Implant Dent Relat Res 1999; 1(1): 2-16.

Branemark PI, Hansson BO, Adell R, Breine U, Lindstrom J, Hallen O, Ohman A. Osseointegrated implants in the treatment of the edentulous jaw. Experience from a 10 year peirod. Scand J Plast Reconstr Surg Suppl 1977; 16: 1-132.

Branemark PI, Lindstrom J, Hallen O, Breine U, Jeppson PH, Ohman A. Reconstruction of the defective mandible. Scand J Plast Reconstr Surg 1975; 9: 116.

Branemark PI. Tooth replacement by oral endoprostheses: clinical aspects. Int J Oral Implantol 1988; 5(2): 27-29.

Branemark R, Branemark PI, Rydevik B, Myers RR. Osseointegration in skeletal reconstruction and rehabilitation: a review. J Rehabil Res Dev 2001; 38(2): 175-181.

Brien EW, Terek RM, Healey JH, Lane JM. Allograft reconstruction after proximal tibial resection for bone tumors. An analysis of function and outcome comparing allograft and prosthetic reconstructions. Clin Orthop 1994; 303: 116-127.

Brown LF, Lanir N, McDonagh J, Tognazzi K, Dvorak AM, Dvorak HF. Fibroblast migration in fibrin gel matrices. Am J Pathol 1993; 142(1): 273-283.

Brown RD. Ed 1983, Antler development in Cervidae. Caesar Kleberg Wild. Res. Inst. Texas A and I University, Kingsville.

Brunette DM. Fibroblasts on micromachiened substrata orient hierarchically to grooves of different dimensions. Exp Cell Res 1986; 164: 11-26.

Brunette DM. Interactions of epithelial cells with foreign surfaces. CRC Crit Rev Bioeng 1986; 1: 323-370.

Brunette DM. The effect of surface topography on the behavior of cells. Int J Oral Maxillofac Impls 1988; 3: 231-246.

Buchanan RA, Rigney ED Jr, Williams JM. Wear accelerated corrosion of Ti6AL4V and nitrogen ion implanted Ti6AL4V: mechanisms and influence of fixed stress magnitude. J Biomed Mat Res 1987; 21: 367-377.

Buis AW, Convery P. Calibration problems encountered while monitoring stump/socket interface pressures with force sensing resistors: techniques adopted to minimize inaccuracies. Prosthet Orthot Int 1997; 21(3): 179-182.

Burn JF, Brockington C. Quantification of hoof deformation using optical motion capture. Equine Vet J Suppl 2001; 33: 50-53.

Burridge K, Fath K, Keely T, Nuckolls G, Turner C. Focal adhesions: transmembrane junctions between the ECM and cytoskeleton. Ann Rev Cell Biol 1988; 4: 487-525.

Burwell RG. The function of bone marrow in the incorporation of a bone graft. Clin Orthop 1985; 200:125-141.

Butler DL, Awad HA. Perspectives on cell and collagen composites for tendon repair. Clin Orthop 1999; 367 Suppl: S324-S332.

Butts TE, Peterson LJ, Allen CM. Early soft tissue ingrowth into porous block hydroxyapatite. J Oral Maxillofac Surg 1989; 47(5): 475-479.

Cambell CE, von Recum A. Microtopography and soft tissue response. J Invest. Surg. 1989; 2: 51-74.

Canale (ed). Campbell's Operative Orthopaedics. Ninth edition (1998) Vol.1 Mosby.

Cannon SR. Massive prostheses for malignant bone tumours of the limbs. J Bone Joint Surg 1997; 79(Br): 497-506.

Caplan AI. Mesenchymal stem cells. J Orthop Res 1991; 9: 641-650.

Carpenter JE, Thomopoulos S, Soslowsky LJ. Animal models of tendon and ligament injuries for tissue engineering applications. Clin Orthop 1999; 367 Suppl: S296-S311.

Chao EY, Inoue N, Ikeda K, Aro H, Frassica F. Formation of Pseudo-Subchondral Bone Plate for Tendon Attachment to Metallic Implant Via Osteoinduction. Trans ORS 1997; 22 Suppl: 1-1.

Chapman DI. Antlers, bones of contention. Mammal Rev 1975; 5: 121-172.

Checketts RG. Surgical treatment of bone tumours. Br J Theatre Nurs 1991; 1(2): 21-25.

Chehroudi B, Gould TR, Brunette DM. Effects of a grooved titanium-coated implant surface on epithelial cell behavior *In Vitro* and *in vivo*. J Biomed Mater Res 1989; 23(9): 1067-1085.

Chehroudi B, Gould TR, Brunette DM. The role of connective tissue in inhibiting epithelial downgrowth on titanium-coated percutaneous implants. J Biomed Mater Res 1992; 26(4): 493-515.

Chehroudi B, Gould TRL, Brunette DM. Effects of a grooved epoxy substratum on epithelial cell behavior *In Vitro* and *in vivo*. J Biomed Mater Res 1988; 22: 459-473.

Chehroudi B, Gould TRL, Brunette DM. Effects of grooved titanium-coated implants on epithelial cell behaviour *In Vitro* and *in vivo*. J Biomat Res 1989; 24: 1067-1085.

Chehroudi B, Gould TRL, Brunette DM. Titanium coated micromachiened grooves of different dimensions affect epithelial and connective tissue cells differently in vivo. J Biomaterial Res 1990; 24: 1203-1219.

Chen PQ, Cheng Ck, Shang HC, Wu JJ. Gait analysis after total knee replacement for degenerative arthritis. J Formos Med Assoc 1991; 90: 160-166.

Ciano PS, Colvin RB, Dvorak AM, McDonagh J, Dvorak HF. Macrophage migration in fibrin gel matrices. Lab Invest 1986; 54: 62-70.

Clark RAF, Henson PM. The molecular Biology of Wound Repair. Plenum Pub Corp 1988 Ed.

Clark J, Stechschulte DJ, Jr. The interface between bone and tendon at an insertion site: a study of the quadriceps tendon insertion. J Anat 1998; 192(Pt 4): 605-616.

Cohen B. The essential nature of periodontal disease. In: Cohen B, Kramer IRH editors: Scientific Foundations of Dentistry Chicago 1976 Year Book Medical Publishers pp: 439-448.

Cook SD, Thomas KA, Kay JF, Jarcl M. Hydroxyapatite-coated porous titanium for use as an orthopaedic biological attachment system. Clin Orthop 1998; 230: 303-312.

Cooper RR, Misol S. Tendon and ligament insertion. A light and electron microscopic study. J Bone Joint Surg 1970; 52(Am): 1-20.

Culp LA, Murray BA, Rollins BJ. Fibronectin and proteoglycans as determinants of cell-substratum adhesion. J Supramol Struct 1979; 11: 401-427.

D'Antonio JA, Capello WN, Crothers OD, Jaffe WI, Manley MT. Early clinical experience with hydroxyapatite-coated femoral implants. J Bone Joint Surg 1992; 74(Am): 995-1008.

Daly B. Development of percutaneous energy transmission systems. Annual Progress Report. National Institute of Health. Report no: NO1-HV-8-2919-2. 1980. National technical Information Service, Accession No: PB 81 10938.

De Groot K, Geesink R, Klein CPAT, Serekian P. Plasma sprayed coatings of hydroxylapatite. J Biomed Mater Res 1987; 21(12): 1375-1381.

Dean WJ, Culbertson KC, D'Angelo AM. Fibronectin and laminin enhance gingival cell attachment to dental implant surfaces *In Vitro*. J Oral Maxillofac Implants 1995; 10: 721-28.

Debreconi AE, Fredrickson JM, Griffiths MU. An implantable electromagnetic sounssource for speech production. Proc 23rd annual meeting ASAIO 1977; 6: 17.

Degasne I, Basle MF, Demais V, Hure G, Lesourd M, Grolleau B, Mercier L, Chappard D. Effects of roughness, fibronectin and vitronectin on attachment, spreading and proliferation of human osteoblast-like cells on Ti surfaces. Calcif Tissue International 1999; 64: 499-507.

Donath K. Reactions of tissue to calcium phosphate ceramics. In: Osseointegrated Implants. Heimke G (ed) CRC Press, Boca Raton, FL, USA1990; 99-125.

Dong J, Uemura T, Kikuchi M, Tanaka J, Tateishi T. Long-term durability of porous hydroxyapatite with low-pressure system to support osteogenesis of mesenchymal stem cells. Biomed Mater Eng 2002; 12(2): 203-209.

Donley TG, Gilette WB. Titanium endosseous implant-soft tissue interface. J Periodontol 1991; 62(2): 153-160.

Ducheyne P, Hench LL, Kagan A, Martens M, Bursens A, Mulier JC. Effect of hydroxyapatite impregnation on skeletal bonding of porous coated implants. J Biomed Mater Res 1980; 14: 225-237.

Ducheyne P, Lemons J. Bioceramics: Material characteristics vs *in vivo* behavior. J Biomed Mater Res 1987; 21(A2): 219-236.

Dunn MG, Liesch JB, Tiku ML, Zawadsky JP. Development of fibroblast-seeded ligament analogs for ACL reconstruction. J Biomed Mater Res 1995; 29: 1363-1371.

Dyce KM, Sack WO, Wensing CJG. The hindlimb of the ruminants (Chapter 33). In: Textbook of Veterinary Anatomy 2nd Ed. 1996. WB Saunders Company.

Eckardt JJ, Matthews JG, Eilber FR. Endoprosthetic reconstruction after bone tumor resections of the proximal tibia. Orthop Clin North Am 1991; 22: 149-160.

Eisenbarth E, Meyle J, Nachtigal W, Breme J. Influence of the surface structure of titanium materials on the adhesion of fibroblasts. Biomaterials 1996; 17(1): 1399-1403.

El Sayegh TY, Pilliar RM, McCulloch CA. Attachment, spreading, and matrix formation by human gingival fibroblasts on porous-structured titanium alloy and calcium polyphosphate substrates. J Biomed Mater Res 2002; 61(3): 482-492.

El-Ghannam A, Starr L, Jones J. Laminin-5 coating enhances epithelial cell attachment, spreading and hemidesmosome assembly on Ti-6AL-4V implant material *In Vitro*. J Biomed Mater Res 1998; 41: 30-40.

Elliott DH. Structure and function of mamalian tendon. Biol Rev 1965; 40: 392-421.

Elton A. Surgical treatment of bone tumours. Prof Nurse 1988; 3(9): 330-334.

Emerson RH Jr, Head WC, Malinin TI. Extensor mechanism reconstruction with an allograft after total knee arthroplasty. Clin Orthop 1994; 303: 79-85.

Emerson RH Jr, Head WC, Malinin TI. Reconstruction of patellar tendon rupture after total knee arthroplasty with an extensor mechanism allograft. Clin Orthop 1990; 260: 154-161.

Engstrom A. Aspects of the molecular structure of bone. In: The biochemistry and physiology of bone. Bourne GH (ed)2nd New York NY Academic press 1972; 237-257.

Enneking WF, Spanier SS, Gordman MA. Current concepts review: The surgical staging of musculoskeletal sarcoma. J Bone Joint Surg 1980; 62(Am): 1027-1030.

Evans EJ, Benjamin M, Pemberton DJ. Fibrocartilage in the attachment zones of the quadriceps tendon and patellar ligament of man. J Anat 1990; 171: 155-162.

Evans EJ, Benjamin M, Pemberton DJ. Variations in the amount of calcified tissue at the attachments of the quadriceps tendon and patellar ligament in man. J Anat 1991; 174: 145-151.

Fernie GR, Kostuik JP, Lobb RM, Pilliar E, Wong E, Binnington AG. A percutanoeus implant using a porous metal surface coating for adhesion to bone and a velour covering for soft tissue attachment: Results of trials in pigs. J Biomed Mater Res 1977; 11: 883-890.

Folkman J, Moscona A. Role of cell shape in growth control. Nature 1978; 273: 345-349.

Forward AD, Cowan RJ. Tendon Suture to Bone. J Bone Joint Surg 1963; 45(Am): 807-823.

Frank C, Amiel D, Woo SL, Akeson W. Normal ligament properties and ligament healing. Clin Orthop 1985; 196: 15-25.

Frank CB, Hart DA, Shrive NG. Molecular biology and biomechanics of normal and healing ligaments; a review. Osteoarthritis. Cartilage 1999; 7(1): 130-140.

Freels DB, Kilpatrick S, Gordon ES, Ward WG. Animal model for evaluation of soft tissue ingrowth into various types of porous coating. Clin Orthop 2002; 397: 315- 322.

Freidman MA, Carter SK. The therapy of osteogenic sarcoma: Current ststus and thought for the future. J Surg Oncol 1972; 4: 482.

Fu W, Lu Y, Piao Y. Culture and pluripotentiality of human marrow mesenchymal stem cells. Zhonghua Xue Ye Xue Za Zhi 2002; 23(4): 202-204.

Gage JR, DeLuca PA, Renshaw TS. Gait analysis: principle and applications with emphasis on its use in cerebral palsy. Instr Course Lect 1996; 45: 491-507.

Galante JO, Lemons J, Spector M, Wilson PD, Wright TM. The biologic effects of implant materials. J Orthop Res 1991; 9: 760-775.

Galante J, Rostoker W, Lueck R, Ray RD. Sintered finer metal composites as a basis for attachment to implants to bone. J Bone Joint Surg 1971; 53(Am): 101.

Gao J, Rasanen T, Persliden J, Messner K. The morphology of ligament insertions after failure at low strain velocity: an evaluation of ligament entheses in the rabbit knee. J Anat 1996; 189(1): 127-133.

Geesink RG. Hydroxyapatite-coated total hip prostheses. Two-year clinical and roentgenographic results of 100 cases. Clin Orthop 1990; 261: 39-58.

Geesink RGT, de Groot K, Christel PAKT. Chemical implant fixation using hydroxyapatite coatings. Clin Orthop 1987; 225: 147-170.

Geesink RGT, de Groot K, Klein CPAT. Bonding of bone to apatite coated implants. J Bone Joint Surg 1988; 70(Br): 17-22.

Gelberman RH, Vandeberg JS, Manske PR, Akeson WH. The early stages of flexor tendon healing: A Morphologic study of the first fourteen days. J Hand Surg (Am) 1985; 10: 776-784.

Ghosh P, Read R, Armstrong S, Wilson D, Marshall R, McNair P. The effects of intraarticular administration of hyaluronan in a model of early osteoarthritis in sheep. I. Gait analysis and radiological and morphological studies. Semin Arthritis Rheum 1993; 22: 18-30.

Gillard GC, Reilly HC, Bell-Booth PG, Flint M. The influence of mechanical forces on the glycosaminoglycan content of the rabbit flexor digitorum profundus tendon. Conn Tiss Res 1979; 7: 37-46.

Giori NJ, Beaupre GS, Carter DR. Cellular shape and pressure may mediate mechanical control of tissue composition in tendons. J Orthop Res 1993; 11: 581-591.

Gocke R, Rafalzyk B, Seyfarth M, Sonnenburg I, Gundlach KK. Components of antibacterial and fibrinolytic activity of human saliva in normal and disordered wound healing Mund Kiefer Gesichtschir 1999; 3(1): 38-42.

Goldring SR, Flannery MS, Petrison KK, Evins AE, Jasty MJ. Evaluation of connective tissue cell responses to orthopaedic implant materials. Connect Tissue Res 1990; 24(1): 77-81.

Gonzales M, Haan K, Baker SE, Fitchmun M, Todorov I. A cell signal pathway involving laminin-5, alpha3beta1 integrin and mitogen-activated protein kinase can regulate epithelial cell proliferation. Mol Biol Cell 1999; 10(2): 259-270.

Goodnight JE, Bargat WL. Limb sparing surgery for extrimity sarcomas after preoperative intra-arterial doxorubicin and radiation therapy. Am J Surg 1985; 150: 109-113.

Gosheger G, Hillmann A, Lindner N, Rodl R, Hoffmann C, Burger H, Winkelmann W. Soft tissue reconstruction of megaprostheses using a trevira tube. Clin Orthop 2001; 393: 264-271.

Goshima J, Goldberg VM, Caplan AI. The osteogenic potential of culture-expanded rat marrow mesenchymal cells assayed *in vivo* in calcium phosphate ceramic blocks. Clin Orthop 1991; 262: 298-311.

Goss RJ. Deer antlers, regeneration, function and evolution. Academic Press 1983

Goss RJ. Tissue differentiation in regenerating antlers. In: Biology of deer production. Fennessy PF and Drew KR. Eds. Royal Society of New Zealand. Bull 22. 1985; 229-238.

Gottsauner-Wolf F, Egger EL, Giurea A, Antosch M, Olsen D, Rock MG, Sim FH. Biologic attachment of an allograft bone and tendon transplant to a titanium prosthesis. Clon Orthop 1999; 358: 101-110.

Gottsauner-Wolf F, Egger EL, Markel MD, Schultz FM, Chao EY. Fixation of canine tendons to metal prosthesis. Acta Orthop Scand 1994; 65: 179-184.

Gottsauner-Wolf F, Egger EL, Schultz FM, Sim FH, Chao EY. Tendons attached to prostheses by tendon-bone block fixation: an experimental study in dogs. J Orthop Res 1994; 12: 814-821.

Gould TRL, Brunette DM, Westbury L. The attachment mechanism of epithelial cells to titanium *In Vitro*. J Periodontal Res 1981; 16: 611-616.

Gould TRL, Westbury L, Brunette DM. Ultrastructural study of the attachment of human gingiva to Ti *in vivo*. J Prosthet Dent 1984; 52: 418-20.

Graf J, Iwamoto Y, Sasaki M, Martin GR, Kleinman HK, Robey FA, Yamada Y. Identification of an amino acid sequence in laminin mediating cell attachment, chemotaxis and receptor binding. Cell 1987; 48: 989-996.

Gray RJ, Elves MW. Donor cells' contribution to osteogenesis in experimental cancellous bone grafts. Clin Orthop 1982; 163: 261-271.

Grinnell F, Feld M, Minter D. Fibroblast adhesion to fibrinogen and fibrin substrata: Requirement for cold-insoluble globulin (plasma fibronectin). Cell 1980; 19: 517-525.

Gristina AG. Biomaterial-centered infection: microbial adhesion versus tissue integration. Science 1987; 237(4822): 1588-1595.

Grosse-Siestrup C, Affeld K, Loppnow H, Bucherl ES. Artificial percutaneous leads allowing permanent epithelial ingrowth. Proceedings of the First Meeting of the International Society for Artificial Organs Tokyo Japan 1997; 1: 86-90.

Grosse-Siestrup C, Affeld K. Design criteria for percutaneous devices. J Biomed Mater Res 1984; 18: 357-382.

Grosse-Siestrup C, Krautzberger W, Burcherl ES. Arterio-venous shunt with percutaneous leads in calves for long term *in vivo* testing of blood contact materials. J Biomed Mater Res 1979; 13: 15-22.

Grundmann E, Ueda Y, Schneider-Stock R, Roessner A. New aspects of cell biology in osteosarcoma. Pathol Res Pract 1995; 191(6): 563-570.

Hacking SA, Bobyn JD, Toh K, Tanzer M, Krygier JJ: Fibrous tissue ingrowth and attachment to porous tantalum. J Biomed Mater Res 200; 52: 631-638.

Hadley MA, Byers SW, Suarez-Quian CA, Kleinman HK, Dym M. Extracellular matrix regulates sertoli cell differentiation, testicular cord formation and germ cell development *In Vitro*. J Cell Biol 1985; 101: 1511-1522.

Hall C, Adans I, Ghidoni J. Development of skin interfacing cannula. Trans Am Soc Artif Intern Organs 1975; 21: 281-288.

Hardy DCR, Frayssinet P, Guilham A, La Fontaine MA, Delince PE. Bonding of hydroxyapatite-coated femoral prosthesis. Histopathology of specimens from four cases. J Bone Joint Surg 1991; 73(Br): 732.

Harrison RG. On the stereotropism of embryonic cells. Science 1911; 34: 279.

Hattersley G, Cox K, Soslwsky LJ, Thomopoulous S, Hewick R, Joyce ME, Rosen V. Bone morphogenic proteins 2 and 12 alter the attachmnet of tendon to bone in a rat model: A histological and biomechanical investigation. Trans Orth Res Soc 1998; 23: 96-16.

Hausman M, Bain S, Rubin C. Reluctance of Metaphyseal Bone to Heal to Tendon: Histologic Evidence for Poor Mechanical Strength. Trans.O.R.S. 14, 277. 1989.

Haynesworth SE, Goshima J, Goldberg VM, Caplan AI. Characterization of cells with osteogenic potential from human marrow. Bone 1992; 13: 81-88.

Heaney TG. A histological investigation of the influence of adult porcine gingival connective tissues in determining epithelial specificity. Arch Oral Biol 1977; 22(3): 167-174.

Heimark RL, Schwartz SM. The role of membrane-membrane interactions in the regulation of endothelial cell growth. J Cell Biol 1985; 100(6): 1934-1940.

Heimark RL, Twardzik DR, Schwartz SM. Inhibition of endothelial regeneration by type-beta transforming growth factor from platelets. Science 1986; 233(4768): 1078-1080.

Hess GP, Cappiello Wl, Poole RM, Hunter SC. Prevention and treatment of overuse tendon injuries. Sports Med 1989; 8: 371-384.

Hildebrand KA, Woo SL, Smith DW, Allen CR, Deie M, Taylor BJ, Schmidt CC. The effects of platelete-derived growth factor-BB on healing of the rabbit medial collateral ligament. An *in vivo* study. Am J Sports Med 1998; 26: 549-554.

Holgers KM. Characteristics of the inflammatory process around skin-penetrating titanium implants for aural rehabilitation. Audiology 2000; 39(5): 253-259.

Holgers KM, Bjursten LM, Thomsen P, Ericson LE, Tjellstrom A. Experience with percutaneous titanium implants in the head and neck: Clinical and histological study. J Invest Surg 1989; 2(1): 7-16.

Holgers KM, Roupe G, Tjellstrom A, Bjursten LM. Clinical, immunological and bacteriological evaluation of adverse reactions of skin penetrating titanium implants in the head and neck region. Contact Dermatitis 1992; 27: 1-7.

Holgers KM, Thomsen P, Tjellstrom A, Bjursten LM. An immunohistochemical analysis of the soft tissue around long-term skin-penetrating titanium implants. Biomaterials 1995; 16(ii): 611-616.

Holgers KM, Thomsen P, Tjellstrom A, Ericson LE. Electron microscope observations on the soft tissue around clinical long-term percutaneous titanium implants. Biomaterials 1995(i); 16(2): 83-90.

Holgers KM, Tjellström A, Bjursten LM, Erlandsson BE. Soft tissue reaction around percutaneous inplants: a clinical study on skin-penetrating titanium implants used for bone-anchored auricular prostheses. Int J Oral Maxillofac Implants 1987; 2: 35-39.

Holgers KM, Tjellström A, Bjursten LM, Erlandsson BE. Soft tissue reaction around percutaneous inplants: a clinical study of soft tissue condition around skin-penetrating titanium implants used for bone anchored hearing aids. Am J Otology 1988; 9: 56-59.

Holmes RE, Roser SM. Porous hydroxyapatite as a bone graft substitute in alveolar ridge augmentation: a histoometric study. Int J Oral Maxillofac Surg 1987; 16(6): 718-728.

Hormia M, Kononen K, Kivilahti J, Virtanen I. Immunolocalisation of proteins specific for adherens junctions in human gingival epithelial cells grown on differently processed titanium surfaces. J Peridontal Res 1991; 26(6): 491-497.

Hormia M, Owaribe K, Virtanen I. The dento-epithelial junction: cell adhesion by type I hemidesmosomes in the absence of a true basal lamina. J Periodontol 2001; 72(6): 788-797.

Hormia M, Sahlberg C, Thesleff I, Airenne T. The epitheium-tooth interface – a basal lamina rich in laminin-5 and lacking other known laminin isoforms. J Dent Res 1998; 77(7): 1479-1485.

Hormia M. Immunolocalization of fibronectin and vitronectin receptors in human gingival fibroblasts spreading on titanium surfaces. J Periodontal Res 1994; 29(2): 146-52.

Horowitz SM, Lane JM, Otis JC, Healey JH. Prosthetic arthroplasty of the knee after resection of a sarcoma in the proximal end of the tibia. A report of sixteen cases. J Bone Joint Surg 1991; 73(Am): 286-293.

Houglum PA. Soft tissue healing and its impact on rehabilitation. J Sports Rehab 1992; 1: 19-39.

Hulbert SF, young FA, Matthews RS, Klawitter JJ, Talbert CD, Stelling FH. Potential of ceramic materials as permanently implantable skeletal prostheses. J Bone Joint Surg 1970; 4(Br): 433.

Hunter A, Archer CW, Walker PS, Blunn GW. Attachment and proliferation of osteoblasts and fibroblasts on biomaterials for orthopaedic use. Biomaterials 1995; 16: 287-95.

Hynes RO. Fibronectins. Scientific Americian 1986; 254(6): 42-51.

Inoue N, Ikeda K, Young DR, Aro H, Frassica F, Ma CB, Waltrip RL, Chao EY. Tendon Fixation to Porous Metallic Implant Using Autogenous Bone Graft Augmentation.Trans ORS 1996; 21: 352.

Inoue N, Ikeda K, Aro H, Frassica F, Sim F Chao E. Biologic tendon fixation to metallic implant augmented with autologous concellous bone graft and bone marrow in a canine model. J Orthop Res 2002; 20: 957-966.

Inoue N, Young DR, Ikeda K, Gottsauner-Wolf F, Egger EL, Chao EY. Fibre Orientation in Soft Tissue Attachment to Metallic Prosthesis. Trans ORS 1995; 20: 615.

Inoue T, Cox JE, Pilliar RM, Melcher AH. Effect of the surface geometry of smooth and porous-coated titanium alloy on the orientation of fibroblasts *In Vitro*. J Biomed Mater Res 1987; 21(1): 107-126.

Ishikawa H, Koshino T, Takeuchi R, Saito T. Effects of collagen gel mixed with hydroxyapatite powder on interface between newly formed bone and grafted achilles tendon in rabbit femoral bone tunnel. Biomaterials 2001; 22(12): 1689-1694.

Jaffe N, Knapp J. Osteosarcoma: Intra-arterial treatment of the primary tumour with cis-diamine dichloroplatinum II: Angiogenic, pathologic and pharmacologic studies. Cancer 1983; 51: 402-407.

Jaffe A, Ehrlich J, Shoshan S. Biological anchoring of acrylic tooth implants in the dog using enriched collagen solutions. Arch Oral Biol 1978; 23(5): 415-419.

James RA, Schultz RL. Hemidesmosomes and the adhesion of junctional epithelial cells to metal implants – a preliminary report. Oral Implantology 1974; 4: 294-302.

Jansen JA, De Wijn JR, Wolters-Lutgerhorst JM, Van Mullem PJ. Ultrastructural study of epithelial cells attachment to implant materials. J Dental Res 1985; 64(6): 891-896.

Jansen JA, Van Der Waerden JPCM, De Groot K. Epithelial reaction to percutaneous implant materials: *In Vitro* and *In Vivo* experiments. J Invest Surg 1989; 2: 29-49.

Jarcho M. Biomaterial aspects of calcium phosphates; Properties and application. Dent Clin North Am 1986; 30: 25-47.

Jarcho M. Calcium phosphate ceramics as hard tissue prosthetics Clin Orthop 1981; 157: 259-278.

Jensen JS. Resection arthroplasty of the proximal tibia. Acta Orthop Scand 1983; 54: 126-130.

Jeon DG, Kawai A, Boland P, Healey JH. Algorithm for the surgical treatment of malignant lesions of the proximal tibia. Clin Orthop 1999; 358: 15-26.

Jevens DJ, DeCamp CE, Hauptman J, Braden TD, Richter M, Robinson R. Use of force-plate analysis of gait to compare two surgical techniques for treatment of cranial cruciate ligament rupture in dogs. Am J Vet Res 1996; 57: 389-393.

Jones JR, Smibert JG, McCullough CJ, Price AB, Hutton WC. Tendon implantation into bone: an experimental study. J Hand Surg 1987; 12(Br): 306-312.

Jozsa LG, Kannus P. In: 1997 Ed Human Tendons – Anatomy, Physiology and Pathology. Pub Human Kinetics. Ch 2 Structure and Metabolism of Normal Tendons.

Karagianes MT, Westerman RE, Hamilton AI, Adams HF, Wills RC. Investigation of long-term performance of porous metal dental implants in nonhuman primates. J Oral Implantology 1982; 10: 189-207.

Karring T, Lang NP, Loe H. The role of gingival connective tissue in determining epithelial differentiation. J Periodontal Res 1975; 10(1): 1-11.

Kastelic J, Palley I, Baer E. A structural mechanical model for tendon crimping. J Biomech 1980; 13: 887-893.

Katenkamp D, Stiller D, Schulze E. Ultrastructural cytology of regenerating tendon. Exp Pathol 1976; 12: 25-37.

Kato K, Aoki H, Tabata T, Ogiso M. Biocompatibility of apatite ceramics in mandibles. Biomater Med Devices Artif Organs 1979; 7(2): 291-297.

Katsumura T, Koshino T, Saito T. Viscous property and osteogenesis induction of hydroxyapatite thermal decomposition product mixed with gelatin implanted into rabbit femurs. Biomaterials 1998; 19: 1839-1844.

Kawahara H, Kawahara D, Hashimoto K, Ong JL. Morphological studies on the biological seal of titanium dental implants. Report 1: *In Vitro* study on the epithialization mechanism around the dental implant. Int J Oral Maxillofac Implants 1998; 13: 457-464.

Kawahara H, Kawahara D, Mimura Y, Takashima Y, Ong JL. Morphologic studies on the biologic seal of titanium dental implants. Report II. *In vivo* study on the defending mechanism of epithelial adhesions/attachment against invasive factors. Int J Oral Maxillofac Implants 1998; 13(4): 465-473.

Kawahara H, Moriwaki S, Takashima Y, Iwao T. Studies on the reconstruction and function of tissue under the heterogeneous environment. Report 1: effect of the heterogeneous environment upon the morphological and functional behavior of cells *In Vitro*. J Oromaxillofac Biomech 1995; 1: 11-16.

Kent JN, Homsy CA, Gross BD, Hinds EC. Pilot studies of a porous implant in dentistry and oral surgery. J Oral Surg 1972; 30(8): 608-615.

Kernwein GA. A Study of Tendon Implantation into Bone. Surgery, Gynaecology and Obstetrics 1942; 75: 794-796.

Kienapfel H, Sprey C, Wilke A, Griss P. Implant fixation by bone ingrowth. J Arthroplasty 1999; 14: 355-368.

Kirschenbuam IH. Basic principals of hydroxyapatite in joint replacement surgery. Sem Arthrop 1991; 2: 252.

Klein CPAT, Driesson AA, de Groot K, Vander Hoff A. Biodegradation behavior of various calcium phosphate materials in bone tissue. J Biomed Mater Res 1983; 17: 769-784.

Kleinman HK, Cannon FB, Laurie GW, Hassell JR, Aumailley M, Terranova VP, Martin GR, DuBois-Dalcq M. Biological activities of laminin. J Cell Biochem 1985; 27: 317-25.

Knabe C, Grosse-Siestrup C, Gross U. Histologic evaluation of a natural permanent percutaneous structure and clinical percutaneous devices. Biomaterials 1999; 20(6): 503-510.

Knese KH, Biermann H. Die knockenbildung an sehnen-und bands a tzen im bereich urspr u nglich chondraler apophysen. Z Zellforsch. 1958; 49: 142-187.

Kobayashi K, Rose GG, Mahan CJ. Ultrastructure of the dento-epithelial junction. J Periodont Res 1976; 11: 313.

Kodama T. Study on biocompatibility of titanium alloys. Kokubyo Gakkai Zasshi 1989; 56(2): 263-288.

Kohler P, Lindh L, Bjorklind A. Bacteria on stumps of amputees and the effect of antiseptics. Prosthet Orthot Int 1989; 13(3): 149-151.

Kononen M, Hormia M, Kivilahti J, Hautaniemi J, Thesleff I. Effect of surface processing on the attachment, orientation, and proliferation of human gingival fibroblasts on titanium. J Biomed Mater Res 1992; 26(10): 1325-1341.

Kornu R, Maloney WJ, Kelly MA, Smith RL. Osteoblast adhesion to orthopaedic implant alloys: effects of cell adhesion molecules and diamond-like carbon. J Orthop Res 1996; 14: 871-877.

Korvick DL , Cummings JF, Grood ES, Holden JP, Feder SM, Butler DL. The use of an implantable force transducer to measure patellar tendon forces in goats. J Biomech 1996; 29: 557-561.

Kumagai J, Sarkar K, Uhthoff HK, Okawara Y, Ooshima A. Immunohistochemical distribution of type I, II and III collagens in the rabbit supraspinatus tendon insertion. J Anat 1994; 185(Pt 2): 279-284.

Kummer FJ, Rose RM. Corrosion of titanium/cobalt-chromium alloy couples. J Bone Joint Surg 1983; 65(Am): 125-1126.

Laassel EM, Loslever P, Angue JC. Patterns of relations between lower limb angle excursions during normal gait. J Biomed Eng 1992; 14: 313-320.

LaBerge M, Bobyn JD, Rivard CH, Drouin G, Duval P. Study of soft tissue ingrowth into canine porous coated femoral implants designed for osteosarcomas management. J Biomed Mater Res 1990; 24(7): 959-971.

Lanir N, Ciano PS, Van de Water L, McDonagh J, Dvorak AM, Dvorak HF. Macrophage migration in fibrin gel matrices II. Effects of clotting factor XIII, fibronectin and glycosaminoglycan content on cell migration. J Immunol 1988; 140: 2340-2349.

Laros GS, Tipton CM, Cooper RR. Influence of physical activity on ligament insertions in the knees of dogs. J Bone Joint Surg 1971; 53(Am): 275-286.

Lavos-Valereto IC, Wolynec S, Deboni MC, Konig B. *In Vitro* and *in vivo* biocompatibility testing of Ti-6Al-7Nb alloy with and without plasma-sprayed hydroxyapatite coating. J Biomed Mater Res 2001; 58: 727-733.

Leadbetter WB. Cell-matrix response in tendon injury. Clin Sports Med 1992; 11: 533-578.

Lee VSP, Solomonidis SE, Spence WD. Stump-socket interface pressure as an aid to socket design in prosthesis for trans-femoral amputees-a preliminary study. Proc Instn Mech Engrs 1997; 211(H): 167-180.

Lehto M, Józsa L, Kvist M, Järvinen M, Bàlint BJ, Rèffy A. Fibronectin in the ruptured human achilles tendon and its paratenon. An immunoperoxidase study. Ann Chir Gynaecol 1990; 79: 72-77.

Letson AK, Dahners LE. The effect of combinations of growth factors on ligament healing. Clin Orthop 1994; 308: 207-212.

Levy SW. Amputees: skin problems and prosthesis. Curtis 1995; 55: 297-301.

Lewis CG, Jones LC, Hungerford DS. Effects of grafting on porous metal ingrowth. J Arthroplasty 1997; 12(4): 451-460.

Li C, Suttie JM. Light microscope studies of pedicle and early first antler development in the Red Deer (Cervus elaphus). The Anatomical Record 1994; 239: 198-215.

Lindholm TC, Lindholm TS. New bone and connective tissue ingrowth in a hydroxyapatite block repairing a rabbit skull defect. Ann Chir Gynaecol Suppl 1993; 207: 109-115.

Linter F, Zweymuller K, Brand G. Tissue reactions to titanium endoprostheses. Autopsy studies of four cases. J arthroplasty 1986; 1: 183-195.

Liotta LA, Weiner UM, Rao CN, Bryant G. Laminin receptors. In; The Cell In Contact ed GM Edelman, JP Thiery. New York: Wiley 1985; pp: 333-344.

Listgarten MA. Electron microscopic study of the gingivo-dental junction of man. Am J Anat 1966; 119(1): 147-177.

Listgarten MA, Lai CH. Ultrastructure of the intact interface between an endosseous epoxy resin dental implant and host tissue. J Bio Buccale 1975; 3: 13.

Listgarten MA, Lang NP, Schroeder HE, Schroeder A. Periodontal tissues and their counterparts around endosseous implants. Clin Oral Impl Res 1991; 2: 1-19.

Liu SH, Panossian V, al Shaikh R, Tomin E, Shepherd E, Finerman GA, Lane JM. Morphology and matrix composition during early tendon to bone healing. Clin Orthop 1997; 339: 253-260.

Liu SH, Yang RS, al Shaikh R, Lane JM: Collagen in tendon, ligament, and bone healing. A current review. Clin Orthop 1995; 318: 265-278.

Lo IKY, Randle JA, Majima T, Thornton G, Rattner JB, Shrive NG, Frank CB, Hart DA. New directions in understanding and optimizing ligament and tendon healing. Current Opinion in Orthopaedics 2000; 11: 421-428.

Löe H. The structure and physiology of the dento-gingival junction. In: Structural and chemical organization of teeth. Volume 2. E.A.W Miles Ed, Academic Press. New York/London 1967; pp: 415-455.

Lowenberg BF, Pilliar RM, Aubin JE, Sodek J, Melcher AH. Cell attachment of human gingival fibroblasts *In Vitro* to porous surfaced titanium alloy discs coated with collagen and platelet-derived growth factor. Biomaterials 1988; 9(4): 302-309.

Lundberg F, Schliamser S, Ljungh A. Vitronectin may mediate adhesion of coagulase-negative staphylococci to biomaterials exposed to cerebrospinal fluid. J Med Microbiol 1997; 46: 285-296.

MacDonald DE, Markovic B, Allen M, Somasundaran P, Boskey AL. Surface analysis of human plasma fibronectin adsorbed to commercially pure Ti materials. J Biomed Mater Res 1998; 41: 120-130.

MacGregor DC, Wilson GJ, Lixfeld W, Pilliar RM, Bobyn JD, Silver MD, Smardon S, Miller SL. The porous-surfaced electrode: a new concept in pacemaker lead design. J Thorac Cardiovasc Surg 1979; 78(2): 281-291.

Mackenzie IC, Fusenig NE. Regeneration of organised epithelial structure. J Invest Dermatol 1983; 81(1): 189-194.

Mackenzie IC, Hill MW. Maintenance of regionally specific patterns of cell proliferation and differentiation in transplanted skin and oral mucosa. Cell Tissue Res 1981; 219(3): 597-607.

Majeska RJ, Port M, Einhorn TA. Attachment to extracellular matrix molecules by cells differing in the expression of osteoblastic traits. J Bone Miner Res 1993; 8: 277-289.

Majors AK, Boehm CA, Nitto H, Midura RJ, Mushler GF. Characterization of human bone marrow stromal cells with respect to osteoblastic differentiation. J Orthop Res 1997; 15: 546-557.

Malawer M. Surgical technique and results of limb sparing surgery for high grade bone sarcomas of the knee and shoulder. Orthopaedics 1985; 8(5): 597-607.

Malawer MM, McHale KA. Limb-sparing surgery for high-grade malignant tumors of the proximal tibia. Surgical technique and a method of extensor mechanism reconstruction. Clin Orthop 1989; 239: 231-248.

Manley Mt. Calcium phosphate biomaterials: a review of the literature. In: Hydroxyapatite Coatings in Orthopaedic Surgery. Geesink RGT, Manley MT (eds). New York NY: Raven Press 1993; 1-23.

Marks SC Jr, McKee MD, Zalzal S, Nanci A. The epithelial attachment and the dental junctional epithelium: ultrastructural features in porcine molars. Anat Rec 1994; 238(1): 1-14.

Martin GR. Laminin and other BM components. Ann Rev Cell Biol 1987; 3: 57-85.

Massaro C, Baker MA, Cosentino F, Ramires PA, Klose S, Milella E. Surface and biological evaluation of hydroxyapatite-based coatings on titanium deposited by different techniques. J Biomed Mater Res 2001; 58: 651-657.

Mast BA. Healing in other tissues. Surg Clin North Am 1997; 77: 529-547.

Matsuno H, Yokoyama A, Watari F, Uo M, Kawasaki T. Biocompatibility and osteogenesis of refractory metal implants, titanium, hafnium, niobium, tantalum and rhenium Biomaterials 2001; 22(11): 1253-1262.

McHugh WD. The keratiniztion of gingival epithelium. J Periodontol 1964; 35: 338-348.

McKinney RV, Steflik DE, Koth DL. Evidence for a junctional epithelial attachment to ceramic dental implants. J Periodontol 1985; 56: 579-91.

Mears DC. Materials and Orthopaedic Surggery, Williams and Wilkins, Baltimore, MD, 1979; pp: 725.

Meffert RM. Do implant surfaces make a difference? Curr Op Periodont 1997; 4: 104-108.

Meffert RM. The soft tissue interface in dental implantology. Int J Oral Implantol 1988; 5(1): 55-58.

Meriam C, Beynnon BD, Fleming BC, Nichols CE, Johnson RJ, Renstrom PA. The Effect of Screw Insertion Torque on Tendons Fixed with Spiked Washers. Trans ORS 1995; 20: 614.

Meyle J, Gultig K, Wolburg H, Von Recum A.F. Fibroblast anchorage to microtextured surfaces. J Biomed Mater Res 1993; 27: 1553-1557.

Michaels CM, Keller JC, Stanford CM. *In Vitro* periodontal ligament fibroblast attachment to plasma-cleaned Ti surfaces. J Oral Implantol 1991;17(2): 132-9.

Mow VC, Hayes WC. In: Basic Orthopaedic Biomechanics. Second Edition 1997. Pub; Lippincott Williams and Wilkins pp 413.

Muir P, Johnson KA, Cooley AJ, Manley PA. Force-plate analysis of gait before and after surgical excision of calcified lesions of the supraspinatus tendon in two dogs. Vet Rec 1996; 139: 137-139.

Nakahara H, Bruder SP, Goldberg VM, Caplan AI. *In vivo* osteochondrogenic potential of cultured cells derived from the periosteum. Clin Orthop 1990; 259: 223-232.

Natsu-Ume T, Nakamura N, Shino K, Morishita R, Nakata K, Horibe S, Mae T, Matsumoto K, Nakamur T, Kaneda Y, Ochi T. *In vivo* introduction of hepatocyte growth factor/ scatter factor (HGF/SF) into healing patellar ligament. Trans ORS 1998; 23: 94.

Nowicki B, Runyan RS, Smith N, Krouskop TA. Kinetics of colonization of a porous vitreous carbon percutaneous implant. Biomaterials 1990; 11(6): 389-392.

Nuttleman CR, Mortisen DJ, Henry SM, Anseth KS. Attachment of fibronectin to poly (vinyl alcohol) hydrogels promotes NIH3T3 cell adhesion, proliferation and migration. J Biomed Mater Res 2001; 57(2): 217-223.

Oguma H, Murakami G, Takahashi-Iwanaga H, Aoki M, Ishii S. Early anchoring collagen fibres at the bone-tendon interface are conducted by woven bone formation: light microscope and scanning electron microscope observation using a canine model. J Orthop Res 2001; 19: 873-880.

Ohgushi H, Goldberg VM, Caplan AI. Heterotopic osteogenesis in porous ceramics induced by marrow cells. J Orthop Res 1989; 7: 568-578.

Ohgushi H, Goldberg VM, Caplan AI. Repair of bone defects with marrow cells and porous ceramic. Acta Orthop Scand 1989; 60(3): 334-339.

Ohtera K, Yamada Y, Aoki M, Sasaki T, Yamakoshi K. Effects of periosteum wrapped around tendon in a bone tunnel: A biomechanical and histological study in rabbits. Crit Rev Biomed Eng 2000; 28: 115-118.

Oikarinen J, Korhonen LK. The bone inductive capacity of various bone transplanting materials used for treatment of experimental bone defects. Clin Orthop 1979; 140: 208-215.

Okuda Y, Gorski JP, An KN, Amadio PC. Biochemical, histological and biomechanical analyses of canine tendon. J Orthop Res 1987; 5: 60-68.

Oreffo RO, Driessens FC, Planell JA, Triffitt JT. Growth and differentiation of human bone marrow osteoprogenitors on novel calcuim phosphate cements. Biomaterials 1998; 19: 1845-1854.

Otis JC, Lane JM, Kroll MA. Energy cost during gait in osteosarcoma patients after resection and knee replacement and after above-the-knee amputation. J Bone Joint Surg Am 1985; 67(Am): 606-611.

Ozaki T, Kunisada T, Kawai A, Takahara Y, Inoue H. Insertion of the patella tendon after prosthetic replacement of the proximal tibia. Acta Orthop Scand 1999; 70: 527-529.

Ozawa N. Histological and mechanical observations of interconnection between sintered porous hydroxyapatite and Achilles tendon in rats. Nippon Seikeigeka Gakkai Zasshi 1991; 65(11): 1091-1098.

Panni AS, Milano G, Lucania L, Fabbriciani C. Graft healing after anterior cruciate ligament reconstruction in rabbits. Clin Orthop 1997; 343: 203-212.

Paquay YC, de Ruijter JE, van der Waer den JP, Jansen JA. Tissue reaction to Dacron velour and titanium fibre mesh used for anchorage of percutaneous devices. Biomaterials 1996; 17(12): 1251-1256.

Park JC, Kim HM, Ko J. Effects of extracellular matrix constituents on the attachment of human oral epithelial cells at the titanium surface. Int J Oral Maxillofac Implants 1998; 13(6): 826-836.

Perek D, Jurczyk-Procyk S. Role of chemotherapy in treatment of osteosarcoma. Pediatr Pol 1995; 70(11): 939-947.

Pilliar RM, Cameron HU, Welsh RP, Binnington AG: Radiographic and morphologic studies of load-bearing porous-surfaced structured implants. Clin Orthop 1981; 156: 249-257.

Prigent H, Pellen-Mussi P, Cathelineau G, Bonnaure-Mallet M. Evaluation of the biocompatibility of titanium-tantalum alloy versus titanium. J Biomed Mater Res 1998; 39(2): 200-206.

Pritham CH. Biomechanics and shape of the above-knee socket considered in light of the ischial containment concept. Prosthetics and Orthotics Int 1990; 14: 9-21.

Radcliffe CW. Functional considerations in the fitting of above-knee prosthesis. Artificial Limbs 1955; 2(1): 35-60.

Rae T. A study on the effects of particular metals of orthopaedic interest on murine macrophages *In Vitro*. J Bone Joint Surg 1975; 57(Br): 444-450.

Ralphs RJ, Benjamin M, Thornett A. Cell and matrix biology of the supropatella in the rat: A structural and immunocytochemical study of fibrocartilage in a tendon subject to compression. Anat Rec 1991; 231: 167-177.

Ralphs JR, Tyres RNS, Benjamin M. Development of functionally distinct fibrocartilages at two sites in the quadriceps tendon of the rat: The suprapatella and the attachment to the patella. Anat Embryol 1992; 185: 181-187.

Rempel D, Abrahamsson SO. The effects of reduced oxygen tension on cell proliferation and matrix synthesis in synovium and tendon explants from the rabbit carpel tunnel: an experimental study *In Vitro*. J Orthop Res 2001; 19: 143-148.

Richards RG. The effect of surface roughness on fibroblast adhesion *In Vitro*. Injury 1996; 27(3) suppl: 38-43.

Robertson DB, Daniel DM, Biden E. Soft tissue fixation to bone. Am J Sports Med 1986; 14: 398-403.

Robertson DM, Pierre L, Chahal R: Preliminary observations of bone ingrowth into porous materials. J Biomed Mater Res 1976; 10: 335-344.

Rodeo SA, Arnoczky SP, Torzilli PA, Hidaka C, Warren RF. Tendon-healing in a bone tunnel. A biomechanical and histological study in the dog. J Bone Joint Surg 1993; 75(Am): 1795-1803.

Rodeo SA, Suzuki K, Deng XH, Wozney J, Warren RF. Use of recombinant human bone morphogenetic protein-2 to enhance tendon healing in a bone tunnel. Am J Sports Med 1999; 27: 476-488.

Rolf HJ, Enderle A. Hard fallow deer antler: a living bone till antler casting? The Anatomical Record 1999; 225: 69-77.

Rosen G, Marcove RJ. Primary osteogenic sarcoma: Eight years' experience of adjuvant chemotherapy. J Cancer Res Clin Onc 1983; 106: 55-67.

Rosen G, Nirenburg A. Neoadjuvant chemotherapy for osteogenic sarcoma: A five year follow-up (T-10) and preliminary report of new studies (T-12). Prog Clin Biol Res 1985; 201: 29.

Rowe RWD. The structure of rat tail tendon fascicles. Conn Tiss Res 1985; 14: 21-30.

Ruano R, Jaeger RG, Jaeger MM. Effect of a ceramic and a non-ceramic hydroxyapatite on cell growth and procollagen synthesis of cultured human gingival fibroblasts. J Periodontol 2000; 71(4): 540-545.

Rubin LR. Metal implants: Historical background and biological response to implantation. In: Biomaterials in reconstructive surgery. Rubin L.R (ed) 1971; 46-61.

Rufai A, Ralphs JR, Benjamin M. Structure and histopathology of the insertional region of the human Achilles tendon. J Orthop Res 1995; 13: 585-593.

Ruoslahti E, Pierschbacher MD. New perspectives in cell adhesion: RGD and integrins. Science 1987; 238: 491-497.

Rust PA, Kalsi P, Cannon SR, Briggs TW, Blunn GW. Improved osteogenic properties of bone allograft by the use of human mesenchymal stem cells. Trans ORS 2003; 49: 295.

Sakou T. Bone morphogenic proteins: from basic studies to clinical approach. Bone 1998; 22: 591-603.

Salama R, Burwell RG, Dickson IR. Recombined grafts of bone and marrow. J Bone Joint Surg 1973; 55(Br)(2): 402-417.

Salo S, Haakana H, Kontusaari S, Hujanen E, Kallunki T, Tryggvason K. Laminin-5 promotes adhesion and migration of epithelial cells: identification of a migration-related element in the lambda2 chain gene (LAMC2) with activity in transgenic mice. Matrix Biol 1999; 18: 197-210.

Sato S, Koshino T, Saito T. Osteogenic response of rabbit tibia to hydroxyapatite particle-Plaster of Paris mixture. Biomaterials 1998; 19: 1895-1900.

Schroeder A, Van der Zypen E, Stich H. The reactions of bone, connective tissue and epithelium to endosteal implants with titanium sprayed surfaces. J Maxillofac surg 1981; 9: 15-25.

Schroeder HE. Ultrastructure of the junctional epithelium of the human gingiva. Helv Odontol Acta 1969; 13: 65.

Schuch CM, Pritham CH. Current transfemoral sockets. Clin Orthop 1999; 361: 48-54.

Seymour GJ, Gemmell E, Lenz LJ, Henry P, Bower R, Yamazaki K. Immunohistochemical analysis of the inflammatory infiltrates associated with osseointegrated implants. Int J Oral Maxillofac Implants 1989; 4: 191-197.

Shaieb MD, Singer DI, Grimes J, Namiki H. Evaluation of tendon-to-bone reattachment: a rabbit model. Am J Orthop 2000; 29: 537-542.

Sherman RA. Utilization of prostheses among US veterans with traumatic amputation: a pilot survey. J Rehabil Res Dev 1999; 36(2): 100-108.

Shin Y, Akao M. Tissue reactions to various percutaneous materials with different surface properties and structures. Artif Organs 1997; 21(9): 995-1001.

Shrive N, Damson E, Loitz B, Frank C, Marchuk L, Hwang W. Compression or shear alters cell morphology in ligament scar *in vivo*. Trans ORS 1993; 18: 58.

Sim FH, Beauchamp CP, Chao EY. Reconstruction of musculoskeletal defects about the knee for tumor. Clin Orthop 1987; 221: 188-201.

Simon M. Causes of increased survival of patients with osteosarcoma: current controversies. J Bone Joint Surg 1984; 66(Am): 306-310.

Simon MA, Aschliman MA, Thomas N. Limb salvage treatment vs amputation for osteosarcoma of the distal end of the femur. J Bone Joint Surg 1986; 68(Am): 1331-1337.

Singer II, Kazazis DM, Scott S. SEM of focal contacts on the substratum attachment surface of fibroblasts adherent to fibronectin. J Cell Sci 1989; 93: 147-154.

Skoog T, Persson B.H. An Experimental Study of the Early Healing of Tendons. Plastic and Reconstructive Surgery 1954; 13: 384-399.

Snik FM, Dreschler WA, Tange RA, Cremers CWRJ. Short and long term results with implantable transcutaneous and percutaneous bone conduction devices. Arch Otolaryngol Head Neck Surg 1998; 124: 265-268.

Soballe K, Hansen ES, Brockstedt-Rasmussen H, Pedersen CM, Bunger C. Hydroxyapatite coating enhances fixation of porous coated implants. A comparison in dogs between press fit and noninterferential fit. Acta Orthop Scand 1990; 61: 299-306.

Soballe K, Hansen ES, Rasmussen H, Jorgensen PH, Bunger C. Tissue ingrowth into titanium and hydroxyapatite-coated implants during stable and unstable mechanical conditions. J Orthop Res 1992; 10: 285-299.

Solar RJ, Pollack SR, Korosto E. *In Vitro* corrosion testing of titanium surgical implant alloys: an approach to understanding titanium release from implants. J Biomed Mater Res 1979; 13: 217-250.

Spindler KP, Imro AK, Mayes CE, Davidson JM. Patellar tendon and anterior cruciate ligament have different mitogenic responses to platelet-derived growth factor and transforming growth factor β. J Orthop Res 1996; 14: 542-546.

Springfield DS, Schnidt R, Graham-Pole J, Marcus RB, Spanier SS, Enneking WF. Surgical treatment of osteosarcoma. J Bone Joint Surg 1988; 70(Am): 1124-1130.

Squier CA, Collins P. The relationship between soft tissue attachment, epithelial downgrowth and surface porosity. J Periodont Res 1981; 16: 434-440.

Squier CA, Kammeyer GA. The role of connective tissue in the maintenance of epithelial differentiation in the adult. Cell Tissue Res 1983; 230: 615-630.

Steflick DE, McKinney RV, Parr GR, Sisk AL, Koth DL. What we know about the interface between implants and soft tissues. Oral Maxillofac Surg Clin North Am 1991; 3: 775-793.

Stiflik DE, Sisk AL, Parr GA, Lake FT, Hanes PJ. Experimental studies of the implant-tissue interface. J Oral Implantol 1993; 19: 90-94.

Stern IB. Electron microscope observations of oral epithelium. I. Basal cells and the basement membrane. Periodontics 1965; 3: 224-238.

Sundaram J, McGuire MH. Magnitic resonance imaging in planning limb salgave for primary malignant tumours of bone. J Bone Joint Surg 1986; 68(Am): 809-819.

Sweetnam R, Knowlelden J, Jennen H. Bone sarcomas: Treatment by irradiation, amputation, or a combination of the two. Br Med Jour 1971; 2: 363-367.

Tamura RN, Oda D, Quaranta V, Plopper G, Lambert R, Glaser S, Jones JC. Coating of Ti alloy with soluble laminin-5 promotes cell attachment and hemidesmosome assembly in gingival epithelial cells : potential application to dental implants. J periodontal Res 1997; 32: 287-94.

Tang L, Tsai C, Gerberich WW, Kruckeberg L, Kania DR. Biocompatibility of chemical-vapour-deposited diamond. Biomaterials 1995; 16: 483-488.

Thomas DB, Inoue N, Cosgarea A, Chao EYS. A histomorphometric analysis of the human patellar tendon insertion. Trans ORS 1999; 24: 1090.

Thompson RC Jr, Cheng EY, Clohisy DR, Perentesis J, Manivel C, Le CT. Results of treatment for metastatic osteosarcoma with neoadjuvant chemotherapy and surgery. Clin Orthop 2002; 397: 240-247.

Tjellstrom A. Percutaneous Implants in Clinical Practice. CRC Critical Reviews in Biocompatibility 1985; 1(3): 205-228.

Tryggvason K. The laminin family. Curr Op Cell Biol 1993; 5: 887-882.

Tsuji T, Aoki H, Shin Y, Togawa T. Hydroxyapatite percutaneous devices implanted in forearms of three volunteers for more than five years. Apatite Vol 1. Proceedings of the 1st national symposium on apatite. Mishima Japan 1991; 361-365.

Turner CE, Glenney JR, Burridge K. Paxillin: a new vinculin binding protein present in focal adhesions. J Cell Biol 1990; 111: 1059-68.

Uludag H. Osteoinductive alternatives and bone substitutes. Curr Op Orthop 1998; 9(VI): 31-37.

Van Best JA, Pronk CAN, Meschelse K, Pompe R, van Eijndhovem JHM. A method for two dimensional multi-segment kinematic and kinetic analysis of normal and pathological human gait. Medical Progress Through Technology 1984; 10: 143-159.

Van Blitterswijk CA, Kuijpers W, Daems WT, Grote JJ. Epithelial reactions to hydroxyapatite. An *in vivo* and *In Vitro* study. Acta Otolaryngol 1986; 101(3-4): 231-241.

Varshney AC, Sharma DN, Singh M, Sharma SK, Nigam JM. Therapeutic value of bovine saliva in wound healing: a histomorphological study. Indian J Exp Biol 1997; 35(5): 535-537.

Vaudaux P, Pittet D, Haeberli A, Lerch PG, Morgenthaler JJ, Proctor RA, Waldvogel FA, Lew DP. Fibronectin is more active than fibrin or fibrinogen in promoting Staphylococcus aureus adherence to inserted intravascular catheters. J Infect Dis 1993; 167(3): 633-641.

Von der Mark K, Kuhl U. Laminin and its receptor. Biochem Biophys Acta 1985; 823: 147-160.

Von der Mark K, Mollenhauer J, Kuhl U, Bee J, Lesot H. In; The role of extracellular matrix in development, ed. R Trelstad, New York Liss 1984; pp: 67-87.

Von Recum AF, Park JB. Permanent percutaneous devices. CRC critical reviews in bioengineering 1981; 5(1): 37-77.

Von Recum AF. Applications and failure modes of percutaneous devices: a review. J Biomed Mater Res 1984; 18(4): 323-336.

Von Recum AF. New aspects of biocompatibility: motion at the interface. In: Heimke G, Soltesz U, Lee AJC eds. Clinical implant materials. Amsterdam Elsevier 1990; 297-302.

Waggett AD, Ralphs JR, Kwan AP, Woodnutt D, Benjamin M. Characterization of collagens and proteoglycans at the insertion of the human Achilles tendon. Matrix Biol 1998; 16: 457-470.

Walker DJ, Usher K, O'Morchoe M, Sandles L, Griffiths ID, Pinder IM. Outcome from multiple joint replacement surgery to the lower limbs. Br J Rheumatol 1989; 28(2): 139-142.

Wang J, Liu B, Lu C. The influence of basement membrane matrix on the attachment of human gingival epithelial cell to titanium: a scanning electron microscope study. Hua Xi Kou Qiang Yi Xue Za Zhi 1997; 15(1): 11-12.

Wang J, Wang D, Liu B. An experimental study of expediting the early attachment of human gingival epithelial cells to titanium with laminin. Hua Xi Kou Qiang Yi Xue Za Zhi 1998; 16(1): 8-9.

Wang RR, Li Y. *In Vitro* evaluation of biocompatibility of experimental titanium alloys for dental restorations. J Prosthet Dent 1998; 80(4): 495-500.

Watt I. Radiology in the diagnosis and management of bone tumours. J Bone Joint Surg 1985; 67(Br): 520-529.

Welbourn E, Champion RH, Parrish WE. Hyposensitivity to bacteria in eczema: Bacterial culture, skin tests and immunofluorescent detection of immunoglobulins and bacterial antigens. Br J Dermatol 1976; 94: 619.

Whiston TB, Walmsley R. Some observations on the reaction of bone and tendon after tunnelling of bone and insertion of tendon. J Bone Joint Surg 1960; 42(Br)(2): 377-386.

Whittager P, Canham PB. Demonstration of quantative fabric analysis of tendon collagen using two-dimensional polarized light microscopy. Matrix 1991; 11: 56-62.

Winter G. Transcutaneous Implants. J Biomed Mater Res Symp 1974; 5(1): 99-113.

Wolke JGC, Klein CPAT, de Groot K. Bioceramics for maxillofacial applications. In: Bioceramics of the human body. Ravagliol A, Krajewk A (eds). Elsevier Appli Sci London 1992; pp: 166-180.

Woo SLY, Gomez MA, Sites TJ, Newton PO, Orlando CA, Akeson WH. The biomechanical and morphological changes in the medial collateral ligament of the rabbit after immobilization and remobilization. J Bone Joint Surg Am 1987; 69(Am): 1200-1211.

Woo SLY, Hildebrand K, Watanabe N, Fenwick JA, Papageorgiou CD, Wang JH. Tissue engineering of ligament and tendon healing. Clin Orthop 1999; 367 Suppl: S312-S323.

Woo SL-Y, Suh J-K, Parsons IM, Wang J-H, Watanabe N. Biologic intervention in ligament healing Effect of Growth Factors. Sports Medicine and Arthroscopy Review 1998; 6: 74-82.

Wooley PH, Petersen S, Song Z, Nasser S. Cellular immune responses to orthopaedic implant materials following cemented total joint replacement. J Orthop Res 1997; 15(6): 874-880.

www.bekart.com/dymonics/coatings/eng/E-deklagen.htm

www.gordonengland.co.uk/ps.htm

www.ortho-u.net/05/187.htm

Yan WQ, Nakamura T, Kawanabe K, Nishigochi S, Oka M, Kokubo T. Apatite layer-coated titanium for use as bone bonding implants. Biomaterials 1997; 18: 1185-1190.

Yaw KM, Wurtz LD. Resection and reconstruction for bone tumors in the proximal tibia. Orthop Clin North Am 1991; 22: 133-148.

Zachrisson BU, Schultz-Haudt SD. A comparative histological study of clinically normal and chronically inflamed gingivae from the same individuals. Odontol Tidskr 1968; 76(2): 179-192.

Zarb G.A, Symington JM. Osseointegrated dental implants: preliminary report on a replication study. J Prosthet Dent 1983; 50(2): 271-276.

Zlatopolsky AD, Chubukina AN, Berman AE. Heparin-binding fibronectin fragments containing cell-binding domains and devoid of hep2 and gelatin-binding domains promote human embryo fibroblast proliferation. Biochem Biophys Res Commun 1992; 183(2): 383-389.